Cytoprotective mechanisms of erythropoietin and erythropoietin derivatives in peripheral arterial disease

Rebekah Sian Hwee Yu

Thesis submitted for the degree of

Doctor of Philosophy

2014

University College London
Division of Surgery and Interventional Science
Hampstead Campus
Royal Free Hospital
Pond Street
London
NW3 2QG

Statement of Contribution

I, Rebekah Sian Hwee Yu, confirm that the work presented in this thesis is my own. Where information has been derived from other sources, I confirm that this has been indicated in the thesis.

Rebekah Yu

Abstract

A third of patients with critical limb ischaemia (CLI) eventually require amputation. Inconsistencies between successful revascularisation and functional outcomes exist, and underlying musculopathy in CLI patients has been identified. Erythropoietin (EPO) has tissue-protective effects in response to ischaemic injury, but its clinical use is often precluded by thromboembolic side effects.

Non-haematopoietic EPO-derivatives have been designed to retain only tissue-protective functions of EPO. We hypothesised that ARA-290 (EPO-derivative) may have tissue-protective potential that could represent a novel therapeutic adjunct in patients with CLI.

The effect of EPO and ARA-290 in mediating cytoprotection in an *in vitro* simulated ischaemia model of skeletal muscle was assessed firstly in the immortalised murine C2C12 myoblast cell line and subsequently in skeletal myoblasts isolated from CLI and control donors. In human and murine cells, simulated ischaemia alone demonstrated a detrimental effect on cell function and survival. Addition of EPO or ARA-290 demonstrated significant improvements in function and survival and utilised JAK2/STAT3, PI3k/Akt and NFκB signalling molecules.

Isolation of human skeletal myoblasts from CLI patients has not previously been described. Comparison of CLI and control myoblasts elucidated significant differences in their function and survival under both normoxic and simulated ischaemic conditions. CLI myoblasts and myotubes exhibited increased proliferative capacity but reduced migratory and contractile function and importantly a reduced susceptibility to a second ischaemic-insult compared with control myoblasts and myotubes.

Evaluation of several variations in the hindlimb ischaemia model allowed the creation of a model which closely recapitulated the muscular pathology observed in human CLI patients. ARA-290 demonstrated improved functional, histological and perfusion outcomes compared to EPO or vehicle-control treated animals.

These studies demonstrate the potential of ARA-290 to protect tissues and cells from ischaemic-injury and encourages the development of novel pharmacological therapies for use in patients with “no option” CLI or severe functional deficit.

Acknowledgements

My deepest thanks go to my supervisor, mentor and role model, Ms Janice Tsui for her continuous support, kindness, guidance and most importantly friendship throughout this study. I am also appreciative of the experience and intelligence of Professor David Abraham, my secondary supervisor, who performed this role with diligence and humour.

I would like to acknowledge the vital financial support from UCL Grand Challenges Studentship and the Centre for Rheumatology and Connective Tissue Diseases, UCL, for the provision of laboratory space and general reagents during the completion of this thesis. In addition, this work could not have been completed without the invaluable knowledge and wisdom of Drs Xu Shi-Wen, Alan Holmes, Pia Moinzadeh, Markella Ponticos, Ioannis Papaioannou and Richard Stratton and all the past and present staff within Centre for Rheumatology for their willingness to share their expertise.

Acknowledgements also to Dr Anthony Cerami and Dr Michael Brines of ARAIM pharmaceuticals, NY, USA, who kindly donated ARA-290 peptide for use in this study.

I am grateful to Mr Daryll Baker, Mr Shyam Kolvekar and the theatre staff at the Royal Free Hospital, Hampstead and The Heart Hospital, London for their help in patient recruitment and sample collection.

Finally, I would like to thank my family, in particular my mum, and close friends for their constant encouragement during this period, as always. I dedicate this thesis to my late father who removed all obstacles in the path of learning, and gave so much but took so little in return.

Table of Contents

List of Figures

List of Tables

List of Abbreviations

ABC	Avidin-biotin complex
ABPI	Ankle : brachial pressure index
ADP	Adenosine diphosphate
ANOVA	Analysis of variance
Akt	Protein kinase B
ARA-290	Erythropoietin pyroglutamate helix-B surface peptide
ATP	Adenosine triphosphate
βcR	Beta-common receptor
Bp	Base pair
BFU-E	Erythroid blast-forming unit
BMS	Basso mouse scale of locomotion
BSA	Bovine serum albumin
CAD	Coronary artery disease
CD	Cluster differentiation
C:F	Capillary : fibre ratio
CFA	Common femoral artery
CFU-E	Erythroid colony-forming unit
CK	Creatine kinase
CLI	Critical limb ischaemia
CRP	C-reactive protein
CTA	Computed-tomography angiography
DAB	3,3’ diaminobenzidene
DAPI	4’, 6-diamidino-2-phenylindole
DMEM	Dulbecco’s modified eagles medium
DMSO	Dimethyl sulphoxide
DNA	Deoxyribonucleic acid
DSA	Digital subtraction angiography
DTT	Dithiothreitol
DUS	Duplex ultrasound
EDTA	Ethylenediamine tetraacetic acid
EGTA	Ethylene glycol tetraacetic acid
ELISA	Enzyme-linked immunosorbant assay

EPO	Erythropoietin
EPOR	Erythropoietin receptor
ESA	Erythropoiesis stimulating agents
ETC	Electron transport chain
EuCTR	European clinical trials registry
FCS	Foetal calf serum
FDA	Food and drug administration
FFPE	Formalin-fixed paraffin embedded
GM-CSF	Granulocyte-macrophage colony stimulating factor
H&E	Haematoxylin and eosin
HbA1c	Glycated haemoglobin
HIFs	Hypoxia inducible factors
HRE	Hypoxia regulatory elements
HRP	Horseradish peroxidase
HS	Horse serum
IC	Intermittent claudication
IgG	Immunoglobulin G
IGF-1	Insulin-like growth factor 1
IL	Interleukin
IP	Immunoprecipitation
IRI	Ischaemia reperfusion injury
IV	Intravenous
JAK	Janus kinsase
kDa	Kilo Dalton
KCl	Potassium chloride
LDPI	Laser Doppler perfusion image
LDS	Lithium dodecyl sulphate
MCA	Middle cerebral artery
MEPO	Mutant erythropoietin
MHC	Major histocompatibility complex
MI	Myocardial infarction
MMC	Mitomycin-C
MRA	Magnetic resonance angiography

MRI	Magnetic resonance imaging
MRS	Magnetic resonance spectroscopy
MnSOD	Manganese superoxide dismutase
MTT	3-(4,5-dimethylthiazol-2-yl)-2,5-diphenyl tetrazolium bromide
NFκB	Nuclear factor kappa-light-chain-enhancer of activated B-cells
NMDA	*N*-Methyl-D-aspartic acid
NSF	Nephrogenic systemic fibrosis
NTR	Netherland's trial registry
pVHL	Von Hippel-Lindau tumour suppressor protein
PAD	Peripheral arterial disease
PBS	Phosphate buffered saline
PCR	Polymerase chain reaction
PHD	Prolyl hydroxylase domain
PI	Propidium iodide
PI-3k	Phosphatidylinositide 3-kinases
qRT-PCR	Quantitative reverse transcription polymerase chain reaction
rHuEPO	Recombinant human erythropoietin
RIPA	Radioimmunoprecipitation assay
RNA	Ribonucleic acid
ROS	Reactive oxygen species
SC	Subcutaneous
SDS-PAGE	Sodium dodecyl sulphate polyacrylamide gel electrophoresis
SEM	Standard error of the mean
SMM	Skeletal muscle medium
STAT	Signal transducers and activators of transcription
TASC	TransAtlantic Intersociety Consensus
TBPI	Toe-brachial pressure index
$TcPO_2$	Transcutaneous oxygen pressure
TLR	Toll-like receptor
TNF-α	Tumour necrosis factor alpha
VEGF	Vascular endothelial growth factor

CHAPTER 1
General Introduction

1.1 Peripheral Arterial Disease

Peripheral arterial disease (PAD) encompasses a continuum of disease states that result from the narrowing or obstruction of any artery excluding the coronary or intra-cranial vessels. Most often, narrowing or obstruction of these vessels is due to build up of atherosclerotic plaques, which perturbs and eventually prohibits blood flow.

1.1.1 Epidemiology, risk factors and natural history

PAD is a significant healthcare problem in the Western world, where prevalence increases sharply with age. PAD will affect less than 5% of the general population 60 years of age and less [1, 2], however in those aged over 75 years, prevalence will have risen to 20% of the population [1-3]. It is estimated however that the true prevalence of PAD may be three or four times higher, when taking into account those individuals who are asymptomatic [4]. The age-adjusted prevalence of PAD is approximately 12% [5], which equates to approximately 27 million individuals with PAD in Europe and North America [6]. Although male gender is a well-recognised risk factor for atherosclerosis, some disparity exists in the literature to exact rates of PAD affliction, at all stages of disease, with regards to gender. Various reports will suggest higher prevalence in one or other gender, as well as both genders being equally affected with PAD [1, 2, 5, 7, 8].

As a result of population aging, increased life expectancy, better management of traditional cardiovascular risk factors (discussed below) and the increasing prevalence of diabetes mellitus, it is likely that the burden of PAD will increase in the coming years [9].

Risk factors

Atherosclerotic lesions of limb arteries are the most common factor underpinning development of PAD. Various risk factors for developing and accelerating the formation of atherosclerotic plaques have been identified, and these are almost identical to the risk factors for developing PAD. They include increasing age (over 40

years), diabetes mellitus, dyslipidaemia, hypertension [10, 11], and cigarette smoking [12-17]. Other associations for developing PAD include hyperhomocysteinaemia, raised C-reactive protein, chronic renal insufficiency and hyperviscosity and hypercoagulable states [14, 18]. Considering the numerous shared risk factors for PAD and coronary artery disease (CAD), as well as the similarities in disease pathogenesis, there is a significant association between PAD and CAD, with approximately 21–33% of patients undergoing surgical management of CAD found to have PAD [14, 19] and conversely, between 60–92% of PAD patients who have concomitant CAD [20-24].

Natural history

The natural history of PAD is a slow progression of symptoms over time. This is due in part to the nature of atherosclerotic development and evolution. As an atherosclerotic plaque continues to accumulate, narrowing of the artery becomes critical until the entire lumen may become occluded. This explains the diversity in the spectrum of PAD, where it is estimated the prevalence is underestimated due to the initial asymptomatic nature of PAD [15]. Even after symptoms begin to present, the time-course of progression tends to be highly variable, and can be prolonged significantly on strict modification of risk factors. The spectrum of PAD therefore ranges from asymptomatic disease to intermittent claudication (IC) to critical limb ischaemia (CLI). One third of patients with PAD in the lower limbs will have IC. Within this group, approximately 30% of patients will have disease progression towards CLI. The incidence of CLI is estimated at between 500–1000 per million population per year in Europe and North America [25]. Of those patients who progress to CLI, 40% will require an amputation within 6 months, due to various reasons (discussed below) including patient co-morbidities, or anatomical lesion difficulties, and 20% will have died within a year [4]. There is a cumulative amputation rate of approximately 10% at 10 years [26].

1.1.2 Clinical presentation and classification

Approximately one third of patients with PAD will present with typical symptoms of IC, which is defined as “leg pain sufficient to cause the patient to stop walking, which is produced by exercise and relieved by rest, and is caused by arterial occlusive disease” [5, 27]. Limb pain will often be localised to the calf muscle; however the

affected muscle group will depend on the distribution of the atherosclerotic lesion. Disease of the abdominal aorta or iliac arteries can result in calf, thigh or buttock claudication, whereas disease of the superficial femoral artery in the thigh will present with calf pain.

In those individuals who are initially asymptomatic and manage to escape detection of IC and progress onto CLI, the first presentation will be with constant and intractable pain at rest, with tissue loss of non-healing ulcers. Approximately 2% of patients will have an initial presentation with symptoms of CLI without previous IC symptoms [4]. The clinical definition of CLI is "chronic ischaemic rest pain, ulcers or gangrene attributable to objectively proven arterial occlusive disease" [27, 28].

Figure 1.1: Typical features of PAD

Early features of PAD include intermittent claudication, causing pain on exertion (A). As PAD progresses to CLI, patients will often suffer from chronic ulcers and gangrene (B and C), occasionally requiring amputation (D and E).

Classification

Classification of PAD is most commonly represented by the Fontaine stages and the Rutherford categories (Table 1.1). The Fontaine classification was introduced in 1954 by René Fontaine for ischaemia [29]. A more recent classification system, the Rutherford categories, was developed in 1997 [30]. Both classification systems are used clinically to determine improvements following treatment. An upward shift of at least one category is required to denote symptomatic improvement, the exception being patients with tissue loss, who must improve to a stage of claudication for treatment to be considered as improved.

Table 1.1: Classification of PAD: Fontaine's stages and Rutherford's categories

Fontaine's Stages		Rutherford's Categories		
Stage	Clinical description	Grade	Category	Clinical description
I	Asymptomatic	0	0	Asymptomatic
IIa	Mild claudication	I	1	Mild claudication
IIb	Moderate to severe claudication	I	2	Moderate claudication
		I	3	Severe claudication
III	Ischaemic rest pain	II	4	Ischaemic rest pain
		III	5	Minor tissue loss
IV	Ulceration or gangrene	IV	6	Ulceration or gangrene

Mild claudication is described as the distance moved before symptoms of claudication (claudication distance) > 50m. Moderate claudication = claudication distance < 50m or completion of treadmill test with ankle pressures post-test > 50mmHg. Severe claudication = unable to complete treadmill test or ankle pressure post-test < 50mmHg.

1.1.3 Diagnostic modalities

Differentiating between symptoms of claudication and other mechanical (e.g. hip arthritis) or medical (e.g. nerve root compression or spinal stenosis) leg conditions is essential for the prompt and accurate diagnosis of PAD necessary to ensure appropriate management of PAD symptoms and risk factors. A comprehensive and detailed clinical history and examination will usually identify those individuals with classical symptomatic IC who refer to a history of pain on exertion, relieved by rest. Similarly, symptomatic CLI individuals will complain of pain at rest with or without

the presence of gangrene, ulcers or tissue loss. In addition, both groups on examination may reveal a pale limb with absent distal pulses.

Systematic history-taking and thorough clinical examination is usually adequate to give a diagnosis of PAD, however often further objective testing is required to either confirm the presence or reveal the location and severity of disease. This will usually fall into two categories: 1. Non-invasive, surrogate markers of blood flow or 2. Imaging of the peripheral vasculature, which can be both invasive and non-invasive.

1.1.3.1 Surrogate markers of blood flow

Simple diagnostic tests which allow easy measurement of haemodynamics and therefore underlying limb perfusion are useful to identify those patients at risk, with disease, as well as providing an indicator of disease location and severity. Included in these tests are the ankle-brachial pressure index (ABPI), toe-brachial pressure index (TBPI), segmental limb pressures and transcutaneous oxygen pressure ($TcPO_2$).

ABPI and TBPI: The ABPI is an important and commonly used diagnostic tool in the evaluation of PAD, which is inexpensive and simple to perform in the majority of clinical settings. It is measured using a handheld continuous-wave Doppler ultrasound probe and a blood pressure cuff: the highest systolic pressure reading from either the dorsalis pedis or posterior tibial artery (in each leg) is divided by the highest brachial artery pressure reading taken from both arms, with the patient lying in a supine position. The ABPI is useful in providing a measure of the severity of PAD, as well as excluding individuals with other exercise-related leg pain (e.g. osteoarthritis), and for the detection of PAD of the contralateral limb, which may be masked by more severe symptoms in the symptomatic leg. The normal range of ABPI is between 0.91–1.31 [31, 32]. ABPI values between 0.41 and 0.90 are usually indicative of mild to moderate claudication disease, whilst values less than 0.40 tend to correlate with patients who have CLI with ischaemic rest pain [33]. In patients who have a ratio greater than 1.31, PAD cannot be excluded, as this is likely to be due to the presence of incompressible, calcified arteries, which tends to be more prevalent in patients with concomitant PAD and diabetes or end-stage renal disease [3, 34]. In these patients, the toe-brachial pressure index provides a more accurate measure as the digital vessels are usually spared from calcification [35, 36].

Toe-brachial pressure index (TBPI) utilises small occlusive cuffs, placed around usually, the proximal portion of the 1st and 2nd digits, to provide a more accurate systolic pressure reading. TBPI should be greater than 0.75 in healthy individuals. A TBPI value of less than 0.7 is considered abnormal and a value less than 0.25 is suggestive of CLI in patients [37].

The ease of ABPI measurement, as well as the high sensitivity (80–95%) and specificity (95–100%) of ABPI has established its role in the initial evaluation of PAD patients [28, 38].

Segmental limb pressures: Information on the anatomical location of disease can be gained using segmental limb pressures. Based upon the same methodology as ABPI, the blood pressure cuff is used to take a brachial blood pressure reading, and then sequential leg pressures. Measurement by Doppler ultrasound is taken at the most obvious ankle arterial signal as the blood pressure cuff is placed at various points from the upper thigh down to the lower thigh, upper calf, ankle and metatarsal. A comparison of the pressures obtained at different levels allows initial detection of the location of arterial occlusion [33]. Whilst this technique is useful to localise lesions, it is less sensitive and specific when there is multi-level disease, calcified arteries or long-segment lesions. In addition artefacts may occur due to inappropriate cuff sizes or positioning [26, 39].

Both ABPI and segmental limb pressures are useful for the first-line identification of disease severity and general location, but tend to need supplementation with more advanced laboratory imaging such as duplex ultrasound (DUS).

Transcutaneous oxygen pressure ($TcPO_2$): is performed using small electrodes consisting of a central platinum cathode surrounded by a circular silver-silver chloride anode which are placed directly onto the skin of the lower limbs. Oxygen that diffuses to the skin is reduced at the cathode to produce a current proportional to the partial pressure of oxygen (PO_2) within the sensor [33]. $TcPO_2$ is usually measured on the dorsum of the foot or anteromedial aspect of the calf. A $TcPO_2$ of <30mmHg is used as an indication of CLI according to TASC II guidelines [4]. Measurement of $TcPO_2$ is useful in assessing the severity of limb ischaemia and to identify those with ulcers that would benefit from revascularisation. It is not routinely performed however, due to the sensitive and time-consuming nature of the test, which is easily influenced and

affected by numerous factors, including skin temperature, sympathetic tone, metabolic activity, cellulitis, hyperkeratosis and oedema [33].

1.1.3.2 Imaging of the peripheral vasculature

Due to the often complex nature of disease in patients with CLI, it is useful to image the vascular tree from the renal arteries to the pedal arch, in order to identify precise anatomical location and extent of disease, and the amenability of obstructions to revascularisation therapies and to guide treatment.

Duplex ultrasound (DUS): DUS is useful in identifying and delineating the anatomical location, as well as the degree of disease. It combines a B-mode ultrasound with a colour Doppler ultrasound in order to assess narrowings in the vessel and the impact on blood flow. The B-mode ultrasound allows visualisation of vessel architecture, and therefore shows the direct interaction of a plaque with the vessel in areas with narrowings or obstruction. The colour Doppler then adds to this image by allowing visualisation of blood flow through the artery. Blood flow velocity tends to increase in areas of stricture, and this allows correlation of increased velocity with an area of narrowing. This is also the cause of certain limitations of DUS in multi-level disease analysis where the detection of downstream stenoses is less sensitive, as the more proximal lesions tend to slow onward flow [40]. It is also a highly operator-dependent imaging modality, with artefact also prominent in supra-inguinal lesions when patients are of certain body habitus, or due to overlying bowel gas [41]. DUS is useful in identifying the anatomical location, which can help decide on the feasibility of different interventions, and is non-invasive and less expensive than other imaging techniques. It is also frequently used for post-revascularisation surveillance of bypass grafts and endovascular stents [42, 43].

Computed tomography angiography (CTA): CTA enables scanning of the entire vascular tree at high spatial resolution within a very short period of time. This reduces the amount of contrast medium required, as well as radiation exposure. However, the requirement for iodinated contrast media is associated with a 16.8% risk of contrast-induced nephropathy in high-risk patients (including those with underlying renal impairment or diabetes). Fortunately only 1% of these progress to require renal replacement therapy [44]. Exposure to radiation is estimated as approximately 7.47mSv, though some centres have reported higher doses, but it has been suggested

that the risk of radiation dose in patients with advance PAD is of less concern due to their already shortened life expectancy. However physicians need to be aware of CTA use in younger patients, where the latent-period of radiation-induced malignancy is within their life expectancy. Meta-analysis of CTA has shown its utility with high sensitivity (95%) and specificity (96%) for greater than 50% stenosis, as well as excellent inter-observer agreement [45].

Magnetic resonance angiography (MRA): In similar fashion to both DUS and CTA, MRA of the peripheral vasculature is useful in the anatomical localisation as well as investigating the extent of PAD. Technological advances have also enabled multiple imaging platforms such as 2-dimensional time of flight, 3-dimensional with or without contrast-enhanced visualisation of the vascular system amongst others. These imaging techniques can also be used in combination, allowing fairly robust and accurate imaging of the lower extremity vascular system, and any disease which may be present [46]. 3D contrast-enhanced MRA (ceMRA) has been extensively reviewed and compared within the MRA umbrella to other MRA techniques, as well as to other imaging techniques, such as CTA. MRA showed superior sensitivity and specificity, 95% and 97% respectively, when compared to other imaging modalities [47]. In addition the potential side effects tend to be lower – less than 1% of all patients had anaphylactic reactions to the gadolinium contrast [48], and MRA avoids the use of radiation. MRA can also be performed in the outpatient setting, unlike CTA, which requires a short in-patient stay. Certain scenarios prevent the use of MRA however, such as individuals with pacemakers, implantable cardiac defibrillators or aneurysm clips where the magnetic force used makes it unsafe to scan patients [49, 50].

In patients with severe renal impairment care should be taken to optimise individuals prior to gadolinium contrast-enhanced MRA due to the rare, but serious complication of nephrogenic systemic fibrosis (NSF). Recent studies have suggested a causal relationship between gadolinium-based contrast agents and NSF in patients with chronic kidney disease stage 4 or 5, between 3–7% [51]. In patients on dialysis, some recent studies have reported 30% who receive gadolinium-based contrast agents developed NSF [52]. Patients with NSF develop rapidly progressive, widespread tissue fibrosis, affecting the skin, joints and internal organs (including the heart, lung, diaphragm, oesophagus and skeletal muscle). The risk of developing NSF can be

reduced in patients with severe renal disease by increased hydration prior to administration of contrast, and prompt initiation of dialysis.

Intra-arterial angiography: Digital subtraction angiography (DSA) has been a gold-standard imaging investigation in PAD diagnosis against which many of the more modern imaging modalities is often compared with. The technique is more invasive than a lot of the newer techniques, and involves administration of contrast to enhance visualisation of vessels, as well as exposure to radiation.

Angiography carries a 0.1% risk of severe reaction to contrast medium, and a 0.16% mortality risk [4].

1.1.4 Medical and Interventional treatment and prognosis

The highly progressive nature of PAD, a growing ability for primary care detection and the increased morbidity and mortality associated with disease have highlighted the importance of treating those with disease immediately and with multiple approaches. The majority of treatments can be categorised into medical or interventional management. The requirement for more invasive intervention is usually reserved for those at the more severe end of the PAD spectrum, and those who are unresponsive to conservative medical management.

1.1.4.1 Medical management

The principal approach for treating patients with PAD is the aggressive modification of the risk factors of atherosclerosis, to slow the progression of PAD as well as the underlying atherosclerotic process. In addition, treatment to provide symptomatic relief (pain and tissue loss) may also be required. Risk factor modification is an absolute requirement due to the significant risk to patients with PAD of developing severe cardiovascular complications. As described previously, greater than 60% patients with PAD will often have CAD. As PAD progresses (and ABPI value decreases) risk of a major cardiovascular event – myocardial infarction or ischaemic stroke – as well as risk of mortality, increases [53-55].

The primary aim of cardiovascular risk factor management includes smoking cessation, treatment of dysplipidaemia using medical therapy as well as lifestyle and dietary modifications, and aggressive management of hypertension and diabetes.

Smoking cessation advice should be offered to patients with PAD due to the correlation of cigarette smoking with disease severity rates, mortality, graft-patency and rates of lower limb amputation [16, 56, 57]. In addition, meta-analysis has shown decreased patency rates of bypass grafts in smokers, but the ability to ameliorate patency rates when smoking is significantly reduced or stopped [58, 59].

Evidence for managing dyslipidaemia in PAD is in vast abundance. A Cochrane review of 18 randomised control trials (RCTs) involving patients with PAD demonstrated a significantly reduced risk of cardiovascular events, especially coronary events whilst receiving statin therapy (odds ratio [OR]: 0.8; 95% confidence interval [CI]: 0.7-0.9) [60]. In patients with PAD and hypertension, current guidelines recommend a target blood pressure of ≤140/90 mmHg, or ≤130/80 mmHg if patients also have concomitant diabetes or renal insufficiency [61, 62].

In patients with concomitant diabetes, rigorous blood glucose control is key to preventing the known microvascular complications. In comparison however, the effect of strict blood glucose control on improving the risk of macrovascular complications is less well evidenced. The aim in diabetic PAD patients is currently to achieve a glycated haemoglobin (HbA1c) of <7% (53mmol/mol), or as close to normal, <6% (42mmol/mol), as an individual patient can achieve. In addition, multi-disciplinary involvement of podiatric services, to ensure adequate foot care and advice can help minimise the risk of developing diabetic foot complications. The United Kingdom Prospective Diabetes Study, compared intensive pharmacological treatment with sulphonylureas or insulin with diet control alone, and showed a significant reduction in MI, but no significant reduction with regards to risk of death or amputation rate due to PAD (relative risk [RR]: 0.6; 95% CI 0.4-1.2) [63].

Medical therapy for other PAD risk factors and earlier stages of disease is also advocated. In patients who are not at risk of bleeding, and also have evidence of other atherosclerotic processes, anti-platelet therapy should be deliberated, as well as in those individuals undergoing infra-inguinal endovascular stenting, drug-eluting balloon angioplasty or below the knee open bypass surgery [53]. A meta-analysis of trials assessing the efficacy of anti-platelet therapy in patients with high-risk vascular disease demonstrated a 23% reduction in adverse cardiovascular incidents, including MI, stroke and vascular death. Similar beneficial results were seen in patients with IC,

or those who had already undergone revascularisation therapies (angioplasty or bypass grafts) [64, 65].

Although no pharmacological agent has proved significantly efficacious alone to supersede surgical revascularisation, a number of drugs have been investigated, and are commonly used as an adjunctive therapy (in combination with revascularisation) or to aid in symptomatic relief where procedures have failed, or as a therapeutic alternative in patients not suitable for revascularisation [66]. The majority of the adjunctive therapies utilised in the treatment of PAD patients rely upon their ability to modulate the vasculature – so called 'vasoactive' drugs. These include prostaglandin analogues (iloprost) and phosphodiesterase inhibitors (cilostazol and pentoxifylline). Iloprost, and other prostanoid-derived drugs demonstrated efficacy in treating rest pain (RR: 1.32, 95% CI 1.10 to 1.57) and ulcer healing (RR: 1.54, 95% CI 1.22 to 1.96), and iloprost treatment showed a reduction in major amputations (RR: 0.69, 95% CI 0.52 to 0.93) in recent meta-analysis and systematic review [67]. The use of cilostazol in the treatment of PAD symptoms has been demonstrated to improve microvascular circulation [68], as well as improve rates of amputation-free survival but not overall survival or the need for repeat revascularisation [69].

In patients with claudication, the principal non-pharmacological treatment is a formal exercise-training program. A Cochrane review of 22 trials with PAD patients with IC demonstrated that exercise programs conferred significant benefit in terms of walking distance and time for up to two years in comparison to routine medical therapy [70]. However, exercise programs need to be supervised for the benefit to be observed, and last for a minimum of 6 months [28].

1.1.4.2 Interventional Management

As peripheral arterial lesions progress and blood flow to the peripheries becomes compromised, vascular intervention is required to preserve both limb function as well as the limb itself. Surgical intervention has two purposes therefore, firstly, to revascularise the limb, using various endovascular, surgical or hybrid techniques, and secondly, when vascular supply to the limb goes beyond a critical life-threatening stage, amputation of the limb to preserve life and remove non-viable tissue.

Revascularisation

The decision to revascularise PAD patients is based on a number of factors including disease location and morphology, as well as the amenability of individuals to undergo revascularisation intervention. With the constantly improving endovascular as well as hybrid fields, greater numbers of patients are suitable. Determining the best method of revascularisation therapy to treat symptomatic PAD patients can loosely be modelled upon the TransAtlantic Intersociety Consensus II (TASC II) classification guidelines [18] summarised in tables 1.2 and 1.3 and figure 1.2 and 1.3. In general, TASC 'A' lesions are deemed the most amenable to treatment using endovascular procedures; 'B' type lesions would benefit from endovascular treatment, unless concomitant open procedure is required for other lesions in the same anatomical region (e.g. endarterectomy); 'C' type lesions are best treated with open surgical revascularisation, with endovascular techniques reserved for patients at high-risk for open repair; 'D' type lesions should not primarily be treated with endovascular techniques, as it does not yield adequate results compared to open surgical treatment.

Table 1.2: TASC II classification of aorto-iliac lesions

Lesion type	Characteristic features
A	• Unilateral or bilateral stenosis of CIA • Unilateral or bilateral single short EIA stenosis (≤3cm)
B	• Short stenosis of infrarenal aorta (≤3cm) • Unilateral CIA occlusion • Single or multiple stenosis (3–10 cm) involving EIA, not extending into CFA • Unilateral EIA occlusion not involving origins of IIA or CFA
C	• Bilateral CIA occlusions • Bilateral EIA stenosis (3–10 cm) not extending into CFA • Unilateral EIA stenosis extending into the CFA • Unilateral EIA occlusion involving origins of IIA and / or CFA • Heavily calcified unilateral EIA occlusion with or without involvement of IIA and / or CFA origin
D	• Infra-renal aortic occlusion • Diffuse disease involving the aorta an both iliac arteries • Multiple, diffuse stenoses involving unilateral CIA, EIA and CFA • Unilateral occlusions of both CIA and EIA • Bilateral occlusions of EIA • Iliac stenoses in patients with AAA requiring treatment not amenable to endovascular stent grafting, or other lesions requiring open surgery

CIA – common iliac artery, EIA – external iliac artery, CFA – common femoral artery, IIA – internal iliac artery, AAA – abdominal aortic aneurysm. Modified from [4].

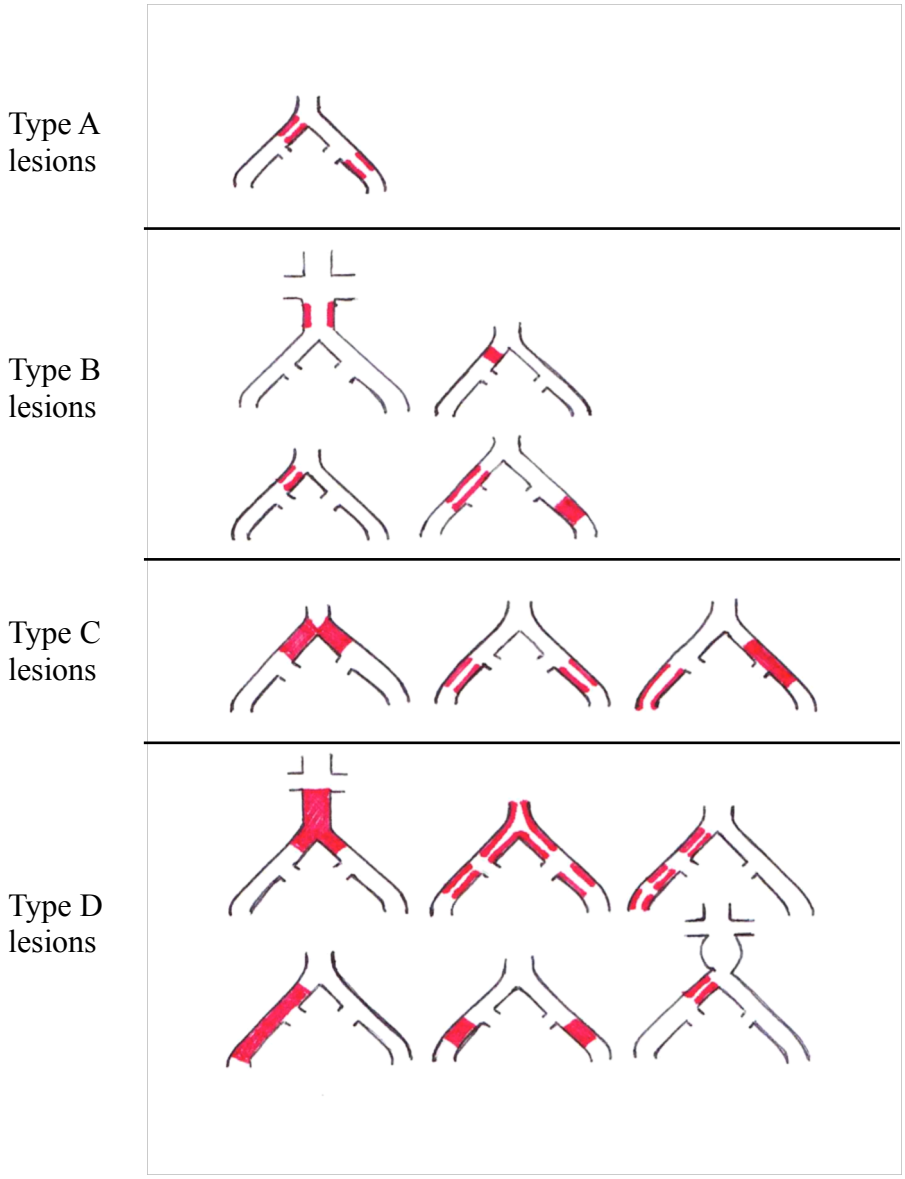

Figure 1.2: Diagram of TASC II classification of aorto-iliac lesions

Type A lesions are most amenable to endovascular techniques. Type D lesions are most amenable to surgical interventions. Type B and C lesions can be managed using either endovascular or open surgical techniques depending on the requirements and risk factors of individual patients.

Table 1.3: TASC II classification of femoral-popliteal lesions

Lesion type	Characteristic features
A	• Single stenosis ≤ 10cm in length • Single occlusion ≤ 5cm in length
B	• Multiple lesions (stenoses or occlusions) each ≤5cm • Single stenosis or occlusion ≤15cm not involving the popliteal artery below the knee • Single or multiple lesions in the absence of continuous tibial vessels to improve inflow for a distal bypass • Heavily calcified occlusion ≤5cm in length • Single popliteal lesion
C	• Multiple stenoses or occlusions totalling > 15 cm with or without heavy calcification • Recurrent stenosis or occlusions that require treatment following two endovascular interventions
D	• Chronic total occlusion of CFA or SFA (>20cm involving the popliteal artery) • Chronic total occlusion of popliteal artery and proximal trifurcation vessels

CFA – common femoral artery, SFA – superficial femoral artery. Modified from [4].

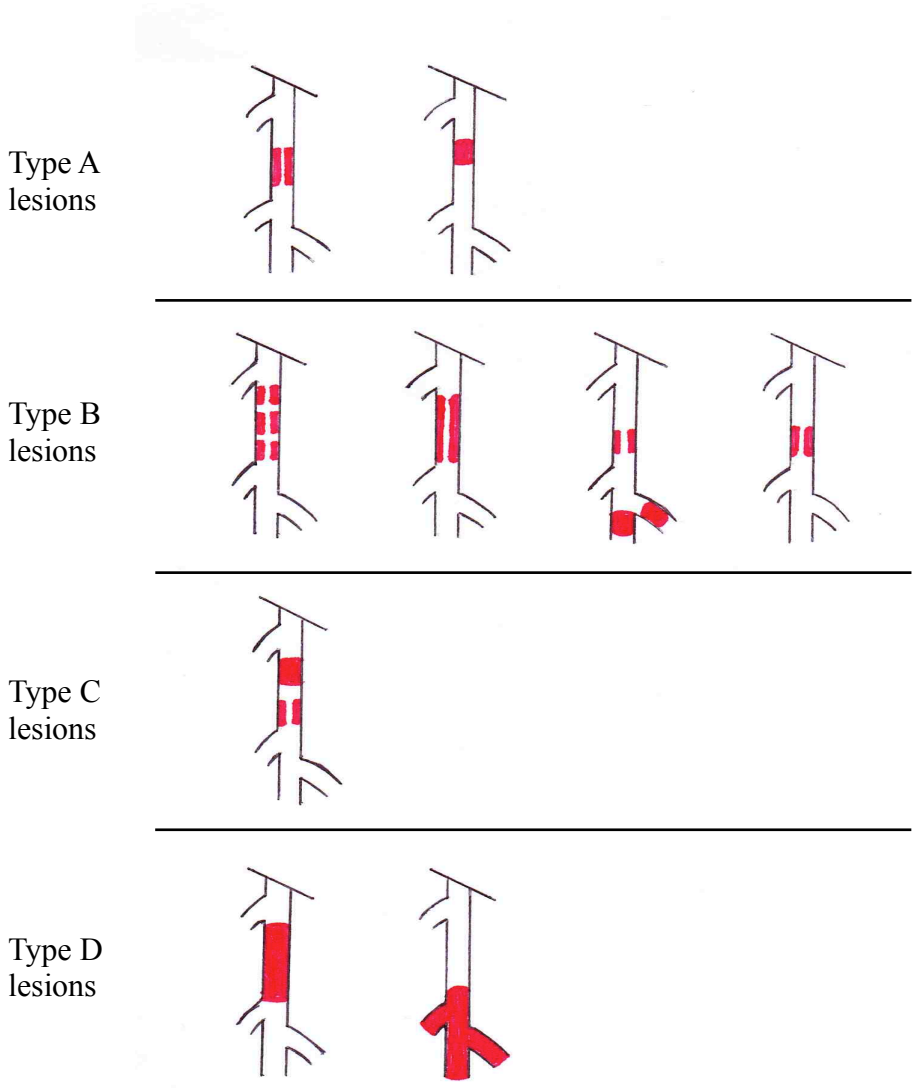

Figure 1.3: Diagram of TASC II classification of femoral popliteal lesions

Type A lesions are most amenable to endovascular techniques. Type D lesions are most amenable to surgical interventions. Type B and C lesions can be managed using either endovascular or open surgical techniques depending on the requirements and risk factors of individual patients.

The decision to treat patients, based on TASC II classification, has limitations as the majority of PAD patients have multi-level disease lesions, which may not be represented by the classification system.

Advances in endovascular techniques have increased the treatment options for patients to undergo minimally invasive percutaneous therapies. Currently available endovascular revascularisation techniques include percutaneous transluminal angioplasty with balloon dilatation, subintimal angioplasty, stenting (using bare metal

or drug-eluting stents), laser atherectomy, cryoplasty and thermal angioplasty [71]. Whilst early and mid-term outcomes demonstrate highly promising limb salvage rates of greater than 80%, substantial evidence of outcomes has also demonstrated a high proportion of restenosis and need for re-intervention [72-74]. Currently the only, multi-centre prospective randomised trial comparing traditional surgical bypass with endovascular angioplasty, the BASIL (Bypass versus Angioplasty in Severe Ischaemia of the Limb) trial, has demonstrated that at both 3 and 7-year follow-up, bypass surgery using autologous vein provides the best long-term amputation-free survival [75, 76].

Traditional surgical techniques – endarterectomy or bypass – are more commonly required to treat patients with significant symptoms despite medical management and where anatomy of arterial lesions is amenable to bypass surgery. Where possible, when performing infra-inguinal bypasses, autologous vein is used as the bypass conduit. Synthetic grafts have a higher risk of graft occlusion and lower patency rates in comparison, and are therefore not recommended [28]. Meta-analysis of CLI patients undergoing infra-inguinal bypass reported 5-year primary graft patency at 64%, secondary patency rate of 71% and limb salvage as 78% [77].

Hybrid interventions – a combination of endovascular and open surgical techniques – are being used more frequently for complex multi-level arterial lesions of the lower limb in specialist centres, with excellent technical success rates. However long-term outcomes are less clear at present. Early reporting on mid-term outcomes following hybrid procedure have suggested patency rates of greater than 70% at 1 year and 60% at 5 years, as well as limb salvage rates greater than 83% [78-82].

Amputation

Despite advances in endovascular and hybrid techniques, many patients will still go on to require lower limb amputation for non-viable limbs or where the arterial disease is not amenable to revascularisation. Indications that identify patients requiring amputation include unreconstructable peripheral vascular disease, usually due to the lack of runoff vessels distally, fixed flexion deformities or extensive tissue loss [83]. The incidence of major lower limb amputation varies from 120–500 per million/year, with almost equal rates of above-knee or below-knee amputations [18, 84].

1.1.4.3 Prognosis

The natural history of PAD is a slow progression of symptoms over time; however the time-course of progression is highly variable, and can be prolonged significantly on strict modification of risk factors. Limb-loss in patients suffering from claudication symptoms is a major fear, however in these patients, the risk of suffering from an adverse cardiovascular or cerebrovascular event is much greater. Recent studies have suggested a 5-year risk of major amputation in IC patients of only 1–3.3% [4]. In contrast however, once symptoms of CLI appear (rest pain, frank tissue-loss, gangrene and non-healing ulcers), prospects become far bleaker, with approximately 40% requiring major amputation and a mortality rate of up to 20% within 6 months [4]. The prognosis following amputation continues to deteriorate. The peri-operative mortality for below-knee and above-knee amputation is between 5–10%, and 15–20%, respectively. Of those who survive the post-operative period, less than half of amputees will have regained full mobility by two years, approximately 40% will die within 2 years of their amputation and 30% will require a second amputation [85-87].

Whilst clinical, or physician-orientated outcomes, demonstrate successful revascularisation therapy, evidence details that patients do not observe functional benefits, and continue to show deterioration in their quality of life, and independence, and limitations in activities of daily living when surveyed. This suggests a disparity between clinical and patient-orientated outcomes, which has been previously described [88-94]. These findings indicate that the underlying cause of the functional impedance patients with PAD describe may be due to more than haemodynamic compromise to the limb alone. Attempts to improve muscle function and survival especially in ischaemic conditions may provide an additional avenue of treatment that could increase patient-orientated outcomes.

1.1.5 Pathology of muscle dysfunction

Although it is widely accepted that PAD is a manifestation of systemic atherosclerotic disease – and the narrowing and obstruction of vessels is the primary catalyst that leads to an impairment of blood flow to tissues – the resultant haemodynamic alteration does not entirely explain the pathophysiology or mechanisms of functional impairment in PAD patients [95, 96].

Research conducted in the last decade has implicated ischaemia-related pathological changes within various limb muscle groups, and in particular calf muscle, which may contribute to the functional decline patients' experience including functional changes, histomorphological changes such as muscle fibre type shift, mitochondrial dysfunction and metabolic alterations, oxidative stress and neuropathy in PAD skeletal muscle.

1.1.5.1 Functional changes

The functional impairment experienced by PAD patients usually manifests as claudication, either intermittently or also experienced at rest. This results in significantly reduced walking speed and distance as well as pain in muscle groups – either at rest or during exercise. Whilst the obvious explanation would appear to be the effect of poor blood flow and therefore oxygen delivery to tissues, various groups have established that there is very little correlation between haemodynamic flow limitations in the limb and claudication-associated functional disability [39, 97-99]. In addition, various invasive revascularisation therapies do not completely improve exercise performance (a measure of functional benefit) despite observable improvement in haemodynamic capacity [100, 101], whereas conversely, prescribed exercise rehabilitation has some amount of established efficacy [102-104].

Measurement of muscle strength in PAD patients using a 5-second maximal isometric strength assessment – a test which is entirely blood flow-independent – demonstrated significantly reduced muscle strength in PAD patients suggesting that there was in addition an intrinsic muscle weakness unaffected by any acute haemodynamic restriction [105].

1.1.5.2 Histomorphological changes and muscle fibre type shift

Examination of PAD skeletal muscle using both light and electron microscopic evaluation has revealed numerous myopathic and neuropathic changes that appear to correlate with disease severity. Characteristic alterations observed in PAD muscle tissue include fibre size diversity, central nuclei, endomysial fibrosis, apoptosis and necrosis, phagocytosis and type II muscle fibre atrophy [106-110].

Adult skeletal muscle is composed of repeated sarcomeres – a basic functional unit that contains the protein filaments actin and myosin that gives skeletal muscle its characteristic striated appearance. These two components then interact when necessary to allow contraction. Skeletal muscle can be categorised depending on the

type of myosin present in the muscle fibres. Broadly speaking there are two categories of myosin heavy chain (MHC) classes: type I and type II [111]. They differ in terms of appearance as well as activity. Type I fibres appear red due to a greater presence of myoglobin – an oxygen binding protein, that therefore makes type I fibres well-adapted to a role in oxidative or aerobic metabolism in order to generate adenosine triphosphate (ATP) an "energy unit" utilised by muscle, that can provide prolonged muscle contractions. On the other hand, type II muscle fibres (of which there are 3 isoforms) [112] appear white due to the relative absence of myoglobin, which means they are better at very intense, fast or powerful movements, which are short lasting, through anaerobic glycolysis in order to provide ATP. These fibres tend also to fatigue much faster. Skeletal muscle fibres have a great capability to change both size and fibre type composition in order to meet with changing demands.

A variety of methods now exist in order to determine fibre type, each stain exploiting one of the differences between the two fibre types. These include myofibrillar ATPase staining – which exploits the difference in ATP generation by type I and II fibres, succinate dehydrogenase – which takes advantage of differences in oxidative potential, and α-glycerophosphate dehydrogenase which depends on differences in glycolytic activity. In addition antibodies against specific MHC isoforms have also been developed with some finding popular commercial use [113].

In human skeletal muscle, though it varies depending upon the exact muscle under analysis, both muscle fibre types will be present. In the majority of muscle groups there tends to be a roughly equal distribution of both fibre types, however some muscles will have a more polarised representation by one fibre type.

In addition to generalised variation in muscle fibre diameter and atrophy, various groups have demonstrated a shift in muscle fibre type in chronic PAD sufferers towards type I fibres [108, 114-116]. Although these differences have been noted, it is not entirely understood whether the plasticity in muscle fibre type is as a consequence of PAD cellular pathology (especially the notable mitochondrial and metabolic dysfunction), or whether it results from the simple deconditioning that often occurs as PAD severity and patient inactivity increases.

1.1.5.3 Mitochondrial dysfunction and metabolic alterations

Evidence of abnormal mitochondrial activity was suggested as far back as 1975 when a study into the effects of carbohydrate supplementation on exercise time in claudication PAD patients demonstrated a significant increase in the glycogen content of their muscle, as well as increased exercise tolerance. Leading on from this work, various groups have since demonstrated that the mitochondria from chronically ischaemic leg muscle have an aberrant dysregulation of a number of metabolic processes. Isolation of mitochondria from the calf muscle of claudicants demonstrated that the rates of pyruvate dehydrogenase-dependent oxidation of carbohydrates was positively correlated with walking performance and increased with exercise training [117]. This suggested that although mitochondrial carbohydrate oxidation is abnormal in claudication PAD, the mitochondrial function is not entirely impaired, and is amenable to exercise-training.

Further studies into the mitochondrial ability to oxidise other metabolites (including lipids, proteins and carbohydrates) by examining acylcarnitine levels also established an imbalance in PAD patients. In normal states, fat, protein and carbohydrate substrates will first be converted into acyl-coenzymeA (acyl-CoA) intermediates before entering into and undergoing complete catabolism through a series of oxidative steps which make up the Kreb's cycle. When mitochondrial metabolism is interrupted, incomplete oxidation of acyl-CoAs occurs, causing their accumulation, which acts in a negative-feedback fashion to inhibit their continued production. However, the presence of the carnitine system, which acts as a buffer for acyl-CoAs, allows the existence of excess acyl-CoAs by collecting their acyl groups to become acylcarnitine. This in turn causes a rise in acylcarnitine concentration, which can be measured in both tissue and plasma, and acts as a biomarker for poor mitochondrial uptake and oxidation of acyl-CoA in PAD [118]. Other groups have also demonstrated that acylcarnitine levels are associated with walking performance in PAD patients, and are amenable to exercise training [119-121].

In vivo analysis looking for evidence of a mitochondriopathy uses techniques of ^{31}P nuclear magnetic resonance spectroscopy (MRS). ^{31}P MRS is a non-invasive tool that provides information on the relative intracellular concentrations of various phosphorous metabolites (including ATP, adenosine diphosphate (ADP) and phosphocreatine) as well as pH in order to allow the calculation of the rate of

phosphoenergetic reactions, which gives an indication as to the bioenergetics occurring. Various pathological conditions can therefore be characterised by their different metabolic signatures. In PAD patients after maximal exercise testing, ^{31}PMRS has displayed a prolonged rate of recovery suggestive of alterations in the oxidative phosphorylation processes, as well as evidence in support of a genuine dysfunction of mitochondria. In addition, evaluation of human PAD limbs with different severity of ischaemic disease revealed the greatest level of mitochondrial dysfunction in the most severely affected limbs [118, 122].

1.1.5.4 Oxidative stress

In addition to the specialised role mitochondria play in ATP-production, mitochondria also produce reactive oxygen species (ROS), which can directly and indirectly affect other cellular activity. In normal resting state, more than 90% of the ROS found in a cell is produced by mitochondria [123] at 2 main sites – electron transport chain (ETC) complexes I and III [124, 125]. However, if damage occurs at these sites, ROS generation is exponentially enhanced [126, 127]. Various groups, using various techniques to study the different aspects of ROS generation, as well as clearance by intracellular antioxidants (such as manganese superoxide dismutase (MnSOD)) have shown that in PAD patients, there is a deficiency of electron transport chain (ETC) complexes I, III and IV [123, 128]. Coupled with the potential increase of ROS production due to damaged complexes, PAD patients also exhibit a scarcity of the antioxidant MnSOD [129]. Evidence of these two imbalanced forces being present in the mitochondria was also shown by analysis of ROS damage to lipids and proteins in PAD muscle, which demonstrated consistently increased protein oxidation and lipid peroxidation products [124].

1.1.5.5 Neuropathy

Whilst the most noticeable symptom for patients with CLI is pain, this can often mask the presence of a general leg weakness, suggestive of an insidious neuromuscular dysfunction. In addition to the histological changes mentioned above, muscle of PAD patients also demonstrates features of focal denervation of the muscle fibres (seen as muscle fibre group atrophy), and denervation-reinnervation characteristics (seen as grouping of fibre types). Muscle fibre group atrophy occurs when a motor neuron becomes incapable of supplying a muscle fibre with its required excitatory and trophic stimuli, so that after a period of denervation, the muscle fibres become locked in the

flaccid state, and without stimuli from a nearby motor neuron begins to lose the majority of their contractile apparatus seen as a muscle fibre atrophy. If however, the muscle fibre is 'rescued' by a neighbouring, healthy motor neuron, then the reinnervated fibre will begin to function like the new motor neuron which supplies it. This gives rise to the characteristic denervation-reinnervation morphology of fibre type grouping.

Objective testing using nerve conduction and electromyographic techniques also identified a number of similar issues in muscle function in PAD patients including axonal neuropathy, demyelination and denervation-reinnervation. The neuropathy observed in PAD whilst appearing predominantly to be motor neuropathy, has also been identified as causing a sensory deficit [118, 130].

1.2 Erythropoietin and erythropoietin-derivative (ARA-290)

In 1906 Carnot and Deflandre first postulated the idea of a hormone that was secreted into the blood stream that was responsible for the regulation of erythropoiesis [131] with its particular name, erythropoietin, introduced in 1948 [132]. EPO was first purified from the urine of patients suffering from aplastic anaemia [133]. With the purified urinary hormone, it was possible to partially identify the amino acid sequence, which was a major step forward in the process of producing recombinant human EPO (rHuEpo). However, it took almost 8 decades before the gene encoding erythropoietin (EPO) was identified, cloned and expressed in 1985 [134, 135].

Since Food and Drug Administration (FDA) approval was granted in 1989 for the use of erythropoietin in the treatment of renal anaemia, over several million patients with chronic kidney disease have benefitted from the numerous erythropoiesis stimulating agents (ESAs) available for correcting haemoglobin levels, reducing the requirement for transfusions, and improving quality of life and symptoms of anaemia, in particular fatigue [136]. Since then, a multitude of alternative actions of EPO have been discovered. Amongst these novel roles, the cytoprotective properties of EPO in situations of ischaemia and metabolic stress have gathered significant interest from a

variety of different clinical specialities, linked via a common interest in ischaemia-induced injury, such as ischaemic stroke and myocardial infarction [137-140].

Cells in the mammalian body have a requirement for oxygen when undergoing oxidative respiration, as well as many other biochemical reactions. However oxygen concentrations in cells need to be finely balanced, as excessive oxygen can lead to undesirable oxidative damage of numerous cellular components, resulting in cell death. Haemoglobin, contained within erythrocytes is responsible for oxygen delivery to tissues. Usually, in healthy individuals, the fine balance between oxygen demand and delivery to all the tissues of the body will be maintained within strict parameters by the number of circulating erythrocytes. The average life of a red blood cell is approximately 120 days, and each day approximately 1% of the circulating pool of erythrocytes will be removed [141], and replaced by an equal number of reticulocytes (immature erythrocytes). As the increased numbers of reticulocytes replete the circulating numbers of erythrocytes, the rate of new reticulocyte production is retarded so that a rebound polycythaemia may not occur. EPO is the principal mediator of this delicately tuned homeostatic process.

1.2.1 Structure and expression of erythropoietin and erythropoietin receptor

Erythropoietin

The glycoprotein hormone EPO is a member of the type I cytokine superfamily. Other members of the type I cytokine superfamily include interleukin (IL) –2, –3, –4, –5 and –6, granulocyte colony stimulating factor and granulocyte – macrophage colony stimulating factor (GM-CSF), leukaemia inhibitory factor and ciliary neurotrophic factor. EPO is able to promote the growth, differentiation and survival of erythroid progenitors in the bone marrow, for the purposes of regulating red blood cell mass in circulation. In embryonic development, hepatocytes and stellate cells within the liver are the primary site of EPO production. Slowly after birth, hepatic production of EPO decreases until in the adult human, the peritubular fibroblasts of the renal cortex almost exclusively produce erythropoietin [142, 143]. However, EPO mRNA is also detectable in the brain, retina, heart, liver, spleen, lung and testis, confirming the presence of locally produced EPO [144-147]. Indeed, upregulation of hepatic EPO production can be as great as 20 – 50% of total EPO production, when stimulated by hypoxia [148, 149].

The human EPO gene is located on the long arm of chromosome 7 (q11–q22) and contains 5 exons and 4 introns. The exons encode a 193-amino acid prohormone that undergoes cleavage of a 27 amino acid leader sequence prior to secretion. The secreted EPO hormone has a molecular mass of 30.4kDa. This is composed of a peptide core and a glycosylated carbohydrate portion. The carbohydrate portion of EPO accounts for approximately 40% of the mass of circulating EPO, and contains 4 glycosylated chains [150], including 3 *N*-linked oligosaccharides at asparagines 24, 38 and 83 and 1 *O*-linked oligosaccharide chain at serine 126 [151, 152]. The carbohydrate composition is necessary to increase the solubility and stability of the EPO glycoprotein *in vivo* [153, 154]. The peptide portion of the EPO protein is composed of approximately 165 amino acids arranged into a compact globular structure, due to its hydrophobic 4 α-helices (named A through D), which are responsible for receptor-binding. Nuclear magnetic resonance spectroscopy has revealed that, like many other members of the type I cytokine superfamily, EPO shares the typical structure represented by four anti-parallel α-helices [155].

The coding region of the EPO gene, on analysis of both nucleotide and amino acid sequence, appears to be well conserved across mammalian species [156], with 91% sequence homology with monkeys [157], 85% identical with cats and dogs, and 80 – 82% homology with mice, rats pigs and sheep [158, 159]. It is not surprising, therefore that there is a marked cross-reactivity between mammalian EPOs.

Erythropoietin receptor

The erythropoietin receptor (EPOR), like its cognate ligand, is part of the type I cytokine receptor superfamily. Classically, this superfamily of receptors is composed of an extracellular domain, with highly conserved regions, a single hydrophobic transmembrane spanning region, and a highly variable cytoplasmic portion, with constitutively bound Janus kinases (JAK), due to the lack of intrinsic kinase activity, characteristic of this superfamily. Mature human EPOR contains 484 amino acid residues, and has a calculated weight of 52.6kDa, which increases to approximately 59kDa due to glycosylation and phosphorylation [160].

The extracellular domain of the EPOR is composed of approximately 230 amino acids. In addition, in keeping with other type I cytokine receptors, the extracellular domain contains four conserved cysteine residues and the WSXWS motif. In the EPOR, this

corresponds to WSAWS. The extracellular portion is also composed of 2 major fibronectin type III subdomains, which form a hinge-like structure where the two domains interact at 90° [161, 162]. Crystallographic analysis has demonstrated that the EPOR homodimerises through the hinge domain [161, 163], where they are separated by 73Å. Ligand binding causes conformational alterations, which bring the two domains to within 39Å, crucial for subsequent signal transduction [164].

The intracellular, or cytoplasmic domain of the EPOR, like the majority of receptors within its superfamily, lacks enzymatic activity. Comparison of the cytoplasmic domain sequence within the superfamily of receptors identifies regions within the proximal portion of the cytoplasmic domain that are conserved. These regions – named box 1, box 2 and a region between box 1 and 2 are thought to be areas of EPOR association with JAK2, to compensate for the lack of kinase activity [164, 165].

The presence of the EPOR outside of erythroid precursor cells has been detailed. EPOR mRNA and protein expression has been described in various tissues, many of which have already been noted above, due to the concomitant expression of EPO mRNA. Additional regions demonstrating EPOR expression are pancreatic islet cells, renal mesangial and epithelial cells, skeletal muscle and the placenta [166-172].

1.2.2 Hypoxic regulation of erythropoietin

Hypoxia – a reduction in oxygen tension below the body's needs – is the primary physiological stimulus of EPO gene expression in humans. This is mediated via a family of transcription factors; known as hypoxia inducible factors (HIFs), which are specific DNA-binding transcription factors. HIFs are responsible for oxygen homeostasis by utilising a spectrum of genes capable of providing hypoxic adaptation including angiogenesis, apoptosis, erythropoiesis, energy metabolism and vasomotor control [173, 174]. HIF is comprised of an oxygen-labile α-subunit and a constitutively expressed β-subunit. In conditions of normal oxygen tensions, these subunits are found individually, but will form a heterodimer under conditions of low oxygen tension. Three HIF-α splice variants exist, each targeting different transcriptional targets, although HIF-1 and HIF-2 share many common targets. The vast majority of present knowledge regarding EPO regulation is based on *in vitro* studies using human hepatoma cell lines (HepG2 and Hep3B) [143], but work is now moving into looking at the regulation of EPO synthesis in the kidneys. Until quite

recently it was believed that HIF-1 was entirely responsible for the regulation of EPO production, but HIF-2 has since emerged as the principal regulator of EPO production in adults [175-179].

Under conditions of normal oxygen tension, the oxygen-sensitive HIF-α subunits undergo hydroxylation of conserved proline residues by prolyl-4-hydroxylase domain (PHD) containing enzymes [180-182]. Oxygen is required as a co-factor for PHDs catalytic activity. This marks them for rapid proteasomal degradation by the von Hippel-Lindau tumour suppressor protein (pVHL). pVHL acts as a substrate for E3-ubiquitin ligase, and hence the subsequent ubiquitylation of HIF-α, in complex with pVHL, targets it for degradation by the 26S proteasome [183, 184]. In conditions of hypoxia, the lack of oxygen restricts the ability of PHDs to hydroxylate HIF-α, preventing their recognition by pVHL, and allowing the stabilised HIF-α to accumulate and associate with HIF-β in the nucleus [185]. Following the heterodimerisation of the two molecules, they are then capable of binding with hypoxia responsive elements (HRE), which are contained in various hypoxic adaptation genes, including the EPO gene. Interestingly, some of the PHDs (PHD2 and 3) are themselves under the regulation of HIF. During chronic hypoxic exposure, as the expression of PHDs increases, HIF-1α levels decline [143].

Besides the HRE, other regulatory components exist within the EPO gene, including GATA sites. In conditions of normoxia, EPO gene upregulation is suppressed by GATA-2 [186]. GATA-2 levels are then reduced in hypoxic conditions [187].

1.2.3 Erythropoietin mode of action

Erythrocyte precursor cells, so called erythrocyte-blast forming and colony forming units (BFU-E and CFU-E), located within the bone marrow are the principal targets of EPO. Under healthy physiological conditions, the replenishment of the red blood cell circulating pool is held under tight regulation by the low concentration of EPO available. This allows for only a small number of BFU-E to differentiate and give rise to CFU-E and only a small number of CFU-E to undergo maturation and become erythrocytes. The remaining erythrocyte progenitor cells undergo apoptosis. The primary mechanism therefore, whereby EPO maintains haematopoiesis is by the prevention of programmed cell death, or apoptosis, of erythroid progenitor cells. The binding of the EPO ligand to its cognate receptor, as described previously, induces

homodimerisation of EPOR [188, 189] and causes a conformational change within the $(EPOR)_2$ homodimer, which allows the constitutively associated JAK2 to phosphorylate itself, as well as 8 tyrosine kinase residues within the cytoplasmic portion of the EPOR [190]. This creates docking sites for various kinase substrates with Src homology-2 (SH2) domains, including signal transducer and activator of transcription 1, 3 and 5 a/b (STAT), mitogen-associated protein kinase/extracellular signal-related kinase (MAPK/ERK), phosphatidyl-inositol-3 kinase (PI-3K/Akt) and protein kinase C, which are some of the signal transduction pathways, proposed to have a role in the EPO-mediated prevention of apoptosis [162, 191-195].

1.2.4 EPO-derivatives

The major step towards the production of EPO-derivatives first occurred in 1983 when the *EPO* gene was cloned for the first time, and then followed a few years later with the subsequent production of the EPO glycoprotein. Since then, with the aid of many modern technologies, the EPO protein has been studied in-depth, with particular emphasis on structure-activity relationships. The focus of both industry and academia has been the potential to improve or re-engineer EPO, with the result being the advent of many EPO-derivatives, produced by investigating the EPO molecule from different perspectives. Although initially the focus was the generation of EPO-derivatives that could stimulate production of red blood cells for the treatment of anaemia, once cytoprotective effects were observed, there has been a shift towards the development of non-haematopoietic EPO-derivatives. EPO-derivatives have been crafted by altering glycosylation sites, chemically modifying or adding peptides to the EPO glycoprotein, as well as looking at the primary, secondary and tertiary structure of EPO to generate derivatives based on certain parts of the EPO molecule.

Recombinant DNA derived-human EPO

The development of recombinant human EPO (rHuEPO) was made possible by the identification of the *EPO* gene. It allowed a biotechnological advance, which has, and still continues to, revolutionise the treatment and prognosis of anaemia associated with chronic kidney disease, as well as other chronic diseases. This group of EPO-derivatives are also known as erythropoiesis stimulating agents (ESAs) and treatment with any rHuEPO is intended to drastically reduce the number of allogeneic blood transfusions required by stimulating the body's own infant reticulocytes into mature

erythrocytes. It therefore also reduced the risk in these patients over time of having a transfusion reaction.

Many commercial forms of rHuEPO are now available, produced and marketed by different pharmaceutical companies under different trade names. They are generally classified into epoetin alpha (Darbepoetin, Epogen, Eprex), beta (NeoRecormon), delta (Dynepo), omega (Epomax) and zeta (Retacrit). Similarities between the different forms of rHuEPO include their amino acid sequence (except Darbepoetin) and production through recombinant-DNA cell culture. Epoetin alpha and beta utilise Chinese hamster ovary cell lines to produce the recombinant protein, but epoetin omega is produced in baby hamster kidney cells. Epoetin delta utilises a human fibrosarcoma cell line to produce the recombinant protein [196], with the result that glycosylation of the protein is more characteristic of human cells. In addition, a dimer of EPO, linked by a 17 amino acid chain, has been produced, demonstrating 8-fold more effective erythropoietic ability, with a prolonged half-life (approximately 8 hours) [197].

All ESAs have the same mechanism of action in terms of EPOR activation, but tend to differ in their receptor binding affinity, plasma half-life, bioavailability, *in vivo* potency and clearance, with the aim of altering certain aspects of their pharmacokinetic or pharmacodynamics profile. Most commonly, the different isoforms of rHuEPO created are able to guarantee market share in the treatment of anaemia due to the subtle differences, which alter the functional profile, mainly by increasing plasma half-life, and therefore are seen as more patient-friendly by reducing the number of doses required each week. There is however potential that the prolonged time of stimulation from newer-generation ESAs can lead to unrequited side-effects of EPO over-stimulation, and therefore all patients on ESAs will have strict monitoring of their haemoglobin and haematocrit levels.

Chemically altered EPO

When it was noted that EPO had potential as a tissue-protective cytokine there was an instant surge in the attempts of different groups to identify novel EPO-derivatives. The aim was to create a derivative that could retain and mediate tissue-protective effects, whilst abolishing the haematopoietic effects, which due to the doses required would often lead to thrombotic side effects.

Even before the protective effects were observed, asialo-EPO was detailed in the literature [198]. EPO is composed of various N-linked and O-linked carbohydrate groups. 14 sialic acid residues mask the galactose residues that make up the terminal residues in each of these branched carbohydrate chains. Nowadays, complete enzymatic desialylation (typically using neuraminidase) yields asialo-EPO. Due to the desialylation, the terminal residue becomes galactose. With terminal galactose residues available, the asialo-EPO is able to bind to galactose receptors in the liver. This hepatic clearance in part explains the very short plasma half-life of asialo-EPO (approximately 1.4 minutes). The lack of modification to the protein backbone of the molecule means that binding and affinity to the EPOR remains unchanged, but the very rapid rate of elimination means there is not sustained stimulation of the EPOR and therefore no haematopoietic effect. Asialo-EPO is however, capable of activating signalling pathways involved in tissue-protection, due to the dynamic nature required in activation of the tissue-protective receptor.

Whilst chemical modification of the EPO molecule can involve any of the lysine, arginine, tyrosine or carboxyl terminals, not all of these have been exploited yet. Modification of lysine residues has however been investigated, and led to the development of another well-known EPO-derivative: carbamylated EPO (CEPO). Under normal physiological conditions in humans, it is possible to find partially carbamylated EPO molecules. This occurs when urea within the plasma is converted to cyanate, which is then able to react with EPO to create partially carbamylated EPO molecules. It can also be produced via the carbamylation of all seven lysine residues in EPO to homocitrulline, with the effect of more than 1000-fold lower binding affinity for the EPOR, and subsequently 1000-fold lower effect in haematopoiesis stimulation assays.

Alterations in EPO primary structure to create Mutant EPO (MEPO)

Following careful examination of the *EPO* gene, in conjunction with its structure, to identify the areas responsible for erythropoiesis, various groups are now in the process of creating mutant EPO-derivatives. These EPO-derivatives have been carefully constructed using site-directed mutagenesis to cause single amino acid mutations within the erythropoietic motif. The result is a MEPO that lacks its former

erythropoietic activity due to a reduction in affinity for the EPOR, but retains its desired tissue-protective effects.

Numerous MEPOs can be found in the literature, and below is a table (Table 1.4) summarising their site of mutation, amino acid change and the arena in which they have been identified for potential therapeutic benefit. In general, following site-directed mutagenesis, the mutant gene will be subcloned into a plasmid, and then either inserted to create a recombinant viral vector and injected for *in vivo* analysis or inserted into a competent cell line which will express sufficient volumes of the MEPO to conduct *in vitro* and *in vivo* analysis.

Table 1.4: Mutant erythropoietin (MEPO) derivatives

MEPO name	Amino acid residue	Initial → mutated amino acid	Tissue-protection area
EPO-R76E	76	Arginine → Glutamic acid	*In vivo* MPTP-induced Parkinsonism [199] *In vivo* optic nerve crush [200] *In vivo* photoreceptor cell damage [201]
EPO-R103E	103	Arginine → Glutamic acid	*In vitro* NMDA-neuron toxicity [202] *In vivo* retinal degeneration [203, 204]
EPO-S71E	71	Serine →Glutamic acid	*In vivo* MPTP-induced Parkinsonism [199]
EPO-S100E	100	Serine → Glutamic acid	*In vitro* NMDA-neuron toxicity [202] *In vivo* MCA occlusion [205] *In vivo* photoreceptor cell damage [203, 206] *In vivo* retinal degeneration [200]
S104I-EPO	104	Serine → Isoleucine	*In vitro* NMDA-neuron toxicity [202] *In vivo* MCA occlusion [207]

NMDA: N-methyl-D-aspartate, MCA: middle cerebral artery, MPTP: 1-methyl-4-phenyl-1,2,3,6-tetrahydropyridine.

Peptide addition

Following on from the discovery that EPO-derivatives with additional glycosylation sites had increased plasma half-life, investigators have looked at other ways of increasing plasma half-life by the addition of other moieties. The rationale for pursuing peptide addition to the EPO molecule came from observed increases in plasma half-life (and a resultant increase in bioactivity) when the carboxy terminal peptide of the β subunit of human chorionic gonadotrophin (hCG) was added to other glycoproteins (e.g. thyrotropin) [208]. Progressing with this idea, successful Epo-fusion peptides have included the use of peptide-derivatives of the carboxy-terminal region of hCG [209-211] and human thrombopoietin (hTpo). The fusion of these selected peptides to the EPO molecule saw the advent of chimeric EPO-derivatives with 28 additional amino acids when hCG peptide was added and either 17 or 178 additional amino acids when hTpo carboxy terminal (or a shortened form) was added.

All of these chimeric proteins demonstrated prolonged plasma half-life, and marked improvement in haematopoietic activity, compared to commercially available EPO-derivatives [209].

Thus far, the resultant EPO-peptide fusion derivatives have mainly been concerned with creating EPO-derivatives that maintain and prolong their haematopoietic activity via increased plasma half-life, and in some cases even further protracted efficacy due to decreased clearance as well. They have not yet been investigated for a role in tissue-protection, but this is likely to follow soon, as well as the potential to create other tissue-protective chimeric fusion proteins using EPO-derivatives that already exhibit solitary tissue-protective functions.

EPO-derivatives based on tertiary structure

Analysis of the tertiary structure of EPO using x-ray crystallography or nuclear magnetic resonance tools has provided a vast quantity of knowledge about the protein structure, and also interaction with its receptor to provide structure-function clues. Analysis of EPO tertiary structure has also given rise to EPO-derivatives. An EPO-derivative based on the helix-C motif has been created (Epotris) and trialled as a neuroprotective agent in an *in vivo* model of kainic acid-induced neurotoxicity [212]. Epotris demonstrated better cytoprotective survival and regenerative profiles compared to EPO, but no evidence of erythropoietic ability. Epotris has subsequently been trialled in a second neurological setting, in an *in vivo* electrically–induced status epilepticus model where it demonstrated more modest cellular protective capability, but did attenuate cellular consequences of status epilepticus [213].

Further scrutiny of the tertiary structure of EPO and structure-function analysis gave rise to an EPO-derivative based on helix-B of EPO. This molecule is discussed in chapter 1.2.6 in further detail.

1.2.5 Erythropoietin and EPO-derivatives as pleiotropic cytokines

The theory that EPO may possess roles outside of the promotion of haematopoiesis and red blood cell maturation was suggested more than 2 decades ago. In the well-designed study, Anagnostou *et al* demonstrated first, using radio-iodinated-labelled EPO, binding of the ligand to a receptor of approximately 79kDa (subtraction of EPOR molecular mass then gave a molecular mass of 45kDa for the putative receptor).

EPO was then observed to stimulate migration as well as proliferation in two endothelial cell types (human umbilical vein and bovine adrenal capillary endothelial cells) [214]. This first report of the non-haematopoietic effects of EPO was followed shortly with numerous publications reporting either presence of the EPOR or a non-haematopoietic effect of EPO in several organ systems. Of note, the presence of functional EPOR or EPOR mRNA was demonstrated in the brain, heart, lung [215], liver stromal cells [216], bone marrow, adrenal cortex, megakaryocytes [217], spleen and testis [218]. Pleiotropic effects of EPO demonstrated in these various tissues, in addition to chemotactic and mitotic promotion noted above, include stimulation of differentiation, increased DNA synthesis [219, 220] as well as neurotropic effects supporting the survival of injured neurons [221].

Unfortunately, the ability of EPO to stimulate red blood cell production has proven to be the limiting factor in its clinical application. In clinical scenarios of ischaemic tissue injury, there is evidence that EPO administration can lead to negative side effects caused by a rise in haemoglobin and haematocrit causing adverse cardiovascular thrombotic events [222, 223]. However structure-function analysis of EPO binding to the EPOR identified specific areas of the EPO molecule essential for stimulating erythrocyte maturation. In addition, studies of EPO-derivatives that have lacked haematopoietic effect have shown the ability to retain previous observed tissue-protective effects [202]. Taken together, these two pieces of information suggest not only that different regions of the EPO molecule have different functional roles, but also, there may be alternative receptors through which EPO mediates tissue protection.

Tissue-protective receptor

The cytokine common beta receptor (βcR) subunit, is so named due to its mutual role as the signal transducing component of many cytokine receptors, including GM-CSF, IL-3R and IL-5R. All of these cytokine receptors are composed of a cytokine-specific α-subunit, and share the βcR subunit [224, 225]. Hence alternative names for the βcR include IL-3Rβ, IL-5Rβ or CD131. Importantly for functionality, it is required that two of the βcR subunits are brought together in order to autophosphorylate JAK2, which similar to the EPOR, is constitutively bound to the cytoplasmic domains of the βcR subunit [226].

Typically, members of the type I cytokine family of receptors are known for forming heteroreceptors, making EPOR unique due to its homodimer conformation. However, EPOR and βcR have previously demonstrated associations *in vitro* [227]. Confirmation of the two receptors forming heterodimers in a tissue-protective setting was provided in a variety of tissues enriched by passage across CEPO – an EPO derivative that does not display any haematopoietic functionality. EPOR / βcR heterodimer complex was demonstrated in preparations of brain, heart, liver and kidney tissue [228].

Identification of a proposed tissue-protective receptor has largely sought to refocus attention back on to EPO and EPO-derivatives, and their pleiotropic capabilities. The use of EPO, and more recently EPO-derivatives, is far-reaching in terms of its clinical potential, and a summary of current clinical applications is delivered below. The initial discovery of EPO inducing mitosis and migration, has been replicated time and again in many different cell types, including stem cells (endothelial, neuronal, renal progenitor cells and mesenchymal stem cells) [229-232].

Further pleiotropic functions of EPO have been demonstrated including anti-apoptotic effects, beyond simply erythroid precursor stem cells, in numerous other cell types, including astrocytes, cardiomyocytes, endothelial cells, epidermal cells, glial cells, neurons, renal tubular epithelial cells, retinal ganglion cells and skeletal myotubes [200, 231, 233-238].

Other lesser-described pleiotropic effects of EPO include improved contractility witnessed in vascular smooth muscle cells and cardiac myocytes [239-241] and an anti-inflammatory effect, by modulating pro-inflammatory cytokines, of which, IL-6 and TNF-α have been the most publicised.

1.2.6 Discovery of ARA-290

Analysis of the tertiary structure of EPO and the interaction of EPO with the erythropoietin receptor $(EPOR)_2$ revealed significant information about the regions of the EPO molecule which are required to bind with the $(EPOR)_2$ in order to initiate haematopoiesis. These regions include helices A, C and D as well as the loop connecting helices A and B [155, 242, 243]. Interestingly, chemical modification of amino acid residues located within any of those regions eliminated binding of the EPO ligand to the $(EPOR)_2$ and therefore saw a reduction in the haematopoietic effect.

Modification did not however, eliminate the tissue-protective properties of the molecule [202]. This led to intensive analysis of the other regions of the EPO molecule in the search for potent tissue-protective molecules. The remaining portions of the EPO molecule (helix B and parts of the loops between helices A/B and C/D) came under scrutiny. When EPO is bound to $(EPOR)_2$ these regions face the aqueous medium, away from the homodimer binding site. Initial work using a 24 amino acid synthetic peptide composed of the peptide sequence of helix B (amino acids 58 – 82) revealed that the EPO-derivative was not capable of promoting the growth of erythrocytes in the UT-7 EPO cell assay. It was however still able to offer neuroprotection (comparable to EPO) in a rat motor neuron *in vitro* model [244] as well as *in vivo*, in a model of ischaemic stroke by reducing infarct size [245].

Further crystallographic study of EPO binding to its homodimer receptor offered guidance as to the exact residues in helix B (8 residues at the surface of the aqueous medium) which may possess specific tissue-protective biological activity. In addition, observation of the amphipathic nature of helix B, as well as other surface amino acids of the B/C loop (exposed due to the rigid structure of the associated A, C and D helices) led to the generation of a new 11 amino acid peptide, called helix B surface peptide (HBSP) [245]. HBSP, due to the incorporation of three additional residues from the B/C loop, is dissimilar in primary sequence to EPO, however, as intended, mimics the 3-dimensional structure of the EPO molecule believed to be cytoprotective. This compound again showed no erythropoietic activity *in vitro* or *in vivo*, but tissue-protective activity in a model of sciatic nerve injury, comparable to EPO and other EPO-derivatives [245].

Spontaneous cyclisation of N-terminal glutamine residues into pyroglutamate, even at room temperature, occurs [246]. Analysis of the HBSP product revealed it consisted of a mixture of two peptides – around 90% of the product had a free N-terminal, whilst the remaining 10% had cyclised into what is now known as ARA-290 – pyroglutamate HBSP (pHBSP) [245]. Initial studies using ARA-290 exhibited no haematopoietic activity. ARA-290 was used *in vivo* in a murine model of renal ischaemia-reperfusion injury and demonstrated a dose-dependent renoprotective effect, similar to prior investigation using EPO as the tissue-protective modality [245, 247]. Its role in a model of ischaemic stroke injury also revealed significant reduction in infarct volume,

even when administered 24 hours post stroke induction, as well as improved neurological function.

ARA-290 synthetic peptide, is now manufactured using standard F-moc solid phase peptide synthesis and purified by HPLC and ion exchange chromatography [248].

1.2.7 ARA-290 in animal models

Evolving analysis of the utility of ARA-290 in the treatment of a wide-ranging number of conditions has relied upon pre-clinical animal models of those various diseases to assess both safety and efficacy.

Cardioprotection

In a rat model of myocardial infarction (MI) – through ligation of the left anterior descending artery – ARA-290 was able to attenuate a number of important features, such as apoptosis, inflammation, cardiac failure and ventricular remodelling. ARA-290 significantly reduced the degree of apoptosis and inflammatory infiltrate within the myocardial area at risk. Echocardiography of the animals 4 weeks after induction of MI also demonstrated greater ejection fractions compared to untreated controls, and a lesser degree of ventricular dilatation [233].

Using a hamster strain of dilated cardiomyopathy (J2N-k), ARA-290 was assessed for its ability to protect cardiomyocytes from TNF-α induced apoptosis. ARA-290 significantly prevented apoptosis, and was shown to do so via activation of the Akt and ERK1/2 pathways. Creatine kinase (released during muscle injury) and atrial natriuretic peptide (a prognostic marker for cardiac failure) were both significantly reduced with ARA-290 treatment [234].

ARA-290 has also been trialled at an earlier stage of cardiac disease, to assess whether or not it has potential to delay progression of coronary atherosclerosis. Using a rabbit model of heritable hyperlipidaemic spontaneous MI, ARA-290 was capable of significantly supressing the progression of coronary atherosclerotic lesions and prevented apoptosis of coronary artery endothelial cells, again utilising the Akt pathway. In addition ARA-290 facilitated a reduction in TNF-α as well as the pro-inflammatory (M1) phenotype of macrophages. Interestingly though, M2 (anti-inflammatory) macrophage numbers were not altered, there was also a significant

reduction in the M1/M2 ratio, suggesting a positive effect of ARA-290 on pro-inflammatory cytokines [249].

Diabetic neuropathy and retinopathy

Using the Akita murine model of diabetic autonomic neuropathy, ARA-290 was employed to determine its ability to reverse established, well-described features of neuritic dystrophy and neuronopathy classical to this model. Akita mice reproducibly develop severe diabetes at 3-4 weeks of age following β-islet cell death, followed by disturbances in blood glucose, HbA1c levels and body weight [250]. Although ARA-290 was unable to demonstrate any positive effect on the described metabolic features or ongoing neuronopathy, it significantly reduced neuritic dystrophy compared to controls [250].

Using the streptozotocin-induced diabetes model, the potential of ARA-290 to ameliorate features of diabetic retinopathy was explored. ARA-290 was able to significantly reduce glial fibrillary acidic protein expression, the concentration of pro-inflammatory cytokines (TNF-α and IL-6) and diabetes-induced DNA damage [251]. Using the same streptozotocin diabetic model, another group demonstrated the potential of ARA-290 to reduce retinal leakage [245].

Neuroprotection

EPO has demonstrated many neuroprotective functions within the brain, following exogenous administration, as well as after local, endogenously produced EPO has been demonstrated to increase. ARA-290 has similarly shown a wide-ranging effect of neuroprotective characteristics in several settings. ARA-290 has shown benefit in modulating pain originating from a variety of causes, including diabetes, inflammation, neuropathic pain and sarcoidosis where it led to improved functional and behavioural pain testing measures [250, 252-254].

In models of traumatic brain injury, ARA-290 administration was capable of significantly reducing contusion volume and improving functional outcome assessments in rats [255, 256].

Using electrical stimulation to initiate a self-sustained status epilepticus episode, ARA-290 intervention demonstrated a significant neurogenic effect as well as improvement in cognitive deficits and functional outcomes [257].

Renal protection

Acute kidney injury due to ischaemia reperfusion of the renal pedicle in rats was created to assess the ability of ARA-290 to reduce glomerular and tubular dysfunction, and prevent renal injury. Renal ischaemia reperfusion injury (IRI) was created by clamping the renal pedicle (renal artery, vein and nerve) for a 30-minute period before releasing the clamp. ARA-290 was able to significantly improve glomerular and tubular dysfunction, measured by serum creatinine and urea, creatinine clearance and excretion of sodium, compared to controls. In addition plasma biomarkers of renal injury (clusterin and osteopontin) were reduced by ARA-290 administration. Subsequent analysis of numerous signalling pathways identified that this amelioration in tissue injury was likely to have involved Akt, GSK-3β and NFκB signalling pathways [258, 259]. Another examination of renal IRI in a larger animal model, using pigs, described similar findings of improved renal function (using glomerular filtration rate as the marker) with ARA-290 treatment. In addition, ARA-290 was able to reduce mRNA expression of the pro-inflammatory cytokines IL-6 and monocyte chemotactic protein-1 (MCP-1), and improve morphological changes of interstitial fibrosis following injury [260].

Further assessment of the signalling pathways utilised in mediating tissue-protection in renal IRI has been undertaken. Using a murine model of IRI, ARA-290 conferred similar anti-apoptotic effects as already described. However, concomitant administration of the PI-3k inhibitor wortmannin, abolished the reduction in apoptosis observed, and additionally worsened serum markers of renal injury, suggesting a key role of the PI-3k signalling pathway [261].

Wound healing

Assessment of thermally induced wounds and the ability of ARA-290 to improve outcomes was assessed by subjecting mice to a partial thickness burn. The partial thickness burn converted into a full-thickness burn within 48 hours due to necrosis of the surrounding tissue, in untreated controls. However, ARA-290 treated animals

were able to maintain microvasculature, and therefore tissue integrity, and demonstrated once again a dampening effect on raised pro-inflammatory cytokines, especially TNF-α [262].

Wounds of both non-ischaemic and recurrent ischaemic origin have also been treated with ARA-290, and each demonstrated a positive role of ARA-290 in ameliorating wound features. In the non-ischaemic wound model, the wound size of ARA-290 treated mice was significantly reduced compared to control. In the recurrent ischaemic wound model (a pre-clinical model for ulcers), ARA-290 reduced the initial wound lesion size, but did not demonstrate a prolonged effect on reducing wound size. This may have been due to experimental procedure, where only 2 doses of ARA-290 were administered on days 1 and 2 of a 14 day total end-point experiment [248].

1.2.8 Current human clinical applications of ARA-290

The role of ARA-290 in a pre-clinical setting, using both *in vitro* and *in vivo* methods, has been complemented with its admittance into clinical trials in multiple fields including inflammatory and rheumatological diseases, neuropathic pain and neuropathic pain in the setting of type 2 diabetes. The current enrolment of ARA-290 for human clinical application will be described below.

Completed clinical trials

Initial safety and toxicity studies on humans were performed by Araim Pharmaceuticals Inc. and revealed no safety concerns at supra-clinical doses in healthy volunteers as well as patients with end-stage renal disease, or sarcoidosis [263].

Investigators in the Netherlands performed a trial to assess the pharmacokinetics of ARA-290 in healthy volunteers. A variety of doses were administered subcutaneously (SC) and a single dose intravenously (IV). SC administrations demonstrated a dose-dependent peak increase in plasma concentration occurring at 6 minutes post-injection. The elimination half-life ($t_{1/2}$) was estimated at approximately 20 minutes [263]. In comparison, IV administration led to peak plasma concentrations within 1 minute, and a $t_{1/2}$ = 2 minutes [263].

The same group of investigators went on to perform a phase IIa and phase IIb clinical trial assessing the use of ARA-290 for small fibre neuropathy (SFN) in a disease setting of sarcoidosis. Both trials are listed as completed, but only one has been

published thus far. 22 patients with sarcoidosis and symptoms of SFN were enrolled in a double-blind, randomised, placebo-controlled study. Primary outcome was pain relief as assessed by SFN screening list. Other outcomes included quality of life, brief pain inventory, depressive symptoms and fatigue. Patients in the ARA-290 treatment group demonstrated significant improvement in SFN screening list scores as well as significant change from baseline pain and physical functioning scores [252].

Clinical trials currently active/recruiting

Numerous clinical trials involving ARA-290 have been registered with the Netherlands trial register (NTR) or the European clinical trials register (EU-CTR). These trials cover a variety of clinical fields, and are at different stages of their clinical trial assessment. The variety of studies therefore involves both healthy volunteers and patients with different disease manifestations [264, 265]. Table 1.5 describes clinical trials currently registered with either EU-CTR or NTR, and their clinical setting.

Table 1.5: Currently active clinical trials investigating clinical applications of ARA-290

Trial Registry Identifier	Scientific Title	Study Group / Study Attributes	Intervention	Primary Outcomes	Secondary Outcomes
2010-023469-22 / NTR2577 [266]	A phase II study of ARA 290 as therapeutic strategy in rheumatoid arthritis	Rheumatoid arthritis Randomised, control study	2mg ARA-290; 1 or 3x/week; IV administration	Disease activity, functional ability, systemic inflammatory markers (ESR, CRP)	Drug tolerance
2010-018584-41 / NTR2685 [267]	A phase II study of ARA-290 as therapeutic strategy in no-option critical limb ischaemia patients	CLI Interventional study	3x/week for 4 weeks	Drug safety and tolerability, pain scores and analgesic use diary, wound healing, inflammatory markers, quality of life	N/A
NTR3575 [268]	Effects of ARA-290 on the regrowth of epidermal nerve fibres in patients with sarcoidosis	Sarcoidosis and SFN Randomised, double-blind, placebo control study	ARA-290 or placebo SC for 28 days	Changes in epidermal nerve fibre density, cutaneous sensitivity, visual tests	Changes in SFN score, pain inventory, 6 minute walk test
2012-005590-32 / NTR3858 [269]	A double blind, placebo controlled Phase II study comparing the effects of ARA-290 on neuropathic symptoms of patients with type 2 diabetes.	Diabetes mellitus type 2 Randomised, double-blind, placebo control study	ARA-290 or placebo SC for 28 days	Drug safety, changes in HbA1c, pain and physical function scores	Changes in sensory testing, epidermal nerve fibre density, 6 minute walk test, visual acuity, heart rate, retinal thickness, glucose control, CRP and microalbuminuria
NTR3131 [270]	ARA-290 and the ventilatory response to hypoxia and pain responses in healthy volunteers	Healthy volunteers Randomised, placebo-control, crossover study	ARA-290, placebo or EPO IV at time of hypoxic induction	Hypoxic ventilatory response, Pulmonary artery pressure	Systolic and diastolic cardiac function, vital and ventilatory parameters, pain threshold under hypoxia

CRP – C-reactive protein, ESR – erythrocyte sedimentation rate, IV – intravenous, SC – subcutaneous, SFN – small fibre neuropathy

1.3 Hypotheses

PAD is a disease of complex pathophysiology and multiple aetiologies. The underlying interplay between haemodynamic compromise and musculopathy has proven the need to better understand the lasting effects of chronic ischaemia on the muscle end-organ, in order to improve current as well as future novel adjunctive treatment options with the aim of improving functional benefit for patients.

Many novel therapeutic agents are brought into the tissue-protective arena, but their utility often needs to be proved via extensive *in vitro* or *in vivo* animal analysis before they can be safely and efficaciously prescribed to patients. EPO has previously been trialled in other hypoxic or ischaemic injury settings, but often its use is prevented due to its pro-thrombotic tendencies following prolonged dosing in people with normal haemoglobin levels. ARA-290 is one of several EPO-derivatives which have since been created which initial studies have suggested retains the tissue-protective properties of EPO but lack any haematopoietic potential.

In terms of the lack of functional benefit often reported by patients following successful revascularisation, it is likely that satellite cells, the principal progenitor component of muscle, may hold the key to elucidating pathological differences due to chronic exposure to a hypoxic environment. For the purposes of this work however, the myogenic differentiated form of satellite cells, myoblasts and myotubes, were isolated and utilised.

This thesis addresses the hypothesis that EPO and the EPO-derivative ARA-290 are capable of mediating cytoprotection when skeletal muscle is subjected to hypoxic insult emulating that seen in critical limb ischaemia.

Experimental approach:

Two experimental approaches were employed to test this hypothesis: initially using an established *in vitro* model of skeletal muscle (derived from mouse) and subsequently primary human skeletal muscle cells, in conjunction with an established model of simulated ischaemia. This provided a useful platform to assess the EPO and ARA-290 compounds ability to reconcile ischaemia-induced apoptosis, as well as determining potential signalling axes being utilised.

Following on from *in vitro* studies, an *in vivo* model of hindlimb ischaemia was used to assess both compounds in a pre-clinical model, with assessment of functional, histological and perfusion outcomes.

1.4 Aims

The aim of this study was to investigate the cytoprotective ability of EPO and the EPO-derivative, ARA-290, in ischaemia-induced injury. In order to achieve this, it was necessary to achieve the following:

1. Demonstrate expression of the tissue-protective receptor in human skeletal muscle.
2. Assess the ability of EPO and ARA-290 to enhance C2C12 myoblast and myotubes function and survival in an *in vitro* simulated ischaemia model.
3. Investigate the functional differences in CLI and control myoblasts and myotubes, and their suitability to form a primary human *in vitro* skeletal muscle model.
4. Assess the ability of EPO and ARA-290 to enhance observed differences in CLI and control myoblast and myotubes function and survival in an *in vitro* simulated ischaemia model.
5. Develop a suitable murine model of hindlimb ischaemia in order to study the ability of EPO and ARA-290 to protect skeletal muscle from ischaemic injury.

CHAPTER 2
Materials and methods

2.1 Patients

Following study approval by the Local Research Ethics Committee (Royal Free and University College Medical School, Hampstead, London) and The Heart Hospital, University College London Hospitals NHS Trust, tissue samples were taken from 2 groups of patients:

Critical Limb Ischaemia group: Patients with CLI

Control group: Patients with no clinical evidence of PAD

Consultations were conducted with patients prior to operative procedure, written and verbal information was provided, and informed consent was obtained from all participants.

CLI Group

Seventeen patients with CLI requiring major lower limb amputation, (i.e. above knee or below knee amputation), were recruited. The Trans-Atlantic Inter-Society Consensus for the management of PAD (TASC guidelines) definition of CLI was used, where patients had chronic ischaemic rest pain for at least two weeks, with or without ulcers or gangrene, attributable to objectively proven arterial disease (e.g. ABPI <0.3). Patients undergoing major lower limb amputation for pathology other than CLI were excluded from the study.

Control Group

Control samples were taken from patients undergoing coronary artery bypass graft (CABG) surgery for coronary artery disease, in which the long saphenous vein was harvested. Patients were assessed pre-operatively by clinical history, physical examination and ABPI measurement to exclude significant PAD. Patients with symptoms and, or, signs of PAD or in whom ABPI measurement was less than 0.9 were excluded from recruitment.

As described in the previous chapter, different muscle groups contain different proportions of myosin heavy chain fibre type. Therefore in order to try and standardise muscle sample collection we obtained all biopsies from the deep belly of the gastrocnemius muscle in both groups of patients. The gastrocnemius muscle is also easily accessible in the control group, and in the CLI group is usually a suitable distance from any infected, ulcerating or gangrenous areas, which were avoided when collecting samples, in order to reduce the confounding effects of concurrent inflammation or infection on our data. The gastrocnemius muscle in CLI patients has been demonstrated to be ischaemic, through presence of HIF-1 as well as by near-infrared spectroscopy in the literature [271]. Demographic details, prevalence of cardiovascular risk factors and information on current medication were also collected from both groups.

2.1.1 Sample collection and preparation

CLI group

Following surgeon-devised operative amputation protocol, the amputated remnant limb was provided to us for access to muscle biopsies. The gastrocnemius muscle was identified, and open muscle biopsies excised.

Excised muscle biopsies were divided into 4 portions. One portion was placed in a microcentrifuge tube and immediately snap frozen in liquid nitrogen, and then stored at –80°C for protein analysis. A second part was collected into RNAlater™ RNA stabilisation reagent (Ambion, Austin, Tx) and stored according to manufacturer's guidelines for later RNA quantitation. A third portion was immersed in 10% formal saline containing 4% formaldehyde (CellPath, UK) for histological processing. The final remaining portion was collected into solution A (30mM 4-(2-hydroxyethyl)-1-piperazineethanesulfonic acid (HEPES), 130mM sodium chloride, 3mM potassium chloride and 10.1mM glucose) for isolation of myoblasts.

Control group

Individuals undergoing long saphenous vein harvest for CABG had the medial aspect of either left or right calf exposed. Once saphenous vein harvest was completed, the gastrocnemius muscle was identified, and an incision in the deep fascia (*fascia*

cruris) was made. Open muscle biopsies (approximately 0.5 cm x 0.5 cm x 0.5 cm) were taken from the surgically exposed gastrocnemius muscle.

Once the muscle sample was excised, the muscle was collected in the same manner as CLI muscle above.

2.2 Tissue analyses

2.2.1 Histological analysis

Preparation of samples collected for histological analysis allowed the muscle biopsy to fix in 10% formal saline containing 4% formaldehyde (CellPath, UK). Samples were allowed to remain in fixing solution for up to 10 days. Fixed tissues were processed and dehydrated overnight and embedded in molten paraffin wax to generate the formalin-fixed paraffin embedded (FFPE) samples. When required, 3µm sections were cut using a microtome (Leica, UK) and mounted onto polylysine-coated slides (VWR, UK) from the FFPE muscle samples. Sections were heated overnight at 42°C and then used to perform staining.

Histology

FFPE sections were dewaxed in xylene (Genta Medical, York, UK) and passed through a series of graded ethanols and then transferred to water. To ensure correct cross-sectional orientation of the embedded muscle tissue, and also to assess tissue architecture, haematoxylin and eosin (H&E) staining was performed using standard protocol. Briefly, FFPE sections were dewaxed and prepared as above. After immersion in running tap water sections were immersed in Harris' haematoxylin for 5 minutes before differentiating by dipping in a weak acid alcohol solution (20mM HCl in 70% ethanol). Sections were then rinsed in running tap water before immersion in eosin for 1 minute. Sections were then rinsed and dehydrated by passing through graded alcohols, cleared in xylene, and then mounted in permanent DePeX mountant (VWR, UK).

Immunohistochemistry

All immunohistochemistry undertaken was performed on FFPE sections. After dewaxing sections, slides were immersed in 0.5% hydrogen peroxide (v/v) in methanol for 10 minutes to quench endogenous peroxidase activity. Antigen retrieval

was performed according to manufacturer's guidelines, but usually entailed either heat-mediated or enzymatic antigen retrieval. Heat-mediated antigen retrieval was achieved by microwave heating of sections submersed in either 10mM Citrate buffer (pH 6.0) or Tris-EDTA (10mM Tris base, 1mM EDTA) buffer (pH 9.0) for 10 – 20 minutes. Alternatively, enzymatic antigen retrieval was performed using either 0.5% trypsin (w/v) or 20μg/ml proteinase k applied directly to the slide for 15-20 minutes. Antigen retrieval protocols were optimised for each antibody used individually.

To reduce nonspecific background staining as a result of binding to non-immunological antigenic sites a blocking step was performed. This involved pre-incubating sections with normal whole serum against the species in which the secondary antibody was raised. Isotype matched control serum (Vector Laboratories, Burlingame, CA) was diluted 1:10 in phosphate-buffered saline (PBS, pH 7.4) and applied to sections for 30 minutes. Endogenous biotin activity was blocked using a commercially available kit (Vector Laboratories) according to manufacturer's instructions. Primary antibodies, dilutions and manufacturer's details were as follows:

Table 2.1: Primary antibodies used for immunohistochemistry

Antibody	Dilution	Manufacturer
Rabbit anti-IL3RB (βcR)	1:250	Abcam
Rabbit anti-IL3RB (βcR)	1:250	Santa Cruz biotechnology
Mouse anti-EPOR	1:40	Abcam
Rabbit anti-EPOR (C-20)	1:500	Santa Cruz Biotechnology
Rabbit anti-EPOR (M-20)	1:500	Santa Cruz Biotechnology
Mouse anti-Pax-7	1:100	Abcam
Rabbit anti-Ki-67	1:100	Abcam
Rabbit anti-CD34	1:100	Abcam

Optimisation of treatment conditions including antibody dilution, length and ambient temperature during staining treatment was performed for each antibody used. An appropriate biotin-conjugated IgG antibody (Vector Laboratories) at 1:200 dilution was applied for 30 minutes at room temperature. Binding was detected using either peroxidase or alkaline phosphatase-based standard immunohistochemical ABC

method (VectaStain, Vector Laboratories). Sections were developed using the corresponding peroxidase-linked chromagen DAB (3,3'diaminobenzidene) or alkaline phosphatase substrate in Tris-HCl (pH 8.2) buffer. In the case of double staining, both DAB and alkaline phosphatase substrates were used following a sequential staining series. Sections were counterstained in Mayer's haematoxylin, and dehydrated in ethanol, cleared in xylene and mounted using the permanent mountant DePeX (VWR, UK).

2.2.2 RNA quantitation and analysis

RNA extraction of tissue samples

Tissue samples were stored in RNAlater™ RNA stabilisation reagent (Ambion, Austin, TX). As per manufacturer's guidelines, samples were stored at 4°C overnight and the solution removed before longer-term storage at -80°C. When required, the samples were thawed, on ice, and adequate weights of tissue samples (approximately 30mg) were immersed in RNeasy RLT lysis buffer containing 10µl/ml (14.3mM) β–mercaptoethanol (RNeasy fibrous tissue mini kit, Qiagen). Tissues were disrupted by lysis for a total of 4 minutes (2 x 2 minutes) at 30 Hz in a TissueLyser (Qiagen). To ensure even homogenisation, samples were rearranged throughout the TissueLyser reaction-tube holder after 2 minutes. After homogenisation, fibrous tissue was digested using proteinase K 0.011% at 55°C for 10 minutes. Samples were centrifuged to remove tissue debris and the supernatant containing RNA mixed with half a volume of 100% ethanol as per RNeasy protocol. RNA was bound within the silica spin column and washed repeatedly. RNA was eluted in 60µl of RNase-free water into microcentrifuge tubes for storage at –80°C. A 16µl aliquot was used for DNase I (Sigma-Aldrich, UK) digestion, to eliminate any contaminating template DNA.

RNA quantification

RNA was quantified using a Nanodrop ND-8000 spectrophotometer (Thermo-Scientific). Briefly, 1µl of each sample was placed on the spectrophotometer and measured for quantity and purity, assessed by the A_{260}:A_{280} and A_{260}:A_{230} ratios. Acceptable A_{260}:A_{280} ratios were between 1.9 – 2.2, and ratios of A_{260}:A_{230} between 2.0 – 2.2.

RNA quality was assessed using the Agilent RNA 6000 nano chips and kit with an Agilent 2100 Bioanalyzer (Agilent Technologies UK Limited) according to manufacturer's instructions (figure 2.1). The RNA integrity algorithm was used to calculate the integrity. For PCR analysis, the minimum acceptable RNA integrity value was greater than 7.0.

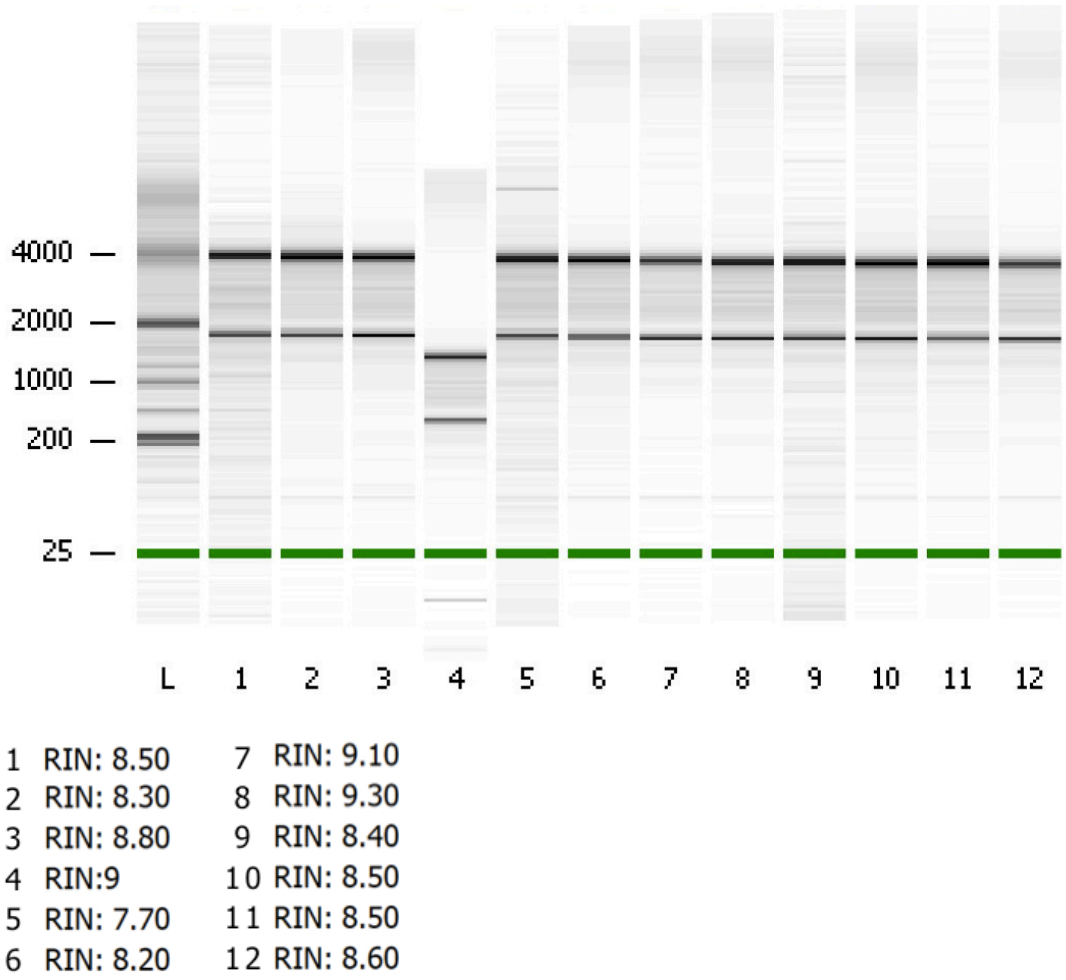

Figure 2.1: Agilent RNA 6000 Nano chip assay results for human skeletal muscle

Representative summary of Agilent RNA 6000 nano chip assessment of RNA quality of RNA isolated from human skeletal muscle. The quality of RNA isolated from human and mouse skeletal muscle was assessed using the Agilent RNA 6000 nano chip set.

Primer design

Primers were designed using NCBI / Primer-BLAST software and human and mouse accession numbers. Human and mouse sequences were aligned to identify conserved areas similar to both species. Primers were designed to span exon-exon junctions

common to both human and mouse. Primers were generated to standard specifications of GC content of 40-50, and a melting temperature of approximately 60°C. All primer sequences were then subjected to BLAST analysis (www.ncbi.nlm.nih.gov/blast) to ensure specificity for the EPOR and βcR genes. No self-annealing or primer dimers were reported on the technical data. Primers were produced by Sigma-Aldrich and are listed in table 2.2.

Table 2.2: Primers used for quantitative PCR

Gene name	Forward primer sequence (5' – 3')	Reverse primer sequence (5' – 3')
βcR	CGTGGAAGGACAGCAAGACC	GCTGTCCCCGAATCCTACAG
EPOR	ATCAATGAAGTAGTGCTCCT	CAGCCACAGCTGGAAGTTA
TBP	AGTGACCCAGCATCACTGTTT	GGCAAACCAGAAACCCTTGC

cDNA synthesis

0.5μg of total RNA was reverse transcribed using the QuantiTect reverse transcription kit (Qiagen). Briefly, the first step requires the elimination of genomic DNA contaminants within each RNA sample. Following this, the RNA was reverse transcribed using the supplied blend of random and oligo-dT primers. The completed cDNA reaction was diluted five-fold with nuclease-free water, giving a final concentration of 100ng/μl.

Quantitative Polymerase Chain Reaction (qPCR)

2μL (final concentration of 100ng) of diluted cDNA was used for real-time quantitative reverse transcription PCR (qRT-PCR) in a 12μL reaction volume using QuantiFast SYBR Green RT-PCR kit (Qiagen). As per manufacturer's guidelines, the reaction mixture also contained 6μL 2x QuantiFast SYBR Green RT-PCR master mix, 0.24μL primer mix (final concentration 1μM), and made up with nuclease-free water to 12μL. A negative, or non-template control was also added into each qPCR cycle by replacing cDNA with nuclease-free water. The reaction mixture was analysed on a Rotorgene-6000 (Corbett Life Sciences, Sydney, Australia) under the following conditions: 95°C for 10 min, followed by 40 cycles of 95°C for 10 seconds, 57°C for 15 seconds and 72°C for 5 seconds. Primer dimers were excluded by melt curve analysis. The reference gene TATA box binding protein (TBP) was analysed

using REST© (Relative Expression Software Tool) from Qiagen to obtain normalisation factors. Gene of interest copy numbers were corrected using these normalisation factors.

2.2.3 Protein quantitation and analysis

Homogenisation of human muscle tissue

Whole muscle samples were homogenised using TissueLyser (Qiagen). Briefly, muscle samples were thawed on ice, and weighed. Between 30 – 50mg of muscle tissue was placed in a 2ml round bottom microcentrifuge eppendorf tube, and 10-volumes of radio-immunoprecipitation assay (RIPA) buffer (150mM NaCl, 1.0% IGEPAL® CA-630, 0.5% sodium deoxycholate, 0.1% SDS, and 50mM Tris, pH 8.0; Sigma-Aldrich, UK) with 1x Complete mini EDTA-free protease inhibitor (Roche) and 10μL/ml each of phosphatase inhibitor cocktail 2 and 3 (Sigma-Aldrich, UK) added. A stainless steel metal ball was added, and the samples arranged in the TissueLyser. Tissue was disrupted by mechanical homogenisation for a total of 6 minutes (2 x 3 minutes) at 30 Hz. To ensure even homogenisation, samples were rearranged throughout the TissueLyser reaction-tube holder after 3 minutes. Homogenised samples were centrifuged at 15,000g for 15 minutes at 4°C. The supernatant was removed and a bicinchoninic acid (BCA) protein assay (ThermoScientific, UK) performed according to manufacturer's protocol to assess protein quantity within each sample. Briefly, standard protein concentrations are created using known albumin protein concentrations, and a 7 fold-serial dilution performed. Equal volumes of standard or samples are added to wells in a 96-well microplate in duplicate. Protein present in the samples will mediate the reduction of Cu^{2+} to Cu^{1+} in a protein concentration dependent manner, which results in a characteristic colour change from green to purple. The absorbance at 560nm of each sample was measured using a microplate reader (Mithras LB940 microplate reader, Berthold Technologies, Germany). Sample protein concentrations were calculated by comparison with the standard curve. Samples were then normalised to the sample with lowest protein concentration, and 4x lithium dodecyl sulphate (LDS sample buffer (Invitrogen, UK) and 50mM dithiothreitol (DTT) added to each sample before denaturing samples by heating at 70°C for 10 minutes. Samples were stored at -80°C when not used.

Western blot analysis

Identification of proteins of interest within muscle or cell lysate samples was performed using Western blot analysis. Equal amounts of protein in LDS sample buffer were fractionated by SDS-polyacrylamide gel electrophoresis using 4-12% bis-tris gels (Invitrogen) or various tris-glycine gradient gels, prepared when required and with a suitable acrylamide composition for the size of the protein of interest. A reference ladder (Novex® Sharp Pre-stained Protein Standard, or SeeBlue® Plus2 Pre-Stained Standard, both Invitrogen) was included, and samples electrophoresed at 180V for 1 hour (bis-tris gels) or 125V for 90 minutes (tris-glycine gels). Proteins were transferred by electro-blotting from each gel onto a nitrocellulose membrane (Hybond-C Extra, GE Healthcare Amersham, UK).

Adequate transfer was assessed by Ponceau S solution (0.1% (w/v) in 5% acetic acid) staining (Sigma-Aldrich, UK) of each membrane. The membrane was washed briefly with phosphate-buffered saline with 0.1% Tween-20 (PBS-T) (Sigma-Aldrich).

Non-specific binding was blocked by membrane incubation with 5% (w/v) non-fat dry milk in PBS-T for 2 hours at room temperature. Membranes were incubated overnight at 4°C with gentle agitation with primary antibodies, listed below with dilutions and manufacturer's details (table 2.3). β-tubulin was used as a loading control in all Western blot analysis.

Before addition of a secondary, species-specific HRP-linked antibody, membranes were washed thoroughly with PBS-T. Secondary antibodies were used at 1:1000 dilution in 5% non-fat dry milk solution and allowed to incubate for 1 hour at room temperature. Signal was detected using a luminescence kit (ECL detection kit; Amersham) followed by exposure to photographic film (Hyperfilm ECL; Amersham) and manual development. Densitometry analysis was performed using VisionWorkLS analysis software (UVP, CA, USA).

Table 2.3: Primary antibodies used for Western blot analysis

Antibody	Dilution	Manufacturer
Rabbit anti-IL3RB (βcR)	1:5000	Abcam
Rabbit anti-IL3RB (βcR)	1:1000	Santa Cruz biotechnology
Mouse anti-EPOR	1:500	Abcam
Rabbit anti-EPOR (C-20)	1:1000	Santa Cruz Biotechnology
Rabbit anti-EPOR (M-20)	1:1000	Santa Cruz Biotechnology
Mouse anti-Pax-7	1:500	Abcam
Mouse anti-myogenin	1:1000	Abcam
Mouse anti-HIF-1α	1:500	Novus Biologicals
Rabbit anti-Cleaved caspase-3	1:1000	Cell Signalling
Rabbit anti-Akt	1:1000	Cell Signalling
Rabbit anti-Phospho Akt (Ser 473)	1:1000	Cell Signalling
Rabbit anti-beta-tubulin	1:50000	Abcam

2.3 Materials

Human EPO protein for all *in vitro* experiments was purchased from Santa-Cruz Biotechnology (CA, USA). The protein was reconstituted in 10% glycerol (v/v in PBS (pH 7.4) at a stock concentration of 120μg ml^{-1}. The stock solution was aliquoted and stored at -20°C. Eprex® (Janssen-Cilag, Buckinghamshire, UK), an erythropoietin alfa analogue, was obtained from the Royal Free Hospital Pharmacy for the purposes of *in vivo* work.

ARA-290 synthetic peptide used in both *in vitro* and *in vivo* work was a kind gift from Professor Anthony Cerami, and Michael Brines of Araim Pharmaceuticals (NY, USA). The peptide was reconstituted in PBS at a stock concentration of 1mg/ml, sterile-filtered, aliquoted and stored at 4°C for up to one month.

2.4 *In vitro* model of simulated ischaemia

In vitro cell culture models are an abundantly used tool to study various signalling pathways, as well as pharmacological interventions and their impact on cellular function. They also provide a useful platform for the initial extensive assessment of novel therapeutic agents.

In order to investigate the effect of ischaemia on a murine myoblast cell line, as well as primary isolated human cells a reproducible model of ischaemia was required. Our group has previously investigated the use of several gas mixtures to find the optimum gas mixture to simulate many of the conditions typically found in the ischaemic limb of CLI patients. Parameters that were similar included pH, partial pressures of oxygen and carbon dioxide as well as lactate dehydrogenase release and induction of HIF-1α and apoptosis of myotubes [238].

A modular incubator (MIC-101, Billups-Rothenberg Inc., Del Mar, CA, USA), and the previously described 20% carbon dioxide balanced in 80% nitrogen (BOC Limited, Guildford, UK) was used in order to simulate aspects of human skeletal muscle ischaemia seen in CLI patients, within our *in vitro* model.

2.4.1 Culture of C2C12 myoblast cell line

C2C12 is an established, immortalised, myoblast cell line of murine origin. The C2 line was first isolated in 1977 by Yaffe and Saxel from the thigh muscles of 1-2 month old mice that had undergone crush injury. The C3H line was then subcloned by H. Blau to produce the C2C12 myoblast line. C2C12 mouse myoblast cell line was obtained commercially (HPA culture collection, #91031101). C2C12 myoblasts were grown in growth medium containing Dulbecco's modified Eagle's medium (DMEM GlutaMAX™) (Invitrogen, Paisley, UK) supplemented with 10% foetal calf serum (FCS) (Gibco®, Paisley, UK), 100 units/ml penicillin and 100μg/ml streptomycin (Invitrogen). The cells were then placed in a humidified incubator with 5% CO_2 atmosphere maintained at 37°C. The medium was changed every 48 hours until cells reached 60 – 70% confluence. Cells were trypsinised – 0.25% trypsin (w/v) in 1mM EDTA (trypsin-EDTA) (Invitrogen) when they reached confluence, and passaged approximately 1:10. All cells required for experiments were used within 10 passages. Following trypsinisation, if cells were required to perform

experiments they were counted using a haemocytometer, and resuspended to a cell density of approximately 25,000 cells/ml. Cells were then seeded into 6-well plates (2ml/well), 24 well plates (500µl/well) or 96-well plates (100µl/well).

Differentiation of C2C12 myoblasts

After seeding C2C12 myoblasts into 6 well plates and allowing them to reach 70-80% confluence, if differentiated myotubes were required, growth medium was exchanged for differentiation medium containing DMEM GlutaMAX™ supplemented with 2% horse serum (Gibco®, Paisley, UK), 100 units/ml penicillin and 100µg/ml streptomycin (Invitrogen). *In vitro* differentiation of C2C12 myoblasts has been well publicised when a change from serum-rich to a less rich serum medium is performed. The medium was changed every 48 hours, and cultures were inspected using a phase-contrast microscope to confirm typical myotube morphology. Cells were maintained in differentiation medium for between 5 and 7 days to ensure adequate differentiation, before being subjected to any experimental procedure.

Pre-treatment with EPO or ARA-290

Stock solutions of both EPO and ARA-290 were made up as detailed above. After assessing the effect of a range of doses on cleaved caspase-3 expression, experimental doses of EPO and ARA-290 were selected. Doses used for EPO pre-treatment ranged from 0.6 – 1200ng/ml, and the optimum dose chosen for future experiments was 60ng/ml. For ARA-290 pre-treatment, doses ranged from 0.05 – 500ng/ml, and the effective dose used for all future experiments was 5ng/ml.

Inhibitor Assessment

Inactivation of key signalling molecules to elucidate important components of the EPO or ARA-290-mediated cytoprotective pathway assessed JAK2/STAT3 (SD-1029), PI3k/Akt (LY294002 and wortmannin) and NFκB inhibitor of activation IV (all Calbiochem, Merck Millipore International, Germany). All inhibitors were reconstituted in DMSO or purchased in solution with DMSO. SD-1029 was used at a final concentration of 10µM. LY294002 was used at a final concentration of 3µM. Wortmannin was used at a final concentration of 10nM and NFκB inhibitor of activation IV was used at a final concentration of 150nM. Vehicle-only (DMSO) at

the highest concentration (1:3000) was added to ensure cell-death was not in response to DMSO content.

2.4.2 Preparation of C2C12 samples for analysis

Cell lysate samples from parallel normoxic control cell cultures, and those that were exposed to pharmacological pre-treatment prior to simulated ischaemia were collected. Supernatant was discarded, the cell monolayer rinsed in PBS, and then RIPA buffer (150 nM NaCl, 1% Triton, 0.1% SDS, 50 mM Tris-HCl pH7.5, 2mM EDTA, protease inhibitor cocktail and 8M urea) with 1x Complete mini EDTA-free protease inhibitor (Roche, UK) and phosphatase inhibitor cocktails 2 and 3 (Sigma-Aldrich, UK) were applied directly to cells. Cells were lysed further using mechanical shearing by a needle and 24-gauge syringe.

2.5 Isolation and culture of human myoblasts and myotubes

2.5.1 Isolation of human myoblasts

The isolation of myoblasts from human muscle tissue was achieved following a protocol from the MRC Centre for Neuromuscular Diseases: *Myoblast isolation from muscle biopsy V4,* kindly offered by Dr Jenny Morgan. Briefly, at the time of muscle biopsy excision, a 0.2 x 0.2 x 0.2cm fragment was placed in 5ml of Solution A and transported on ice, before being processed on the same day. Under aseptic conditions in a class II microbiological safety laminar flow hood the muscle biopsy only was transferred to a petri dish and washed in 5ml fresh Solution A. The muscle biopsy was then placed on an empty petri dish, and all visible adipose and connective tissue removed, before finely mincing the tissue into smaller pieces. 5ml Solution ATE (10% Trypsin-EDTA, Invitrogen, UK in Solution A) was added to the finely minced tissue to help aspirate it into a sterile wheaton flask with a magnetic stirrer. The petri dish was washed a further two times with 5ml Solution ATE to give a final volume in the flask of 15ml. The flask was placed in a pre-warmed beaker of water, at 37°C, placed on top of a hotplate with magnetic stirrer (Stuart Scientific, Bibby Scientific Limited, Staffordshire, UK) and the stirring mechanism initiated to ensure the magnet bounced within the flask disrupting the tissue fragments further. After 15 minutes

solution ATE, with dissociated cells, was aspirated and transferred into a 50ml centrifuge tube containing 20ml 10% FCS-DMEM, with care taken to avoid removing the muscle fragments. 15ml fresh solution ATE was added to the flask to continue the magnet stirring. This process was repeated a third time. Each time the 15ml solution ATE with dissociated cells was placed into 20ml DMEM-10%FCS to neutralise the trypsin-EDTA before centrifuging at 400g for 5 minutes to obtain a pellet of dissociated cells. Each cell pellet was resuspended in 1ml skeletal muscle cell growth medium (PromoCell, Heidelberg, Germany) supplemented with PromoCell skeletal muscle SupplementMix (containing foetal calf serum 0.05 ml/ml, bovine fetuin 50µg/ml, recombinant human epidermal growth factor (EGF) 10ng/ml, recombinant human basic fibroblast growth factor (bFGF) 10ng/ml, recombinant human insulin 10µg/ml, dexamethasone 0.4µg/ml), 10% FCS (Gibco®), 1x GlutaMAX™ (Gibco®, UK), 100 units ml^{-1} penicillin and 100µg ml^{-1} streptomycin (Invitrogen) (SMM complete medium). The cells were pooled and each centrifuge tube rinsed with 2ml SMM complete medium to collect any remaining cells. All 9 ml was filtered across a 40µm sterile cell strainer (BD Falcon™, Oxford, UK) and then plated into a $25cm^2$ tissue culture flask. The flask was then placed in a humidified incubator with 5% CO_2 atmosphere maintained at 37°C. After 3 days, 3ml of fresh SMM complete media was added into the flask. 5 days after initial plating of cells, all medium was removed, and the cells washed gently with 3mls DPBS (Dulbecco's phosphate buffered saline, calcium and magnesium free, Gibco, UK) and 9ml fresh SMM complete medium replaced into the flask. The media was changed every 48 – 72 hours, and cultures were inspected using a phase-contrast microscope to confirm typical myoblast morphology.

2.5.1.1 Culture and differentiation of human myoblasts

Cultures of human myoblasts were maintained in SMM complete medium until 60 – 70% confluent. At this point, to avoid the cells differentiating due to cell-to-cell contact, cells were trypsinised as described above for C2C12 myoblasts, and passaged approximately 1:6. If required for future experiments, human myoblasts were counted using a haemocytometer and resuspended to approximately 30,000 cells/ml. Cells were then seeded into 6-well plate (2ml/well) 24-well plate (500µl/well) or 96-well plates (100µl/well). All experiments using human myoblasts

and myotubes were performed between passages 2 – 5 to ensure cells did not undergo phenotype conversion.

2.5.2 Human myoblast analysis

Cultures of human myoblast isolates were used to explore the differences in function and response to simulated ischaemia. Human myoblast isolates were also assessed for true myogenic lineage and purity. Analysis of differences between CLI and control myoblasts, with regards to their proliferation, migration and contractile characteristics were assessed in the following ways.

2.5.2.1 Assessment of proliferative capability

Several techniques for assessing the proliferative capacity of cells exist. Often these techniques rely upon either the viability or activity of cells in order to estimate their proliferative capacity [272]. In order to accurately identify the proliferative potential of human myoblasts under both normoxic and hypoxic conditions a number of techniques were used in combination.

3-(4,5-dimethylthiazol-2-yl)-2,5-diphenyl tetrazolium bromide (MTT) assay

MTT is a tetrazolium dye that is reduced by cellular mitochondrial dehydrogenase enzymes present in viable cells, to produce an insoluble formazan product. The formazan product can be solubilised using dimethyl sulphoxide (DMSO), and the absorbance of the solution measured using a spectrophotometer at absorbance wavelength 560nm. As only viable cells can reduce the MTT to formazan, it is often used as a surrogate marker for cell proliferation. The MTT proliferation assay was conducted as follows. Following trypsinisation, cells were plated in triplicate at 5,000 cells/well in a 96 well microplate, and allowed to adhere for 6 hours. Medium was exchanged for fresh 1% FCS-DMEM. If the effect of ARA-290 or EPO was under investigation, these were added to the media of the relevant wells. One plate was placed in the hypoxic chamber under simulated ischaemia as detailed above for 12 hours, and a second control plate left in a normal humidified incubator with 5% CO_2 ambient atmosphere. When the ischaemic period was finished, both plates had media exchanged with 100µl fresh media and 10µl 12mM MTT. Both plates were returned to a normal humidified incubator for 4 hours. 85µl of the media-MTT mix was removed, and any formazan by-product produced was solubilised using DMSO, by adding 50µl DMSO to each well. The plates were incubated at 37°C for 10

minutes, shaken gently using a plate shaker and the absorbance read at 560nm using a Mithras LB940 microplate reader.

Crystal Violet assay

In contrast to the MTT assay which is dependent on metabolic activity, crystal violet relies upon the DNA-dye binding [272, 273]. Its accumulation within the nuclei is then solubilised to indicate the relative cell number as a tool to assess cell proliferation. For the purposes of cell proliferation measurement, it was used in the following way. A 0.025% (w/v) crystal violet solution was dissolved in a 10% (v/v) methanol solution. Cells were plated in a similar way as described for MTT proliferation assay, and subjected to the same simulated ischaemia and normoxic conditions. Following the ischaemic period, both plates were prepared by removal of media, and 2 washes with PBS, with care taken not to affect the cell monolayer. 50µl of the working crystal violet solution was added to each well, and allowed to incubate at room temperature for 10 minutes. Following the incubation period, crystal violet solution was removed, and the plate washed 3 times with dH_2O. Following the final wash, to ensure the plate was adequately dried, it was inverted and blotted on tissue paper, before being left inverted and allowed to air dry for 3 hours. After ensuring adequate drying, crystal violet was solubilised using a 33% acetic acid solution, and the absorbance read at 560nm using a microplate reader (Mithras LB940).

CyQUANT® NF Cell Proliferation assay

CyQUANT® NF Cell Proliferation assay (Invitrogen, UK) is based on the principle of measuring DNA content using a proprietary fluorescent DNA-dye which will bind to DNA. The extent of cell proliferation can be determined by assessing cellular DNA content which will be proportional to cell number [274, 275]. Assessment of cell proliferation using this kit was performed as follows. Cells were plated as previously described for MTT assay, and subjected to the same simulated ischaemia and normoxic conditions. Following the ischaemic period, both plates were prepared by removal of media, and 2 washes of PBS, with care taken not to disrupt the cell monolayer. A 1x dye binding solution was prepared by adding 22µl of CyQUANT® NF dye reagent, and 11µl of dye delivery reagent to 11ml of Hank's balanced salt solution. 50µl of the dye binding solution was applied to each well, and the plate incubated at 37°C for 30 minutes. Fluorescence intensity was measured in each

sample using a microplate reader with excitation at ~485nm and emission detection at ~530nm (Mithras LB940).

2.5.2.2 Scratch-wound assay for the assessment of migratory potential

Scratch or wound assays were performed to assess the ability of myoblasts to close an artificial gap made in a monolayer of cells, as a marker of their migratory ability. Preparation for this assay required cells to be plated in a 24-well plate, and allowed to adhere and proliferate until around 70% confluence. An artificial scratch was made into a monolayer of myoblasts using a sterile p10–200 pipette tip and the lid of the plate as a straight-edge ruler [276-278]. The cell monolayer was then washed with DPBS to remove any floating cells from the edge or centre of the scratch-wound. Mitomycin-C (Merck Millipore, UK) was included in all wells to inhibit cell proliferation. A positive control well containing DMEM supplemented with 1% FCS only was also included. All other wells were treated with DMEM supplemented with 1% FCS and 7.5µg/ml mitomycin-C (MMC) as well as EPO or ARA-290 with any inhibitors of interest. All wells were visualised using phase-contrast microscopy to ensure integrity of scratch-wound at time 0 hours. Images were captured after 24 hours (Olympus CDK2 microscope) for analysis of cell migration and scratch-wound closure. Closure of the scratch-wound was expressed as the percentage of cells migrated into the scratch wound at 24 hours.

2.5.2.3 Floating collagen gel cultures and quantitation of gel contraction

Assessment of contractile ability was conducted using the previously described floating collagen gel contraction assay [279, 280]. Briefly, 24-well tissue culture plates were pre-coated with 0.22µm sterile-filtered 2.5% bovine serum albumin (BSA) overnight. Prior to use, the BSA was removed, and the plate washed 3 times with DPBS. Trypsinised human skeletal myoblast cells were counted using a haemocytometer and resuspended in DMEM supplemented with 1% FCS and mixed with a collagen solution, containing one part of 0.2 M N-2-hydroxyethylpiperazine-N'-2-ethanesulfonic acid (HEPES; pH 8.0), four parts collagen (Vitrogen-100, 3 mg/ml, Cohesion Technologies, Palo Alto, CA), and five parts of DMEM-cell suspension yielding a final concentration of 80,000 cells/ml and 1.2mg/ml collagen. 1ml of the collagen-cell suspension was added to each well, and the plate replaced to the humidified incubator with 5% CO_2 atmosphere maintained at 37°C, for 1 hour to allow polymerisation of the collagen gels. After polymerisation, gels were detached

from wells by adding 1ml of 1% FCS-DMEM medium. Supplementing wells with 10% FCS-DMEM medium created a positively contracted gel for comparison. Contraction of the gel was quantified by loss of gel weight and decrease in gel diameter over a 48-hour period.

2.5.3 Preparation of human myotube samples for analysis

2.5.3.1 Differentiation of human myoblasts

Following trypsinisation, human myoblasts were seeded into different tissue culture plates including 6, 24, and 96 well plates as described previously and in addition 4-well chamber slides (15,000 cells/well) (BD Bioscience, Bedford, MA, USA) for later immunofluorescence analysis. Myoblasts were maintained in skeletal muscle cell growth medium until they reached 70-80% confluence, at which point they were induced to differentiate by the addition of differentiation, low-serum media described above (DMEM GlutaMAX™ supplemented with 2% horse serum).

2.5.3.2 Immunofluorescence-immunocytochemistry of skeletal muscle cells

Assessment of human isolated skeletal muscle populations using immunofluorescence analysis was performed using markers to ensure a myogenic population, and also to investigate the effect of simulated ischaemia on cell apoptosis. Immunofluorescence analysis was performed on cells seeded into chamber slides as described above. All isolated myoblasts were subjected to immunofluorescence analysis for the muscle-specific marker desmin (Abcam, Cambridge, UK). Populations that demonstrated less than 5% contamination with other cell-types were used for myotubes analysis.

Immunofluorescence protocol was as follows. Cells were fixed in 10% formal saline containing 4% formaldehyde (CellPath, UK) for 5 minutes at room temperature. If required, a permeabilisation step was performed using 0.05% Triton-X-100 in PBS for 10 minutes at room temperature. Cells were washed thoroughly with PBS and non-specific binding of antibody prevented by incubating samples with isotype-matched normal whole serum against the species in which the secondary antibody was raised. Primary antibody dilution, duration and ambient temperature of incubation were optimised for each antibody including anti-desmin (Abcam) and anti-annexin V (Abcam), both used at 1:250 dilution. Slides were washed and incubated with a suitable Alexa Fluor® fluorescent secondary antibody against primary antibody

species IgG heavy and light chain (Invitrogen, UK) at 1:2000 dilution for 30 minutes at room temperature, shielded from the light. Slides were washed and mounted with Vectashield mounting medium containing DAPI (Vector Laboratories). Fluorescence signal was detected using AxioSkop2 fluorescence microscope and Axiovision v4.8 software (both Carl Zeiss GmbH, Jena, Germany)

2.5.3.3 Preparation of human myotubes cell lysates for analysis

Following experimental procedure, conditioned supernatant media was collected and stored for subsequent quantification. Cell lysates were prepared by first rinsing the cell monolayer using DPBS. Subsequently, RIPA buffer with 1x Complete mini EDTA-free protease inhibitor (Roche, UK) and phosphatase inhibitor cocktails 2 and 3 (Sigma-Aldrich, UK) were applied directly to cells. Cells were lysed further using mechanical shearing by a needle and 24-gauge syringe. LDS sample buffer and the reducing agent DTT was added before samples were heated. Prepared samples were then used for Western blot analysis as previously described.

2.5.3.4 Enzyme-linked immunosorbent assay of human myotubes supernatant

Enzyme-linked immunosorbent assay (ELISA) was performed on conditioned medium of both normoxic samples and those pre-treated with EPO or ARA-290 and the various inhibitors, before being subjected to simulated ischaemia. ELISA quantitation of the conditioned medium for the inflammatory cytokine interleukin-6 (IL-6) was performed using a sandwich-ELISA technique using Human IL-6 Duoset ELISA kit (R&D Systems®, MN, USA) as per manufacturer's protocol. Briefly, 100µl of IL-6 capture antibody, at a concentration of 2µg/ml, was applied to the appropriate number of wells in a 96 well microplate. The microplate was sealed and allowed to incubate overnight at room temperature. Following overnight incubation, the capture antibody was aspirated and discarded, and the wells washed carefully 3 times, ensuring complete removal of liquid at each step. All future washes throughout the ELISA protocol were performed in an identical fashion, as described here, with the previous incubated solution aspirated and discarded, and 3 washes performed, ensuring complete removal of all liquid at each step. The microplate was blocked using 100µl per well of 0.2µm sterile-filtered 1% bovine serum albumin (BSA) in PBS (pH 7.4) for 1 hour at room temperature. Blocking solution was aspirated, and the wells washed. A seven-point standard curve, using 2-fold serial dilutions, with a high standard of 600pg/ml was prepared. 100µl of sample or

standard (duplicates) was added to the appropriate well and allowed to incubate at room temperature for 2 hours. Standards and samples were discarded and the wells washed. Detection antibody was diluted to 50ng/ml, and 100µl applied to each well. The plate was covered and allowed to incubate for 2 hours at room temperature. Detection antibody was discarded and the wells washed. 100µl streptavidin-horseradish peroxidase (HRP) was applied to wells for 20 minutes at room temperature. Streptavidin-HRP was discarded and the wells washed. Glo Substrate Reagent (R&D systems®, MN, USA) was substituted for the frequently used hydrogen peroxide/tetramethylbenzidine substrate for HRP, and used as directed by manufacturer's protocol. Briefly, one part of Glo substrate reagent A (luminol) is mixed with two parts of Glo substrate reagent B (hydrogen peroxide) and 100µl added to each well. The microplate was incubated in the dark for 5 minutes before the luminescence of the microplate was read using Mithras LB940 microplate reader. IL-6 concentration of each sample was calculated by comparison with a 4-parameter logistic curve to create a standard curve.

2.6 *In vivo* murine model of hindlimb ischaemia

2.6.1 Animal housing

All animals were licensed under the UK Home Office Animals (Scientific Procedures) Act 1986 and Home Office approval was obtained prior to commencing all animal procedures (project licence PPL: 70/7087). Strict adherence to institutional guidelines was practiced. All animals were obtained from Charles Rivers Laboratories. Upon arrival, they were housed in a specific pathogen-free conventional colony, with access to food and water *ad libitum,* and were exposed to 12-hour light/dark cycles.

The planning and reporting of the *in vivo* experiments were done according to ARRIVE guidelines [213, 281].

2.6.2 Hindlimb ischaemia model

Unilateral hindlimb ischaemia was induced on BALB/c mice (Charles River, UK). Animals were anaesthetised using Avertin (2,2,2 tri-bromoethanol) dissolved in tert-amyl alcohol (both, Sigma-Aldrich, UK) (0.25–0.5mg/kg) prior to surgery. Once anaesthetised, animals were prepared by shaving over the hindlimbs on both sides.

The mouse was then placed in a supine position on an isothermal heating pad, and the surgical area prepared using alcohol wipe to clean. Under a magnifying glass, a 1 cm vertical incision was made in the groin at the level of the inguinal ligament. The subcutaneous fat pad overlying the groin was repositioned to one side to reveal the femoral artery, vein and nerve, covered by a thin layer of fascia. The fascia was divided to expose the neurovascular bundle. The femoral artery was carefully mobilised, with care taken to avoid damage or injury to the surrounding vein and nerve structures. The common femoral artery, just proximal to bifurcation giving rise to the profunda femoris, superficial femoral and superficial circumflex artery was ligated using a 7-0 vicryl (Ethicon, Johnson & Johnson, UK) suture passed under the artery, and tied with a double knot. The popliteal artery (an extension of the femoral artery) proximal to the knee joint was then identified and ligated in the same way. The artery in between the two ligatures was excised. Closure of the incision was performed using 6-0 vicryl (Ethicon, Johnson & Johnson, UK), interrupted sutures. Immediately after completion of surgery, mice were randomly allocated to a treatment group, and received treatment plus analgesic care – Temgesic (buprenorphine) 0.05mg/kg. Animals in the sham group underwent the same anaesthetic preparation, incision and exploration of the groin area to identify and mobilise femoral artery, but no ligation of the artery. Skin was closed in an identical fashion, and animals received analgesic care. Following surgery, mice were observed until they recovered, and then returned to standard housing conditions with free access to food and water *ad libitum*.

2.6.3 Assessment of blood flow in the ischaemic hindlimb

Blood flow perfusion of the ischaemic hindlimb was assessed using laser Doppler perfusion imaging (LDPI) (Moor Instruments, UK). Measurements were taken pre-operatively, in ¼ of randomly selected animals, and immediately following induction of ischaemia in all animals to ensure greater than 95% blood flow reduction in the operated paw was achieved. At the time of sacrifice, 3, 10 and 21 days after surgery, animals were anaesthetised, allowed to equilibrate in temperature on an isothermal heating pad, at 37°C for 15 minutes, and LDPI measurement taken. Paw perfusion results were analysed using in-program software (Moor LDPI Image Processing v4.0, Moor Instruments, UK). All perfusion images were analysed by an observer blinded to intervention. The extent of residual ischaemia at the various end-points was

expressed as a ratio of perfusion in the left (ischaemic) paw versus the right (control) paw – known as the perfusion index.

2.6.4 Assessment of functional outcome following hindlimb ischaemia

Two observers, blinded to the treatment group of each mouse, assessed functional ability of the mice following hindlimb intervention. Functional assessment was performed using a variety of well validated and detailed scoring systems, each assessing a different aspect of functional capacity, including generalised movement (Tarlov score), specific locomotor function (Basso mouse scale for locomotion (BMS)) and grading of visible ischaemia (Ischaemia and modified ischaemia score).

At pre-determined time-points, all mice from all treatment groups were tested in an open field (30 cm x 20 cm) for 2 minutes, and assessed based on the above mentioned scoring systems, detailed below and in tables 2.4 and 2.5.

2.6.4.1 Tarlov score

The Tarlov score [282] is a widely used tool for assessing functional outcomes in a variety of different fields. It contains graded scoring where at its lowest value 0 always represents no movement. However the Tarlov score has been modified to suit the requirements of different investigators, depending on the animals and scenario being studied. Therefore the upper value can range from the original 6, to lesser or greater values [283]. For the purposes of this work, the original Tarlov score was used, with 0 representing no movement, and 6 indicating the normal full and fast movements seen in mice. A full description of characteristic movement and criteria related to each score can be found in Table 2.4.

2.6.4.2 Ischaemia and Modified ischaemia score

The ischaemia score was devised to evaluate the mobility of mice following hindlimb ischaemia by simple visual assessment [284]. Visual inspection of the ischaemic hindlimb was performed to assess the viability of the foot or whole limb, or the presence of any gangrenous tissue or possible auto-amputation. The ischaemia score was later modified to detect less severe levels of ischaemia, as represented by discolouration of nails or toes [285]. The individual criteria of each score can be found in table 2.4, but collectively allow for the easy visual assessment of greater degrees of hindlimb ischaemia. Both the original and modified ischaemia scores were employed and the animal assessed in the open field.

2.6.4.3 Basso mouse scale of locomotion (BMS)

The BMS evolved from the previously described Basso, Beattie and Bresnahan (BBB) locomotor rating scale, a scale originally designed to assess locomotor competence in rats following spinal cord injury [286]. The BMS was introduced to cater specifically for mice, to be a comprehensive locomotor assessment, which, once assessors were trained would be highly sensitive, and easier to replicate. The detailed scoring system was modified for the purposes of this work, so that evaluations relevant only to spinal cord injury pathology were excluded. The modified BMS used can be found in table 2.5.

Table 2.4: Tarlov, ischaemia and modified ischaemia functional scores

Functional assessment scoring sheet, copied from *Brenes et al 2012 [287]*

Score	Description
Tarlov	
0	No movement
1	Barely perceptible movement, non-weight-bearing
2	Frequent movement, non-weight-bearing
3	Supports weight, partial weight-bearing
4	Walks with mild deficit
5	Normal but slow walking
6	Full and fast walking
Ischaemia	
0	Auto-amputation > half lower limb
1	Gangrenous tissue > half foot
2	Gangrenous tissue < half foot, with lower limb muscle necrosis
3	Gangrenous tissue < half foot, without lower limb muscle necrosis
4	Pale foot or gait abnormalities
5	Normal
Modified Ischaemia	
0	Auto-amputation of leg
1	Leg necrosis
2	Foot necrosis
3	Discolouration of > 2 toes
4	Discolouration of 1 toe
5	Discolouration of >2 nails
6	Discolouration of 1 nail
7	No necrosis

Table 2.5: Basso scale for mouse locomotion

Functional assessment score sheet, modified from [286]

Score	Description
0	No movement in affected limb
1	Slight movement in affected limb
2	Extensive movement in affected limb
3	Plantar placing of the paw with or without weight support –OR– Occasional, frequent or consistent dorsal stepping but no plantar stepping
4	Occasional plantar stepping
5	Frequent or consistent plantar stepping, no coordination
6	Frequent or consistent plantar stepping, some coordination
7	Coordinated plantar stepping (normal)

2.6.5 Sample collection and preparation

2.6.5.1 Post mortem samples

Following whole blood collection, animals were sacrificed by cervical dislocation. 0.3 x 0.3 x 0.3 cm samples of gastrocnemius and tibialis anterior muscles from both right and left hindlimbs was placed in RNAlater™ RNA stabilisation reagent (Ambion, Austin, Tx) and stored according to manufacturer's guidelines for later RNA quantitation. The remaining muscle samples as well as whole heart, lungs, liver and kidney organs were immersed in 10% formal saline containing 4% formaldehyde (CellPath, UK) for histological processing.

2.6.5.2 Histological analysis

As detailed above, formalin-fixed tissues were processed and dehydrated overnight before being embedded in molten paraffin to generate FFPE samples. Sections were cut and mounted on polylysine slides for histological analysis.

Haematoxylin and Eosin stain

H&E was performed on sections from all animals, to ensure correct orientation. The H&E stain is also an excellent stain to display tissue architecture, and demonstrate any areas of muscle regeneration, denervation, necrosis or provide evidence of inflammatory infiltrate – all characteristic features of muscle afflicted with chronic periods of ischaemia. Representative high-powered images, encompassing 3 fields of view per muscle group were taken using Axioscop-2 (Carl Zeiss, Germany), with the observer blinded to the origin of the animal. Following image acquisition, 5 blinded observers were used to score all sections focusing on typical features of muscle pathology previously mentioned. A scoring system based on a standard operating procedure for quantifying skeletal muscle pathology, developed by the neuromuscular diseases network, was created [288] to delineate stages of muscle injury. Representative scoring images can be seen below, along with their associated score, based upon different stages of muscle damage and repair or regeneration (figure 2.2). Normal, or undamaged muscle fibers scored 0. At the other end of the muscle injury spectrum, muscle which showed large areas that had undergone fibro-adipocytic changes, as well as large areas of non-muscle tissue were given a score of 5. A score of 1 was awarded if muscle showed signs of inflammatory infiltrate, with minimal disruption to tissue ultrastructure. A score of 2 corresponded to necrotic myofibres,

showing dense inflammatory infiltrate and, or, variation in muscle fibre size due to hypercontracted and degenerating muscle fibres. A score of 3 corresponded to recently regenerated muscle fibres, as evidenced by small myofibres with centrally located nuclei. Larger diameter fibres with central nuclei was evidence of a regenerated myofibres, which attained a score of 4.

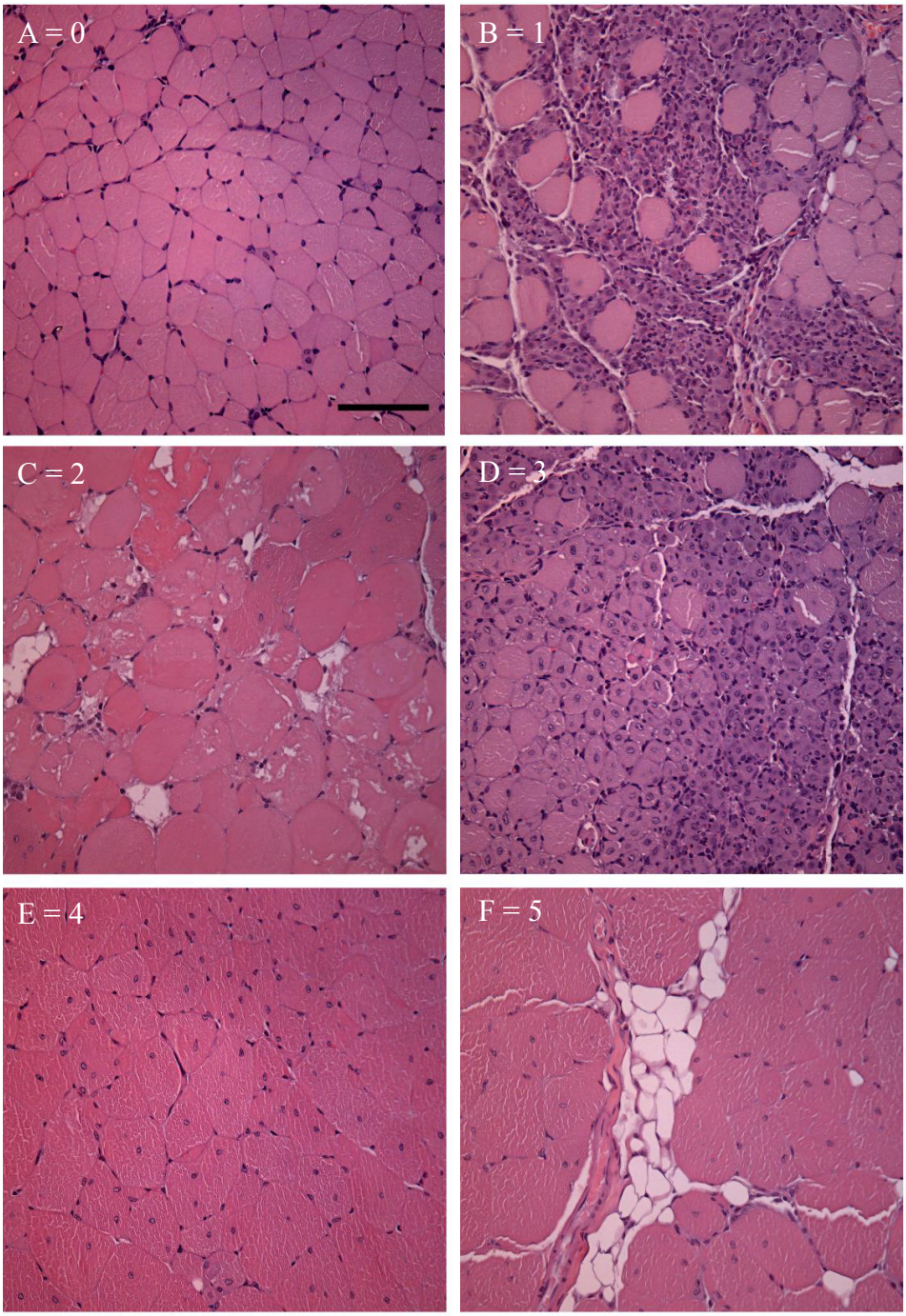

Figure 2.2: Histological features of mouse skeletal muscle pathology stained with haematoxylin and eosin, copied from [288]

Representative images of muscle injury seen following H&E staining of muscle sections. A: Normal myofibres characterised by peripheral nuclei, intact sarcoplasm and regular shape are mainly visible. B: Early inflammation and necrotic myofibres can be seen with severe inflammatory infiltration. There is also loss of sarcoplasm and variation in fibre size. C: Degenerating, necrotic myofibres characterised by a fragmented sarcoplasm, myofibres with irregular shape and few peripheral myonuclei. D: Recent regeneration characterised by many small-diameter myofibres with central nuclei. E: Regenerated myofibres, indicated by larger-diameter myofibres which have retained their central nuclei. F: Fat deposition in injured muscle, between myofibres in the interstitial space is common and can also include fibrotic changes (not shown).

Immunohistochemical analysis to determine the degree of proliferation using the marker Ki-67 was performed. In addition assessment of capillary : fibre (C:F) ratio was performed using CD34 staining. CD34 is commonly utilised as a haematopoietic and endothelial cell surface marker, however it is also capable of identifying both activated and quiescent satellite cells in mice, but not human, tissue [289, 290]. Details of immunohistochemistry methods can be found in chapter 2.2.1.

2.7 Data analyses

2.7.1 Power calculation

Selection of sample sizes was based on calculations performed using preliminary data from validation and optimisation experiments and from published data to provide a 90% power of detecting a difference between the groups at the 5% significance level. This was based on the formula:

$$N \text{ per group} = 2 \times (Z_{\alpha/z} + Z_{\beta})^2 \times \sigma^2/\delta^2$$

Where: δ = difference in mean values

σ = standard deviation of values in either group

α = probability of Type I error occurring = 0.05

β = probability of Type II error occurring = 0.10 (power of 90%)

$Z_{\alpha/z} = 1.96$

$Z_{\beta} = 1.28$

Based on mean values and SD of preliminary EPO and ARA-290 efficacy studies in the literature, required sample sizes were estimated to be approximately 12 patients per group for human tissue analysis, 5 samples per group for human *in vitro* analyses and 6 animals per group for *in vivo* validation.

Further considerations were made based on unit case-load, the time period required to collect adequate samples and the time and costs of laboratory analyses.

2.7.2 Statistical analyses

Statistical analyses were performed using GraphPad Prism version 6.0 for Mac (GraphPad Software). Single comparisons between two groups were analysed using two-tailed Mann-Whitney test for non-parametric unpaired data. Ordinary one-way ANOVA test was used for comparisons between multiple independent groups, followed by Tukey's multiple comparison test. A p-value < 0.05 was considered statistically significant.

CHAPTER 3

Tissue protective receptor in CLI

3.1 Introduction

The ability of EPO to prevent apoptosis is key to its function as a haematopoietic hormone. Endogenous EPO production is mediated by signals of low or impaired oxygen delivery to tissues. Multiple causes of low oxygen tension exist, including anaemia and hypoxemia. This hypoxic stimulates upregulates gene transcription of EPO, mainly in the kidneys – the primary site for EPO production in adults. The main action of EPO is upon erythrocyte-colony forming units (CFU-E) contained within the bone marrow. Once EPO reaches target EPO receptors on CFU-E, it is able to prevent apoptosis of the immature cells, allowing them to mature into reticulocytes and enter the circulation, maturing further into erythrocytes, increasing the circulating pools of erythrocytes and ultimately improve tissue oxygenation.

This anti-apoptotic effect of EPO is what has propagated the belief that EPO could play a pivotal role in mediating cytoprotection in other tissues. Its potential tissue-protective actions have previously been investigated in organs including the brain, heart and kidneys, all of which have also exhibited EPOR expression. Other tissues that have demonstrated EPOR expression include testes and skeletal muscle.

More recently EPO-derivatives have also been created with the specific intention of retaining only those tissue-protective effects of EPO and not its haematopoietic effects, which can lead to thrombotic side effects. The advent of novel EPO-derivatives was deemed possible for numerous reasons, including structural analysis that demonstrated discrete portions of the EPO molecule binding with the EPO receptor homodimer to promote erythrocyte maturation. Additionally, the capacity EPO possesses to provide tissue-protective effects are thought to be mediated via a heterodimer receptor composed of the EPOR in complex with a βcR, and EPO-derivatives preserve the ability to bind with the EPOR / βcR tissue protective receptor complex.

Little published data exists describing the presence of the EPOR or the βcR in human skeletal muscle in detail. Previous reports have described the presence of both receptors in human skeletal muscle, but not investigated their functionality [169, 291]. In this chapter the presence of the EPOR / βcR tissue protective receptor in human skeletal muscle has been explored. Recently, some controversy has arisen over the validity of previously published data with regards to EPOR expression in non-haematopoietic tissue. Much of this debate has stemmed from the proposed lack of specificity of numerous commercially available EPOR antibodies [292].

Skeletal muscle has an intrinsic ability to repair and regenerate itself in response to biological, chemical or mechanical injury. This regenerative potential is largely fulfilled by satellite cells – small mononuclear cells, identified by their characteristic location between the basal lamina and sarcolemma of skeletal muscle fibres. Often referred to as the principal skeletal muscle stem cell, mitotically quiescent satellite cells are activated in response to injury stimuli, resulting in increased proliferation. The new pool of satellite cell progeny giving rise to a significant increase in proliferation will merge with existing myofibres and help to repair or regenerate injured myofibres either by fusing with existing myofibres, one another or replenishing the satellite cell population [293, 294].

Satellite cells in early studies were identified by observation under electron microscope, on the basis of their location. Reliable markers of satellite cells have since been identified, but practical difficulties have arisen, mainly due to the dynamic state of markers in quiescent and subsequently activated cells, as well as significant differences in the presence of several markers between humans and animals, mainly mice, in which much of the current knowledge regarding satellite cells and their markers has ben performed. Examples of specific molecular markers of satellite cells for both humans and mice include Pax7 and M-cadherin [295]. In addition, other commonly used markers in mice include syndecan 4, CD34 and Myf5 [295-297]. In CLI there is evidence of increased numbers of satellite cells and attempts at muscle repair [298].

3.2 Aims

The aims of this chapter were therefore to demonstrate the existence of both the EPOR and βcR and further to determine a functional role of the tissue-protective receptor by identifying its potential to co-localise and interact physically within human skeletal muscle.

3.3 Methods

Written informed consent was obtained from all patients prior to enrolment in this study. Muscle biopsies from CLI patients undergoing lower limb amputation and control patients requiring saphenous vein harvest for CABG were collected for the purposes of this work. Clinical and demographic data on all donors was also collected at the time of biopsy harvest. Subsequent analysis on clinical indicators and patient demographics was performed.

Western blot analysis was performed to detect the presence of the tissue protective heteroreceptor, EPOR and βcR, and to determine differential expression of Pax7 in human skeletal muscle homogenates from CLI and control biopsies. The techniques of muscle homogenisation and Western blot analysis have previously been described in chapter 2.2.3. Protein expression of EPOR in skeletal muscle homogenates was assessed using two commercially available EPOR antibodies.

Immunohistochemistry was performed on human skeletal muscle sections to assess the localisation of EPOR and βcR within skeletal muscle. Subsequent co-localisation of the two receptors was established using immunohistochemistry and immunofluorescence. Expression of the satellite cell marker Pax7 was also assessed on human skeletal muscle sections. A detailed protocol of immunohistochemistry techniques, including double staining, can be found in chapter 2.2. Double immunofluorescence labelling for EPOR and βcR required the use of Zenon Rabbit IgG Labelling kit (Invitrogen, UK) as per manufacturer's protocol. Briefly, 1μg of each antibody was mixed with 5μl of desired Zenon labelling reagent for 5 minutes at room temperature. 5μl of Zenon blocking reagent was added into the mixture and the complete solution incubated for a further 5 minutes at room temperature. The

antibody-fluorescent probe complex was then applied to FFPE human skeletal muscle sections that were dewaxed, prepared using 10mM citrate buffer (pH 6.0) antigen retrieval, and blocked in 0.2% BSA and 5% goat serum in PBS for 30 minutes at room temperature. The antibody-fluorescent probe complex was applied to sections for 1 hour at room temperature followed by three 5-minute washes. A second fixation of the tissue sections was performed using 4% formaldehyde in PBS for 10 minutes at room temperature followed by two 5-minute PBS washes before counterstaining and mounting in mounting medium with DAPI.

3.3.1 Co-immunoprecipitation

To directly assess heterodimerisation of the EPOR and βcR, co-immunoprecipitation and subsequent Western blot analysis was performed. Immunoprecipitation is designed to enrich a protein within a complex mixture (as you would find in a whole tissue homogenate). Co-immunoprecipitation, should, if a physical interaction is present, enrich both proteins of interest. To determine the physical interaction between the EPOR and the βcR co-immunoprecipitation (Co-IP) was performed on snap frozen muscle biopsies. Briefly, 20mg of muscle tissue was placed in a 2ml round-bottomed microcentrifuge tube with 600µl of IP lysis/wash buffer (150mM NaCl, 1% Triton X-100, 10mM Tris pH7.4, 1mM EDTA, 1mM EGTA pH8.0, 1x Complete mini EDTA-free protease inhibitor (Roche), 1% phosphatase-inhibitor cocktail 2 and 3 (Sigma-Aldrich)). The muscle was homogenised using a 5mm stainless steel bead with TissueLyser (both, QIAGEN GmbH, Hilden, Germany) for 2 x 2 minutes at 30 Hz. The steel bead was removed, and samples centrifuged at 13,000 rpm for 15 minutes at 4°C. The supernatant was removed and applied to the pre-clearing antibody-Sepharose bead complex, prepared below.

Antibody-bead preparation

The antibodies of interest were each cross-linked to the protein A-Sepharose beads (Sigma-Aldrich, UK) and in addition a pre-clearing antibody-Sepharose bead complex was also prepared. For the purposes of pre-clearing samples, an anti-collagen IV antibody was used each time. All antibodies were mixed in a 1:10 ratio with Sepharose beads that were pre-washed using lysis buffer. Antibody-bead complexes were incubated for 1 hour with constant rotation at 4°C and then washed

in equal volumes of IP wash buffer, before centrifuging to pellet the antibody-bead complex, and repeating the wash step twice more.

Cross-linking of the anti-βcR and anti-EPOR antibodies to Sepharose beads was performed using 20mM dimethyl pimelimidate (DMP) in 0.2M sodium borate (pH 9.0) in a 1:1 ratio with the pre-mixed antibody-bead complexes. The antibody-bead complex was returned to constant rotation at 4°C for 1 hour, before the cross-linking reaction was quenched using 1ml of 0.2M ethanolamine (pH 8.0). The cross-linked antibody-bead complex was centrifuged and the supernatant removed. To ensure all residual DMP was neutralised, a further 1 ml of 0.2M ethanolamine (pH 8.0) was added before the cross-linked antibody-bead complex was washed 3 times, as described above with IP wash buffer.

Pre-clearing samples

Following preparation of the pre-clearing antibody-Sepharose bead complex, the supernatant from tissue homogenisation was applied and the whole sample incubated at 4°C with rotation for 1 hour. The sample was centrifuged, and the supernatant removed with care taken not to aspirate any of the bead pellet. The supernatant was then divided in two, and applied to either the anti-βcR or anti-EPOR Sepharose bead cross-linked pellet. Samples were incubated at 4°C with constant rotation for 1 hour. Each sample was then divided in two in order to be washed with IP wash buffer of either 150mM (low stringency) or 500mM (high stringency) NaCl concentration. 5 washes in total were performed, before samples were resuspended in LDS-sample buffer, heated at 95°C for 5 minutes, centrifuged to pellet the beads, and the supernatant used for SDS-PAGE Western blot analysis to confirm the presence of the receptor that was immunoprecipitated, as well as the presence of the co-immunoprecipitated protein.

3.4 Results

Table 3.1 shows analysis of clinical and demographic data from all CLI and control donors. Analysis revealed no significant difference in the prevalence of all major risk factors for PAD between the two sample groups. There was also no significant difference in age or cardiovascular risk factor treatment between the two groups. 3 patients in total were receiving ESA therapy, however these samples were only used for tissue analysis, and not isolation of human myoblasts.

ABPI was the only clinical indicator in which there was a significant difference ($P<0.0002$, Mann-Whitney test, n=17 CLI, n=15 control group) between CLI and control patients.

Table 3.1: Clinical and demographic summary of study participants

	CLI	Control
Age	73 ± 18.5	62 ± 10.5
Male:Female	11:6	11:4
ABPI	0.2925 ± 0.1929	0.9974 ± 0.0656
Diabetes Mellitus	6	5
Ischaemic Heart Disease	13	15
Hypertension	15	11
Smoking History	12	10
Aspirin Therapy	11	9
Statin Therapy	13	13
ESA Therapy	2	1

CLI: Critical limb ischaemia, ABPI: ankle-brachial pressure index, ESA: erythropoiesis stimulating agent.

3.4.1 Expression of the tissue protective receptor in human skeletal muscle

3.4.1.1 Multiple EPOR antibodies can detect EPOR expression

Using the same CLI and control sample muscle homogenates two different EPOR antibodies, produced commercially from two separate companies were compared. Both antibodies were capable of detecting a protein band at approximately 60 kDa, and showed a similar pattern of protein expression between identical Western blots performed with CLI and control samples (figure 3.1).

Muscle homogenates from all CLI and control patient samples were used to demonstrate the expression of both components of the tissue protective heteroreceptor complex. Western blot analysis of CLI and control samples revealed a distinct increase in expression of the EPOR and βcR (figure 3.2A). Densitometric analysis of the detected protein bands showed expression of both receptors to be significantly upregulated in CLI muscle samples in comparison to controls (CLI: n=17, Control: n=15; $P<0.001$) (figure 3.2B).

Using RNA isolated from 12 of the patients, qRT-PCR analysis for the βcR and EPOR genes showed significantly upregulated gene activity in CLI samples, correlating with the observed increase in protein expression (CLI: n=6, Control: n=6; βcR: $P<0.030$; EPOR: $P<0.0173$). Figure 3.3 A and B show the normalised gene expression levels in whole muscle RNA from CLI and control samples.

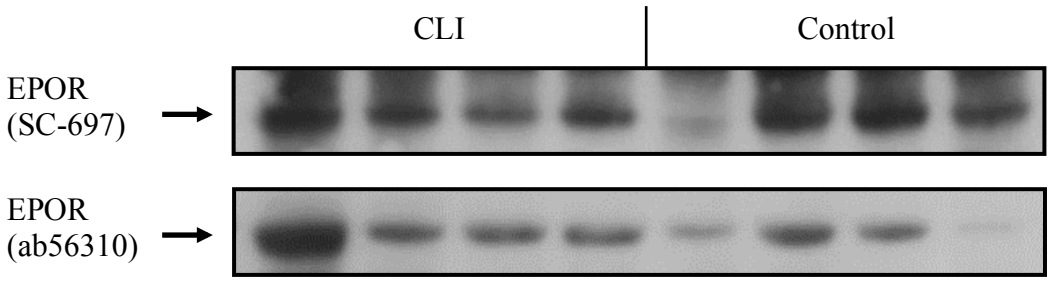

Figure 3.1: Expression of EPOR using 2 antibodies

Western blot analysis was performed to compare two commercially available anti-EPOR antibodies. Both antibodies demonstrated similar expression profiles of identical CLI and control samples.

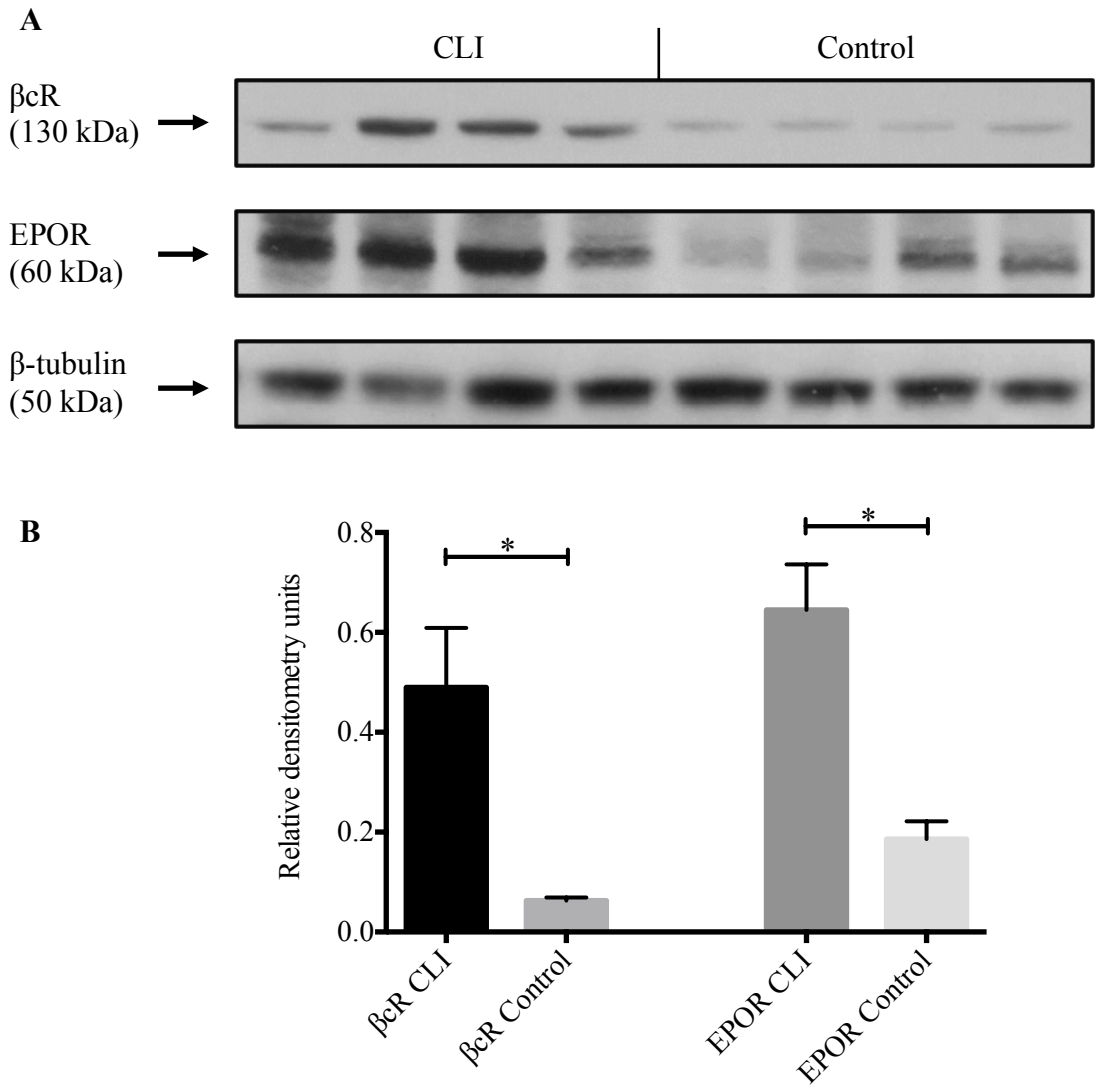

Figure 3.2: Expression of βcR and EPOR in human muscle lysate

*A: A representative Western blot of human skeletal muscle from CLI and control samples demonstrated increased expression of both βcR and EPOR (both antibodies from Abcam) in CLI muscle. B: This was confirmed using densitometric analysis of all Western blots performed on all CLI (n=17) and control (n=15) samples, which concluded an increase in expression of both receptors in CLI muscle (*P<0.001, Mann-Whitney test). Data are expressed as mean ± SEM.*

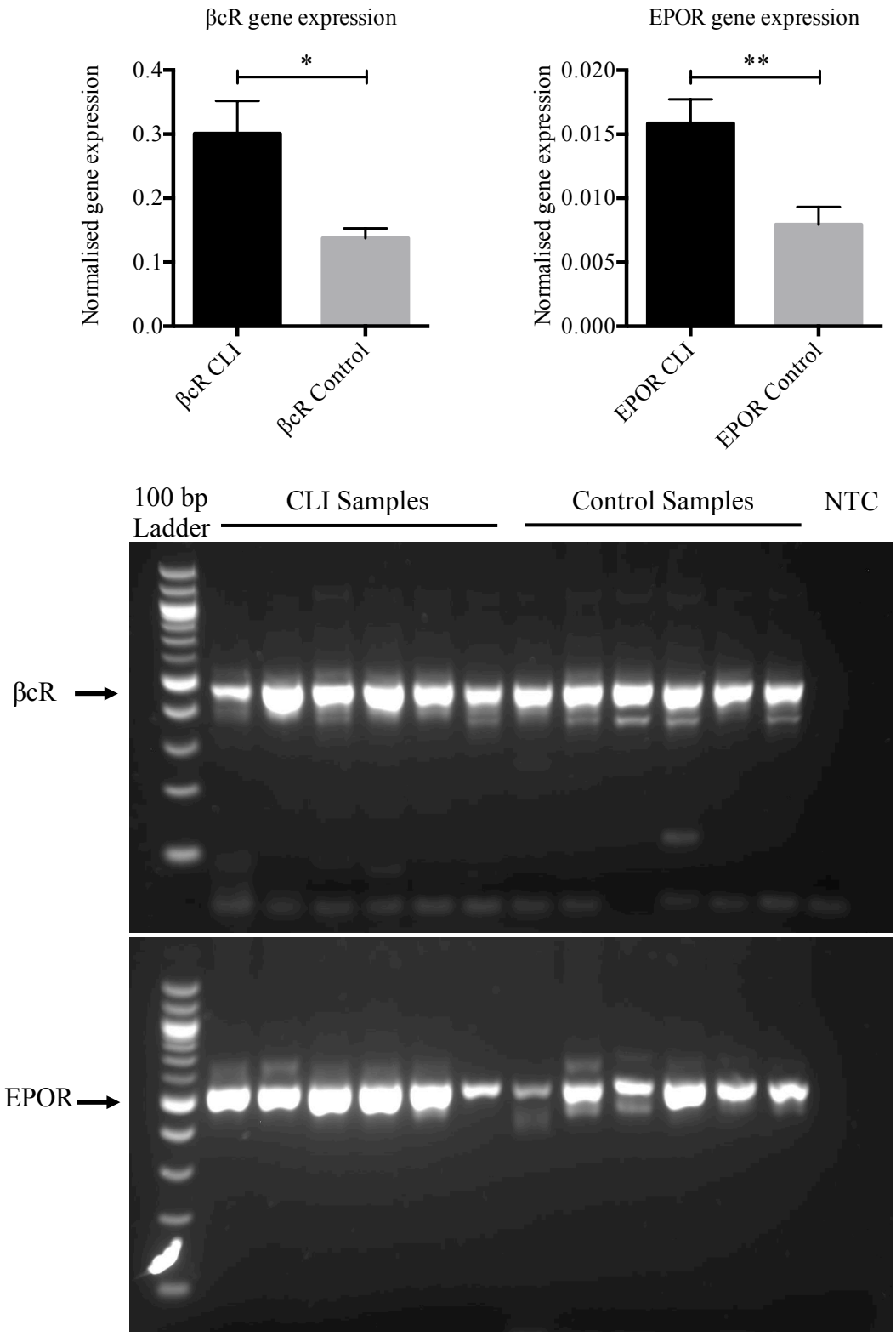

Figure 3.3: βcR and EPOR gene expression in human skeletal muscle

*Differences in βcR and EPOR between CLI and control muscle shows a marked increase in gene expression in CLI muscle samples. (*P<0.05; **P<0.01, both Mann-Whitney test, n=6 both CLI and control groups). Data are expressed as mean ± SEM. NTC: non-template control.*

3.4.2 Interaction of the EPOR and βcR in human skeletal muscle

Following co-immunoprecipitation of our sample with an antibody for each protein of interest, subsequent Western blot analysis demonstrated that the βcR co-precipitated when anti-EPOR antibody was used to immunoprecipitate proteins of interest from a muscle lysate sample. The same finding was observed when a sample was immunoprecipitated for using an anti-βcR antibody, where it was subsequently possible to detect the co-precipitated EPOR (figure 3.4).

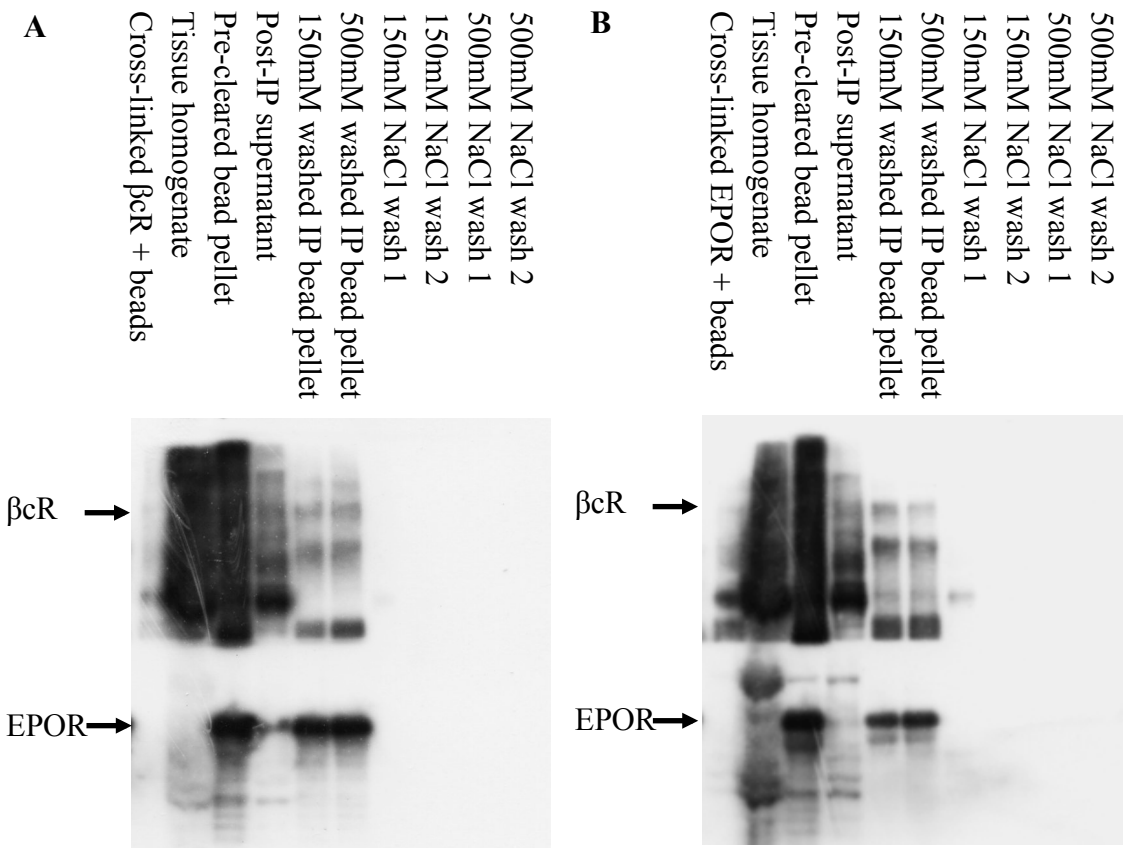

Figure 3.4: Co-immunoprecipitation of βcR and EPOR in human skeletal muscle

A: Co-immunoprecipitation using an anti-βcR antibody to perform immunoprecipitation pull-down. B: Co-immunoprecipitation performed using anti-EPOR antibody to pull-down. Subsequent Western blot analysis for both βcR and EPOR demonstrated the co-immunoprecipitation of both receptors in each sample.

3.4.3 Distribution of the tissue protective receptor

To explore the location of both βcR and EPOR within muscle sections immunostaining was performed. Figure 3.5A shows representative immunostaining of the βcR: a markedly diffuse distribution of staining throughout the cytoplasm of muscle fibres. In comparison, in figure 3.5B, representative immunostaining for the EPOR showed more discrete staining, mainly localised to the periphery of fibres. Double-staining for both βcR and EPOR (both antibodies from Abcam) using the chromagen alkaline phosphatase to stain for the βcR and DAB to display the EPOR, identified areas where the two receptors co-localise with one another (figure 3.5C). An IgG Isotype control for both antibodies was also prepared (figure 3.5D).

Co-localisation of the two receptors in human skeletal muscle sections was more clearly demonstrated using direct immunofluorescence for βcR and EPOR (both antibodies from Santa Cruz Biotechnology). The presence of both receptors co-localising in CLI and control human skeletal muscle was demonstrated. Co-localisation of the two receptors was mainly limited to the muscle fibre membrane (figure 3.6).

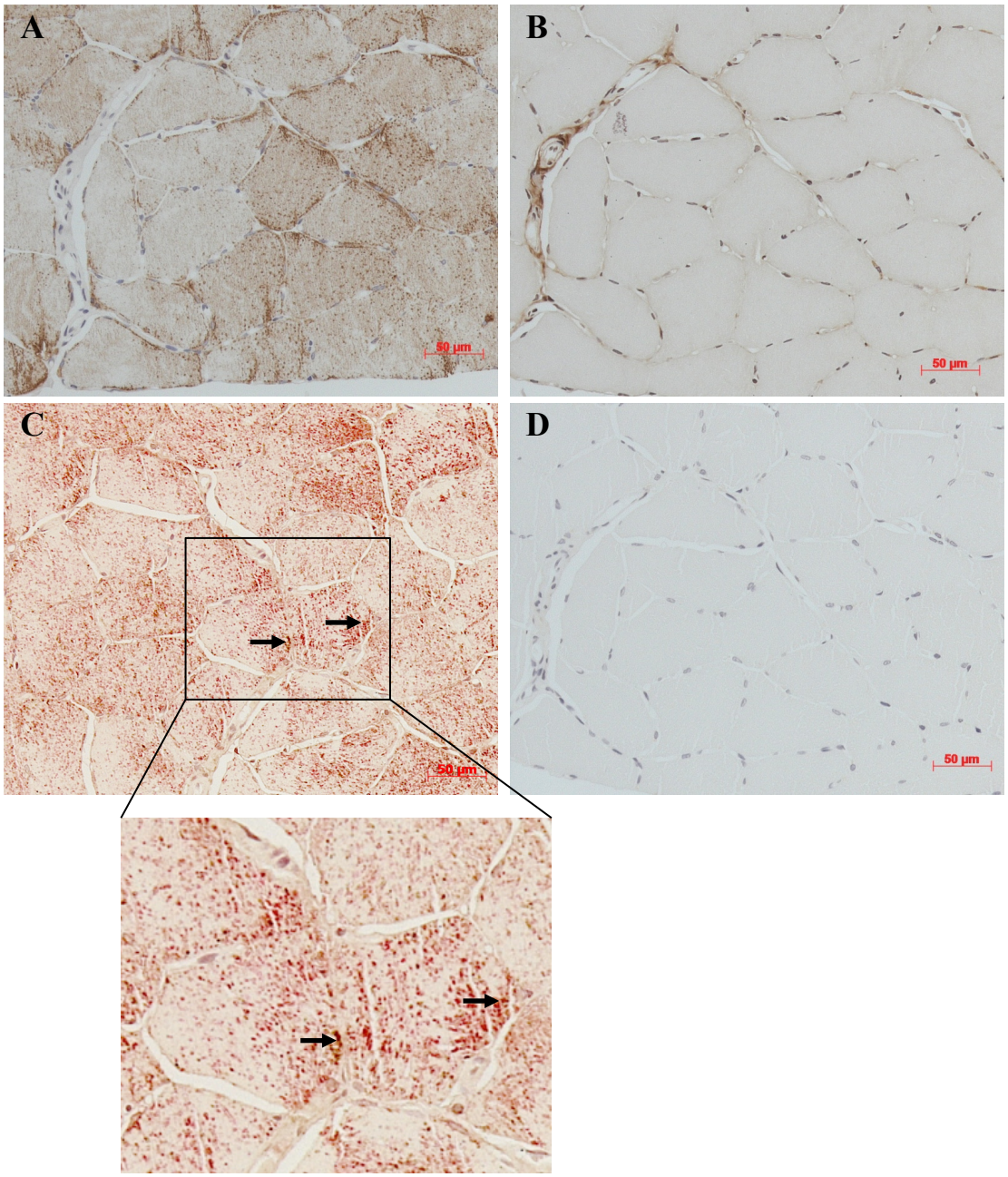

Figure 3.5: Tissue-protective heteroreceptor expression in human skeletal muscle

A: βcR can be found distributed quite ubiquitously throughout the muscle fibre, but greater membrane staining. B: EPOR expression is located discretely around the membrane of muscle fibres. C: Double-staining for the presence of both βcR (alkaline phosphatase, red) and EPOR (DAB, brown) shows co-localisation (black arrows) of the two receptors in human muscle sections. D: IgG isotype (rabbit and mouse) control. Scale bar = 50µm.

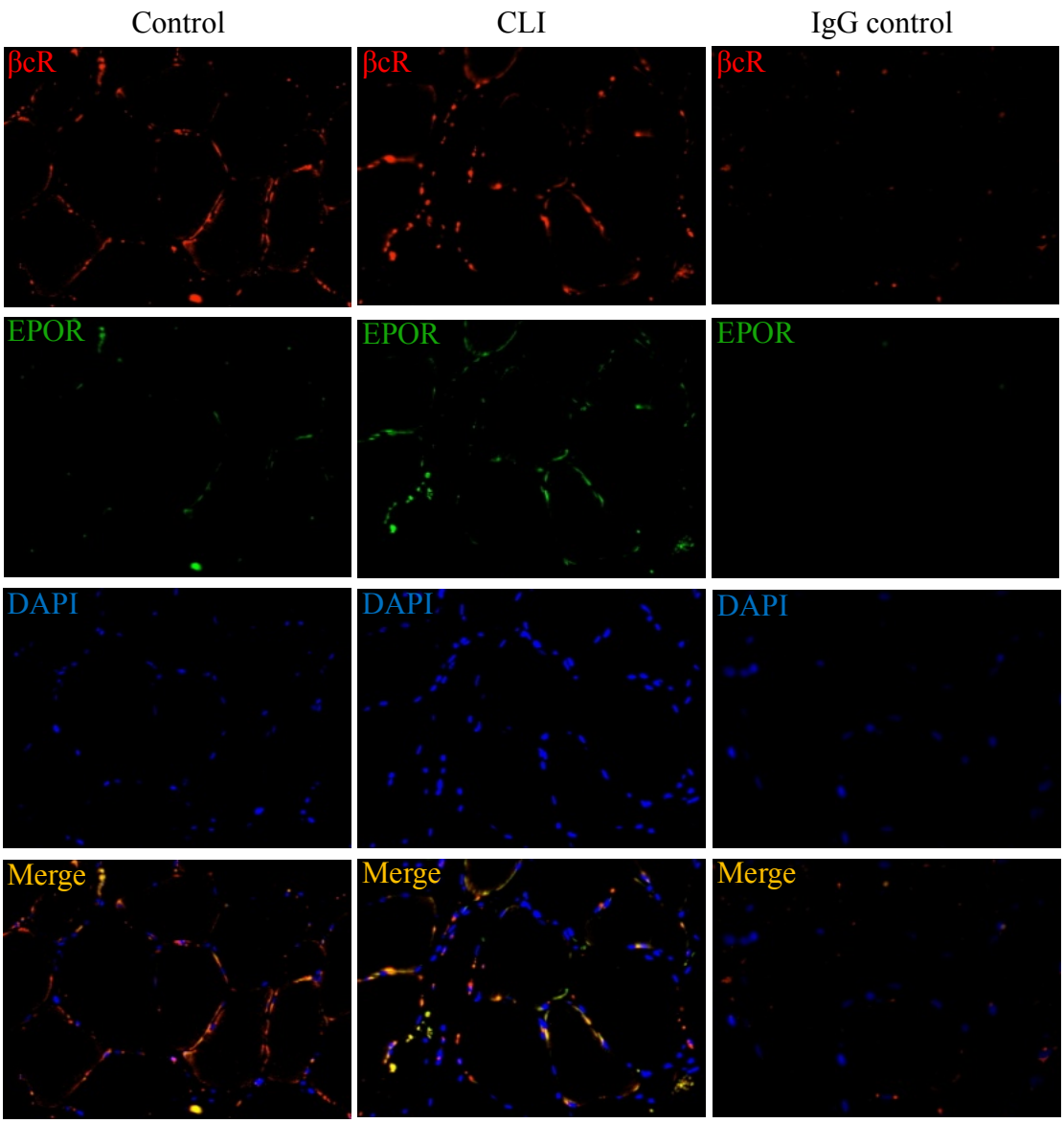

Figure 3.6: Immunofluorescence co-localisation of βcR and EPOR in human skeletal muscle

Double staining for the presence of βcR (red) and EPOR (green) shows co-localisation of the two receptors (orange) in human muscle sections of CLI and control samples. An IgG isotype control (rabbit) was also included.

3.4.4 Regenerative potential of human skeletal muscle in CLI

Western blot analysis of human skeletal muscle lysates for the satellite cell marker Pax7 demonstrated significantly increased expression of Pax7 in CLI samples (lanes 1 – 5) compared to controls ($P<0.05$, Mann-Whitney test, n=5 both CLI and control) (figure 3.7A).

Immunostaining of human skeletal muscle sections identified Pax7 positive nuclei in both CLI and control muscle sections. However, in concordance with Western blot results, CLI muscle sections had a greater number of Pax7 positive nuclei per field of view, compared to control muscle (figure 3.7B). The number of positive nuclei observed in CLI muscle was approximately 3 times greater than that observed in control samples – CLI mean=18.29, control mean=6.11, n=5 per group. The proportion of Pax7 positive nuclei observed within control sections was comparable to the 2–7% reported in the literature [299]. An IgG isotype and non-muscle tissue (tonsil) control was also included to ensure specificity of the anti-Pax7 antibody.

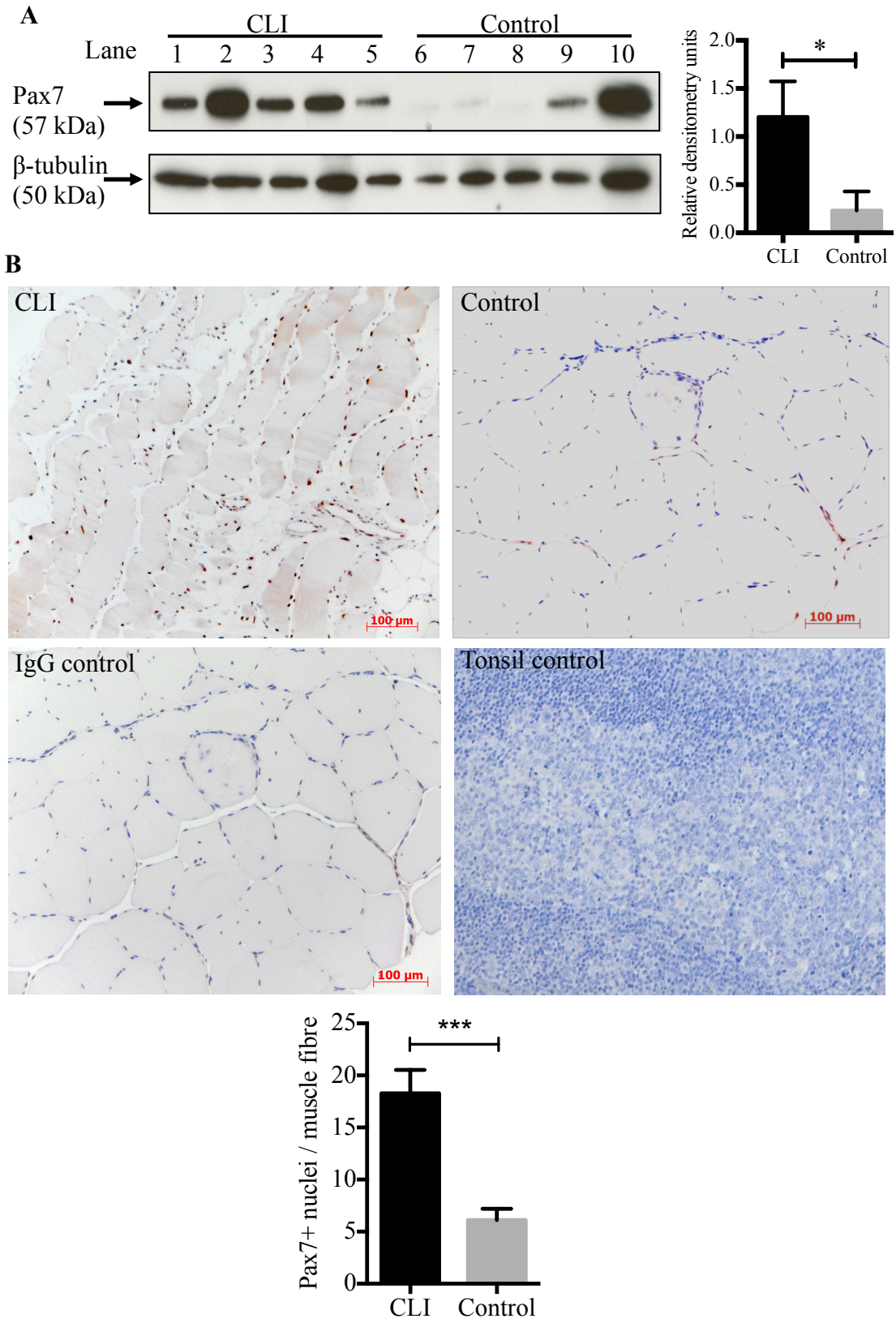

Figure 3.7: Myogenic potential in human skeletal muscle

A: Human skeletal muscle homogenates were assessed using Western blot analysis for the satellite cell marker Pax7. CLI muscle samples (lanes 1–5) demonstrated

*approximately 5-fold greater expression of Pax7 compared to control muscle samples (lanes 6–10; *P<0.05, Mann-Whitney test, n=5 both CLI and control groups). B: Immunohistochemistry performed on skeletal muscle sections from CLI and control samples demonstrated increased expression of Pax7 positive nuclei in CLI muscle sections compared to control. Quantification of the number of Pax7-positive nuclei per muscle fibre demonstrated approximately 3-fold greater numbers of Pax7 positive nuclei in CLI muscle samples (***P<0.0003, Mann-Whitney test n=5 both CLI and control groups). An IgG Isotype specific and non-muscle tissue control were used to ensure specificity of the anti-Pax7 antibody. Scale bar = 100μm*

3.5 Discussion

In this chapter, the presence of the tissue protective receptor, described in chapter 1, has been examined in more detail. Although EPOR expression has been demonstrated in various tissue types beyond erythrocyte precursors in the bone marrow, less literature exists describing its presence in human skeletal muscle. Those reports that do describe the presence of EPOR in muscle have utilised either murine cell lines (C2C12) [172] or skeletal muscle from healthy volunteer subjects [169-171]. Further, expression of the βcR within human skeletal has not been demonstrated previously.

Observation of the presence of the EPOR in human skeletal muscle is in keeping with work by other groups [169, 171]. Previous studies assessing the efficacy of EPO in a setting of ischaemic stroke has demonstrated the presence of EPOR and an upregulation in receptor expression following ischaemic insult, in both pre-clinical, animal models, as well as in human study subjects [300-302]. A similar pattern of expression was observed in our CLI muscle samples when compared to control samples, when gene expression levels were assessed. Whilst there is likely to be a multitude of factors interplaying to result in the increased presence of EPOR observed, one possibility is the hypoxic environment found in CLI muscle initiates HIFs which then respond by upregulating various genes and signalling cascades designed to counteract the hypoxic stimulus, including increasing EPOR expression – similar to the scenario with red blood cells. Another possible explanation for the upregulation of EPOR observed is the role of the innate immune system and its response to pathogen invasion – a common cause of prolonged colonisation of ischaemic ulcers and or gangrene often seen in CLI patients. In order to prevent spread of an infection, the innate immune response is initiated and employs pro-inflammatory cytokines of the type I superfamily to isolate and remove any pathogens. Members of the pro-inflammatory cytokine superfamily include TNF-α, one of a number of genes responsible for the upregulation of EPOR expression in the innate immune response [303]. The roles of the EPOR and TNF-α are antagonistic to one another. Upregulation of EPOR expression is required to regulate the extent of the response mounted by the pro-inflammatory arm by salvaging cells from pro-inflammatory cytokine-induced cell death. This mechanism is designed to ensure

excessive collateral damage is prevented. Therefore the presence of infection and inflammatory stimuli could be another additional reason for the increase in EPOR expression observed in CLI muscle.

Indeed, the importance of the EPOR in embryonic development as well as in mediating tissue-protection has already been investigated, and been shown to play a pivotal role in both of these areas. Firstly, EPOR knockout mice die at around embryonic day 13.5, due mainly to the failure of erythropoiesis, but additionally due to ventricular hypoplasia that is also observed between embryonic day 12-13, likely as a consequence of the general hypoxic state [304]. In addition, the fundamental role of EPOR in mediating tissue-protection has also been demonstrated in models of ischaemic stroke. In these models, upregulation of the EPOR as well as endogenously produced EPO has been observed, and shown to reduce infarct size as a consequence. However addition of a soluble EPOR abolishes this reduction in infarct size by competing for available EPO-ligand leading to greater infarct volume and worse behavioural outcomes [305, 306]. The same outcome can also be observed when an EPOR conditional knockout strain is used, and knockout of EPOR is introduced after initiation of stroke [307].

The presence and distribution of the βcR in human skeletal muscle was also revealed. Due to its nature as a multi-faceted, common receptor subunit, it is not surprising that it was present in skeletal muscle. However, the effect of ischaemia on its expression has not been previously described. The results proceeded to show elevated expression of the βcR in human CLI muscle. Following a similar pattern of expression as the EPOR gene, RNA analysis of muscle isolates for expression of the βcR gene mirrored the increased expression seen in CLI samples. This result was consistently seen on gene as well as protein analysis in all samples analysed. Previous examples of hypoxia inducing expression of the βcR have not been described, and within the current literature, stimuli of βcR mainly revolves around pro-inflammatory cytokines – IFN-α and TNF [308, 309]. Considering the role of IL-3, IL-5 and GM-CSF in regulating key players of the haematopoietic system, including eosinophils, basophils, monocytes and macrophages, it is not surprising that inflammatory cytokines are capable of mediating their upregulation, in order to more effectively mount and maintain an immune response. A proposed mechanism for

upregulation of the βcR in human CLI muscle could be the possibility of increased infection in patients with CLI, as also described for the increase in EPOR.

Although reports exist in the literature with regards to specificity of certain commercially available antibodies, by comparing two antibodies – one from Santa Cruz biotechnology, previously queried in the publication by Elliot *et al* [292] – and a second antibody produced by Abcam Ltd, we were able to detect very similar results with both antibodies on Western blot analysis. Both antibodies detected increased expression of the EPOR in CLI samples. The comparable nature of results yielded may not be true for immunohistochemistry where this antibody was not trialled. The use of this antibody for co-localisation of the EPOR with expression of the βcR by immunofluorescence yielded discrete, membranous staining, comparable to the expression of EPOR demonstrated by the Abcam EPOR antibody on immunohistochemistry. Close examination of the publication by Elliot *et al* clearly reveals that the anti-EPOR (C-20) antibody is capable of specifically detecting EPOR expression in cell lines known to positively express EPOR by Western blot analysis, and queries only the specificity of the antibody for immunohistochemical techniques. Using direct immunofluorescence, co-localisation of the two receptors was revealed in both CLI and control samples more clearly than with immunohistochemistry.

Association, or co-localisation of the two receptors has previously been demonstrated in spinal cord neurons and cardiomyocytes only [228]. Demonstrating this putative tissue protective receptor complex co-localising and physically interacting in human skeletal muscle gives credence to the idea of EPO mediating tissue protection via a novel receptor isoform, distinct from the EPOR homodimer required for haematopoiesis. In addition, it encourages the future development of therapeutic EPO and EPO-derivatives and their use in a setting of tissue-protection following ischaemic injury.

The findings of this study provide a greater platform of evidence into the role of tissue-protective signalling via the βcR and EPOR in ischaemia. It complements previous reports describing the presence and co-localisation of these receptors and by demonstrating the heteroreceptor complex, as well as its upregulation in ischaemic tissue, it suggests a key role for tissue-protection.

The behaviour and response of myogenic precursors following chronic ischaemic muscle injury is poorly understood. The observed increase in satellite cells in CLI muscle suggests an attempt at repair and regeneration in response to ischaemic muscle injury, as would be expected following muscle injury or damage in the normal physiological setting. However this does not appear to translate into a clinical benefit for CLI patients, who have indubitable muscle atrophy and weakness. The 3-fold increase in Pax7 positive nuclei may, in part, be explained by another well-recognised phenomenon that contemporaneously exists in CLI muscle. There is an acknowledged histomorphological change in muscle fibres, with a shift towards the more oxidative, type 1-muscle fibres [114-116]. In addition there have been several reports published identifying a difference in the proportion of satellite cells in relation to type 1 and 2 muscle fibres, with type 1 muscle fibres demonstrating between 4-5 fold greater numbers of associated satellite cells [310-314]. Taken in conjunction, the alteration in proportion of type 1-muscle fibres may provide a partial explanation for the increased number of satellite cells demonstrated in CLI muscle. The presence of Pax7 positive nuclei in association with blood vessels may be explained by their common embryological origin, which forms the foundation of much work looking into the ability of blood vessels and other tissues to provide myogenic cells for muscle regeneration [310]. However, it has not yet been demonstrated that endothelial-derived myogenic precursors are capable of becoming quiescent satellite cells, and opposing views suggest that satellite cells instead share a common origin with myoblasts [310, 315, 316].

Whilst it has not been demonstrated that there is a subsequent increased regenerative drive in patients with CLI, these results do suggest that the normal downstream processes of myogenic commitment, differentiation into myoblasts and fusion with existing myofibres to allow terminal differentiation are more susceptible to ischaemic injury, causing deviations from the physiological muscle repair pathway, rather than a lack of contribution from satellite cells in the first instance. The presence of satellite cells in patients with CLI may therefore provide suitable target to focus future therapies, aimed at improving muscle function to prevent the muscle atrophy frequently observed in CLI patients [109].

3.6 Summary

In conclusion, we have described the presence of the βcR and the EPOR in human skeletal muscle. We report a striking difference in expression of both receptors within human skeletal muscle, at both a protein, as well as transcriptional level between CLI and control muscle. It provides compelling evidence for the role of the EPOR and βcR in mediating a response to ischaemic injury. Thus we propose that the presence, and upregulation of the tissue-protective receptor could be utilised by EPO and EPO-derivatives to mediate tissue-protection as a therapeutic adjunct in an ischaemic setting.

CHAPTER 4
Effect of ARA-290 on C2C12 myoblasts and myotubes *in vitro*

4.1 Introduction

One of the most common and persistent progressive features in patients with PAD is a decline in functional independence and ability to perform activities of daily living due to pain and muscle weakness [114]. Often this is attributed to the lack of perfusion to the affected limb. However, in spite of successful revascularisation many patients will still describe significant functional deficit and morbidity at levels comparable to their pre-operative state [88-92]. The majority of studies assessing novel therapeutics in patients with CLI focus on the aspect of arterial insufficiency, and catalysing angiogenesis in an attempt to improve perfusion to the limb. Although this is likely to partially ameliorate those complications mentioned above, and improve viability of the limb, the effect on functional outcome and underlying detriment to skeletal muscle is less clear.

The musculopathy that exists in PAD has been detailed to involve multiple cellular ultrastructural components and their functioning. This includes changes in muscle fibre type, as well as aberrant mitochondrial function, neither of which demonstrated benefit following successful revascularisation. There is a growing body of evidence supporting the existence of underlying muscle pathology and dysfunction in patients with PAD, which should also be addressed in order to improve functional deficit in patients. Currently, supervised exercise-training programmes have led to improvement in patients' functional ability to an extent.

In vitro models provide a useful platform for the initial assessment of novel hypotheses and therapeutics. C2C12 skeletal-myoblast cells represent a heavily utilised, and therefore extensively characterised, mouse myoblast-derived cell line. They are often used in the study of muscle cell growth, differentiation and function due to similarities in character and behaviour to isolated human cells [317-320].

A novel *in vitro* model system for simulated ischaemia of C2C12 skeletal myotubes has previously been described. The simulated ischaemia model was capable of reproducing many of the physiological parameters known to be abnormal in ischaemic CLI muscle, including pH, partial pressure of oxygen and carbon dioxide [238]. Downstream consequences following simulated ischaemia include increased apoptosis, lactate dehydrogenase, IL-6 and TNF-α release.

EPO has previously demonstrated utility in numerous settings of ischaemic tissue injury, including models of ischaemic stroke and MI [305, 307]. Its protective role in ischaemia or trauma induced injury on skeletal muscle has also been reported [321-325]. In these scenarios, a combination of increased capillary perfusion and proliferation of satellite cells as well as reduced apoptosis of muscle fibres led to favourable results. In keeping with observations of EPO treatment in clinical scenarios, there was a dose-dependent effect over which increasing doses became detrimental. This was due to EPO-mediated side effects on haematocrit.

The development of EPO-derivatives that have removed the haematopoietic capabilities but retained tissue-protective functions has reignited an interest in the potential of EPO and EPO-derivatives to provide tissue-protection. ARA-290 has been assessed in several pre-clinical *in vitro* and *in vivo* models, for a number of conditions, including renal ischaemia, neuropathic pain, myocardial infarction and stroke. In both *in vitro* and *in vivo* assessment ARA-290 did not demonstrate any haematopoietic or angiogenic potential, whilst improving cellular and whole-tissue survival outcomes.

The mechanisms through which EPO and ARA-290 are capable of driving cell survival are incompletely understood. Much of the current knowledge on EPO-mediated tissue survival has been derived from studies assessing EPO-mediated red blood cell survival. As yet, it is unclear how the signalling pathways involved in EPO-mediated red blood cell survival translate into the general cytoprotective domain.

4.2 Aims

In this chapter, using the *in vitro* model of simulated ischaemia on the C2C12 cell line, we aim to assess the effect of simulated ischaemia on both the progenitor

myoblast cell, as well as differentiated myotubes. In addition, the potential role of ARA-290 and EPO in mediating cytoprotection during simulated ischaemia will be investigated. Further investigation aims to identify the importance of potential signalling pathways in mediating cytoprotection.

4.3 Methods

Culture of C2C12 myoblasts and differentiation into myotubes has been described in detail in chapter 2.4. Briefly, culture of myoblasts was always performed using C2C12 myoblast growth medium, consisting of DMEM GlutaMAX™ supplemented with 10% FCS, 100 units/ml penicillin and 100μg/ml streptomycin. When required, C2C12 myoblasts were seeded onto 6, 24 or 96 well plates at a cell density of 25,000 cells/ml.

Under particular conditions of serum removal C2C12 myoblasts will spontaneously differentiate to produce a reliable source of skeletal myotubes [238, 326]. Therefore, when required, C2C12 myoblasts at suitable confluence (70–80%) were cultured in differentiation media consisting of DMEM GlutaMAX™ supplemented with 2% HS, 100 units/ml penicillin and 100μg/ml streptomycin.

The effect of simulated ischaemia on C2C12 myoblast and myotubes survival was assessed using Western blot analysis for the apoptotic marker cleaved caspase-3. MTT and crystal violet assays were performed to investigate the effect of simulated ischaemia on C2C12 myoblast proliferation, and scratch-wound migration assays were performed to investigate the effect of ischaemia on myoblast migration. Subsequently, the addition of EPO or ARA-290 prior to simulated ischaemia was also investigated to identify their potential actions on myoblast survival, proliferation and migration. Comprehensive methods of each of these techniques can be found in chapter 2.5.2.

The potential roles of known mediators of erythrocyte precursor survival were interrogated for their role in mediating cytoprotection following simulated ischaemic injury. This included addition of inhibitors against JAK2/STAT3, PI3k/Akt and NFκB activation following pre-treatment with ARA-290 or EPO and prior to simulated ischaemia.

4.4 Results

4.4.1 Effect of ischaemia on C2C12 myoblast apoptosis, proliferation and migration in ischaemia

Apoptosis

Pooled data from repeated simulated ischaemia procedures on C2C12 myoblasts were assessed using western blot analysis performed looking for the apoptotic marker cleaved caspase-3. Figure 4.1 demonstrates the upregulation of cleaved caspase-3 in ischaemic samples compared to parallel samples left in 'normal' conditions (humidified incubator at 37°C and 5% CO_2).

Proliferation

Assessment of proliferative potential using MTT reagent as a marker of cell number demonstrated an increase in proliferation in cells placed under normoxic conditions. In comparison, cells subjected to simulated ischaemia demonstrated significantly reduced proliferative potential ($P<0.0001$, Mann-Whitney test, n=12 in both conditions; Figure 4.2A). Subsequent analysis using crystal violet protocol demonstrated similar pattern of results to the MTT assay. A significant reduction in proliferative potential occurred in myoblasts subjected to ischaemia ($P<0.0001$, Mann-Whitney test, n=15 in both conditions; Figure 4.2B). Due to the comparable detection of proliferation by MTT and crystal violet assays, subsequent analysis of C2C12 myoblast proliferation employed both assays interchangeably.

Migration

Scratch-wound assays to assess migratory potential of myoblasts under normoxic and simulated ischaemic conditions demonstrated an increased ability of myoblasts to promote migration in normoxic conditions. Assessment of the positive control wells (no mitomycin-C (MMC) added) demonstrated the ability of myoblasts to obtain greater than 80% closure in normoxic conditions, and greater than 70% closure in ischaemic conditions, utilising both proliferation and migration (Figure 4.3 A and B). However, inhibition of proliferation using 7.5μg/ml MMC, as a negative control comparison, displayed an average of 10% closure of the scratch-wound by migration alone in both normoxic and hypoxic conditions (Figure 4.3 C and D).

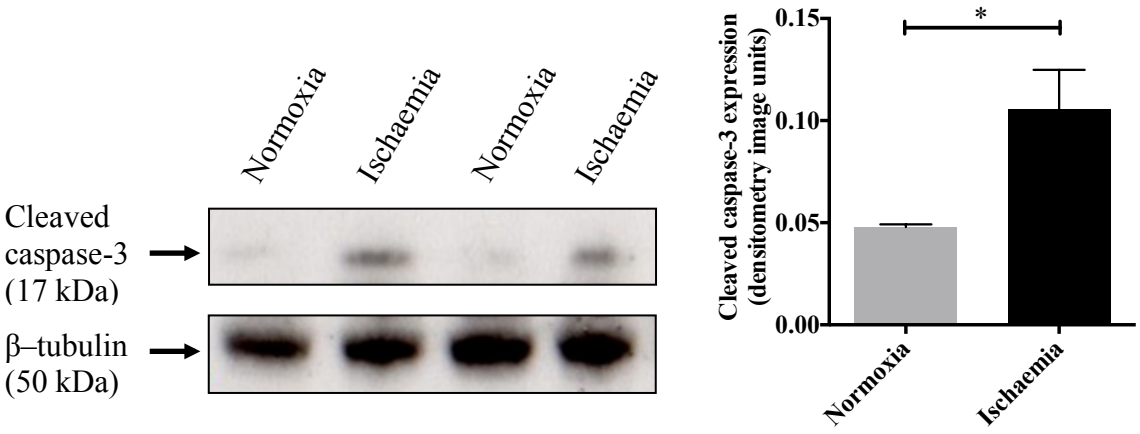

Figure 4.1: C2C12 myoblast apoptosis following simulated ischaemia

*A significant difference (*P<0.05, Mann-Whitney test) was evident in cleaved caspase-3 protein expression from C2C12 myoblast lysates following exposure to simulated ischaemia. Representative Western blot and pooled data from 3 independent simulated ischaemia experiments (n=6). Summary data is expressed as mean ± SEM.*

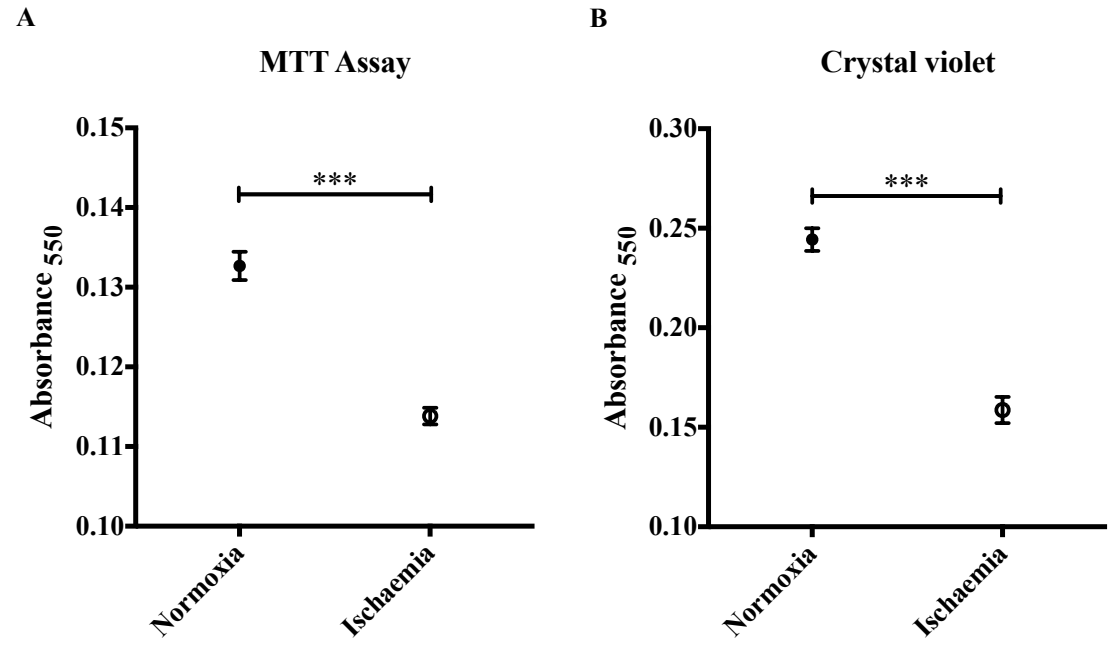

Figure 4.2: Effect of simulated ischaemia on proliferation of C2C12 myoblasts

*Analysis of both MTT (A) and crystal violet (B) assay displayed a significant reduction in C2C12 myoblast proliferation following ischaemic injury (both ***P<0.0001, Mann-Whitney test, MTT assay n=12 per group, Crystal Violet n=15 per group).*

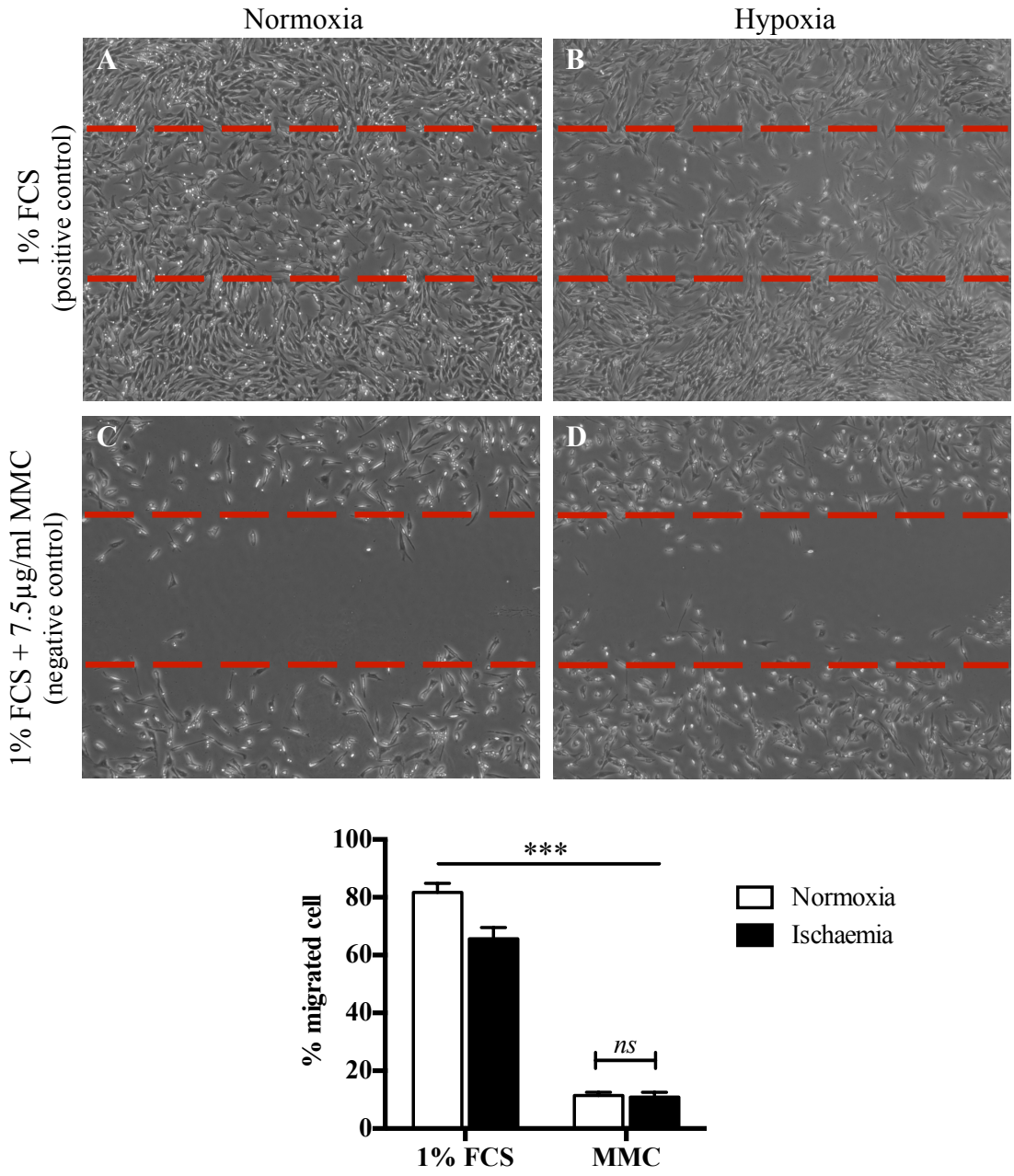

Figure 4.3: Migratory potential of C2C12 myoblasts following simulated ischaemia

Representative phase-contrast images of myoblasts 24 hours after scratch-wound. Myoblasts demonstrated ability to close a scratch-wound through proliferation and migration (A and B) in both normoxic and hypoxic conditions. Addition of the anti-proliferative agent MMC to isolate only migratory effects demonstrated severely reduced closure of the scratch-wound at 24 hours, under both normoxic and hypoxic conditions (C and D).

4.4.2 EPO and ARA-290 mediated reduction in C2C12 myoblast apoptosis

Addition of EPO 12-hours prior to induction of simulated ischaemia demonstrated partial effect on reducing the detection of cleaved caspase-3. Levels of cleaved caspase-3 were approximately half of the levels detected in parallel un-treated ischaemic samples. A similar effect was observed when myoblasts were pre-treated with ARA-290 (figure 4.4).

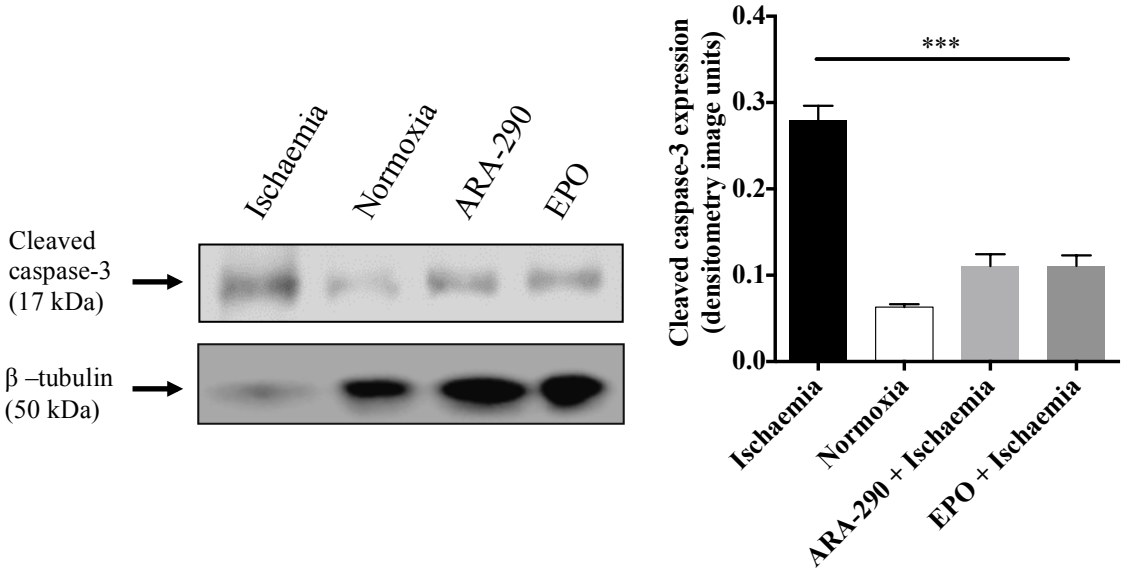

Figure 4.4: Effect of EPO and ARA-290 pre-treatment on C2C12 myoblasts apoptosis following simulated ischaemia

*Representative Western blot demonstrating significant anti-apoptotic effects of EPO and ARA-290 pre-treatment on C2C12 myoblasts prior to simulated ischaemia. EPO and ARA-290 significantly reduced expression of cleaved caspase-3 compared to the ischaemic control (both ***P<0.0001, one-way ANOVA n=6 per group). No significant difference compared to the normoxic samples occurred.*

4.4.3 Effect of EPO and ARA-290 on C2C12 myoblast proliferation

Following initial assessment of the effect of ischaemia on myoblast proliferation, EPO and ARA-290 were investigated for their ability to ameliorate the ischaemia-induced difference in proliferation. Under normoxic conditions, addition of either compound had no significant effect upon proliferation compared to control. EPO, as the traditional cytoprotective agent, demonstrated slight, but non-significant, improvement of proliferative capacity compared to untreated cells in ischaemia.

ARA-290 pre-treatment of myoblasts however, displayed significantly improved proliferative capability compared to untreated cells in ischaemia (P=0.0005, one-way ANOVA, n=15; figure 4.5).

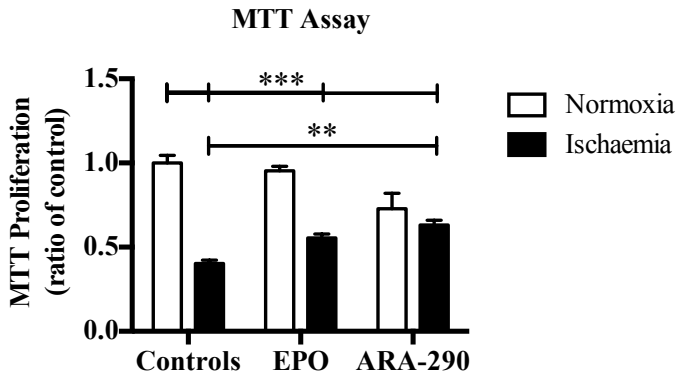

Figure 4.5: Ability of EPO and ARA-290 to improve ischaemia-induced deficit in proliferation

Myoblasts subjected to simulated ischaemia displayed a significantly diminshed proliferative capacity compared to parallel myoblasts in normoxic conditions (P<0.0001, one-way ANOVA, n=7 per group). Under normoxic conditions, pre-treatment with EPO or ARA-290 did not alter proliferative capabilities compared to untreated control (P>0.95). EPO pre-treated myoblasts subjected to ischaemia demonstrated increased proliferation compared to the ischaemic control, however this did not attain significance (P=0.0698, n=15). Pre-treatment with ARA-290 prior to ischaemic injury was able to ameliorate proliferation differences. ARA-290 treated myoblasts demonstrated a significantly improved proliferation potential (P=0.001, one-way ANOVA, n=15).

4.4.4 Effect of EPO and ARA-290 on C2C12 myoblast migration

Following initial assessment of the effect of ischaemia on myoblast migration, EPO and ARA-290 were investigated for their ability to ameliorate the ischaemia-induced differences in migration. Under normoxic conditions, addition of either compound was capable of significantly improving the migration of C2C12 myoblasts greater than the negative control myoblasts which were treated with MMC only. Addition of EPO or ARA-290 led to a 50–70% increase in the number of cells observed to move into the scratch-wound area (figure 4.6).

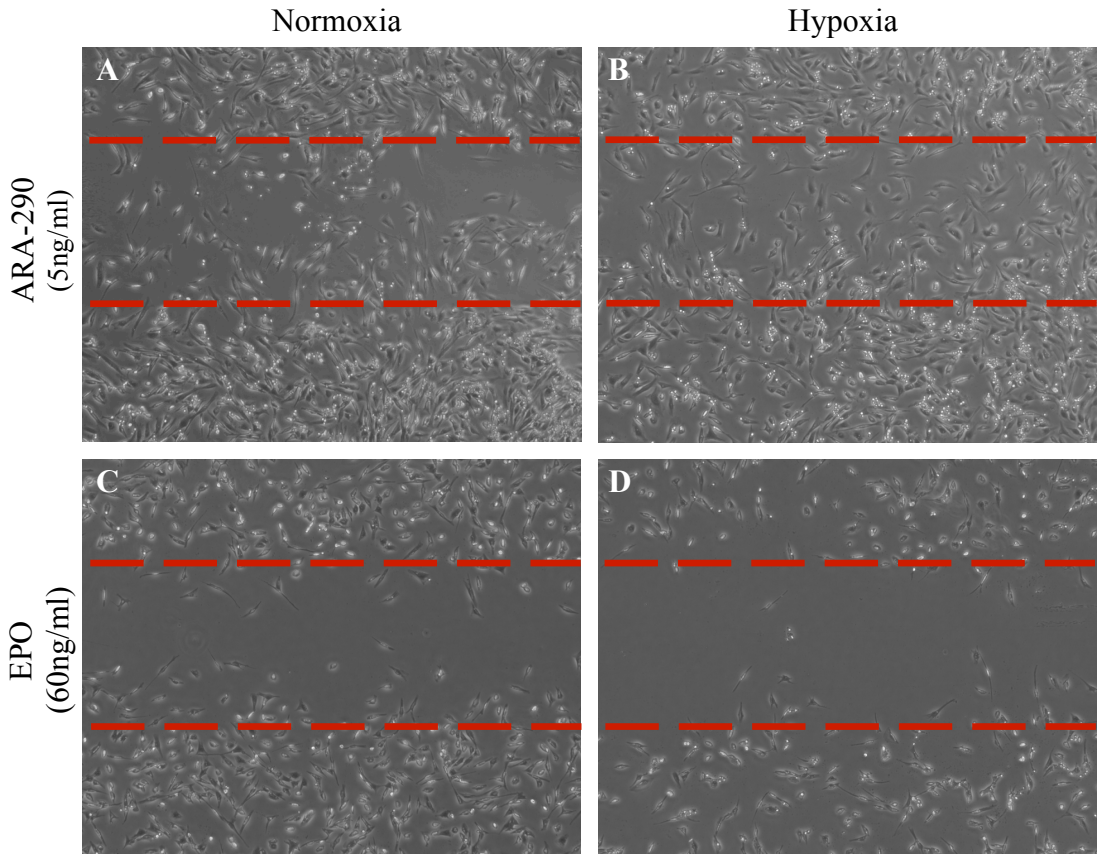

Figure 4.6: Effect of ARA-290 and EPO pre-treatment on C2C12 myoblast migration

ARA-290 (A and B) and EPO (C and D) pre-treatment resulted in increased myoblast migration compared to the negative control samples (1%FCS and MMC only).

4.4.5 Involvement of the Jak2, PI3k/Akt and NFkB signalling pathway

Inactivation of JAK2/STAT3 using the inhibitor SD-1029, PI3k/Akt using the broad-spectrum irreversible inhibitor wortmannin and NFκB using the NFκB inhibitor of activation demonstrated severe reduction in the ability of ARA-290 and EPO to improve myoblast migration in either normoxic or simulated ischaemic conditions. Inhibition using wortmannin or NFκB inhibitor of activation demonstrated the greatest effect upon ARA-290 or EPO mediated myoblast migration (Figure 4.7 B and D, respectively). Inhibition of JAK2/STAT3 also displayed reduced migration of myoblasts, but the difference was not significant in either normoxic or hypoxic conditions (Figure 4.7A).

The broad-spectrum reversible inhibitor LY294002, displayed greater effect upon inhibition of EPO mediated myoblast migration than ARA-290 (Figure 4.7 C). Migration of myoblasts treated with ARA-290 and LY294002 achieved approximately 30% cell migration into the scratch to attain closure of the scratch wound (approximately half the closure achieved by treatment with ARA-290 alone). As with ARA-290 treatment alone, a greater percentage of cell movement was observed under hypoxic conditions. Conversely treatment with EPO and LY294002 did not demonstrate any movement greater than that observed in the negative control samples. This highlights the possible divergence in signalling molecules utilised by EPO and ARA-290 to direct their cytoprotective potential.

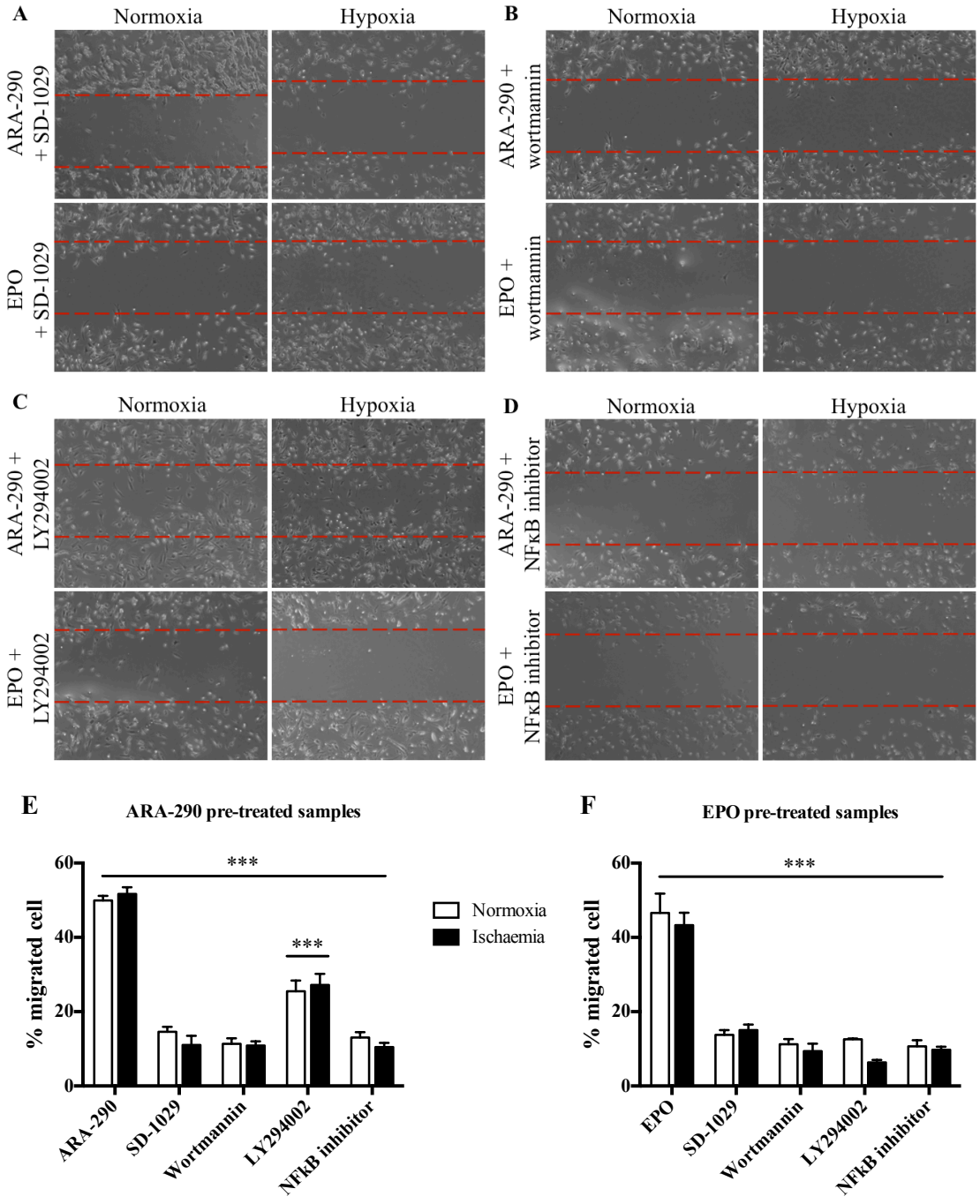

Figure 4.7: Inhibition of signalling molecules on C2C12 myoblast migration

Selective inhibition of (A) JAK2/STAT3, (B and C) PI3k/Akt and (D) NFκB was performed to identify potential molecules utilised by ARA-290 and EPO. Both ARA-290 and EPO treated samples demonstrated significant improvement of myoblast migration compared to negative control samples (1% FCS + MMC only) (P<0.0001, one-way ANOVA, n=6 per group). Subsequent inhibition with any inhibitor demonstrated significant removal of ARA-290 and EPO potentiated myoblast migration, to levels similar to negative control (P<0.0001 ARA-290 vs any inhibitor and EPO vs any inhibitor, one-way ANOVA, n=6 per group). Interestingly,

LY294002 inhibition of ARA-290 pre-treated myoblasts displayed significantly less reduction in migration compared to remaining inhibitors ($P<0.0023$, one-way ANOVA, n=6 per group). Figure 4.7 E and F summarise myoblast migration for ARA-290 and EPO pre-treated samples respectively.

4.4.6 Effect of ischaemia on C2C12 myotube apoptosis

C2C12 myotubes subjected to simulated ischaemia demonstrated increased protein expression of cleaved caspase-3 compared to parallel normoxic controls. This finding indicates greater susceptibility of C2C12 myotubes to ischaemia-induced apoptosis (Figure 4.8 A and B).

4.4.7 Effects of EPO and ARA-290 on C2C12 myotube apoptosis

Addition of EPO or ARA-290 24-hours prior to induction of simulated ischaemia demonstrated a significant reduction of cleaved caspase-3 expression. The role of phosphorylated-Akt was also investigated and demonstrated increased phosphorylated protein in EPO and ARA-290 treated lysates compared to normoxic or ischaemic controls (Figure 4.8 A and B).

4.4.8 Involvement of the Jak2, PI3k/Akt and NFkB signalling pathway

Molecules known to play a role in EPO-mediated erythrocyte precursor survival were interrogated for their role in abolishing the previously observed EPO or ARA-290 mediated cytoprotection in C2C12 myotubes. As phosphorylated-Akt demonstrated a correlation with cleaved caspase-3 expression in early studies, the effect of inhibition of various known upstream and downstream signalling partners on Akt phosphorylation was also analysed. Figure 4.8A demonstrates the effect of EPO (60ng/ml) pre-treatment on C2C12 myotubes, followed by subsequent inhibition of JAK2/STAT3, PI3k/Akt, and NFκB, prior to simulated ischaemia exposure. The effect of EPO pre-treatment on reducing the levels of cleaved caspase-3 expression is abolished upon addition of all inhibitors to a comparable extent. Inhibition of JAK2/STAT3 using SD-1029 also resulted in increased apoptosis with parallel decrease of phosphorylated-Akt. The effect of PI3k/Akt inhibition with wortmannin or LY294002 upon EPO pre-treated myotubes resulted in increased expression of cleaved caspase-3 and decreased expression of phosphorylated-Akt. The effect of LY294002 on ARA-290 pre-treated myotubes was not as apparent. Inhibition of

NKκB activation also resulted in an abolishment of EPO mediated cytoprotection and phosphorylated-Akt decrease.

The effect of the above inhibitors upon ARA-290 pre-treated cells followed a similar pattern of results, with abolishment of anti-apoptotic effects of ARA-290 pre-treatment on C2C12 myotubes undergoing ischaemic injury, with the exception of addition of LY294002. LY294002 is a reversible PI3k/Akt inhibitor. Similar to its effects on C2C12 myoblast migration, addition of LY294002 displayed the least abolishment of ARA-290 effect on ischaemia-induced apoptosis. Though expression of phosphorylated-Akt was also diminished, expression was still apparent, suggestive of incomplete occupation of all relevant ATP-binding domains. In contrast, wortmannin, an irreversible PI3k/Akt inhibitor, caused apoptosis to similar levels observed in the ischaemic, untreated controls, with an additional decrease in phosphorylated-Akt.

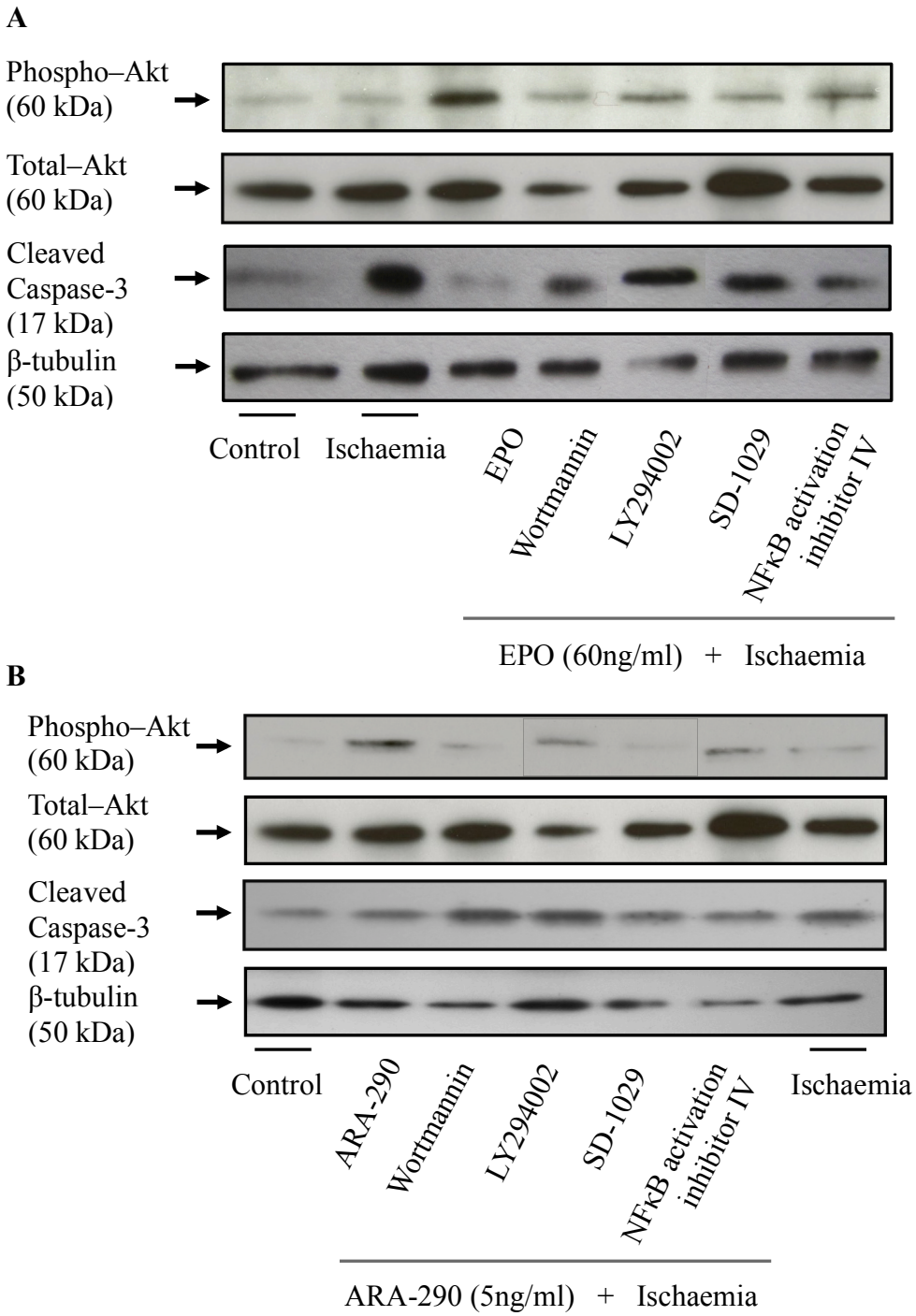

Figure 4.8: Analysis of ARA-290 and EPO pre-treatment on apoptosis in C2C12 myotubes

Representative Western blot of (A) EPO and (B) ARA-290 pre-treated myotubes subjected to simulated ischaemia. Potential pathways utilised by EPO and ARA-290 for mediating cell survival were dissected by inhibiting JAK2/STAT3 (SD-1029), PI3k/Akt (Wortmannin and LY294002) and NKκB activation. Addition of any of these inhibitors in conjunction with ARA-290 or EPO abolished the prior decrease in cleaved caspase-3 expression observed following simulated ischaemia.

4.5 Discussion

In this study, the effect of simulated ischaemia on several cellular and physiological outcomes of the C2C12 murine myoblast cell line has been investigated. Alterations in apoptosis, migration and proliferation in response to simulated ischaemia were identified. Most poignant was the detrimental effect of ischaemia upon myoblast function and survival, as well as myotube survival, features which may contribute to muscle pathology in PAD.

Interestingly, several groups investigating the effect of low oxygen tension on satellite cells have a identified a beneficial effect of low, or physiological, oxygen concentrations, compared to the 5% CO_2 95% air, which contains approximately 20% oxygen. This includes increased rates of proliferation, chemotaxis and survival, as well as maintenance of satellite cells in their quiescent state with replenishment of the self-renewal population [327-330]. Future work may need to be conducted to identify this balancing phenomenon between beneficial and destructive qualities of decreasing oxygen concentrations.

The *in vitro* model of skeletal muscle ischaemia used in this work has also been invaluable in highlighting potential aspects of myoblast function which are most affected following ischaemic insult, suggestive of the underlying pathology in human disease. Evidence from the study also demonstrated the potential of novel therapeutic agents to improve a number of features that occur following ischaemic injury.

Treatment with EPO and ARA-290 demonstrated an ability to 'rescue' myoblasts and myotubes from the detrimental effects propagated by ischaemia. Both agents resulted in similarly effective and significant ability to prevent myoblast and myotube apoptosis. Identification of critical mediators involved in delivering ARA-290 and EPO-mediated tissue protection were explored by inhibition of discrete molecules known to play a role in EPO-mediated erythrocyte precursor survival. Addition of inhibitors in combination with EPO or ARA-290 pre-treated cultures resulted in impedance of previously observed anti-apoptotic effects of both ARA-290 and EPO. Although the signalling cascades involved in EPO-mediated erythrocyte precursor survival has been extensively investigated, less knowledge is available on signalling pathways through the tissue-protective heteroreceptor complex. Interrogating known

molecules to illuminate their role in tissue-protective pathways identified the importance of JAK2, PI3k/Akt, and NFκB.

JAK2, via crystallographic studies, is in direct interaction with the EPOR, and known to be required to mediate the phosphorylation of itself, and several other tyrosine kinases to propagate signalling cascades. Downstream molecules known to interact with JAK2 following EPO-ligand binding include STAT3 and STAT5. The inhibitor SD-1029 (JAK2/STAT3) resulted in reduced migration and increased apoptosis, although the extent of these features suggested incomplete blockade of all downstream signalling pathways. Literature has shown that SD-1029 targets phosphorylation of STAT3 by JAK2 [331-333]. Although the observed effects of inhibition suggest a crucial role of STAT3 in mediating tissue protection, it is likely that some alternative signalling may also occur via other interacting molecules.

The disparity in inhibition between the two broad-spectrum PI3k/Akt inhibitors, wortmannin and LY294002 on ARA-290 treated samples highlights possible deviations in the tissue-protective signalling cascade from those known to be involved in EPO dependent erythrocyte precursor survival and maturation. Differences in the effect of PI3k/Akt inhibition using both inhibitors have also been identified and include differences in cell growth and apoptosis, intracellular calcium homeostasis and action potentials and nitric oxide production [334-337]. A plausible explanation for these observed differences is that although both inhibitors rely upon competitive ATP-binding, LY294002 will bind via a reversible hydrogen bond, whereas wortmannin binding results in an irreversible covalent complex [338, 339].

This study provides compelling evidence of a negative effect of ischaemia on skeletal muscle tissue. The observed decrease in migration and proliferation as well as the increase in apoptosis under ischaemic conditions are all features relevant to human CLI, and support the idea of the occurrence of musculopathy in patients with CLI. Currently, a large focus of CLI treatment aims to target the diminished vascular supply. Understanding and acceptance of underlying muscle pathology is not widely established, providing a vast arena to target for therapeutic benefit.

Functional deficit associated with CLI is a leading cause of morbidity for the majority of patients. Despite successful revascularisation, a corresponding improvement in functional outcomes is often not described. The contribution of myoblasts to the

pathogenesis of musculopathy and functional decline in CLI is uncertain but likely to play a role considering the vast bulk of tissue in the hindlimb is composed of skeletal muscle. In addition, the increased vulnerability of skeletal muscle to ischaemia compared to other components of the limb increases the likelihood that there will be a consequent modulation in myoblast and myotubes behaviour [340]. The ability to observe the behaviour of skeletal muscle cells, including in their precursor state, is highly relevant in this study.

4.6 Summary

In this study, the deleterious effects of ischaemia on a murine skeletal muscle immortal cell line were seen. This suggests the muscle pathology observed in PAD patients may be as a consequence of the chronic ischaemic conditions found in CLI limbs. The cytoprotective properties of EPO and ARA-290 were also demonstrated as evidenced by their ability to reduce ischaemia-induced injury in the C2C12 skeletal muscle *in vitro* model. In conjunction, these results highlight the susceptibility of C2C12 skeletal myoblasts and myotubes to ischaemic injury as well as the possibility of "rescuing" cells from ischaemic injury using novel therapeutic agents.

CHAPTER 5

Effect of ARA-290 on human myoblasts and myotubes *in vitro*

5.1 Introduction

Cell lines represent an invaluable tool in the *in vitro* modelling of human disease pathogenesis. The majority of cell lines provide a domain that is easy to handle, and well established, making the results generated easier to replicate and also more acceptable due to their extensive characterisation. In the assessment of skeletal muscle, the C2C12 cell line retains all these features, and in addition allows for a degree of standardisation through its use across investigating communities. However, whilst cell lines provide a reliable and replicable source of immortalised cells, they are often quite removed from the clinical scenario of interest. Phenotypical differences that have been recognised between the C2C12 cell line and primary human skeletal muscle myoblasts include cell size, growth rate, formation of sarcomeres and the substrates required for optimal growth [341, 342], all of which may have an impact upon different fields of study.

A logical progression, following the use of immortalised cell lines in the study of human disease, is the use of primary cell lines to more closely mimic human cellular behaviour, or pre-clinical *in vivo* models to replicate the entire disease process. In this chapter, the use of human primary myoblasts isolated from patients with CLI, as well as control individuals – for comparison, provides a more pertinent experimental model to assess the underlying human disease pathology.

Isolation of myoblasts from CLI patients has not previously been reported in the literature. Very little knowledge is therefore available on the behaviour of CLI myoblast explants. To counteract possible confounding results, myoblasts were also isolated from control donors to better identify phenotypical differences that may exist as a result of the ischaemic niche present in the CLI limb.

The experimental data from the previous chapter indicated differences in myoblast behaviour as a result of simulated ischaemia. In addition, C2C12 myotubes showed

sensitivity to ischaemia-induced apoptosis. Pre-treatment with EPO or ARA-290 demonstrated potential to provide protection to C2C12 myoblast and myotubes against injury as a result of simulated ischaemia. The response of CLI and control myoblasts and myotubes to simulated ischaemia is uncertain. The effect of ARA-290 on human skeletal myoblasts has also not been established, however work in the field of ischaemic cardiac myocytes may provide evidence for possible therapeutic benefit of EPO and ARA-290. Therefore the cytoprotective effects of ARA-290 on skeletal myoblasts and myotubes were explored. Key signalling molecules of EPO-mediated red blood cell survival, identified in the previous chapter, were subsequently assessed in this study.

5.2 Aims

This study aimed to develop an *in vitro* simulated ischaemia model using myoblasts and myotubes isolated from CLI and control samples which would allow the identification of differences in the functional characteristics of myoblasts from the CLI and control donor populations, as well as their response to simulated ischaemia. In addition, the therapeutic potential of EPO and ARA-290 to provide cytoprotection against ischaemia-induced apoptosis was investigated.

5.3 Methods

In this study, the effect of simulated ischaemia on primary human skeletal myoblasts and myotubes was investigated. Myoblasts were isolated from biopsies of our disease group of interest – CLI patients. In order to allow comparison of myoblasts and myotubes, isolation of myoblasts from the control group was also performed. Isolation of human myoblasts from skeletal muscle biopsies, and their subsequent culture and differentiation into myotubes have been described in detail in chapter 2.5. Briefly, all muscle biopsies from both CLI and control sample biopsies were isolated using the same standard operating procedure. Isolated myoblasts were maintained in specialised skeletal myoblast growth medium (PromoCell) supplemented PromoCell skeletal muscle SupplementMix, 10% FCS (Gibco®), 1x GlutaMAX™ (Gibco®, UK), 100 units/ml penicillin and 100µg/ml streptomycin. When required, human myoblasts were seeded onto 6, 24 or 96 well plates at a cell density of 30,000 cells/ml.

Under particular conditions of serum removal human myoblasts will spontaneously differentiate to produce a reliable source of skeletal myotubes. Therefore, when required, human myoblasts at suitable confluence (70–80%) were cultured in differentiation media consisting of DMEM GlutaMAX™ supplemented with 2% HS, 100 units/ml penicillin and 100µg/ml streptomycin.

Myoblast characterisation

Cultures of primary human myoblasts were inspected using a phase-contrast microscope to confirm typical myoblast morphology. Subsequent characterisation of human myoblasts involved immunocytochemistry/immunofluorescence for the muscle-specific marker desmin, to ensure homogeneous myoblast populations. To ensure myoblast differentiation into myotubes, cell lysates were assessed for the myogenic-regulatory factor, myogenin, using western blot analysis.

Apoptosis

Quantitative assessment of apoptosis in human myoblast and myotubes following simulated ischaemia was performed in order to correlate significant findings from western blot analysis. The luminescent Caspase-Glo® 3/7 Assay (Promega, UK) was

used according to manufacturer's protocol. Briefly, cells of interest were plated at 25,000 cells/ml, in a white-walled 96-well sterile, tissue-culture plate (100µl/well), and allowed to adhere for 4 hours prior to initiation of 8 hours of simulated ischaemia, with a parallel plate left in normoxic conditions. Subsequently, both plates were allowed to equilibrate to room temperature, during which time the Caspase-Glo® 3/7 buffer and substrate were mixed in 1:1 volume. 100µl/well of Caspase-Glo® 3/7 mixed reagents was added to each well, the plates gently shaken, and allowed to equilibrate for 1 hour at room temperature. Luminescence of each plate was then read using a microplate reader (Mithras LB940 microplate reader).

Proliferation

Differences in proliferative capabilities of CLI and control myoblast were investigated using established assays, as well as newer, commercial options. Proliferation assays have been described in detail in chapter 2.5.

All proliferation assays were performed on cells seeded at 30,000 cells/ml into 96-well plates (100µl/well). Every primary cell line was seeded at least in duplicate, and identical plates were seeded for assessment of proliferative differences under both normoxic and simulated ischaemic conditions, using all three assays, to ensure passage number did not affect proliferation (6 plates in total). MTT assay relies on the relationship between mitochondrial activity and cell number to provide an estimate of proliferation potential. The crystal violet and CyQUANT assays use agents which will intercalate with DNA to give a proportional representation of cell number. These assays were used in conjunction to identify similarities and potential differences between CLI and control myoblasts.

Migration

Migration of myoblasts to areas of injury is an important feature of tissue repair. Investigation into potential underlying phenotypic differences in migratory ability of CLI and control myoblasts was performed by introducing a scratch-wound into a monolayer of CLI or control myoblasts.

Contraction

Skeletal muscle has many functions, including mobilisation and movement, through coordinated skeletal muscle group contraction and relaxation. In addition, cell contraction plays an important role in overall cell migration, especially in a co-ordinated response to tissue injury, in order to facilitate repair. To further identify potential causes for alterations in CLI myoblast migration in the above assay, as well as aberrant skeletal muscle repair in CLI patients, contractile ability was investigated using floating type I collagen gel lattices.

Human myotube in vitro model

The lack of oxygen during ischaemia causes consequent alterations in a number of genes encoding proteins designed to counteract the local hypoxia. These genes often share a common mode of regulation that involves activation of the HIF family of transcription factors, and in particular, HIF-1α. HIF-1α, a cellular detector of low oxygen tension becomes stabilised by hypoxia, and promotes transcription of several factors to counteract the low oxygen concentrations. Although upregulation of HIF-1α has previously been demonstrated in C2C12 myobtubes undergoing ischaemic injury [238], this finding was revalidated in the human myotubes *in vitro* model using both control and CLI myotubes. Following simulated ischaemia, cell lysates were assessed for the expression of HIF-1α, compared to paired normoxic lysates using western blot analysis.

Previously, using the C2C12 cell line, EPO and ARA-290 demonstrated an ability to reduce ischaemia-induced apoptosis. In addition, key signalling molecules involved in EPO or ARA-290 mediated reduction of apoptosis were identified. Using these identified molecules, investigation of their role in human primary cells was performed. This included pre-treatment of human myotubes with EPO or ARA290 and the use of inhibitors against JAK2/STAT3 (SD-1029), PI3k/Akt (wortmannin and LY294002) and NFκB (NFκB inhibitor of activation IV).

5.4 Results

5.4.1 Analysis and differentiation of primary human myoblasts

Characterisation

Due to the composition of skeletal muscle (endothelial cells, fibroblast and myoblasts), purity of myoblast populations was investigated to ensure homogeneous myoblast population. Obtaining pure myoblast cultures was of greater difficulty in biopsies from CLI patients, and is likely due to the more fibrotic nature of their muscle tissue. To assess the purity of myoblast populations immunocytochemistry was performed using the muscle-specific marker desmin. Figure 5.1 provides representative phase-contrast images of myoblasts in culture following isolation from muscle biopsy at day 3 (A), 7 (B) and 14 (C), as well as myoblasts that have differentiated, fused and aligned to become myotubes (D). Figure 5.1E shows a representative image of myoblasts with positive desmin staining confirming muscle-derived cells. Desmin staining was performed on all isolated human cultures, and at each passage used, to ensure that the derived population had less than 5% contamination with other cell types when used experimentally.

Confirmation of myoblast differentiation was also achieved by assessment of myoblast and myotubes cell lysates for the myogenic regulatory factor myogenin. Figure 5.2 shows a representative Western blot of myoblast and myotubes lysates, assessed for expression myogenin. Cell lysates, from myotubes, that have undergone myogenic differentiation show an increase in myogenin protein expression.

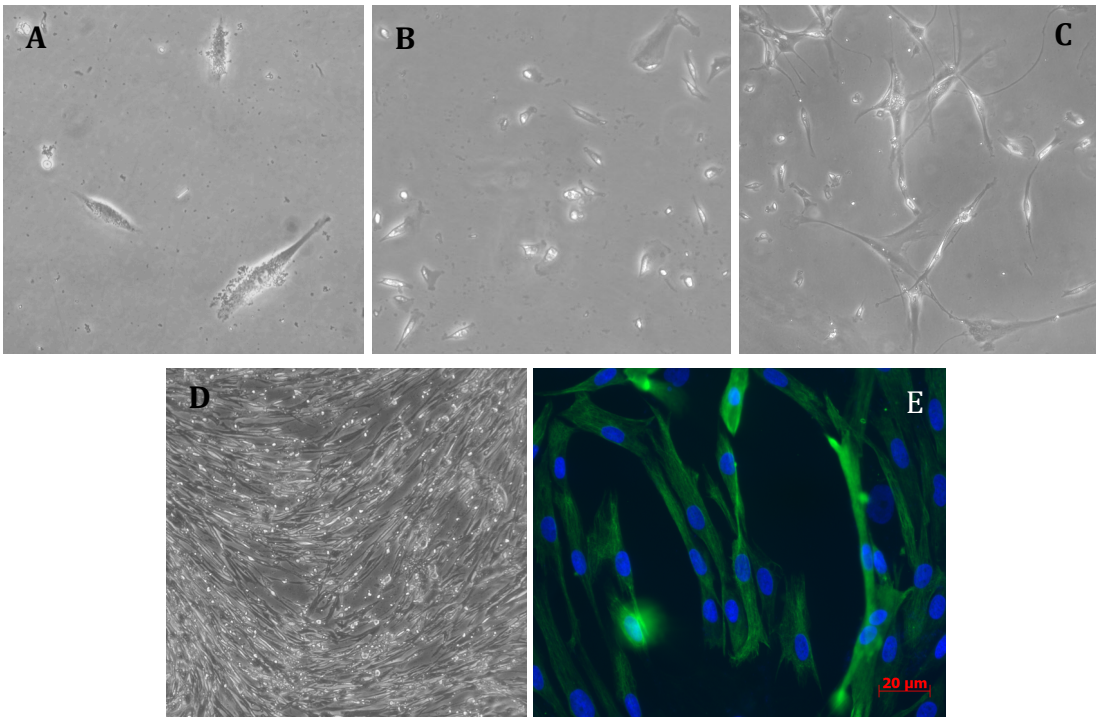

Figure 5.1: Isolation of human myoblasts

Representative phase-contrast photomicrographs of primary skeletal myoblasts at day 3 (A, 100x magnification), 10 (B), and 14 (C) following isolation. Myoblasts were also induced to differentiate (D), and stained with desmin antibody to confirm cell type (E). Phase-contrast magnification = x20 unless otherwise stated. Scale bar=20 µm.

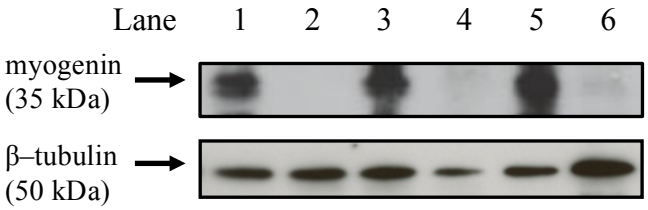

Figure 5.2: Analysis of human myoblast differentiation

Representative Western blot of paired myoblast and myotubes cell lysates assessing differentiation of myoblasts by probing for myogenin expression. Myotube samples demonstrated increased expression of myogenin (lanes 1, 3 and 5) compared to parallel myoblasts (lanes 2, 4 and 6).

5.4.2 Effect of ischaemia on myoblast function

Apoptosis

Myoblasts isolated from CLI and control donors subjected to simulated ischaemia were assessed for caspase-3/7 activity following ischaemic exposure. Under normoxic conditions, myoblasts from CLI and control did not display a significant difference in caspase activity. Parallel samples of myoblasts evaluated following exposure to simulated ischaemia displayed a significant increase in caspase-3/7 activity compared to normoxic controls. Interestingly, caspase-3/7 activity was approximately 2-fold greater in myoblasts isolated from control samples compared to myoblasts from CLI patients under ischaemic conditions, indicative of underlying physiological differences in response to hypoxic injury, likely as a response of their native environment (figure 5.3).

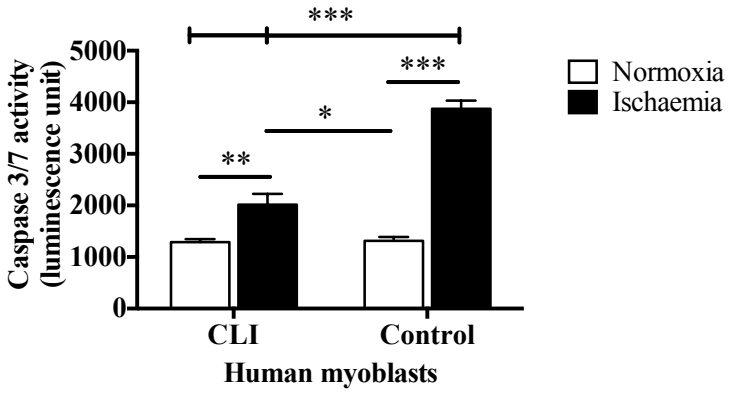

Figure 5.3: Differences in myoblast apoptosis in response to simulated ischaemia

Quantification of apoptotic activity using Caspase-3/7 assay revealed reduced sensitivity of CLI myoblasts to ischaemia induced apoptosis. Control myoblasts showed 2-fold greater caspase-3/7 activity, indicating increased apoptosis, as a result of simulated ischaemia ($P<0.0001$, one-way ANOVA, $n=6$ for CLI myoblasts, $n=5$ for control myoblasts).

Proliferation

Proliferative potential of human myoblasts was evaluated using multiple complementary assays. Whilst all three proliferation assays were able to detect a significant proliferative difference between CLI and control myoblasts, different assays demonstrated different sensitivities for the proliferation capacity of CLI and

control myoblasts under different oxygen tension conditions. Figure 5.4 represents the pooled data from a series of proliferation assays using all three reagents.

Crystal violet assay of CLI and control myoblasts in normoxic and simulated ischaemic conditions highlighted significant differences between their respective proliferative capabilities. Even in normoxic conditions, CLI myoblasts demonstrated a significantly greater (over 1.5-fold greater) proliferative capacity compared to control myoblasts in the same conditions ($P<0.0001$, one-way ANOVA, n=6 for CLI myoblasts; n=5 for control myoblasts). A significant decrease was observed in CLI and control myoblasts that were subjected to an ischaemic period, compared to their normoxic parallel counterparts. Interestingly, even following simulated ischaemia, CLI myoblasts still retained greater proliferative potential than control myoblasts, subjected to either normoxic or ischaemic periods ($P<0.0001$, one-way ANOVA).

The commercial CyQUANT assay yielded similar patterns of proliferation capabilities between CLI and control myoblasts. There was a greater difference under normoxic conditions, approximately 2-fold, between proliferation observed in CLI versus control myoblasts. Similarly to the crystal violet assay, CLI myoblasts, even after an ischaemic period, still demonstrated a significantly higher proliferative potential compared to control myoblasts under any condition. To note however, following simulated ischaemia there was no significant decrease in proliferation observed compared to parallel control myoblasts.

The MTT assay revealed the least difference between CLI and control myoblasts following simulated ischaemia: with no significant difference detected between CLI myoblasts subjected to simulated ischaemia compared to their normoxic counterparts, as the previous two assays suggested. In addition, no significant difference was observed between CLI myoblasts and control myoblasts in normoxic conditions – a significant difference detected by both the previous assays.

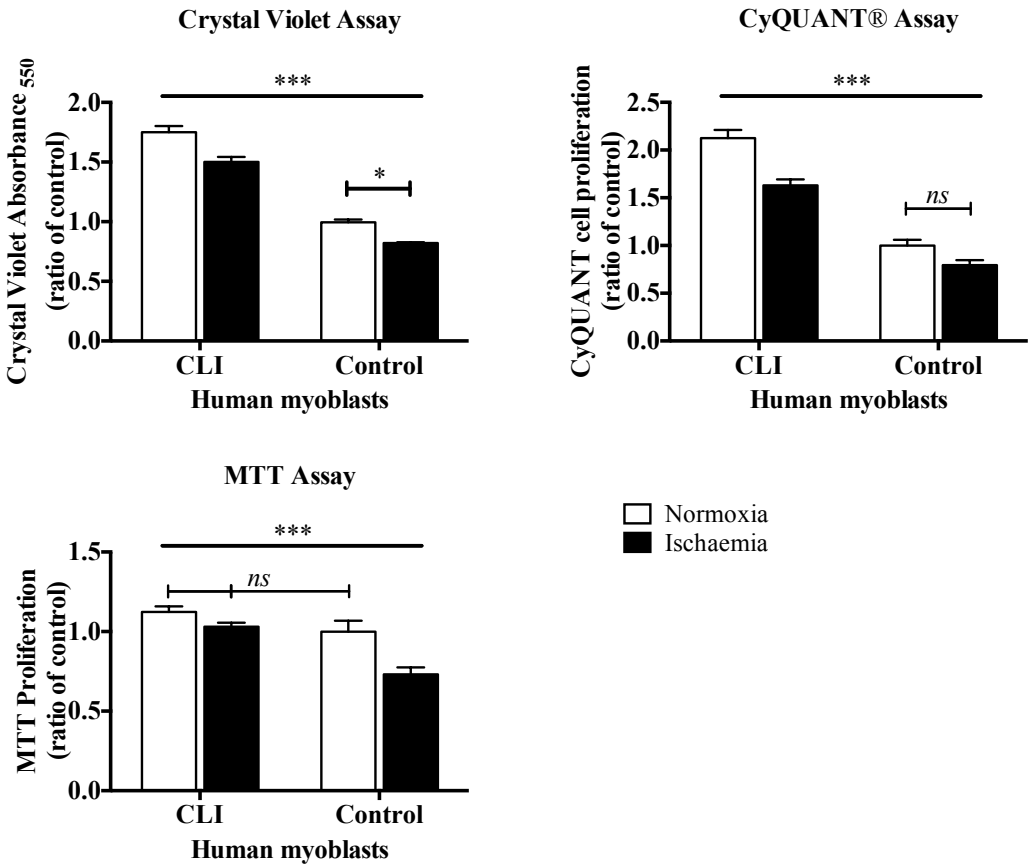

Figure 5.4: Multiple assessment of proliferative capacity of human CLI and control myoblasts

Myoblasts from CLI donors demonstrated significantly greater proliferative potential in crystal violet and CyQUANT assays compared to control myoblasts. This finding was still present after simulated ischaemia ($P<0.0001$, one-way ANOVA, n=6 CLI myoblasts, n=5 control myoblasts). The MTT assay demonstrated a significantly greater proliferative capacity of CLI myoblasts compared with control myoblasts, but was less sensitive at detecting proliferative differences under simulated ischaemic conditions.

Migration

Scratch-wound assays to assess migratory potential of human CLI and control myoblasts under normoxic and simulated ischaemic conditions demonstrated a diminished ability of CLI myoblasts to promote migration alone in hypoxic conditions when the anti-proliferative agent MMC, was added as a negative control comparison. On average CLI myoblasts displayed an average of 16.6 and 5.8% closure of the scratch-wound by migration alone, in normoxic and hypoxic conditions respectively, compared to control myoblasts which achieved 16.3 and 15.9% closure of the scratch-wound under the same respective conditions (Figure 5.5).

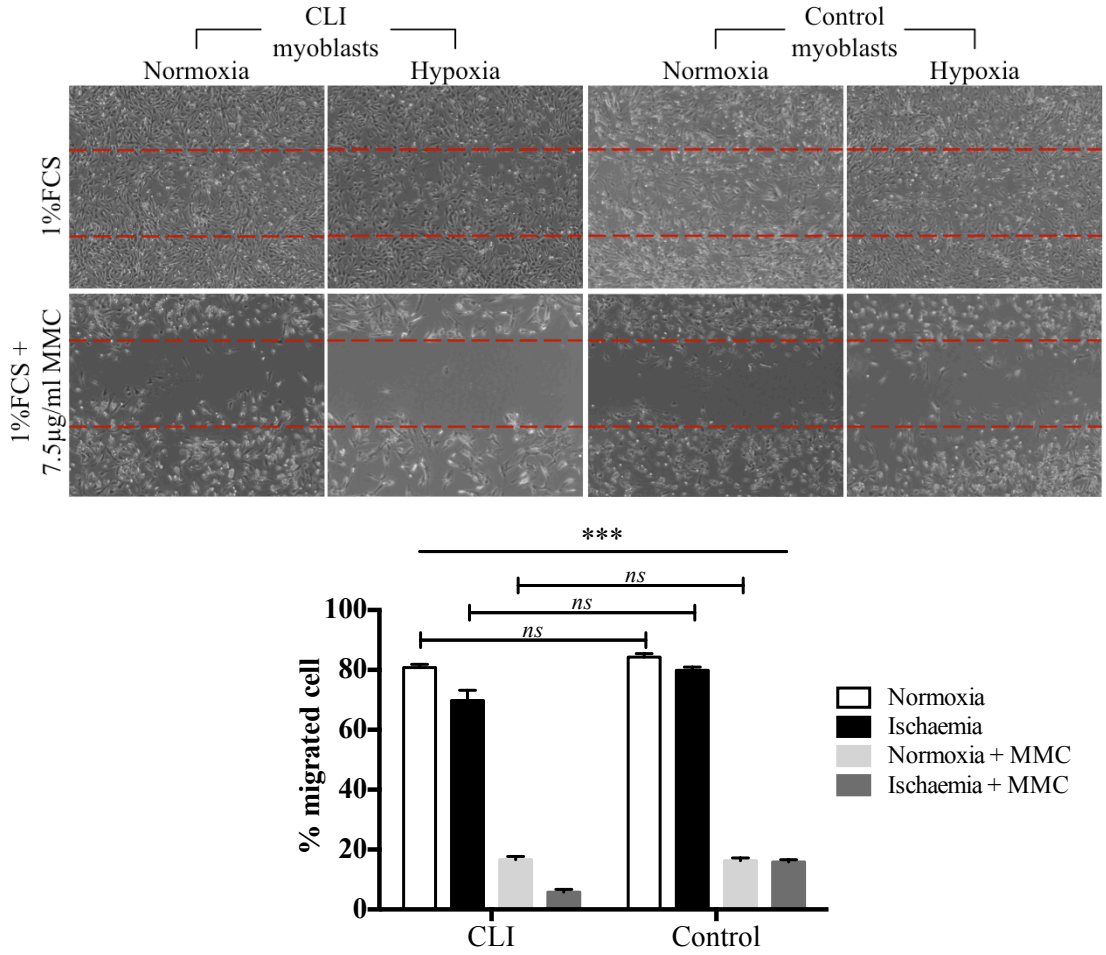

Figure 5.5: Migratory potential of CLI and control myoblasts following simulated ischaemia

Myoblasts from CLI donors demonstrated a diminished ability to migrate into a scratch made in a monolayer of cells compared to control myoblasts. This finding was further exaggerated when myoblasts were subjected to simulated ischaemia.

Contractility and migration

Data from a series of independent contraction assays using type I collagen gel lattices outlined an important, aberrant functional effect of the CLI phenotype, similar to the diminished migratory potential observed above. Figure 5.6 shows contraction assays from myoblasts isolated from CLI patients, compared with controls. Myoblasts from CLI patients were unable to promote the same degree of contraction of the collagen gel lattice as healthy control myoblasts, suggestive of dysfunctional contractile apparatus affecting myoblast migration.

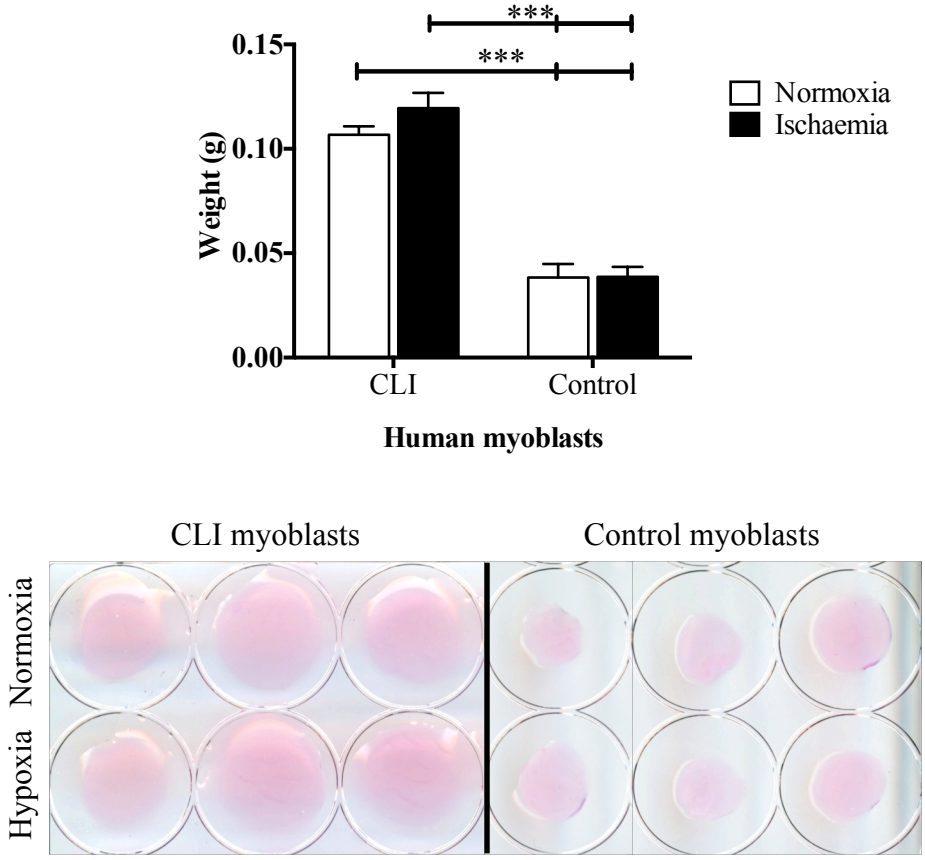

Figure 5.6: Enhanced contraction of collagen gel lattices by control myoblasts

Representative image demonstrating the diminished ability of CLI myoblasts to contract type I collagen gel lattices compared to control myoblasts (P<0.0001, one-way ANOVA, n=5 for both CLI and control myoblasts). There was no significant difference in contractile ability when subjected to simulated ischaemia.

5.4.3 EPO and ARA-290 improvement of human myoblast migration

Treatment of myoblast cultures with EPO or ARA-290 at the time of scratch-wound demonstrated positive effects of both agents on promoting myoblast migration (Figure 5.7). Both EPO and ARA-290 were capable of improving CLI and control myoblast migration, to similar levels. The migration observed in both CLI and control treated samples was significantly higher than migration observed in MMC-only (negative control) wells, under both normoxic and simulated ischaemic conditions.

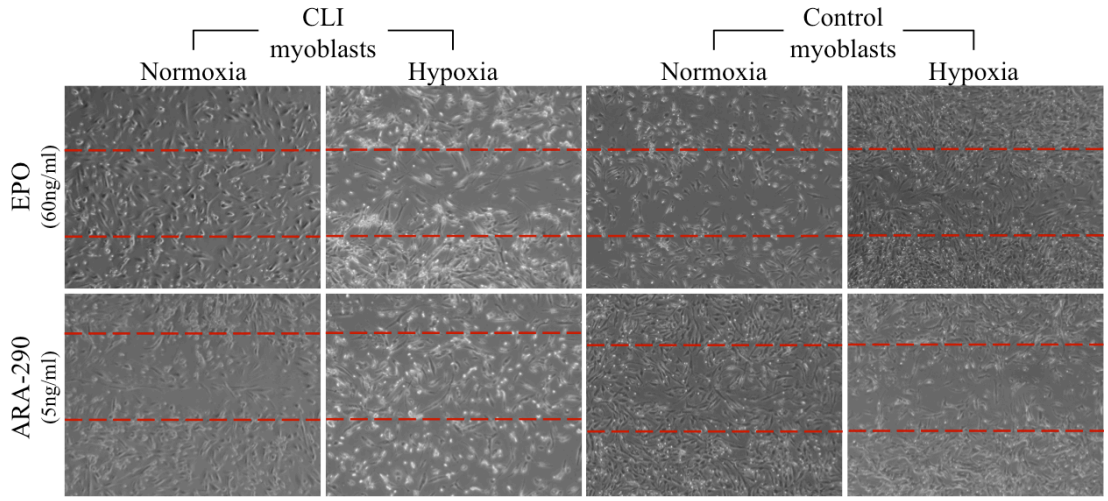

Figure 5.7: Pro-migratory effect of EPO and ARA-290 on human myoblast

Pre-treatment of human myoblasts with EPO or ARA-290 resulted in an increased migration of myoblasts into the scratch wound compared with the negative control scratch-assays (1%FCS and MMC only)

5.4.4 Involvement of the JAK2, PI3k/Akt and NFkB signalling pathway in myoblast migration

Inhibition of EPO treated samples using inhibitors against JAK2/STAT3, PI3k/Akt or NFκB resulted in marked decrease in myoblast migration into the scratch-wound. Under normoxic conditions there was an observable reduction in both CLI and control myoblast migration, but the difference was not significant. However, inhibition of EPO effect using SD-1029, wortmannin, LY294002 or NFκB inhibitor of activation was consistently more prominent on myoblasts subjected to simulated ischaemia, whether from either CLI or control samples (figure 5.8).

Inhibition of JAK2/STAT3, PI3k/Akt using wortmannin and NFκB demonstrated severe reduction in the ability of ARA-290 to improve either CLI or control myoblast migration in either normoxic or simulated ischaemic conditions. All three inhibitors caused significant reduction in ARA-290 mediated migration. The reduction in migration following inhibition ranged between approximately 7 – 50% of migration observed when treated with ARA-290 and MMC alone. Simulated ischaemia did not demonstrate any compounding effect on myoblast migration of ARA-290 with inhibitor-treated wells. The broad-spectrum reversible inhibitor LY294002, similar to previous results, did not entirely abolish improvements in migratory potential of either CLI or control myoblasts. CLI and control myoblasts treated with ARA-290 and LY294002 still achieved greater than 70% migration of ARA-290 only treated samples. This is in comparison to wortmannin-induced PI3k inhibition samples, and those treated with EPO where LY294002 had greater inhibitory effect.

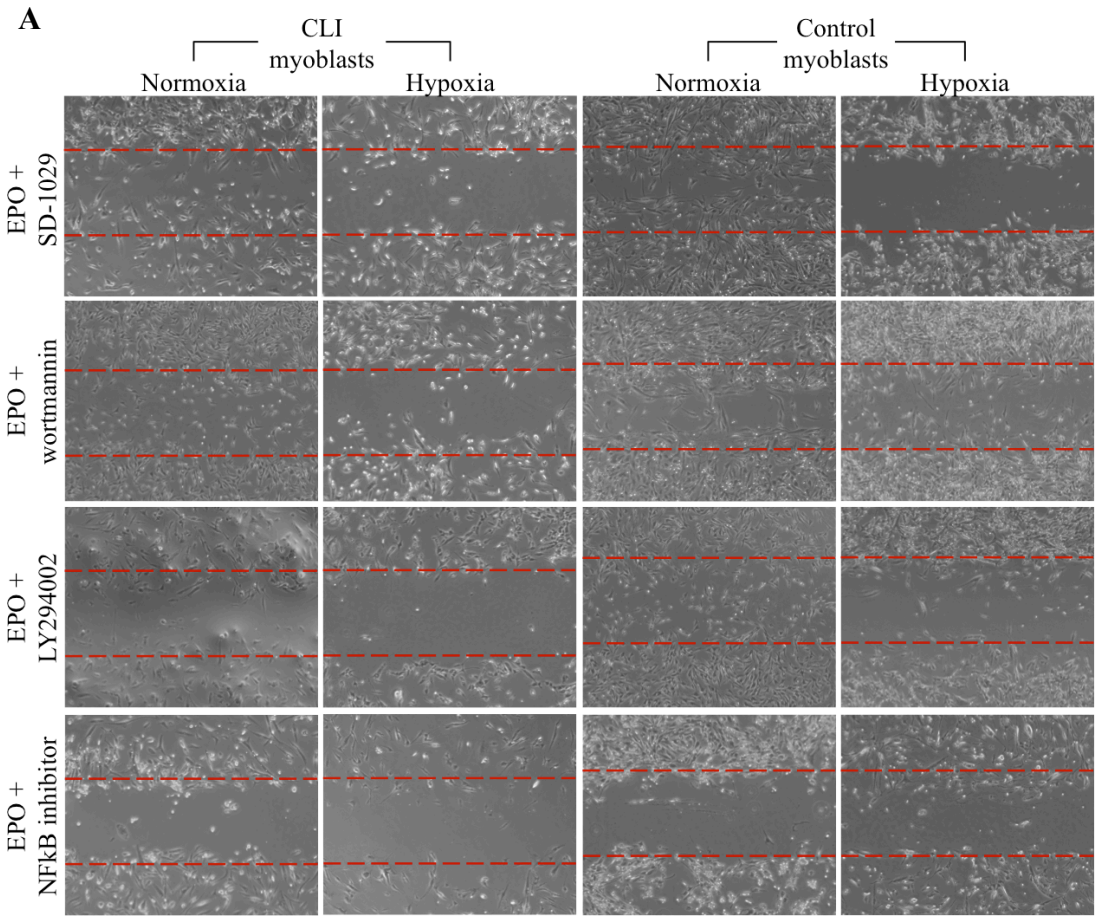
A
CLI myoblasts
Control myoblasts
Normoxia
Hypoxia
Normoxia
Hypoxia
EPO + SD-1029
EPO + wortmannin
EPO + LY294002
EPO + NFkB inhibitor

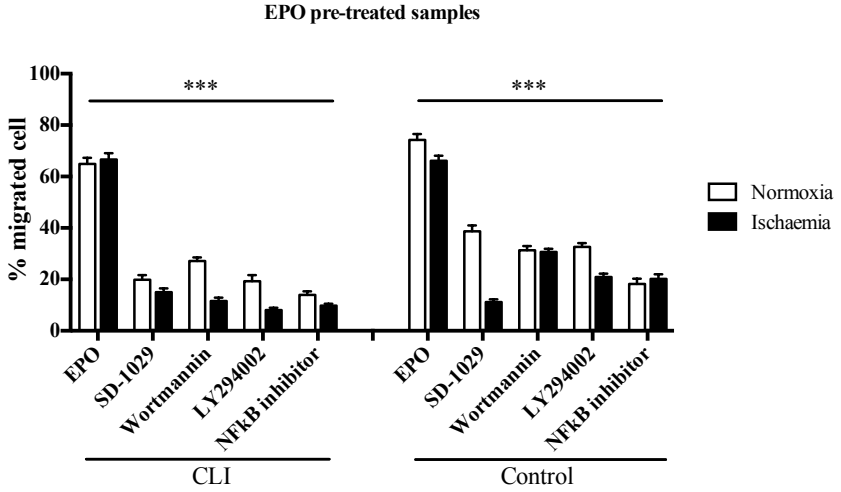
EPO pre-treated samples
% migrated cell
100
80
60
40
20
0
***
***
EPO
SD-1029
Wortmannin
LY294002
NFkB inhibitor
EPO
SD-1029
Wortmannin
LY294002
NFkB inhibitor
CLI
Control
Normoxia
Ischaemia

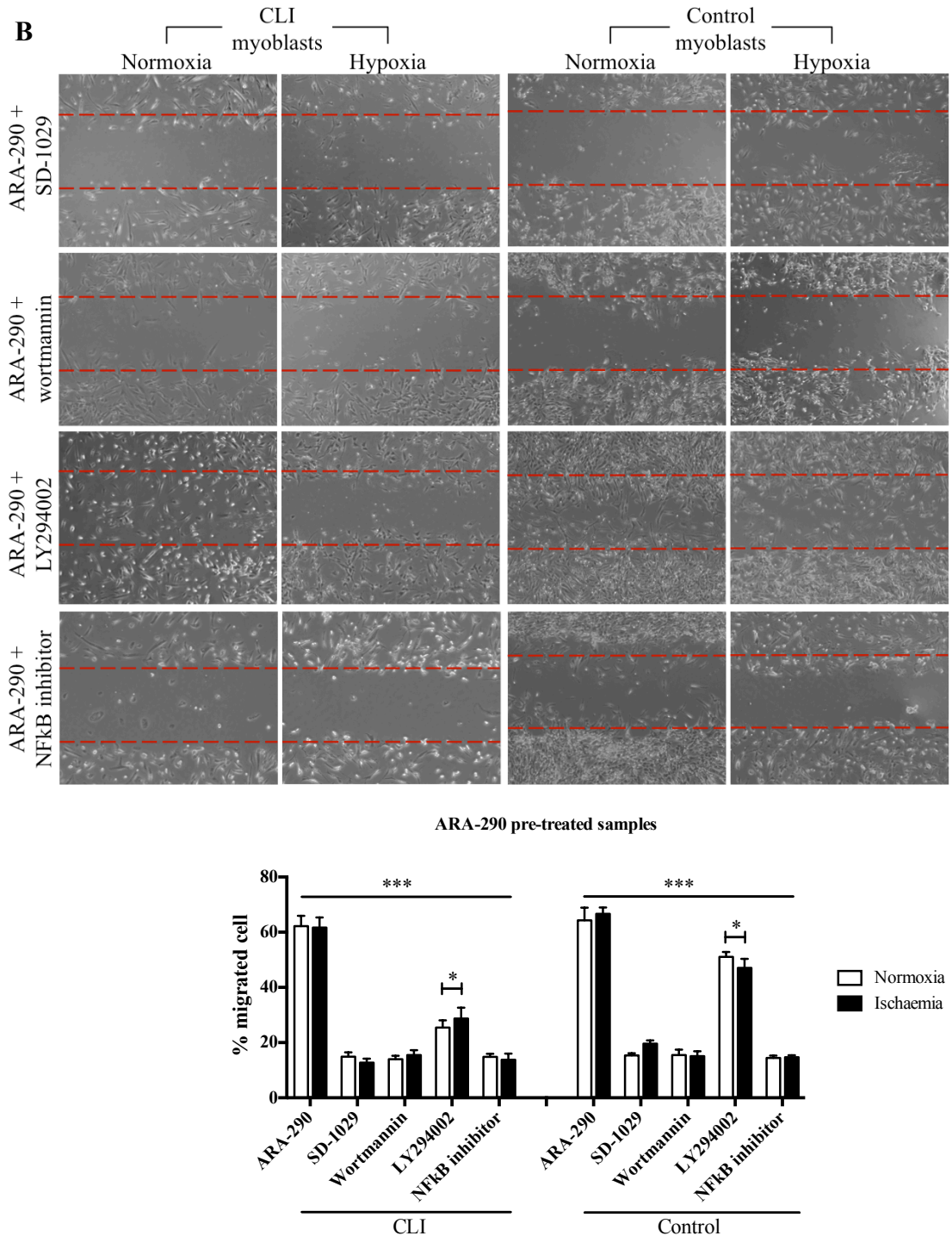

Figure 5.8: Inhibition of EPO and ARA-290 mediated migratory effects

EPO (A) and ARA-290 (B) treated scratch-wounds were concomitantly treated with inhibitors against JAK2/STAT3, PI3k/Akt and NFκB to assess potential signalling cascades in mediating the migratory effects of both compounds. Addition of any inhibitor caused a significant reduction in EPO or ARA-290 mediated improvements in CLI or control myoblast migration ($P<0.05$, one-way ANOVA, $n=5$ both CLI and control).

5.4.5 Effect of ischaemia on human myotube apoptosis and cell death

Western blot analysis of parallel samples of CLI and control myoblasts harvested from normoxic conditions, or following exposure to simulated ischaemia demonstrated an increase in HIF-1α expression in ischaemic samples from both CLI and control myotubes samples (figure 5.9).

Observation of myotubes isolated from CLI and control patients when subjected to simulated ischaemia repeatedly demonstrated lower signal intensity of cleaved caspase-3 in ischaemic samples from CLI myotubes, compared to control myotubes. To quantitatively assess the difference in response to ischaemia of CLI and control myotubes two further techniques were utilised.

Control and CLI myotubes were assessed for caspase-3 and 7 activity using the caspase GLO assay as described above. CLI and control myoblasts in normoxic conditions did not demonstrate any significant difference in levels of apoptosis, as represented by caspase-3/7 activity. Following conditions of simulated ischaemia, both CLI and control myotubes demonstrated a significant increase in caspase-3/7 activity (figure 5.10 A). However, the rise in caspase-3/7 activity between CLI and control myotubes was also significantly dissimilar. CLI myotubes subjected to ischaemia demonstrated approximately 3-fold difference in caspase-3/7 activity compared to normoxic control. On the other hand, control myotubes, following simulated ischaemia, demonstrated approximately 6.75-fold increase in caspase-3/7 activity compared to normoxic control (over 2-fold increase in caspase-3/7 activity compared to CLI myotubes also subjected to ischaemia) (figure 5.10A).

Further assessment of apoptosis and cell death in human myotubes was performed using immunocytochemistry/immunofluorescence techniques. Samples of both CLI and control myotubes subjected to ischaemia were stained for using an anti-annexin V antibodies, in conjunction with propidium iodide (PI) (figure 5.10B).

Control myoblasts exposed to simulated ischaemia demonstrated a greater number of cells positively stained for annexin V – indicating a greater degree of apoptosis in comparison to CLI myotubes under identical conditions. Annexin V staining was most intense in the nuclei, but could also be demonstrated in the cytoplasm. Counterstaining myotubes with PI was used to determine permeability of the plasma membrane to small molecules, indicative of a cell undergoing secondary necrosis.

Similarly to annexin V expression, PI was only detectable in the nuclei of control myotubes following simulated ischaemia. In comparison, CLI myotubes subjected to ischaemia displayed very little nuclear or cytoplasmic annexin V or PI staining, suggesting resilience in apoptotic response to ischaemic injury (figure 5.10 B).

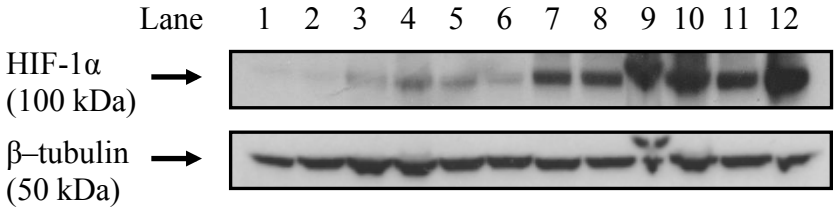

Figure 5.9: HIF-1α expression following simulated ischaemia in human myotubes

Representative Western blot of HIF-1α expression in human cell lysates subjected to ischaemia (lanes 7 – 12), and their parallel normoxic counterparts (lanes 1 – 6). A significant upregulation in HIF-1α expression was observed in ischaemic myotubes. There was no significant difference in HIF-1α expression between myotubes from CLI (lanes 1 – 3 and 7 – 9) or control (lanes 4 – 6 and 10 – 12).

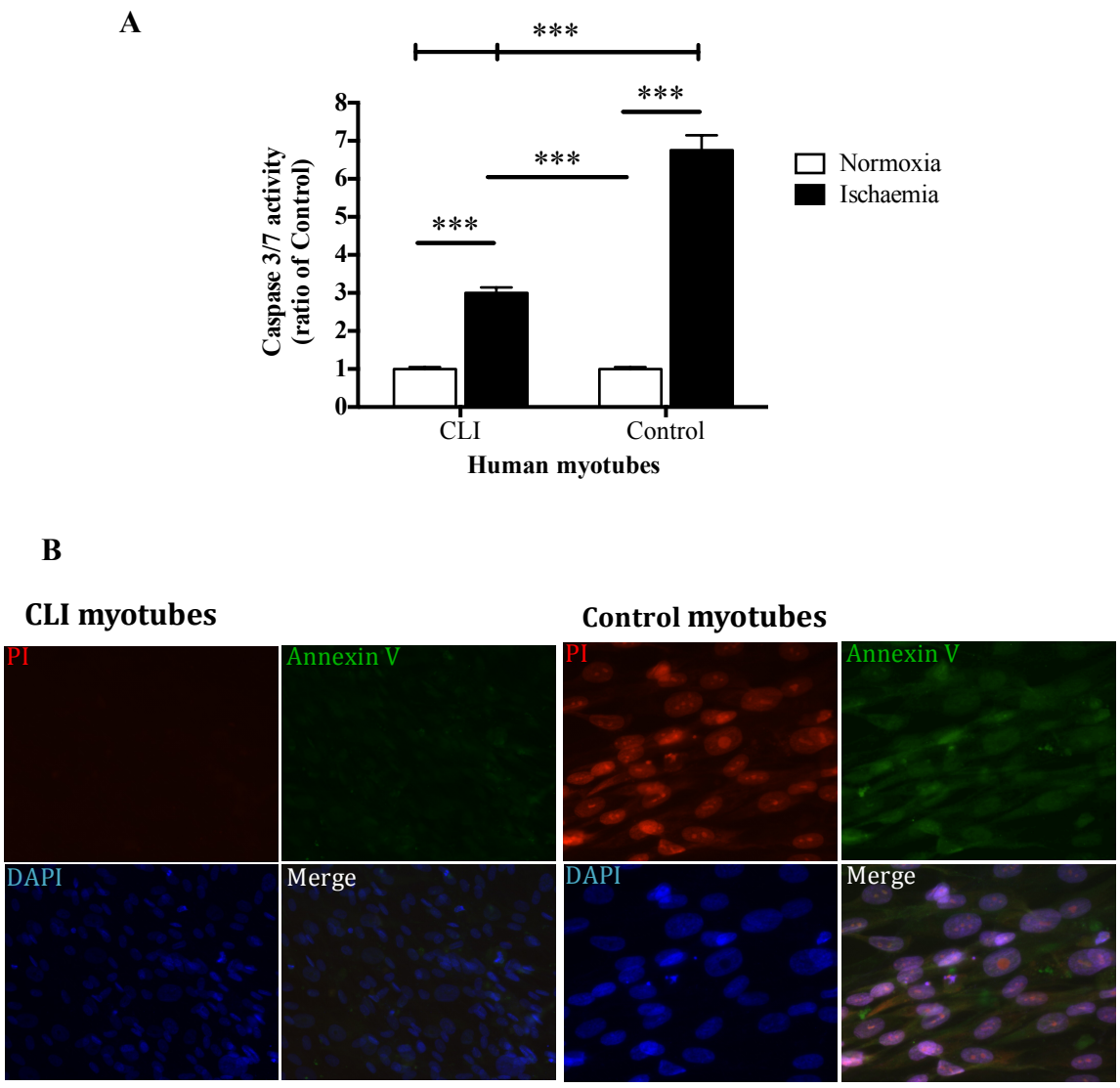

Figure 5.10: Effect of ischaemia on human myotube apoptosis

(A): Quantification of caspase-3/7 activity in CLI and control myotubes demonstrated a significantly reduced susceptibility of CLI myotubes to caspase-mediated apoptosis. Apoptosis was more than 2-fold increased in ischaemic control myotubes, compared to ischaemic CLI myotubes. (P<0.0001 one-way ANOVA, n=6 CLI, n=6 control myotubes)

(B) Immunocytochemistry/immunofluorescence for the apoptotic marker annexin V and PI demonstrated increased apoptosis in control myoblasts. Further there was increased signal of PI suggesting later stages of apoptosis in control myotubes. CLI myoblasts had reduced signal of annexin V staining, and did not counterstain with PI – indicating an intact nuclear membrane.

5.4.6 EPO and ARA-290 mediated reduction in human myotube ischaemia-induced apoptosis and IL-6 release

Pre-treatment of human myotubes with EPO or ARA-290 24-hours prior to induction of simulated ischaemia demonstrated a significant reduction in cleaved caspase-3 expression. The role of phosphorylated-Akt was also investigated and demonstrated increased phosphorylated protein in EPO and ARA-290 treated lysates compared to normoxic or ischaemic controls (Figure 5.11 A and B).

ELISA assessment of cell culture supernatants for release of the cytokine IL-6, demonstrated an increased secretion of IL-6 into supernatant of samples subjected to ischaemia compared to parallel normoxic controls. Pre-treatment with EPO or ARA-290 prior to simulated ischaemia caused a significant decrease in IL-6 concentration compared to ischaemic control samples. A similar trend in IL-6 secretion by either CLI or control myoblasts was detected (Figure 5.12).

5.4.7 Involvement of the JAK2, PI3k/Akt and NFkB signalling pathway

Following EPO pre-treatment a reduction in cleaved caspase-3 expression was observed. Subsequent inhibition using LY294002, wortmannin, SD-1029 or NFκB inhibitor of activation IV demonstrated a significant abolishment of EPO-mediated reduction of apoptosis. As a consequence of inhibition of any of the above molecules there was an increase in cleaved caspase-3 expression above that of the simulated ischaemia control (figure 5.11A).

Following ARA-290 pre-treatment, a reduction in cleaved caspase-3 expression was also observed. Likewise, subsequent inhibition using the above-mentioned inhibitors also caused a decrease in ARA-290 mediated prevention of apoptosis. Similarly to previous findings, inhibition of ARA-290 effect using LY294002 consistently demonstrated less inhibition of PI3k/Akt, coinciding with a reduction in cleaved caspase-3 expression.

The findings described above were consistently found in our human myotube cell lines isolated from CLI or control samples. However, as mentioned earlier, detection of cleaved caspase-3 in CLI lysates required almost 3 times the total quantity of protein to be loaded to adequately detect expression.

Supernatant collected after human myotubes were subjected to simulated ischaemia, prior to myotubes lysis, were assessed for release of the inflammatory cytokine IL-6. Simulated ischaemia caused a significant increase in IL-6 release compared to normoxic controls for each primary human cell line. Pre-treatment of myotubes with EPO or ARA-290 lead to a decrease in IL-6 secretion into cell media as a result of simulated ischaemia. This reduction in IL-6 secretion could be removed when inhibitors against JAK2/STAT3, PI3k/Akt and NFκB were applied to cells prior to simulated ischaemia (Figure 5.12).

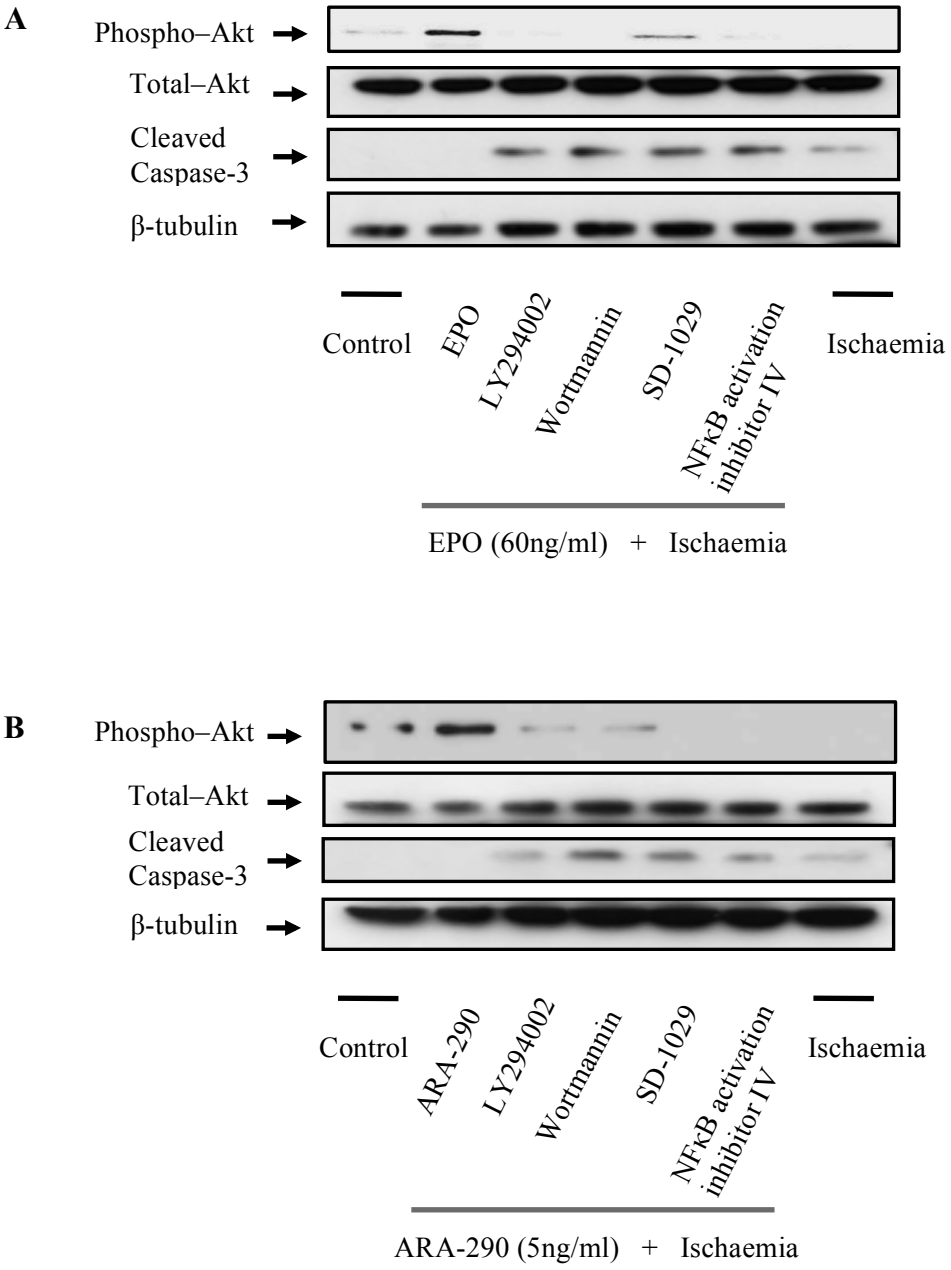

Figure 5.11: EPO and ARA-290 effect on ischaemia-induced apoptosis

Representative Western blots of EPO pre treated human myotubes demonstrating increase expression of cleaved caspase-3 when human myotubes were subjected to ischaemia. Pre-treatment with EPO or ARA-290 cause a reduction in cleaved caspase-3 levels, similar to levels observed in samples not exposed to ischaemia. Further identification of important signalling pathways used by EPO and ARA-290 to mediate myotubes protection revealed important roles of JAK2/STAT3, PI3k/Akt and NFκB, as evidenced by their ability to abolish EPO or ARA-290 mediated improvements in apoptosis.

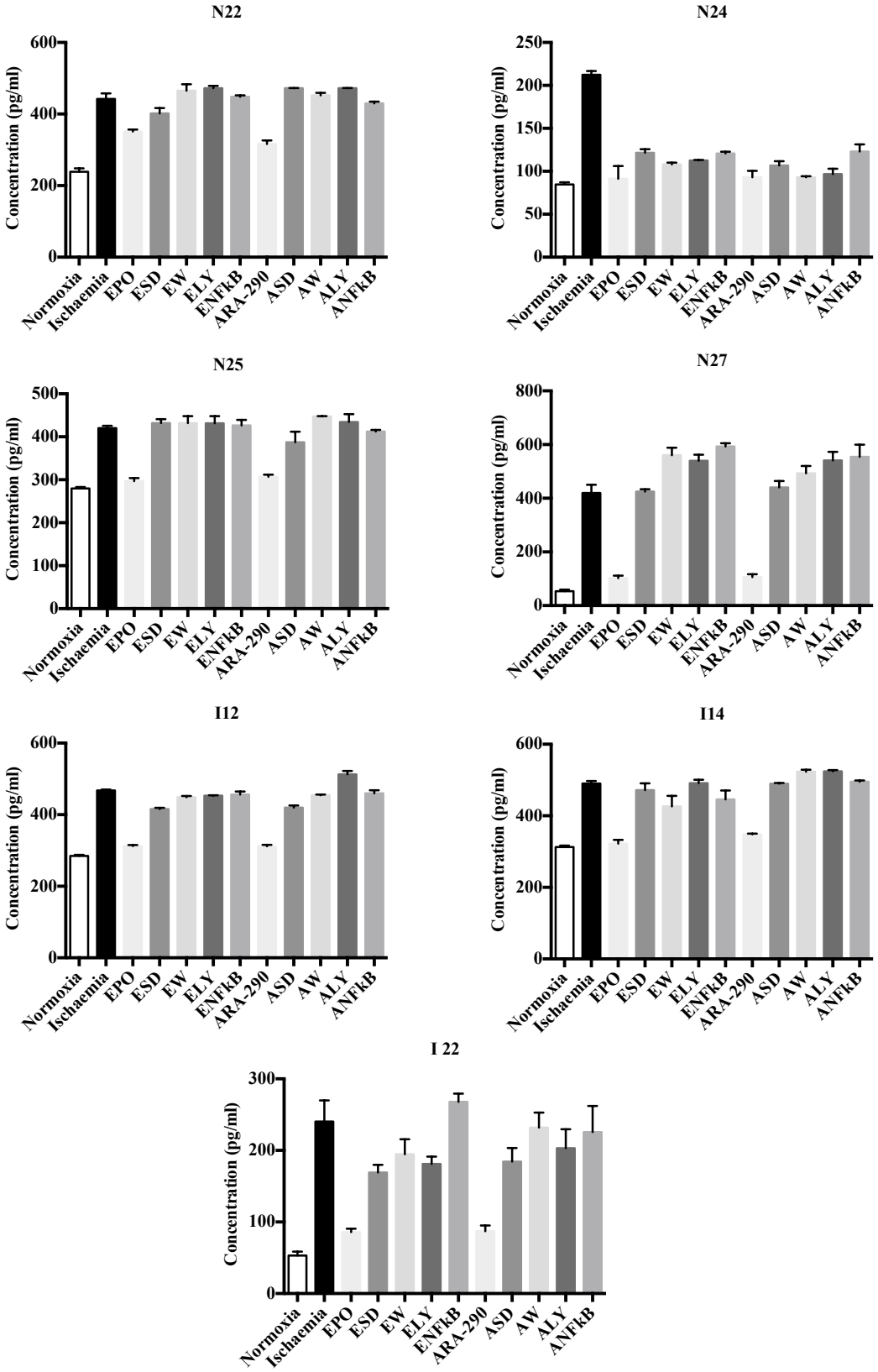

Figure 5.12: ELISA quantification of IL-6 secretion into media following simulated ischaemia, and pre-treatment with EPO or ARA-290.

Simulated ischaemia caused a significant increase in IL-6 production compared to normoxic samples in both CLI and control samples. Pre-treatment with EPO or ARA-290 demonstrated a sustained ability to suppress IL-6 secretion during simulated ischaemia. However, inhibition of JAK2/STAT3, PI3k/Akt or NFκB resulted in a rise in IL-6 secretion.

(N=Control myotubes, I=CLI myotubes, A=ARA-290, E=EPO, SD=SD-1029, W=wortmannin, LY=LY294002, NFκB=NFκB inhibitor of activation IV)

5.5 Discussion

In this study the effect of simulated ischaemia on myoblasts and myotubes from CLI and control patients was investigated. There are no previous reports in the literature of primary isolation of CLI myoblasts – the closest comparison being isolation of myoblasts of healthy individuals after intensive exercise. Therefore, very little investigation has been performed on the fundamental building block of muscle tissue – myoblasts and myotubes – and potential phenotypic alterations as a result of prolonged exposure to ischaemia.

Myoblasts from CLI and control donors demonstrated important functional differences under both normoxic and simulated ischaemia conditions. Leading on from this, differentiated CLI myotubes also demonstrated subtle differences culminating in resistance to simulated ischaemia.

5.5.1 Functional differences in human myoblasts from controls and CLI

Though MTT is often used as a proliferative assay, it relies upon the correlation between cell number and metabolic activity. However metabolic activity within a cell can be influenced by a number of variables – including their response to ischaemic injury – which may account for the lower sensitivity and specificity observed using MTT to highlight potential proliferative differences between human primary myoblasts.

It is a well-recognised fact that skeletal muscle has the ability to repair and regenerate new muscle fibres in response to a variety of injuries (biological, chemical or mechanical) or as a consequence of disease. The processes of repair and regeneration requires the activation of a pool of quiescent muscle stem cells, known as satellite cells, which in response to injury, start to proliferate, and differentiate. Myoblasts are a differentiated form of satellite cells, which in response to myogenic regulatory factors, commit themselves to a myogenic lineage, and then fuse to form myotubes. The differentiation of satellite cells into myoblasts, and their ability to travel to sites of injury is therefore key in the repair and regeneration cycle. Assessment of human skeletal muscle has previously demonstrated an upregulation of satellite cells in CLI muscle, providing evidence of regenerative attempts in response to ischaemic injury [298]. This highlights the possibility that the underlying myopathy observed in CLI

patients is not as a result of a defect in the self-renewal properties of muscle precursor cells, but of later attempts to repair muscle at sites of injury.

Impaired migration and contractile ability of CLI-isolated myoblasts compared to control myoblasts was another significant finding. Though the reasons for this decreased contractile ability in CLI myoblasts are likely to be manifold, a plausible explanation is the reduced mitochondrial activity previously described in CLI patients [118]. Mitochondrial dysfunction has been identified in the skeletal muscle of CLI patients. In addition, defective electron transport chain complexes (mainly ETC I and III) cause increased reactive oxygen species damage to the skeletal muscle [124]. Muscle, under aerobic and anaerobic conditions, has an absolute requirement for ATP in order to contract. In combination, this leads to the idea that CLI myoblasts are likely to exhibit a deficit in myoblast contraction due to their impaired mitochondrial activity leading not only to less forceful contractions but also earlier fatigue and fewer contractions [343, 344]. Another well-known clinical scenario where ischaemia is responsible for impaired functional contractility is myocardial infarction. In this scenario, following the ischaemic period, the infarct becomes invaded with inflammatory cells, and then subsequently myofibroblasts colonise the wounded infarct area and remodelling occurs, creating a stable, but immobile and less contractile scar. CLI muscle at the time of biopsy harvest is macroscopically more fibrotic than healthy non-ischaemic muscle. This is also likely to account for the discrepancy between myoblast purity following isolation between CLI and control myoblasts. However the work conducted above did not specifically focus on myofibril contraction typically associated with muscle function, which would require the differentiated form of myotubes, and is often observed *in vitro* as myofibril twitching, or analysed using techniques which are capable of transducing and measuring a contraction force, such as isometric and eccentric force generated.

A relevant phenomenon is the conferred resistance to ischaemic injury as a result of previous exposure to ischaemia – known as ischaemic pre-conditioning [345, 346]. In those situations, although the exposure to ischaemia is usually for an acute period, the underlying mechanisms may be applicable. The increased resistance of CLI myoblasts and myotubes to simulated ischaemia was a repeated finding in this chapter, and quantification of caspase-3/7 activity and annexin V staining resulted in clear indications of significant difference between the response of CLI and control

myoblasts to ischaemia. Through survival in a chronically ischaemic niche, it is possible that CLI myoblasts have been pre-conditioned, or that additionally they have developed pertinent adaptations which allow them to better withstand a second ischaemic insult.

5.5.2 EPO and ARA-290 influence on human myoblasts and myotubes

Treatment of CLI or control myoblasts and myotubes with EPO or ARA-290 resulted in improvement of observed detrimental responses to simulated ischaemia. This included improved migration of myoblasts, and reduced susceptibility of myotubes to ischaemia-induced apoptosis and subsequent secretion of the pro-inflammatory cytokine IL-6.

The influence of different signalling molecules on EPO and ARA-290 mediated cytoprotection was examined by investigating a number of molecules known to facilitate EPO-mediated erythrocyte precursor survival. In the previous chapter, inhibitors of JAK2/STAT3, PI3k/Akt and NFκB demonstrated a significant inhibitory effect on EPO and ARA-290 cytoprotective effects. Their impact on human myoblasts and myotubes was similarly valid. In both CLI and control myoblasts and myotubes, addition of any of the above inhibitors to EPO or ARA-290 pre-treated samples resulted in reduced migration and increased apoptosis. This identifies key roles of JAK2/STAT3, PI3k/Akt and NFκB in human cell signalling, as well as murine cells. However, the effect of ischaemia on cellular mechanisms is not limited to these molecules only, and recent observations of the JAK1, STAT5, MAPK and TLR signalling cascades are just a handful of other important molecules within the deluge of interacting molecules arbitrating the effects of ischaemia. EPO is known to have interactions with most of these molecules, and therefore the potential interaction with ARA-290 remains to be investigated.

The ability of both EPO and ARA-290 to dampen the secretion of IL-6 may account for their ability to attenuate secondary injury by removing the noxious pro-inflammatory damage often triggered by the primary tissue injury. EPO has already been explored in this role, and evidence has shown its antagonistic effects to TNF-α – a well-known pro-inflammatory cytokine – in order to limit collateral injury [347]. The opposing roles of EPO and TNF-α in inflammation have been identified in other human disease pathologies including rheumatoid arthritis and myelodysplastic

syndromes [348, 349]. Recent studies assessing ARA-290's ability to reduce inflammatory cytokines has also identified efficacy at reducing levels of IL-6, TNF-α and other cytokines (IL-1β, IL-8 and MCP-1) following injury [249, 260, 350].

Although *in vitro* models do not fully recapitulate the *in vivo* environment, the rapid and high-throughput screening of target molecules, oligonucleotides and novel hypotheses and strategies can be easily assessed by cell-culture systems, prior to more extensive validation in animal models, which possess both time and cost implications.

The main drawbacks of using *in vitro* human explant primary cell cultures is their limited proliferative capacity, behavioural heterogeneity due to donor age and genetic composition, and their variation in phenotype as culture and passage progress [351-353]. However, they often yield more valid results than immortal cell lines, and therefore provide a useful bridge to clinical assessment [354, 355].

5.6 Summary

Isolation of human myoblasts from our clinical group of interest provided insight into fundamental adaptations they have accumulated due to a chronically ischaemic environment. Both CLI and control myoblasts offered suitable alternatives to the C2C12 skeletal muscle *in vitro* model, allowing repeated observations of their function and responses to simulated ischaemia.

CHAPTER 6

Effect of ARA-290 *in vivo* in a murine model of hindlimb ischaemia

6.1 Introduction

Whilst there is an evident utility of *in vitro* methods for its amenability to the high-throughput analysis and testing of novel hypotheses and therapies, as well as the ability to finely control numerous parameters, assessment of many diseases is often more complex than the majority of single or co-cultured experimental offerings. An *in vivo* model is also often a pre-requisite to establishing novel therapies before their permitted use in human clinical trials. *In vivo* models, though not usually performed on the end-target species, do provide a more relevant platform for analysis, by incorporating many of the multiple organ-systems, molecular and cellular interactions and associated signalling pathways, and complexities, making it more representative of the human disease pathology being investigated when an appropriate and relevant model is used. In this project, the use of a murine hindlimb ischaemia model as a pre-clinical model of CLI provided a useful means of assessing the potential therapeutic capability of EPO and ARA-290.

In the previous chapters, the cytoprotective potential of EPO and ARA-290 was demonstrated first in an established murine myoblasts – myotubes cell line, and then in a novel *in vitro* model of human myoblasts – myotubes using cells derived from both CLI and control patients. In both models, EPO and ARA-290 demonstrated an ability to prevent ischaemia-induced apoptosis in these single cell-type cultures. Despite its promising role in mediating cytoprotection *in vitro* this needs to be translated into a model that encompasses the multiple aspects often found in occlusive arterial diseases, such as PAD. This includes the response of the occluded vasculature, as well as the impact upon surrounding muscle, which forms the primary bulk of tissue found in the limb and is reported as being the most sensitive and vulnerable tissue in the limb to ischaemia [340].

6.1.1 Severity of hindlimb ischaemia model

A model of CLI was first described in 1953, achieved by injecting thrombin and a sclerosant into the femoral artery of a rabbit hindlimb [356, 357]. Since then, a number of different methods for inducing ischaemia in the hindlimb, both surgical and newer endovascular techniques have been described, each manifesting in slight, but distinct, modifications in terms of vascular injury and potential regeneration as well as consequent surrounding tissue injury observed in the model [285, 358-364]. Most commonly, hindlimb ischaemia is induced by surgical ligation or interruption of the arterial (inflow) vessels of the lower limb. However, there is no standardised method for inducing hindlimb ischaemia, and this may be due, in part, to the relative endpoint being examined by different users. In addition, considering the heterogeneous nature of PAD manifestations, it is desirable to have a model that can likewise, be manipulated to represent all the different pathological features of PAD. The hindlimb ischaemia model is used, in various forms, to assess a variety of different therapeutic options, including angiogenesis, arteriogenesis, and tissue protection potential of different agents, and therefore slight modifications in the protocol make the model more relevant to each area of PAD study. For example, a single ligation of the femoral artery, just distal to the origin of the profunda femoris, without excision will result in milder ischaemia, more comparable to intermittent claudication than CLI [365]. With this model, collaterals are left viable and intact and as a consequence, blood flow to the limb is usually completely restored within 7 days [358].

Alternatively, using a double ligation method, placing the proximal ligature just proximal to the bifurcation that gives rise to the profunda femoris at the inguinal ligament, and excising the intervening segment until the distal ligature, which is placed just proximal to the bifurcation of the popliteal artery around the knee joint, a model of hindlimb ischaemia which is more severe than single ligation is created. This is due to the disruption and removal of much of the collateral bed, which results in far reduced blood flow that is prolonged for up to 28 days [358].

In comparison, a ligature can be placed far more proximally, in the region of the external iliac artery with ligation of all distal branches until the level of the popliteal artery. The region of vessel between the two ligations (external iliac to popliteal

artery) is excised, resulting in a very severe model of ischaemia, which very rapidly leads to necrosis and auto-amputation of the affected limb. This model is at the most severe end of the spectrum, and is not often utilised as a representative model CLI [361].

6.1.2 Modifications of the hindlimb ischaemia model

In addition to alterations in surgical technique, it is possible to influence the severity of the hindlimb ischaemia model by selecting certain laboratory mice strains, using transgenic strains to mimic known risk-factors or co-morbidities associated with disease and aging animals.

Inter-strain variability

Two of the most commonly used mice strains – BALB/c and C57BL/6 – have vastly different responses in natural recovery to hindlimb ischaemia. This is due to differences in distribution of collateral arteries and the response of the collateral circulation as a result of obstruction to arterial flow. BALB/c strains have reduced native collaterals compared with C57BL/6 and therefore show slower recovery after induction of hindlimb ischaemia, providing a larger window of assessment [366, 367].

Co-morbidities

Patients with PAD typically suffer from multiple co-morbidities including diabetes mellitus, hypercholesterolaemia and hypertension. All of these factors have been extensively investigated and are known to contribute to the pathology of PAD through inflammation, endothelial dysfunction and oxidative stress. However transgenic strains modelling the majority of human diseases now exist, and can be used in conjunction with the hindlimb ischaemia model to more accurately mimic the PAD state.

Age

The prevalence of PAD increases with age, whereas the majority of hindlimb ischaemia studies will use mice aged 8-12 weeks. A mouse would need to be aged for approximately 2½ years to age-match a 75-year-old human. This involves considerable cost implications to house and age mice for such a period.

6.2 Aims

Since the first study of hindlimb ischaemia was published there has been a multitude of different techniques described to induce hindlimb ischaemia. It is important to select a model which will result in an adequate degree of ischaemia for the purpose of the study as well as ensuring the period of hindlimb ischaemia is appropriate for the time-course studied, and representative of the disease being modelled.

A preliminary aim was therefore to establish a suitable model of hindlimb ischaemia by assessing a variety of different levels of the double ligation model, commonly used strains, and also the age of animals used and the consequent outcomes. The quantification of the hindlimb ischaemia model was assessed by conventional techniques including LDPI and H&E microscopic assessment of the hindlimb muscles – gastrocnemius and tibialis anterior. In addition to disruption in blood flow, measured by LDPI, it was vital to produce a model of hindlimb ischaemia which was relevant to CLI, and which mimicked characteristic alterations in muscle pathology observed in human disease.

The greater objective of this chapter aims to assess the therapeutic potential of ARA-290 in a pre-clinical CLI model, and compare its tissue-protective potential with EPO which has previously demonstrated tissue-protective functions in other settings of ischaemic injury. Tissue protective capabilities was assessed by outcomes including functional ability, return of blood flow using LDPI, and histological evaluation of ischaemic and inflammatory damage to muscle and attempts at regeneration.

6.3 Methods

All animal studies described in this chapter were licensed under the UK Home Office Animals (Scientific Procedures) Act 1986, project license number 70/7087.

Experimental procedures were designed, first to assess the feasibility of different hindlimb ischaemia models to provide an adequate and representative pre-clinical model of CLI, and secondly to assess the therapeutic potential of a novel synthetic peptide – ARA-290.

6.3.1 Establishing parameters for a model of hindlimb ischaemia

Variations in surgical technique

Two models of hindlimb ischaemia were evaluated. Surgically, both involved double ligation of the arterial inflow supply, but differed in terms of the location of the proximal ligature. Briefly, a 1 cm incision was made in the groin area in both scenarios to gain exposure of the femoral artery around the level of the inguinal ligament. In the less severe hindlimb ischaemia model the femoral artery was ligated just distal to the bifurcation of the profunda femoris and just proximally to the bifurcation of the popliteal artery. The intervening segment (approximately 10 mm) was also excised. In the more severe model, the proximal ligature was placed just proximally to the bifurcation of the profunda femoris, and the distal ligature again placed just proximally to the bifurcation of the popliteal artery. The intervening segment was also excised (approximately 12 mm). In both operative procedures, care was taken to avoid damage to surrounding structures (vein and nerve) and the skin was closed using 6-0 vicryl sutures. Both surgical procedures were performed on the C57BL/6 background strain, with mice aged 8 weeks.

Common laboratory mice strain

The two commonest strains of mice used for assessing hindlimb ischaemia are BALB/c and C57BL/6. Mice from each strain, obtained in-house from UCL comparative biological unit, at 9 weeks of age, were assessed for their ability to provide an acceptable model of hindlimb ischaemia. The more severe hindlimb ischaemia technique discussed above was introduced in animals of each strain, and assessed over a time-course of 21 days.

Age of mice

Incidence of PAD rises sharply with age in human subjects, therefore investigation into the effects of aged mice and the resultant influence on the model was investigated. The hindlimb ischaemia model was performed on aged mice (16 weeks of age) and compared with young animals (6 weeks of age). Both young and old animals were sourced from the BALB/c strain. There is however a trade-off that needs to be made between the costs required to house and age animals and advantages in replication of a disease mainly prevalent in older members of the species.

6.3.2 Assessment of ARA-290 in an *in vivo* hindlimb ischaemia model

Immediately following induction of hindlimb ischaemia, animals were randomised to receive either saline vehicle control (n=4), Eprex® (3000IU/kg; n=6), low-dose ARA-290 (30μg/kg; n=6), or high-dose ARA-290 (60μg/kg; n=6), all via intra-peritoneal injection. Mice received subsequent doses on days 2, 4, 6, 8 and 15 postoperatively until the relevant endpoint. Sham operated animals followed the same anaesthetic and operative procedure but did not undergo ligation of femoral artery. In addition, they received the same post-operative analgesic care, but no subsequent interventions until the relevant endpoint.

At the relevant endpoints, animals were first transferred to an open field for assessment of functional outcomes as described in chapter 2.5.4, then anaesthetised using Avertin for assessment of paw perfusion using LDPI, collection of whole blood, and collection of hindlimb muscles for histological analysis.

Histological analysis of mouse hindlimb muscle included routine H&E stain to assess tissue morphology following ischaemic injury and assessment of C:F ratio using endothelial cell markers (CD34). To investigate the effects of ARA-290 on ameliorating ischaemia-induced tissue injury, images were recorded of the stained sections. 2 high-powered fields of view were taken of both the gastrocnemius and tibialis anterior muscles of the operated limb and 1 high-powered field of view for both the gastrocnemius and tibialis anterior muscles of the non-operated limb for comparison. Scoring of the muscle sections was conducted in a blinded fashion by 5 assessors for H&E sections, and 3 assessors for all other staining. Assessment of proliferative index was performed using immunohistochemistry to detect the Ki-67

protein – known to be strictly associated with cell proliferation. Using sections stained for Ki-67 all images were analysed using ImageJ software, and the 'cell-counter' plug-in (v1.47, http://rsbweb.nih.gov/ij). Ratios of proliferative (positive staining): resting (no staining) cells were calculated and assessed.

6.4 Results

6.4.1 Initial assessment of hindlimb ischaemia model

In the preliminary study, a number of different permutations of animal, age and surgical technique were explored, yielding quite varied impact upon the duration of flow disruption, and muscle fibre injury, as evidenced by histological analysis, as detailed below.

Surgical technique

With the less severe model, analysis of LDPI results demonstrated resolution of blood flow disruption to almost 75% or normal, or full, flow by day 7. By day 21 blood flow had achieved 95% in the ligated limb, compared to the contralateral un-operated limb. In comparison, using the modified, more severe hindlimb ischaemia model, by day 7, blood flow had returned to only 40% of full flow, and 80% of full flow by day 21 (Figure 6.1).

Histological analysis of FFPE sections, stained with H&E, demonstrated slight variation in muscle fibre damage observed in each operative technique. In the less severe model at day 7 tissue architecture looks normal, and at day 21 there is some muscle fibre size variation but nuclei still reside around the periphery of each fibre. In comparison, in the more severe ligation, tissue architecture looks abnormal. At day 7, there is evidence of inflammation and muscle fibre necrosis, in addition to loss of peripheral nuclei. By day 21, tissue structure remains abnormal, a number of fibres have centrally located nuclei, indicative of muscle fibres attempting regeneration (figure 6.2).

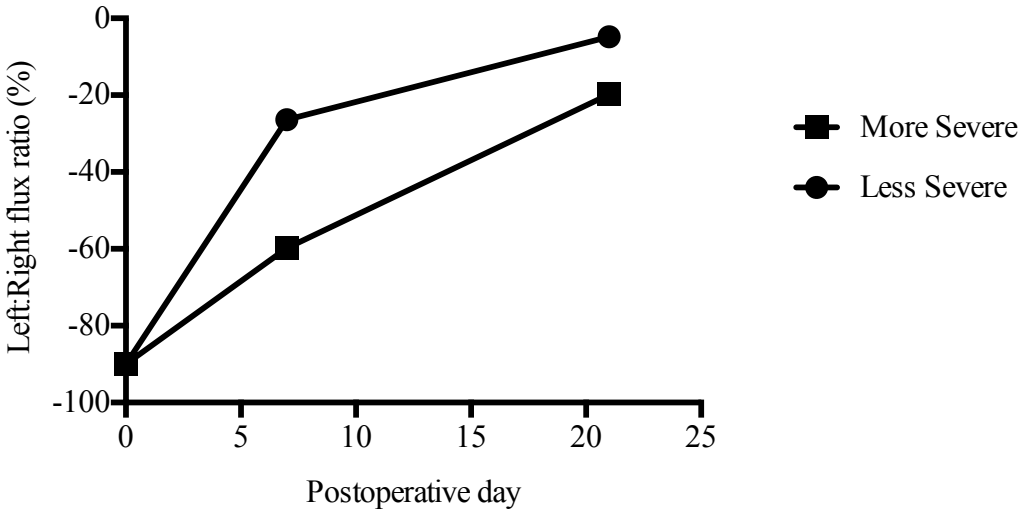

Figure 6.1: Recovery of paw perfusion following different severity of hindlimb ischaemia

Paw perfusion appears to recover faster and to a greater extent in the less severe femoral artery ligation model compared to the more severe ligation (n= 2 per group and at each time point).

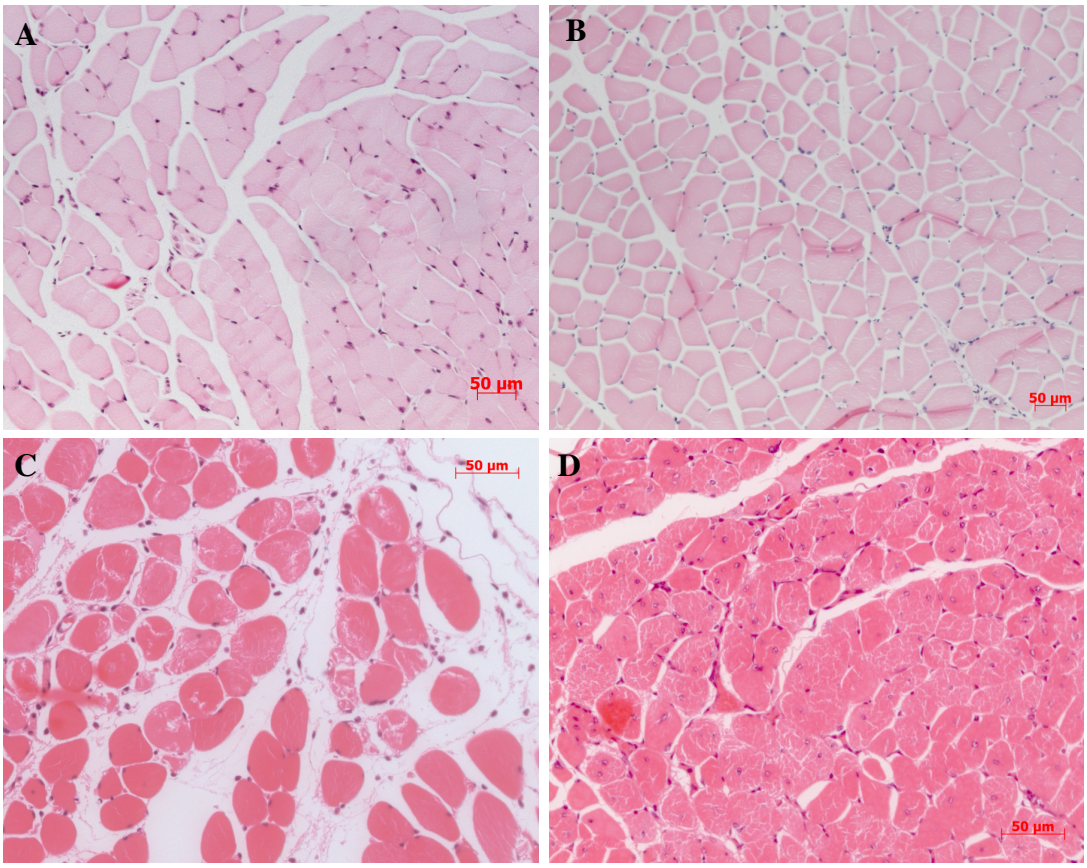

Figure 6.2: Muscle injury following different severity of hindlimb ischaemia

A and B: Representative H&E sections from less severe hindlimb ischaemia model at day 7 (A) and 21 (B). Tissue architecture maintains features of normal skeletal muscle at both the early and late time points, with little evidence of muscle injury. C and D: Representative H&E sections from a more severe hindlimb ischaemia model at day 7 (C) and day 21 (D). Muscle sections show features of muscle injury at both early and late time points including variation in fibre size and sarcoplasmic destruction. Scale bars = 50µm.

Background strain of mouse

Comparison of LDPI results between the BALB/c and the C57BL/6 strains at day 7 demonstrated a significant difference in the perfusion ratio between ischaemic and non-ischaemic limbs, with the BALB/c strain showing less resolution of perfusion. The C57BL/6 strain demonstrated approximately 20% greater perfusion ratio compared to BALB/c mice at the day 7 (Figure 6.3). This finding was sustained, and the difference in perfusion ratio between the two strains increased to 30% greater perfusion in C57BL/6 animals at the day 21 endpoint. The BALB/c animals demonstrated 68% perfusion in the operated limb in comparison to the non-operated limb at day 21.

In both strains of mice histological analysis using routine H&E of samples displayed typical feature of skeletal muscle injury in muscles isolated from the operated limb. These features included signs of necrosis with gross infiltrating inflammatory cells and sarcoplasmic destruction as well as variation in muscle fibre size. There was however, some difference in the severity of the muscle injury displayed. Animals from the BALB/c strain showed diffuse inflammatory infiltrate in comparison to C57BL/6 mice, which showed little, or very discrete areas of inflammation, at any time point. The BALB/c animals also showed greater susceptibility to muscle necrosis, observed as large pyknotic nuclear clumps. Progression of ischaemic injury in the BALB/c mice also lead to adipogenic and fatty connective tissue areas, whereas the C57BL/6 strain did not demonstrate such features (figure 6.4).

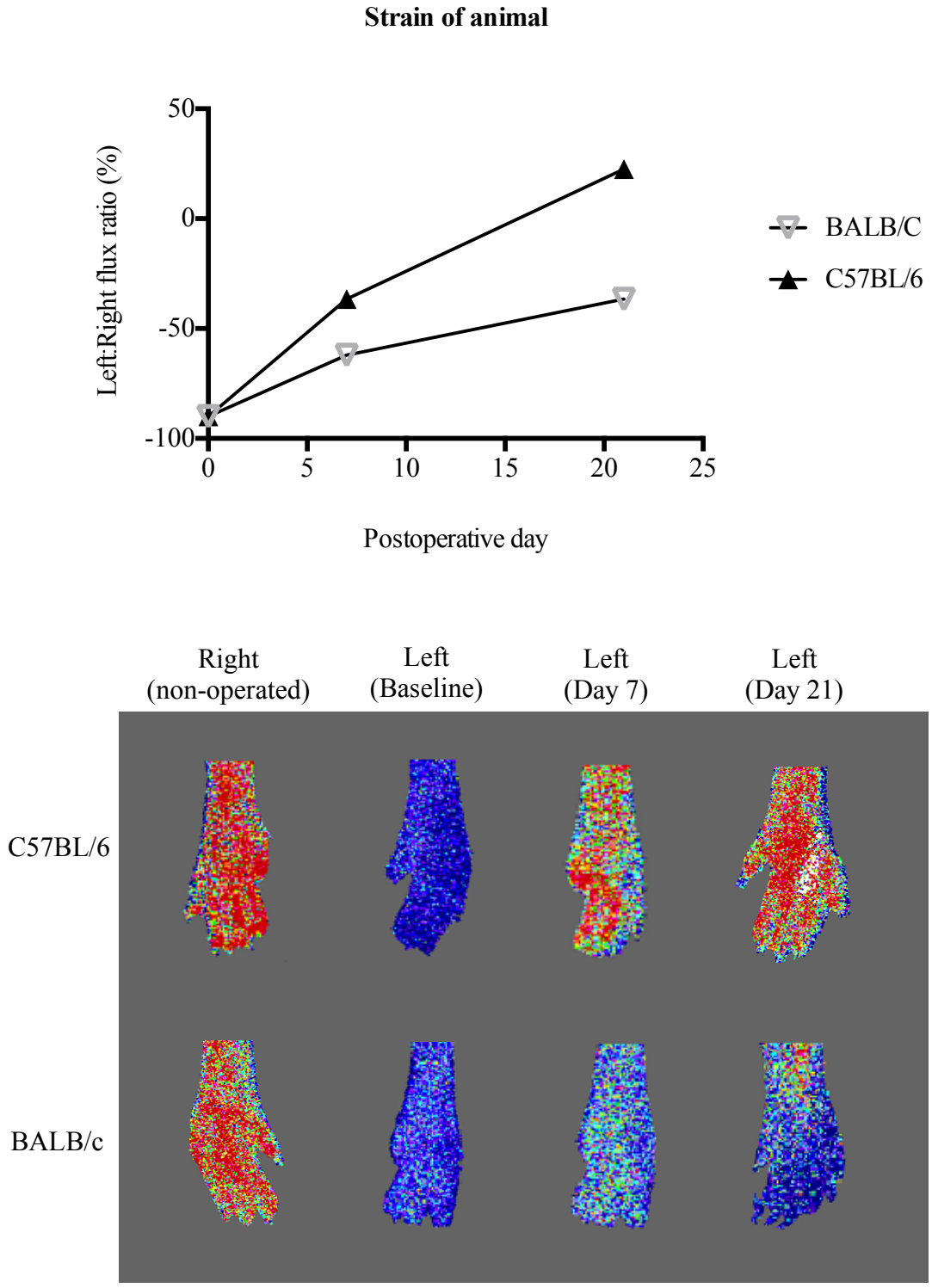

Figure 6.3: Natural recovery of paw perfusion in different strains of laboratory mice

Paw perfusion appears to recover faster and to a greater extent in the less severe femoral artery ligation model compared to the more severe ligation (n= 2 per group and at each time point).

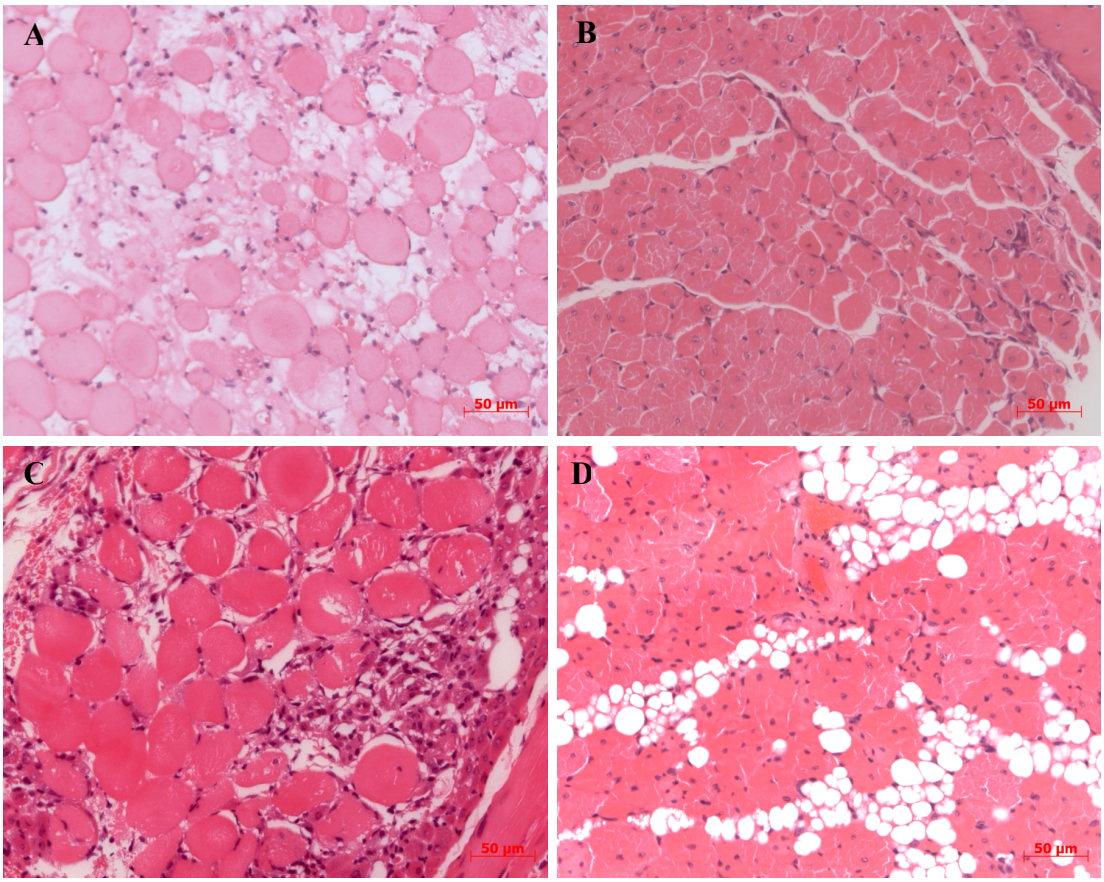

Figure 6.4: Effect of common laboratory strains of mice on hindlimb ischaemia model

A and B: Representative H&E sections from C57BL/6 hindlimb muscle at day 7 (A) and 21 (B). Tissue retains structural architecture, with evidence of muscle injury including sarcoplasmic destruction and variation in fibre size. C and D: Representative H&E sections from BALB/c hindlimb muscle at day 7 (C) and day 21 (D). Muscle sections show features of muscle injury at both early and late time points including gross inflammatory infiltrates, variation in fibre size and replacement of muscle fibres by fibrotic fatty tissue. Scale bars = 50µm.

Age of mice

Analysis of the hindlimb ischaemia model in 6 weeks old mice (young) compared to 18 weeks old mice (old) displayed markedly prolonged disruption in re-perfusion in the older animals. At day 7, a 20% difference in perfusion ratio was observed between the young and older mice. This finding was persistent and increased at the day 21 endpoint, when the difference in perfusion ratio between the young and old animals increased to 36%, with the older animals achieving only 48% perfusion in the operated limb, compared to the non-operated limb (Figure 6.5).

Figure 6.6 shows observations following H&E staining of muscle sections from the operated limb. Younger animals had milder signs of muscle injury, both in the early and late phases analysed. It was only possible to detect very defined regions of muscle regeneration (Figure 6.6A), or infiltration of inflammatory cells (Figure 6.6 B), and at all time points observed, the majority of each muscle area did not display overt features of ischaemic injury. In contrast, observations of the older animals following hindlimb femoral artery ligation showed gross tissue abnormalities which became more severe with progression of time. In the initial stage following ligation, there was evidence of muscle fibre necrosis as seen by pyknotic nuclear clumps and infiltration of muscle tissue by inflammatory cells (Figure 6.6C). The muscle damage observed progressed into fibrotic changes towards day 21, and those areas where muscle fibres remained showed attempts at regeneration (Figure 6.6D).

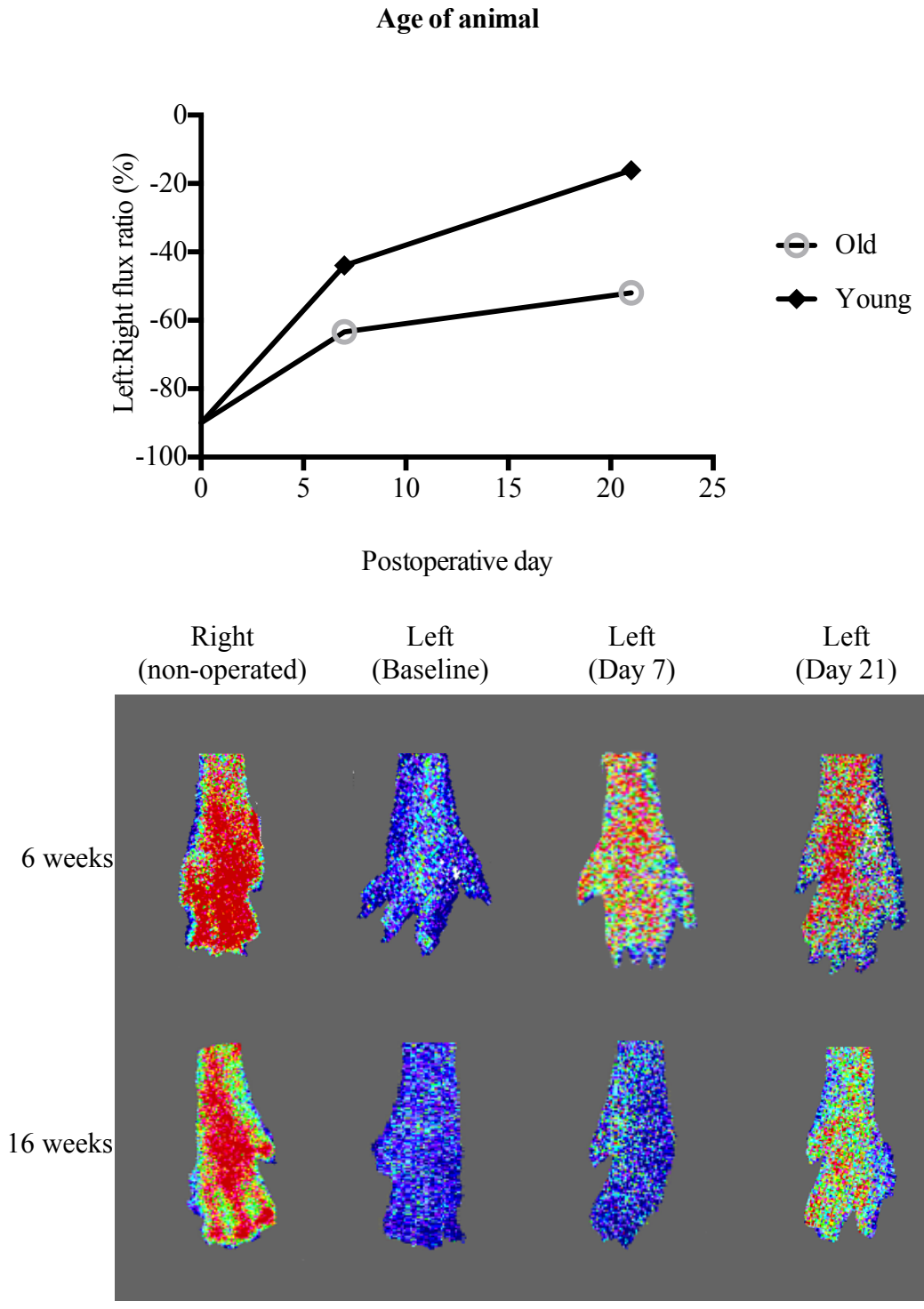

Figure 6.5: Natural recovery of paw perfusion following hindlimb ischaemia induction in mice of different ages

Paw perfusion appears to recover faster and to a greater extent in younger mice (6 weeks of age) compared to older (16 weeks of age) mice (n=2 per group and at each time point).

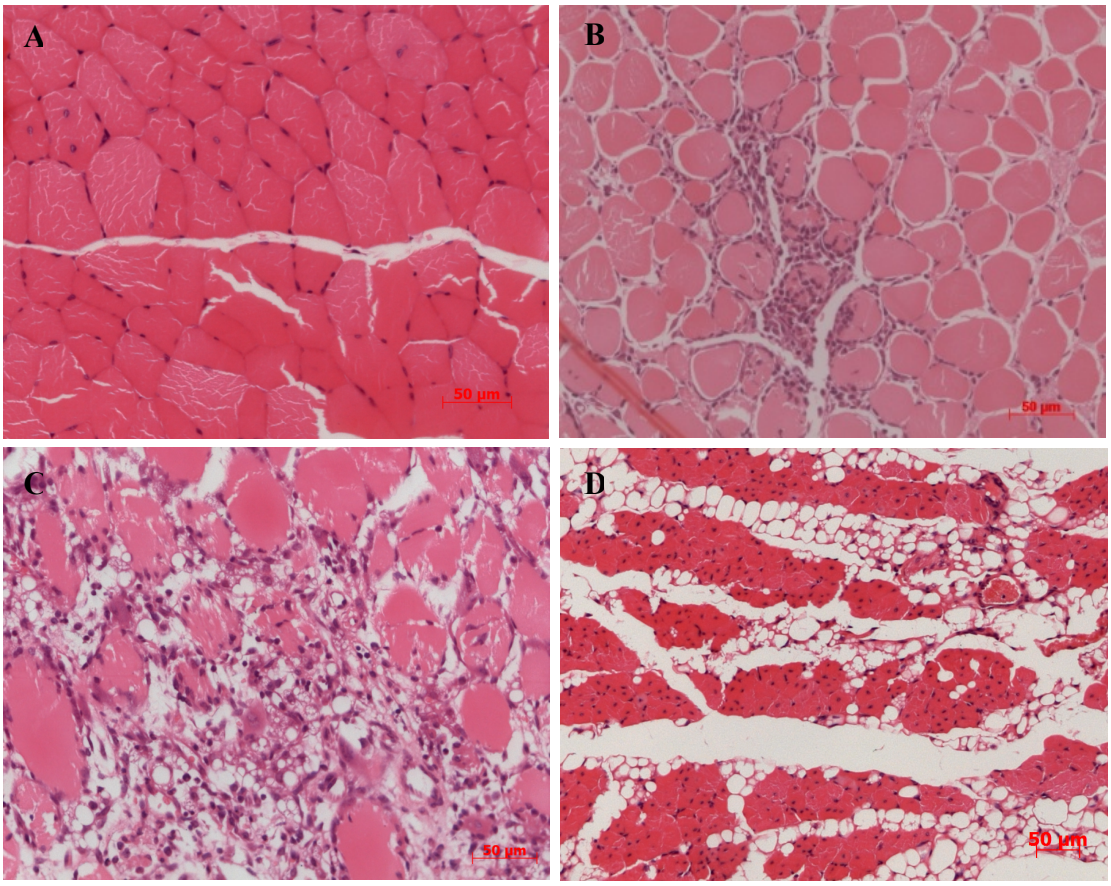

Figure 6.6: Effect of animal age on hindlimb ischaemia model

A and B: Representative H&E sections from young mice hindlimb muscle at day 7 (A) and 21 (B). A: Tissue retains structural architecture, and demonstrates little evidence of muscle besides a small number of fibres with central nuclei. Even at later stages (B), a small degree of localised inflammatory infiltrate can be observed. C and D: Representative H&E sections from older mice hindlimb muscle at day 7 (C) and day 21 (D). Muscle sections show features of severe inflammatory infiltrate and necrosis of muscle fibres in the early stages (C), which appears to lead to muscle fibre necrosis and replacement of extensive areas with fibrotic fatty tissue. Scale bar = 50µm.

Summary of hindlimb ischaemia model development

Comparison of LDPI perfusion images identified the more severe ligation technique, BALB/c strain and older mice as demonstrating the most prolonged period of perfusion mis-match between left and right limbs (Figure 6.7). A similarly increased degree of muscle tissue damage was also evident on comparison of H&E sections from the various hindlimb groups. Therefore for subsequent experiments, the severe ischaemia model on 12 weeks old BALB/c strain was used.

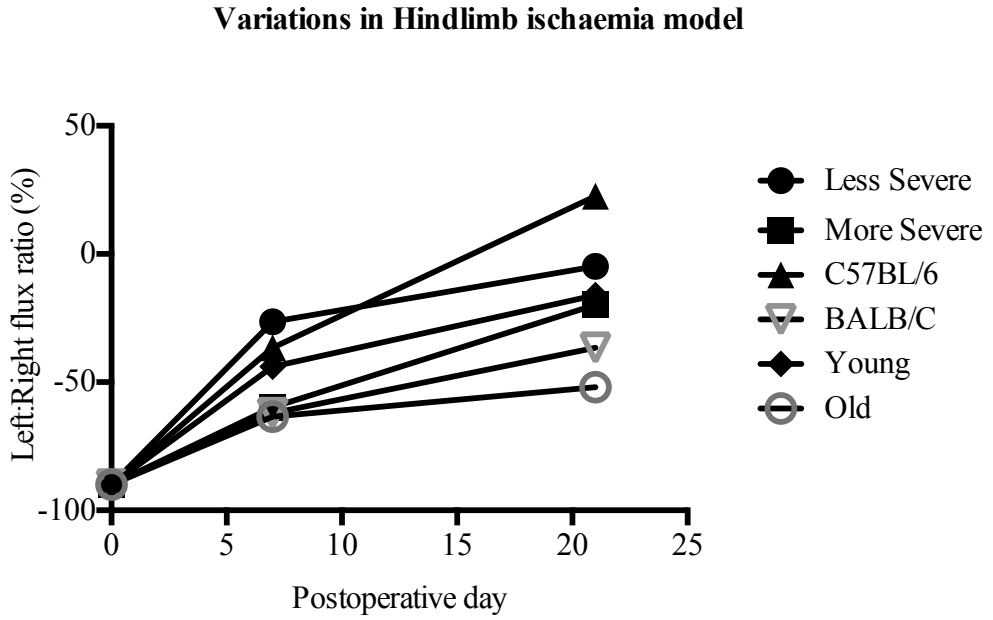

Figure 6.7: Comparison of paw perfusion following variations in hindlimb ischaemia model

Summary graph of all preliminary studies assessing variability in the hindlimb ischaemia model through alterations in technique, animal strain and age (n=2 per group and at each time point). The more severe surgical ligation provided a more suitable model of hindlimb ischaemia. In subsequent comparisons between mice strain and age the more severe ligation was used.

6.4.1.1 Applicability of hindlimb ischaemia model to human disease

The relationship between human PAD and the murine hindlimb ischaemia model was assessed to ensure a robust model was used that replicated classical features of the disease of interest. The comparisons relied on histological techniques to assess muscle morphology (routine H&E stain) as well as connective tissue fibrosis – a histopathological feature of more chronic and severe disease – using picro-sirius red stain.

Figure 6.8 A, B and C shows representative images of human skeletal muscle taken from control patients and patients with different stages of PAD. This can be compared to skeletal muscle samples taken from the BALB/c hindlimb ischaemia model, which shows normal muscle from the non-operated limb, as well as muscle from a middle and late time point (Figure 6.8 D, E and F). Characteristic features in early stage of disease observed by H&E analysis include infiltration of inflammatory cells, attempts of muscle fibres to regenerate as well as evidence of past regeneration (central nuclei) and muscle fibre size heterogeneity. At terminal stages of disease, replacement of muscle fibres with fatty, fibrotic tissue can be observed, as well as loss of peripheral nuclei, and centrally located nuclei as muscle fibres attempt to regenerate.

Following observations of fibrotic regions in CLI muscle, human skeletal muscle sections were assessed for collagen deposition in both control and CLI disease patients, using picro-sirius red staining. Analysis of sections under brightfield, and subsequent polarised light microscopy confirmed little collagen present around muscle fibres of control samples but increased deposition of collagen in CLI muscle. In brightfield images, collagen around the muscle fibres was stained red, which when viewed under polarised light, demonstrates both larger collagen fibres (orange and yellow staining) as well as smaller reticular fibres (green staining). Analysis of mouse hindlimb ischaemia sections demonstrated similar features of endomysial fibrosis previously observed in human CLI sections.

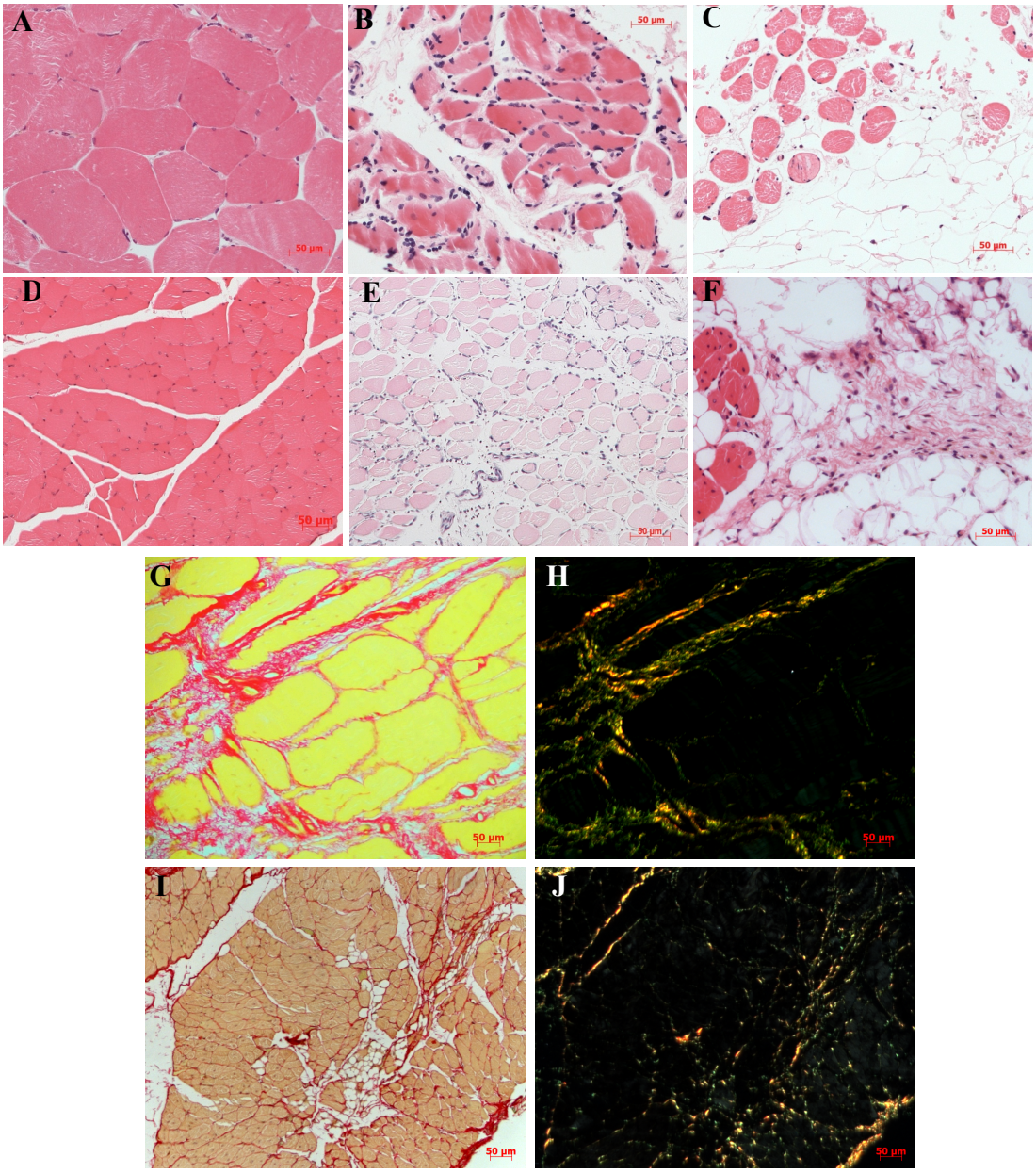

Figure 6.8: Comparison of human and mouse skeletal muscle following prolonged ischaemia

A and D: Representative H&E sections from adult, non-ischaemic human (A) and mouse (D) gastrocnemius. Structure of the muscle tissue is composed of a mosaic of muscle fibres in contact with one another. Each fibre has a peripherally located nucleus. B and E demonstrates muscle injury in the early ischaemic period, with characteristic sarcoplasmic destruction and variation in fibre size. C and F demonstrate severe muscle injury following chronic ischaemia, with loss of muscle fibre and replacement with adipocytic connective tissue. Analysis of connective tissue seen in later stages of PAD (G and H), and the hindlimb ischaemia model (I

and J) using picro-sirius red staining identified the endomysial and perimysial distribution of collagen.

6.4.2 ARA-290 treatment improves functional and physiological outcomes in the murine hindlimb ischaemia model

Following induction of unilateral hindlimb ischaemia in 12-week old BALB/c female mice, daily monitoring revealed mice that were less active in comparison to sham-operated animals in the days immediately after hindlimb ischaemia was induced. This decrease in movement and activity was only evident for three to four days post operation, after which all animals were observed to be freely moving around.

Qualitative assessment of functional (Tarlov and modified BMS) and ischaemia-related (ischaemia and modified ischaemia) scoring systems was therefore performed to identify differences in physiological outcomes between the different animals.

All scoring platforms identified operated mice as being less ambulatory, and demonstrating features of ischaemic injury in the first 3 days post operation compared to sham operated mice. Natural recovery of all physiological outcomes was also observed to an extent by the vehicle-control treated animals by day 21 (Figure 6.9).

High-dose ARA-290–treated mice showed significantly accelerated improvement in comparison to vehicle-control mice, in all scoring systems as early as day 10 ($P=0.0075$ Tarlov score; $P=0.0052$ Ischaemia score; $P=0.0002$ modified ischaemia score; $P=0.0121$ modified BMS score, all by one-way ANOVA, post-hoc Tukey's test, $n=6$ mice/group). These observations were prolonged until day 21, compared with vehicle-control mice in all scoring systems except the ischaemia score. A similar pattern of improved physiological scores was exhibited in low-dose ARA-290–treated mice by day 21 in the Tarlov, modified ischaemia and BMS scoring systems only. Improvement in physiological scores were also observed following EPO treatment however the trend was not significant, and was also less pronounced in comparison to ARA-290 treated animals. Representative images of both normal and ligated paws showing nail and digital necrosis can be seen in figure 6.10.

Animals were also assessed for changes in weight, which may affect recovery. All animals were weighed pre-operatively and on days 3, 10 and 21, before anaesthesia

was administered. There were no significant changes in weight between the animals at any time point (figure 6.11).

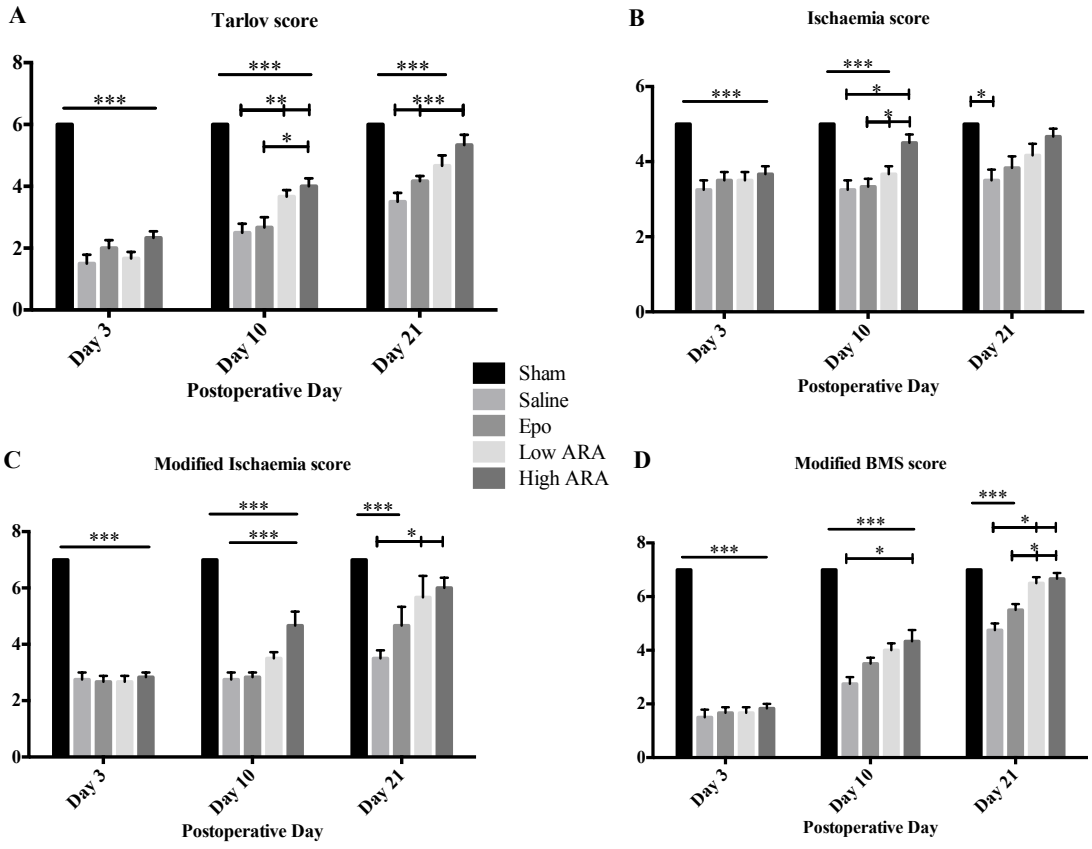

Figure 6.9: Assessment of functional outcomes following hindlimb ischaemia

Analysis of functional scoring systems demonstrated variation in extent of recovery following hindlimb ischaemia. Vehicle-control treated animals recovered the least across all scoring platforms. In comparison, ARA-290 treated animals receiving either low or high-dose treatment showed significantly improved functional and ischaemia-related scores. Summary data is expressed as mean ± SEM.

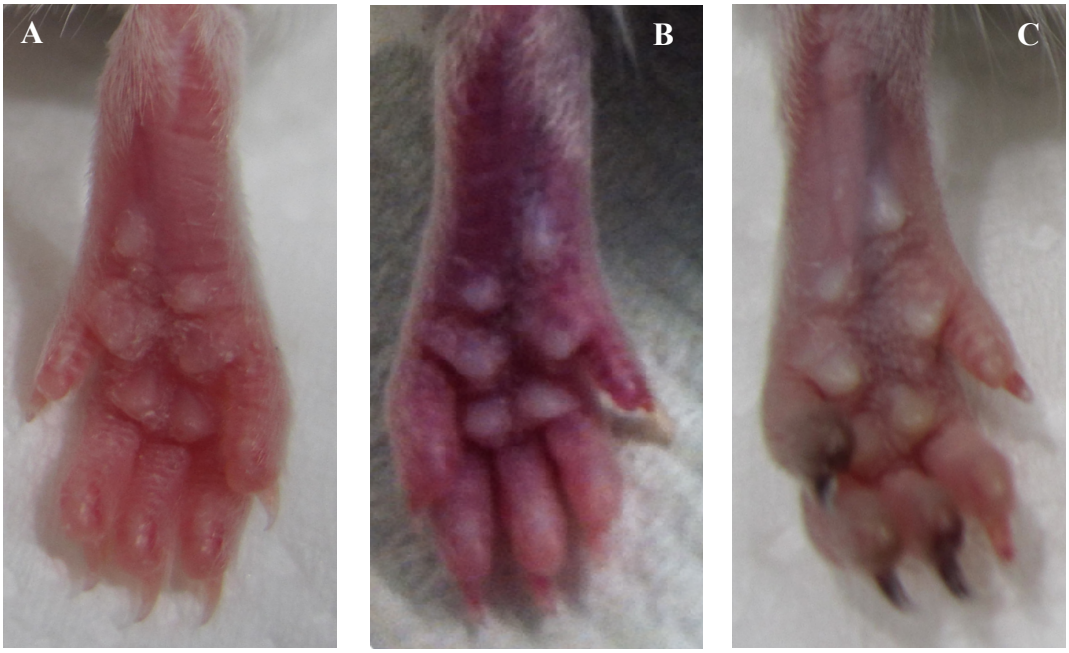

Figure 6.10: Hindlimb paws following induction of hindlimb ischaemia

Representative image of normal paw (A), ischaemic 'dusky' paw (B) and nail and digit necrosis (C).

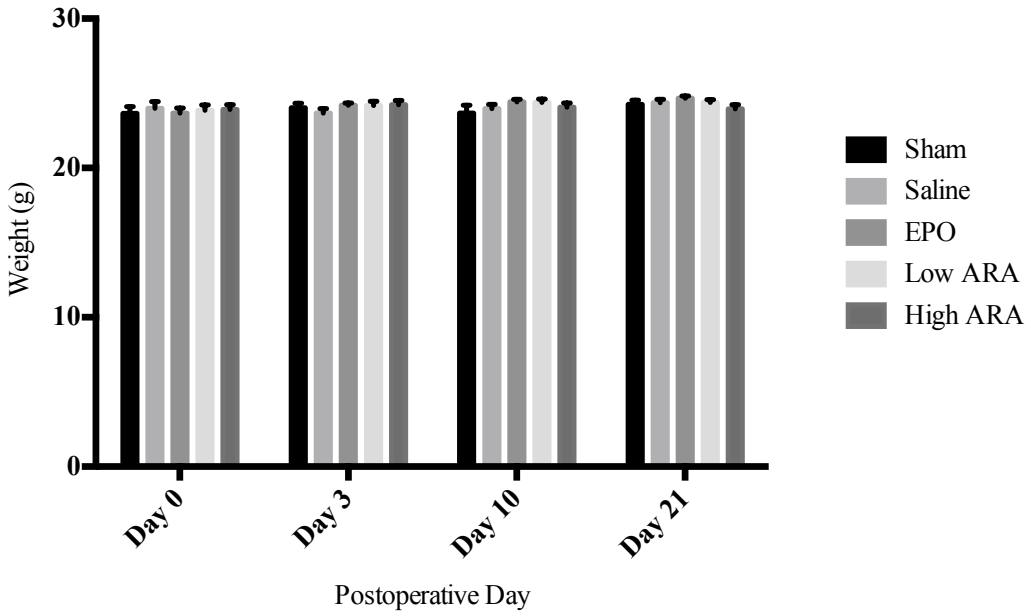

Figure 6.11: Assessment of weight pre and post-operatively in all animals

All animals were weighed prior to ligation of femoral artery, and also prior to the relevant end-point. There was no significant alterations in weight in any treatment or control group nor at different time points.

6.4.3 Effect of ARA-290 on blood flow

The effect of EPO and EPO-derivative administration on limb perfusion following surgical induction of hindlimb ischaemia was measured over 21 days. Vehicle-control treated animals demonstrated natural recovery of blood flow to the affected limb of approximately 50% compared to the unaffected limb by day 21. The degree of paw perfusion was still significantly reduced compared to sham operated animals (Figure 6.11).

In comparison, at day 21, animals treated with either EPO or ARA-290 demonstrated significantly greater improvements of paw perfusion, compared to vehicle-control treated animals ($P=0.0009$ EPO-treated; $P=0.0001$ low-dose ARA treated; $P=0.0003$ high-dose ARA-290 treated, all by one-way ANOVA, n=6 mice/group). Treatment with either low or high-dose ARA-290 demonstrated accelerated recovery of limb perfusion, as early as day 10. At this time, paw perfusion in both groups was not significantly different to sham operated animals ($P>0.55$ both ARA-290 treatment groups, one-way ANOVA). In addition the improvement in paw perfusion was significantly attenuated compared to vehicle-control mice ($P=0.042$ low-dose ARA; $P<0.0001$ high-dose ARA, one-way ANOVA).

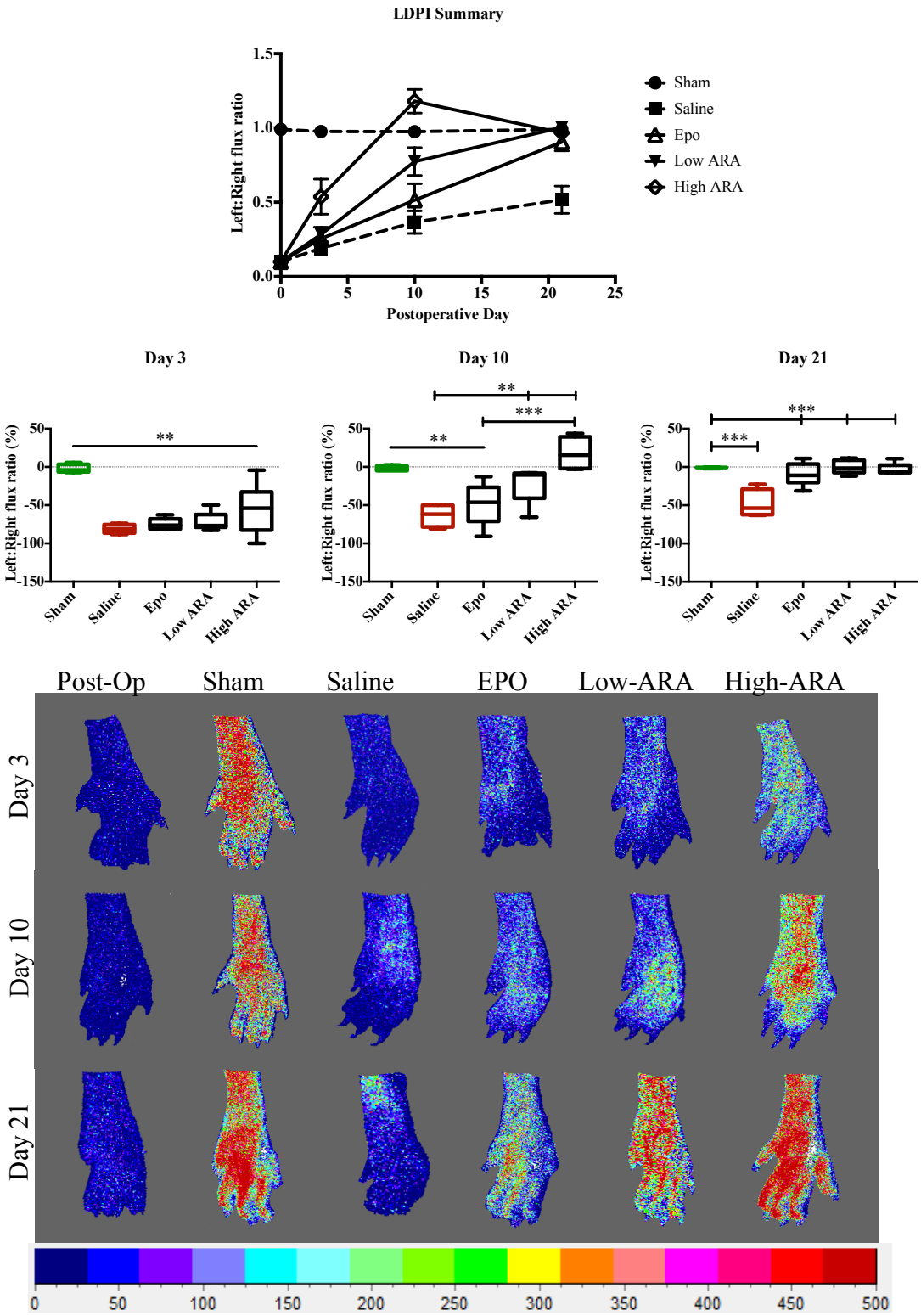

Figure 6.12: Recovery of hindlimb ischaemia following EPO and ARA-290 treatment

(A) Analysis of recovery in paw perfusion forllowing hindlimb ischaemia. (B) Representative Laser Doppler images of paw perfusion at all time points and intervention groups. Summary data are expressed as mean ± SEM.

6.4.4 Effect of ARA-290 on muscle injury

The effect of hindlimb ischaemia on muscle damage was assessed using H&E analysis of muscles harvested from the hindlimb. The pre-defined grading system, which takes into account characteristic features of muscle injury and its evolution, clearly displayed a detrimental effect of hindlimb ischaemia on skeletal muscle at day 3. Typical features seen in the affected limb of all operated animals at day 3 include infiltration by inflammatory cells, centrally located nuclei, muscle fibre shrinkage and variation in fibre size (Figure 6.13). Vehicle-control treated animals tended to progress towards greater severity of muscle damage, which was prolonged until experimental end-point (Figure 6.12).

In comparison, treatment with low-dose ARA-290 maintained a similar level of muscle injury observed at day 3, across all time points. Treatment with high-dose ARA-290 did not appear to have as great a benefit on preventing the natural progression of muscle damage at day 10, especially in the more distal tibialis anterior muscle, but subsequently, ameliorated the progression of disease by day 21. Treatment with EPO similarly, did not show initial benefit in counteracting ischaemia-induced muscle injury evolution at day 10. However, tissue-protective properties were demonstrated, by day 21, when the level of muscle injury observed was comparably lower. Protracted treatment with EPO caused slight muscle damage in the contra-lateral, non-operated limb in 1 animal from the EPO-treatment group (n=6). This finding may be consistent with known thrombotic side effects of high-dose EPO treatment.

Figure 6.13 exhibits representative H&E images of characteristic features observed in the progression of ischaemic-muscle injury. Muscle sections from the non-operated limb all displayed normal architecture, with single peripherally located nuclei (A). At day 3 post-operative hindlimb ischaemia the operated limb had inflammatory cell infiltration (B). Progression of muscle injury was variable across the different treatment groups, but other characteristic features of muscle injury observed included muscle fibre diameter shrinkage, variation in fibres size, denervation and loss of peripheral nuclei (C), attempts at muscle regeneration and centrally located nuclei (D and E), muscle necrosis and pyknotic nuclear clumps, with replacement of muscle fibres with adipogenic tissue (E and F).

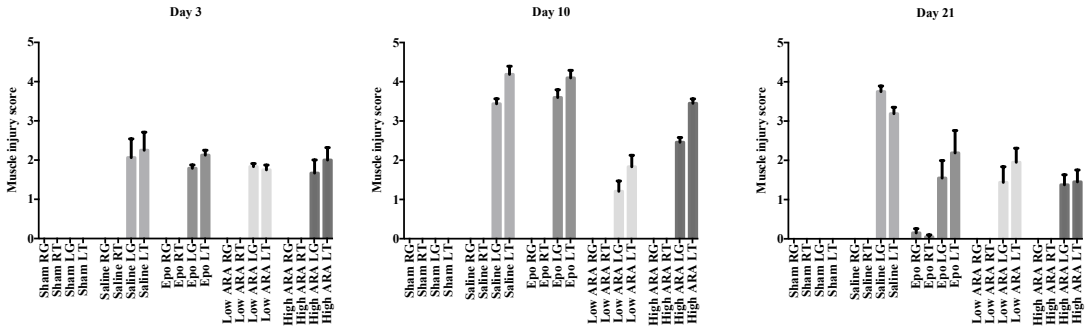

Figure 6.13: Evaluation of muscle injury following hindlimb ischaemia

Analysis of blinded scores of muscle H&E sections for all animals and timepoints revealed an increase in mean muscle injury score in vehicle-control treated animals at day 21. EPO treated animals demonstrated worsening muscle injury scores, comparable to saline-treated animals at day 10. Resolution in muscle injury occurred towards day 21. ARA-290 treated animals demonstrated less severe muscle injury, and significantly improved muscle injury scores by day 21. Summary data is expressed as mean ± SEM.

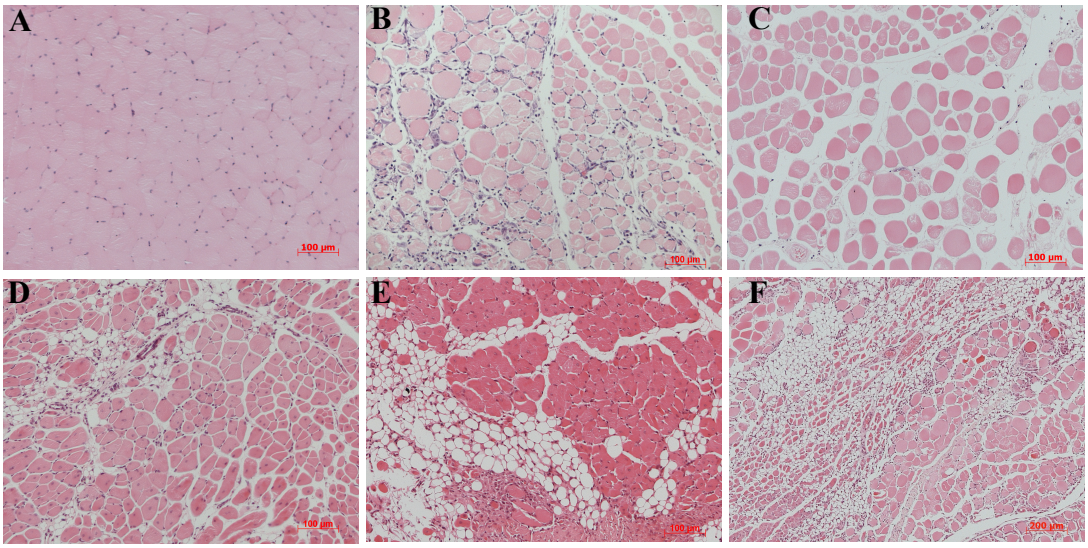

Figure 6.14: Features of ischaemic muscle injury

Representative images of H&E stained muscle sections showing normal (A) and pathological muscle tissue (B-F). In the early ischaemic period there is an increased infiltration of inflammatory cells (B). Loss of myofibre innervation, peripheral nuclei and variations in size also occur (C). Attempts by muscle to regenerate are characterised by centrally located nuclei (D). Necrosis of vast numbers of muscle fibres leads to pyknotic nuclear clump (E) and replacement of normal myofibres with adipogenic and fibrous connective tissue (E and F).

6.4.5 Effect of ARA-290 on myofibre proliferation

Assessment of muscle fibre nuclei for the proliferative marker Ki-67 revealed EPO and ARA-290 treatment groups had accelerated induction of proliferation – evidenced by the increased percentage of Ki-67^{+} nuclei – at day 3. There was a significantly higher percentage – greater than two-fold higher – of positive nuclei in the EPO and ARA-290 treated groups at this early time point (figure 6.14 and 6.15). The vehicle-control treated group demonstrated an increase in positively stained cells between day 3 and 10, to a comparable level observed in the EPO and ARA-290 treated groups. By day 21 all treatment groups had less than 20% positively stained cells, with no significant difference between vehicle and EPO or ARA-290 treated groups. All treatment groups demonstrated significantly increased proliferation compared to the contralateral limb, as well as sham operated animals, at all time points.

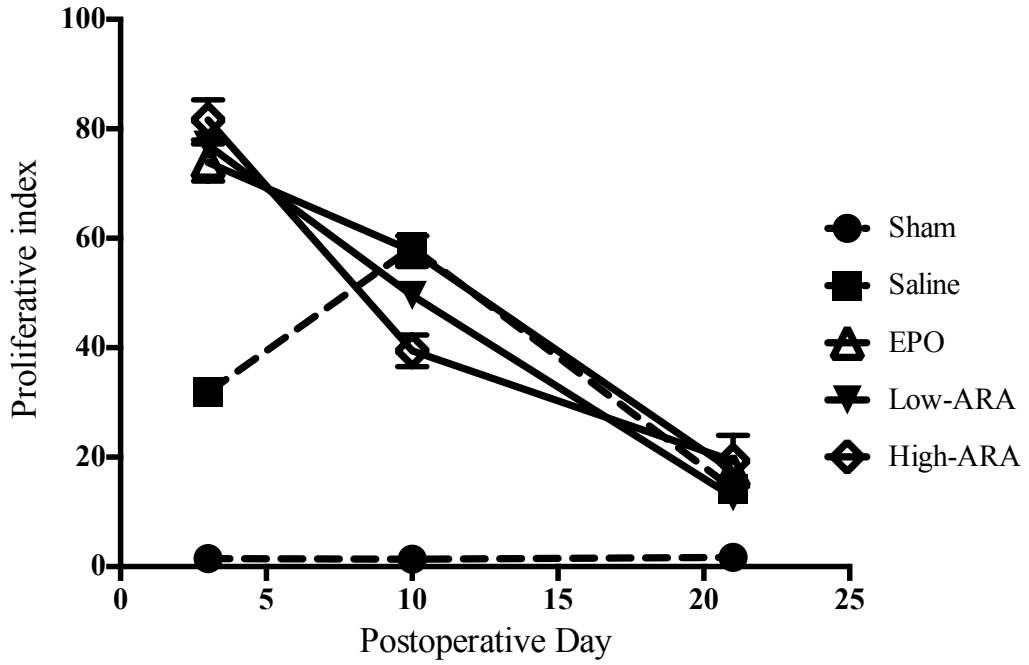

Figure 6.15: Analysis of proliferation index following hindlimb ischaemia

ImageJ analysis of muscle sections stained for Ki-67 demonstrated an increase in proliferation positive cells in animals subjected to hindlimb ischaemia. There is an initial increase in proliferative nuclei, which during our time course peaked at day 10, followed by a steady decline. EPO and ARA-290 treated animals demonstrated an accelerated increase in positive cells, followed by a steady decline. Summary data is expressed as mean ± SEM.

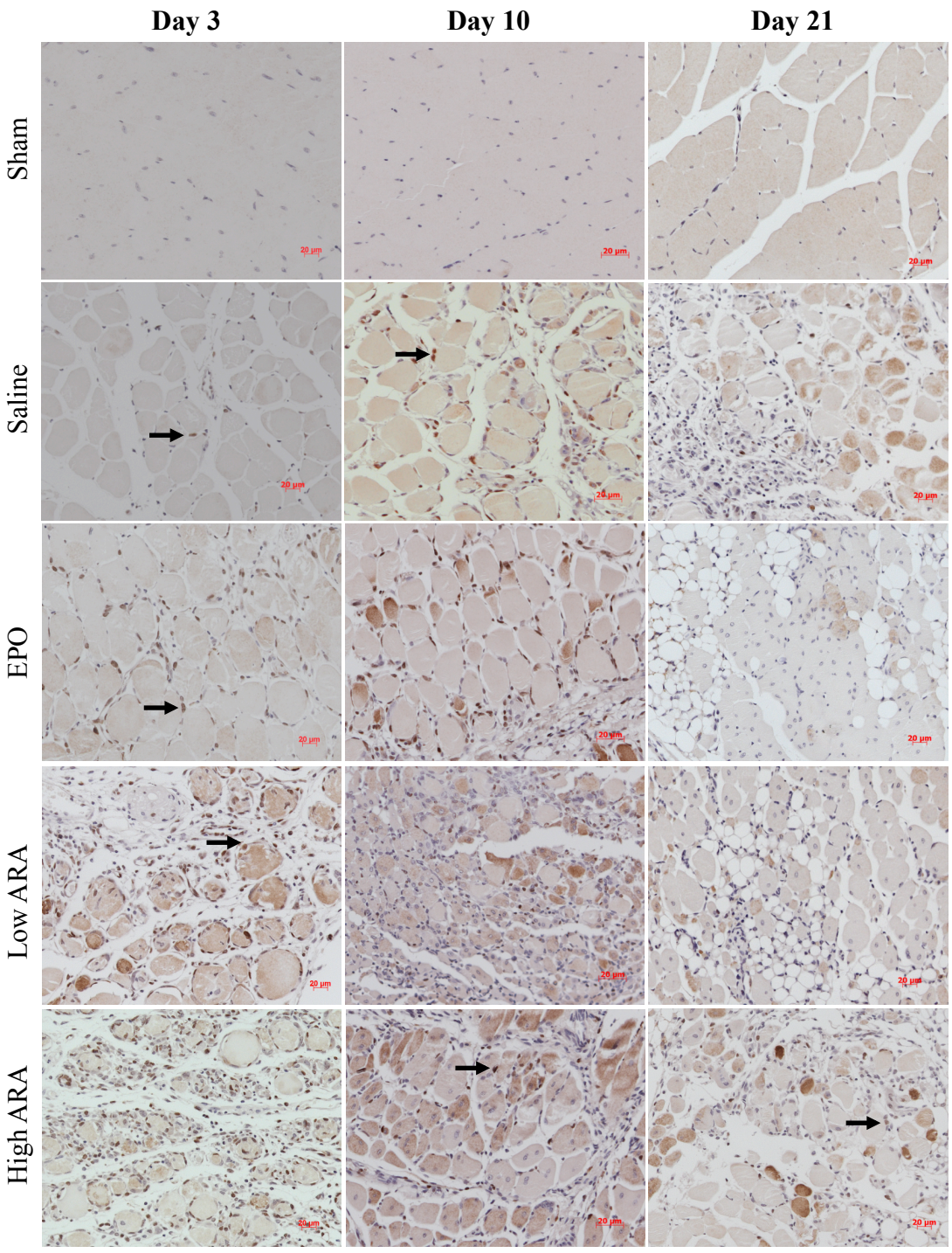

Figure 6.16: Histological analysis of proliferation following hindlimb ischaemia

Representative images used for cell counting of both positively and negatively stained Ki-67 nuclei (in brown (DAB)) to assess proliferative index. Arrow indicates Ki-67 positive nucleus. Scale bars = 20µm.

6.4.6 Effect of ARA-290 on ischaemia-induced angiogenesis

Analysis of C:F ratio over the time-course of the experiment demonstrated a slight decrease in the C:F ratio in all operated animals compared to sham operated animals at day 3. Observation of vehicle-treated animals as an indication of natural recovery demonstrated an increase in C:F ratio to approximately 1.5-fold greater than sham operated animals, indicating a degree of neoangiogenesis occurred following hindlimb ischaemia. Treatment with either low or high-dose ARA-290 demonstrated a similar reduction in C:F ratio at day 3, followed by an increase to approximately 1.1 by day 10, after which a plateau was observed (Figure 6.16).

EPO treated animals demonstrated a greater than 3-fold increase in C:F ratio between day 3 and 10. A further, slight, increase in C:F ratio was observed at day 21 (Figure 6.16). This finding is in keeping with known observations of the angiogenic capabilities of EPO.

Representative images of CD34 staining for assessment of C:F ratio are shown in Figure 6.13. An increase in CD34 staining can be seen in operated animals at day 10 and 21. EPO-treated animals display a far greater proportion of CD34 positive stained cells, indicating an increase in the number of capillaries present. This increase in CD34 staining is prolonged until day 21 (Figure 6.16).

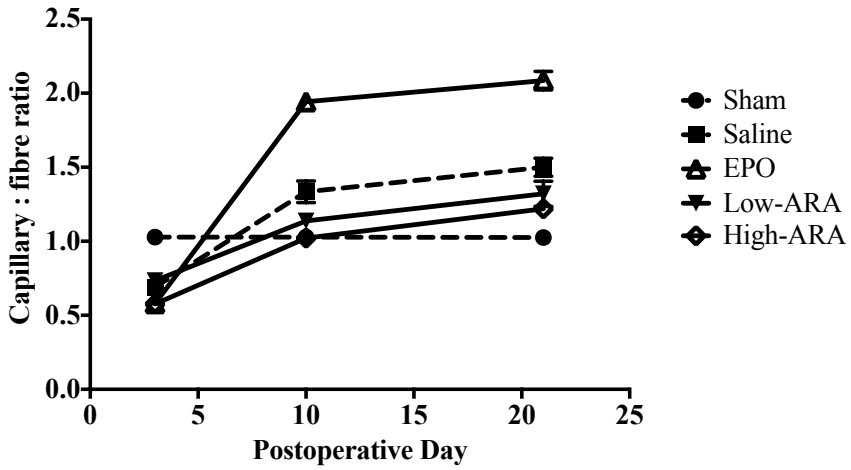

Figure 6.17: Evaluation of capillary : fibre ratio following hindlimb ischaemia

A gradual increase in C:F ratio is observed in ischaemic muscle as perfusion recovers. EPO-treated animals demonstrate greater increase C:F ratio by day 10, which is sustained until the experiment end-point. Summary data is expressed as mean ± SEM.

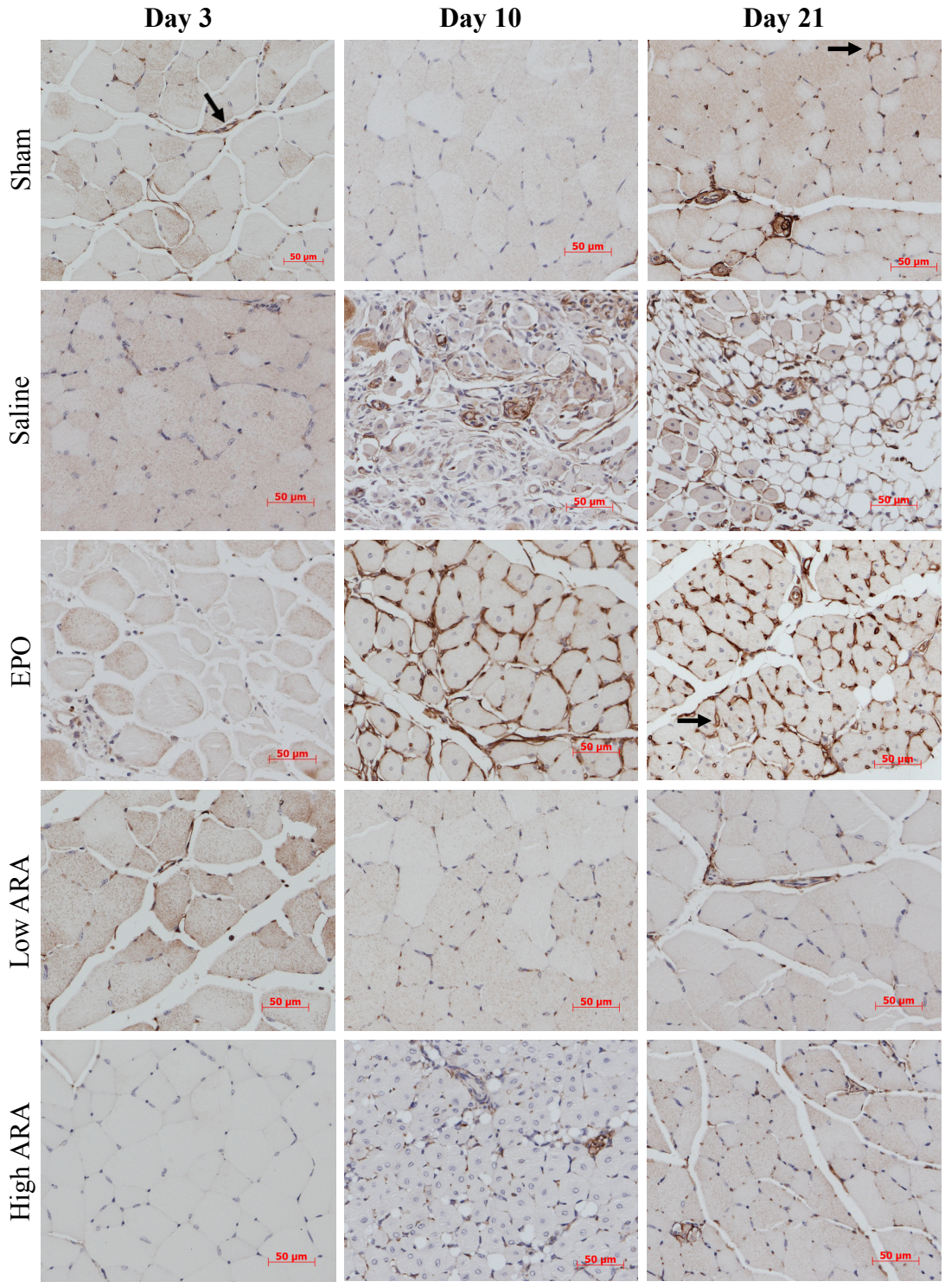

Figure 6.18: CD34 immunohistochemistry for C:F assessment

Representative images of CD34 immunohistochemistry performed on muscle from the ischaemic hindlimb, used to calculate the C:F ratio in the different treatment groups at different time points. Arrow demonstrates a capillary. Scale bars = 50µm.

6.5 Discussion

In this study, establishing a murine model of hindlimb ischaemia which closely mimics characteristic features of human CLI and PAD was made possible through modulation of a number of common variables of the technique and animals used. Variation in the surgical technique, mouse strain and age all had consequent effects on the severity of the hindlimb ischaemia produced. Developing a robust pre-clinical model was a pre-requisite in order to test the novel EPO-derivative, ARA-290, as a potential tissue-protective agent following ischaemic injury to the hindlimb.

6.5.1 Establishing a suitable model of hindlimb ischaemia

Initiation of hindlimb ischaemia model: Severity of hindlimb ischaemia

The mouse hindlimb is known to have an extensive innate collateral system, and for this reason, is remarkably resistant to ischaemia, with models utilising single ligation of the femoral artery often documenting no severe ischaemic change, and resolution to normal parameters within 7–28 days [358, 368, 369]. For this reason, development of a chronic ischaemia model will often employ techniques involving double ligation, or gradual occlusion of the femoral artery – using balloon dilation devices – to induce, and maintain a prolonged ischaemic period. In this study, we varied the length of femoral artery ligated to increase the severity of ischaemia induced. As expected, the more severe surgery resulted in a hindlimb that showed greater evidence of ischaemia, including more pronounced reduction in paw perfusion, and histological features suggestive of more severe ischaemic injury. In comparison, the less severe technique failed to provide a prolonged window of reduced paw perfusion, with resolution in perfusion achieving 75% of the non-ischaemic limb within 7 days. Histological analysis demonstrated only mild features of muscle injury in localised areas, with the majority of muscle not overtly dissimilar in appearance to muscle from the contralateral, normal limb.

Initiation of hindlimb ischaemia model: C57BL/6 vs. BALB/c strains

Comparison of two common laboratory mice strains – C57BL/6 and BALB/c were also considered for the innate ability to recuperate following femoral artery ligation to render the limb ischaemic. Following interruption or occlusion to arterial inflow,

there is significant variation in the response of the collateral circulation between these strains. Analysis of the animals after surgery displayed considerable variation in the natural response to hindlimb ischaemia. BALB/c animals demonstrated a greater susceptibility to ischaemic injury following surgery, as evidenced by a prolonged period of reduced paw perfusion in the affected limb, and more pronounced histological features of muscle inflammation, injury, attempted regeneration, and necrosis, with subsequent fibrotic fatty tissue replacement. C57BL/6 animals, in comparison, also demonstrated sensitivity to hindlimb ischaemia, but a greater propensity for recovery of both paw perfusion and muscle tissue injury, within a shorter timeframe. This could be due, in part to previous observations that C57BL/6 mice have a large repository of native collaterals compared to BALB/c mice [370, 371]. As a consequence, the recovery times of C57BL/6 mice tends to be significantly reduced whereas BALB/c mice exhibit a prolonged recovery period – a potentially desirable feature, providing a greater period for analysis of interventions [372]. Both strains are highly inbred with minimal genetic heterogeneity within each strain. In addition, a vast number of knockout mice are based on a background utilising one of these strains, making them ideal to devise appropriate, replicable pre-clinical models of hindlimb ischaemia.

Initiation of hindlimb ischaemia model: Age

A key feature of PAD is its increased prevalence with age. The majority of patients with PAD are elderly, with impaired regenerative capacity and dynamic response to everyday stimuli and mechanical or other trauma. The effect of mouse age on natural recovery rates in the hindlimb ischaemia model was assessed. Young mice (6 weeks old) displayed a remarkable capacity to withstand and recover from ischaemic injury. Histological analysis demonstrated very mild features of muscle damage in very localised areas. In contrast the older mice (16 weeks of age), although not comparable in age to a typical 70-year-old human PAD sufferer, displayed many of the characteristic features of muscle injury, and attempted regeneration, as well as muscle tissue death. The significance of aging mice, for more accurate representation of clinical disease features needs to be balanced with cost-effectiveness of achieving characteristics. To produce a 75 year old human 'age-matched' mouse the mouse would need to be 2½ years old, which has significant housing and maintenance costs implications. Analysis of young and old mice responses to ischaemia emphasised the

significantly slower recovery rates observed in the older animals. Other studies looking at the effects of aging in the hindlimb ischaemia model, using mice that show typical age-related phenotype (Klotho mutant mice) also reported impaired recovery of the ischaemic limb [373].

6.5.2 Effect of ARA-290 on recovery following hindlimb ischaemia

Erythropoietin has previously demonstrated its utility as a multi-tissue-protective agent. Unfortunately, its routine use in chronic diseases other than the treatment of anaemia cannot be justified due to the side effects of repeated administration, including effects on haematocrit, platelets, and blood pressure [374-376]. Assessment of the novel EPO-derivative, ARA-290, was therefore trialled for potential tissue-protective effects *in vivo* following induction of hindlimb ischaemia.

Treatment of mice following induction of hindlimb ischaemia with ARA-290 significantly improved the natural recovery of blood flow, functional and histological outcomes within the ischaemic limb over 21 days. The mechanisms underlying these observations are likely due to the contribution and complex interaction between each of these factors, amongst a multitude of others.

Recovery of blood flow demonstrated improvement when treated with ARA-290. Indeed, treatment with high dose ARA-290, at twice the dose given to the low-dosed animals resulted in accelerated recovery in the early to mid-phase, which normalised and equalled the blood flow recovery observed in the low-dose ARA-290 treated animals by the day 21 endpoint. Interestingly, though there was an increase in blood flow recovery in EPO treated animals, the difference was not as significant compared to ARA-290 mice. Analysis of angiogenic potential of EPO and the EPO-derivative revealed significantly enhanced C:F ratio, indicative of angiogenesis in the EPO treated group only. This explains, in part, the increased improvement in blood flow recovery observed in the EPO treated group, but does not account for the increased and faster recovery seen in ARA-290 treated groups, neither of which displayed capillary fibre ratios above that observed in saline, vehicle-control treated animals. This finding is in keeping with other functional studies of EPO and ARA-290. EPO is known to possess angiogenic potential [377-380], but the design of ARA-290 intentionally focused on harnessing only the tissue-protective potential of the EPO-molecule and discarding all other haematopoiesis-related attributes [245].

Assessment of angiogenic potential *in vitro,* assessing capillary tube formation, demonstrated treatment with ARA-290 did not positively influence angiogenic outcomes [381]. EPO is also capable of promoting blood vessel outgrowth by influencing other cells. Examples of such actions include the role of EPO on stimulating endothelial progenitor cells to mobilise to ischaemic tissue and promote new blood vessel formation [382-384]. In addition EPO has demonstrated an effect upon regulation of nitric oxide, another molecule known to promote angiogenesis in addition to vasodilation [385, 386].

Functionally, all treatment groups demonstrated enhanced recovery of ambulation compared to vehicle-control group with high-dose ARA-290 treated animals improving earlier (by day 10) than low-dose ARA-290 treated animals. Although it might be expected that EPO treated animals, following increased C:F ratio may demonstrate the greatest functional outcomes, this was not the case, and conversely, analysis of functional scores for EPO-treated animals did not reach statistical significance in comparison to vehicle-control. A similar pattern of results was observed when animals were assessed for physiological improvements. ARA-290 treated animals showed statistically significant improvement towards the end of the experimental period in the modified ischaemia score only.

Inter-related with blood flow and functional outcomes is the effect of hindlimb ischaemia on the skeletal muscle which, much like in humans, in mice, also makes up the bulk of the hindlimb. Histological assessment of the effect of ischaemia on the muscle tissue identified many characteristic features of the various stages of muscle injury. As expected, all EPO and ARA-290 treatment groups demonstrated improvement in histological appearance at day 21, and at all time points compared to the saline, vehicle-control treated animals. Interestingly, EPO and high-dose ARA-290 treated animals, similarly to the vehicle control animals showed a progression in muscle damage between day 3 and 10, which begin to show resolution after day 10. Such progression of muscle damage was not observed in low-dose ARA-290 animals

On a macroscopic level, it is logical to assume that an improvement in blood flow would impact upon the degree of muscle injury observed, which in turn alters functional and physiological outcomes, and underpinning a greater resolution of perfusion deficit could be the ability to develop greater numbers of collateral vessels

to improve the perfusion to the ischaemic area. Whilst this may be true for the EPO-treated animals, only a relatively modest increase in C:F ratio was observed in both ARA-290 treatment groups. The C:F ratio observed was also below the levels observed in vehicle-control treated animals, who fared significantly worse on all functional and physiological scores in comparison to ARA-290 treated animals. What is known, is that the ischaemia induced following surgical ligation of the femoral artery to create the hindlimb ischaemia model, catalyses a complex cascade of events including muscle damage, and in response to the hypoxic environment that is created, a degree of angiogenesis to reperfuse the limb. In addition, treatment with EPO or ARA-290 appears to have differential effects on ameliorating muscle damage, angiogenic potential of the muscle and as a consequence the functional benefit observed.

Another possible explanation for the improved functional outcomes observed in EPO and EPO-derivative treated animals is the effect these agents had upon proliferative index following hindlimb ischaemia. In the early period following surgery, EPO and ARA-290 treated animals displayed significantly higher proportion of proliferative nuclei when analysed using immunohistochemistry for the proliferative marker Ki-67, indicative of a regenerative phenotype. Though this higher proliferative index was not maintained across all time points, it is possible that the accelerated initial proliferation might 'kick-start' the regenerative potential of the muscle tissues, hence why the observed staining in each group is not prolonged.

Limitations of the hindlimb ischaemia model

In initialising a hindlimb ischaemia model, a number of factors were considered, besides how closely the model mimicked the human disease of interest. Age of disease sufferers has previously been mentioned, and was assessed as above. Other underlying mechanisms that contribute to PAD, aside from increased age, include hypertension, hypercholesterolaemia and diabetes mellitus. Numerous animal models mimicking each of these diseases exist, and the additive effect of each or any of these factors on the hindlimb ischaemia model has been reported in the literature [386-392].

In diabetic models of hindlimb ischaemia, there is impairment in ischaemia-induced vascular remodelling as well as dysregulation of the inflammatory response. The aberrations in vascular remodelling affect both arteriogenesis and angiogenesis due to

inhibition of mobilisation and integration of bone marrow progenitor cells into the endothelium and impaired signalling of VEGF ligand, respectively [387, 393, 394].

A number of methods exist for producing dyslipidaemic and atherosclerotic animals, including changing their feed to a high-fat diet, but more commonly an ApoE-knockout or a low-density lipoprotein (LDL) receptor knockout mice can be used. These animals get characteristic atherosclerotic lesions in major vessels, including the aorta, carotid, femoral and popliteal arteries. Literature suggests that the dyslipidaemic state affects inflammatory responses [388].

Animal models have constant and undeniable utility and important roles in helping to answer clinical questions, as well as identifying potentially efficacious future therapies. However, no model is capable of exactly replicating the highly evolved and multifaceted disease of interest, and often a scenario will dictate the optimum permutations of factors to use in order to get the most representative disease model. Although not ideal for standardising results and assessments, such is the nature of human disease pathology.

6.6 Summary

The changes seen in human skeletal muscle of patients with CLI can be reproduced using the murine model of hindlimb ischaemia. The model therefore provides a suitable platform to assess the potential therapeutic effects of novel agents. Administration of EPO or ARA-290 resulted in improved functional, histological and perfusion outcomes following induction of hindlimb ischaemia.

CHAPTER 7

General discussion and Future studies

7.1 General discussion

PAD is a syndrome with multiple aetiologies. This complex interaction between several disease pathologies makes the management of individuals with PAD equally as complex. Much of the current clinical research for patients with "no option" CLI has focused on therapeutic angiogenesis – in an attempt to stimulate the development of new blood vessels, and replenish blood flow, and therefore oxygen and key nutrients to ischaemic tissue. Though this represents a promising novel treatment in individuals with CLI, therapeutic angiogenesis has been of interest to investigators since the 1970's, and clinical breakthroughs have remained somewhat elusive, with limited success in phase II and III clinical trials [372]. In addition, there are many facets of CLI that therapeutic angiogenesis does not directly address, and therefore there remains a large scope to develop novel adjunctive therapies.

In the treatment of CLI patients, several recent studies have identified that despite successful revascularisation patients do not always report a return to their pre-morbid functionality. In these cases, it hints at the possibility of additional pathologies affecting CLI individuals, preventing recovery. Study of CLI muscle has indicated a number of changes that occur in the skeletal muscle of CLI patients, which do not appear reversible despite successful revascularisation [88, 90, 118, 124]. Many of the described changes centre on the largest organ supported by the network of arteries in the lower limb – muscle.

This thesis has investigated EPO and the EPO-derivative, ARA-290, in order to determine their potential muscle-protective properties.

7.1.1 Tissue-protective receptor in CLI

The initial aim of the study was to identify the presence of the tissue-protective receptor in human skeletal muscle, especially CLI sample muscle, as the clinical group of interest. This was essential due to recent publications suggesting incorrect

localisation of the EPOR to a number of tissues [292, 395-397]. In addition, expression of the βcR in human skeletal muscle has not been previously described.

Multiple EPOR and βcR antibodies were initially assessed for their ability to accurately detect the presence of both receptors in human whole-muscle homogenates. Following the demonstration of EPOR and βcR protein expression by Western blot analysis in human muscle samples, RNA expression was also demonstrated using qRT-PCR techniques. However, having demonstrated the presence of the receptors individually, determining the nature of their physical interaction was achieved using a combination of techniques. This included co-localisation techniques by immunohistochemistry and immunofluorescence, as well as protein-protein interaction using co-immunoprecipitation. Co-localisation of the EPOR and βcR as well as positive co-immunoprecipitation results suggests these two receptors likely form heteroreceptors in human skeletal muscle.

Assessment of Western blot and qRT-PCR analysis established an increase in expression of both EPOR and βcR in CLI muscle. The underlying reason for this observed increase in expression of both receptors is likely due to their location within an ischaemic niche. Previous work has described an increase in EPOR expression in skeletal muscle following intensive exercise-induced ischaemia in healthy individuals, although this is an acute ischaemic period [169]. In addition, increase in EPOR expression has also been described in other organs following ischaemic injury including the brain, nervous system, eye and heart [300, 301, 398-400].

A limitation of this study was the need to use antibodies previously suggested to be non-specific (anti-EPOR (C-20) from Santa Cruz biotechnology), due to the range of applications required to assess the presence and interactions of the EPOR and βcR in human skeletal muscle. However, careful study of the literature and initial comparison between multiple EPOR antibodies provided evidence of satisfactory specificity of the C-20 EPOR antibody. Its use in co-immunoprecipitation was further validated by subsequent Western blot analysis using a second EPOR antibody to demonstrate the presence of the pull-down product.

The use of EPO in humans is reserved for the treatment of anaemia of chronic disease. In addition, the tissue-protective capacity of EPO has been recognised for some time, but therapeutic side-effects of EPO's native role have often precluded its

use in a clinical setting. Investigation into potential arenas for EPO tissue-protective settings have included cerebral ischaemia (stroke), cardiac and renal ischaemia. Due to haematopoietic side-effects, the search for EPO-derivatives which retain cytoprotective properties, without causing haematopoiesis, has seen great advances, and in addition to developing EPO-derivatives, has identified potential receptors and signalling pathways utilised by tissue-protective EPO-derivatives to mediate their beneficial effects. Identifying the presence of the tissue-protective receptor in human skeletal muscle is an important step towards demonstrating the future potential use of EPO-derivatives in the management of CLI patients.

In order to study the presence of the tissue-protective receptor in human tissue, and isolate primary skeletal muscle cells for *in vitro* analysis of the effect of simulated ischaemia, patients undergoing amputations and CABG were recruited. Access to the lower limb was gained through surgical exposure. The surgical procedure therefore dictated the exact site and timing of sample collections. In samples collected from patients undergoing lower limb amputation, there is a longer acute ischaemic time. This is the time between the vessels (usually the femoral or popliteal artery and vein) to the lower limb extremities being clamped and the lower limb removed, and the remnant passed for research – between 5 and 20 minutes. In contrast, during harvest of the saphenous vein for CABG all branches are ligated, but arterial supply to the muscle is not disrupted. Once the saphenous vein has been removed, a much shorter period of time elapses between muscle biopsy harvest and processing for research – typically less than 5 minutes. An assumption was therefore made that the second, acute, ischaemic period when collecting samples from CLI patients would not be significant, compared with the chronic ischaemia in the limb. Due to natural variation in muscle fibre composition within different muscle groups, a standardised technique was employed when collecting biopsies from CLI or control patients. Biopsies were always collected from the deep belly of the gastrocnemius muscle in order to reduce the confounding effect of natural fibre composition.

An alternative source of control muscle is the proximal muscles in CLI patients. However, as mentioned already, variations occur in fibre composition depending on location, making direct comparison more challenging. In addition, proximal muscle from CLI patients, which may still be clinically viable is unlikely to be entirely normal due to the systemic effect of pathological changes in the distal muscle, such

as the release of endogenous ligands affecting the proximal muscles. Obtaining muscle biopsies from control patients without objectively proven PAD provided a more reliable source of 'normal' control tissue.

7.1.2 *In vitro* assessment of EPO and ARA-290 cytoprotective function

In vitro assessment of the tissue-protective capacity of EPO and ARA-290 was made possible through a previously described *in vitro* simulated ischaemia C2C12 skeletal muscle model [238]. Pre-treatment of C2C12 myotubes with EPO or ARA-290 demonstrated a distinct ability of both to reduce ischaemia-induced apoptosis of myotubes. Importantly, the functionality of phosphorylated Akt in mediating cytoprotection was also identified. In addition, inhibition of potential signalling molecules involved in cytoprotection, JAK2/STAT3, PI3k/Akt and NFκB demonstrated a dampening effect of EPO or ARA-290 mediated reduction of apoptosis. Whilst these molecules had quite severe effect upon EPO and ARA-290 cytoprotective ability it is likely there are many more potential signalling cascades that will need to be interrogated to fully appreciate the complex tissue-protective pathways utilised by both agents, and also to propagate further development of tissue-protective therapies. Based on observations in the literature of signalling pathways required for EPO-mediated red blood cell survival, it is likely that following JAK2 phosphorylation STAT 1 and 5, MAPK and protein kinase C may also be activated to promote tissue-protection. The diversity of molecules regulated by STAT 1, 3 and 5, as well as the cross-talk between MAPK, PI3k/Akt and NFκB will likely be investigated in the future to assess their contribution to EPO and ARA-290 mediated cytoprotection.

Besides the effect of EPO and ARA-290 on rescuing myotubes from ischaemia-induced apoptosis, both had positive effects on C2C12 myoblasts and ischaemia-induced aberrations in function. These effects included improving C2C12 myoblast migration, proliferation and apoptosis. These observations are supported by other studies that have noted similar functional benefit in alternative cell types, as well as myoblasts, following administration of EPO [172, 401-404].

Following the observation of promising results in the C2C12 myoblast and myotubes model of skeletal muscle, this thesis attempted to produce more clinically relevant results by assessing the utility of EPO and ARA-290 on skeletal myoblasts isolated

from our disease group of interest. As with all disease entities, usually there are several cellular attributes that, in becoming abnormal, lead to the disease state. In order to compare therefore, myoblasts were also isolated from control donors who did not demonstrate arterial pathology of the lower limbs.

Primary isolated human myoblasts and myotubes yielded a suitable model of skeletal muscle, showing characteristic features when subjected to simulated ischaemia, such as differentiation of myoblasts, as evidenced by increased expression of myogenin, and upregulation of the hypoxia responsive protein HIF-1α. Both CLI and control myotubes demonstrated these features. However, observation of their behaviour in culture and during simulated ischaemia provided novel insights into potential functional differences between CLI and control myoblasts and myotubes.

7.1.3 Functional differences between CLI and control myoblasts

Myoblasts from patients with CLI demonstrated enhanced proliferative activity compared with myoblasts from control individuals. However, myoblasts from CLI patients also demonstrated suppressed migratory activity, and reduced ability to contract collagen gel lattices *in vitro*. In conjunction, these results identify cellular mechanisms that are differentially affected as a result of chronic exposure to ischaemia.

The increased proliferative activity of myoblasts from CLI patients in both normoxia and simulated ischaemia is likely due to the increased requirement of muscle repair and regeneration in CLI patients due to the loss of muscle tissue under chronically hypoxic conditions. In addition, patients with CLI often have concomitant infection in the lower limb extremities, and inflammation and infection, through TNF-α, IFN-γ and downstream effects on IGF-1 are known to cause an increase in myofibre regeneration. This was also evident when human skeletal muscle was probed for the expression of myogenic precursors. There was significantly increased expression of Pax7 on Western blot and immunohistochemical examination. Although the process of myogenic repair and regeneration in CLI is incompletely understood the results assessing prevalence of myogenic precursors yields promising results that the underlying defect is not attributable to a dysfunction in proliferative potential of satellite cells or myoblasts.

The impaired migratory and contractile activity of myoblasts from patients with CLI may provide some insight into the functional impairment often described by CLI patients, even after successful revascularisation. These findings suggest that underlying alterations in cellular apparatus responsible for myofibre contraction and migration occur when muscle is subjected to chronic periods of ischaemia. Even after isolation of myoblasts, and their prolonged culture under normoxic conditions, those alterations, are not amenable to improvement. Interestingly, control myoblasts subjected to simulated ischaemia maintained superior migratory and contractile ability compared to CLI myoblasts, although ischaemia caused slightly diminished migratory potential.

Differences observed between CLI and control myoblasts and their response to simulated ischaemia highlights the key role ischaemia plays in inducing lasting pathology. Understanding the cellular mechanisms that govern muscle regeneration during and after ischaemia will improve treatment alternatives for those individuals who are unsuitable for revascularisation, and help those who do not benefit functionally after successful revascularisation.

The effect of EPO and ARA-290 pre-treatment on human myoblasts and myotubes demonstrated similar findings to those observed in C2C12 myoblasts and myotubes. EPO and ARA-290 were able to reduce ischaemia-induced apoptosis in both CLI and control myotubes. Inactivation of JAK2/STAT3, PI3k/Akt and NFκB signalling molecules demonstrated their key roles in mediating the beneficial effects of EPO and ARA-290 treatment against apoptosis, as well as release of the inflammatory cytokine IL-6. CLI and control myotubes subjected to simulated ischaemia demonstrated a significant release of IL-6 into the medium, compared to normoxic controls, as assessed by ELISA methods. The response of CLI and control myotubes to EPO and ARA-290 treatment however was less uniform, and is likely due to subtle differences in the susceptibility of myotubes to EPO and ARA-290 effect, as well as the initial injurious ischaemic period. Although only small numbers were assessed in each disease group, there was no correlation between disease versus control, gender or other co-morbidities and effect of EPO or ARA-290 treatment on IL-6 release. Absolute concentration of IL-6 secretion was also variable, and it is likely that all of these observations are due to the natural heterogeneity between individuals.

The combination of observations, including the ability of EPO and ARA-290 to reduce apoptosis and inflammatory cytokine secretion add to the understanding of their mechanisms of action. It is important to remember however, that muscle damage as a result of ischaemia is a culmination of myofibre injury, oxidative stress and inflammation. It is therefore important that therapeutic strategies are developed that aim to treat more than one aspect of the disease pathology and support the regenerative potential of myofibres.

7.1.4 *In vivo* hindlimb ischaemia model

Having observed the potential of EPO and ARA-290 to improve skeletal myoblast and myotube function following ischaemia-induced dysfunction, it was important to assess their role in a pre-clinical assay, and as such, the hindlimb ischaemia model was selected. Preliminary studies with small numbers of animals were performed to identify a suitable technique that would provide a significant degree of muscle damage, akin to changes observed in CLI muscle biopsies. This involved assessing the effect of age, strain and surgical technique on variation in the resultant severity and period of hindlimb ischaemia.

The hindlimb ischaemia model identified the ability of EPO and ARA-290 to improve functional outcomes, perfusion and proliferation of muscle fibres. In animals treated with EPO, this was likely due to the angiogenic potential of EPO, as evidenced by the increased capillary:fibre ratio. ARA-290 did not demonstrate an increase in C:F ratio, and therefore the underlying mechanism for observed improvements needs to be further interrogated in order to validate the potential use of ARA-290 for use in human subjects. However, considering the safety of ARA-290 prescription in both healthy individuals and those with sarcoidosis has already been reported [252], confirming ARA-290 mechanism of therapeutic benefit in a setting of ischaemic injury will endorse its clinical application for patients with CLI.

The majority of pre-clinical models for CLI induce hindlimb ischaemia by ligation of lower limb vessels. It is important to realise however, that there are several limitations to the use of this model, and therefore, care needs to be taken in making direct comparison with human clinical benefit. Most importantly, the hindlimb ischaemia model does not adequately take into account the natural progression of PAD, and the complex interaction between multiple co-morbidities. In patients with

PAD, atherosclerotic lesions tend to develop over time, in multiple locations, giving rise to diffuse lesions, and a more insidious onset of ischaemia, with greater opportunity for the limb to develop a collateral circulation. Most animal models of CLI fail to mimic these features. In addition all surgical ligation models of hindlimb ischaemia represent more of an acute ischaemic insult due to the sudden loss of arterial supply to the limb. This partly explains the extensive inflammatory response observed. Other techniques exist to mimic CLI in hindlimb ischaemia model. This includes slow occlusion of the vessel with constrictors or balloon dilation, which is less reproducible, with high-costs associated with the constrictor and the prolonged period of experimental intervention. Other techniques include double ligation of the femoral artery twice, separated by approximately 12 weeks to produce a more chronic hindlimb ischaemia. Assessment of muscle injury is not widely available in these alternative models however, and would therefore need to be assessed in greater detail to explore their relevance as a model to mimic the muscle pathology observed in human CLI disease. PAD patients also tend to have multiple co-morbidities, which influence disease state and progression. Although transgenic strains for the majority of co-morbidities found in PAD patients exists, little work has been done assessing the hindlimb ischaemia model with transgenic animals to assess the resultant effect on muscle.

Laser Doppler measurement of 'perfusion' is a reliable and easily reproducible technique for assessment of recovery of ischaemia, and is often complemented with histological analysis of C:F ratio. However, LDPI assesses blood flux rather than true tissue perfusion, and relies on the standardisation of ambient conditions, including the temperature of the animal and surroundings.

In addition, much information can be accrued by observing other aspects in the field of muscle biology. The investigation of muscle degeneration and weakness, both age or disease related is likely to highlight many potential dysregulated pathways applicable to muscle dysfunction in CLI. An example of this is the IGF-1 axis, which has for sometime been known to play a role in cancer cachexia and muscle wasting, as well as driving muscle regeneration [405, 406]. Recently, components of the IGF axis have been associated with both the presence and severity of PAD, identifying it to have an underlying pathophysiological role [407].

In summary, the work contained in this thesis has attempted to assess the protective functions of EPO and ARA-290 for the application in CLI. In order to do this, human myoblasts were isolated from both our disease group of interest and control donors. Comparison of their behaviour and function identified significant differences between them. This study also sought to identify a clinically relevant hindlimb ischaemia model which mimicked features of muscle pathology found in human patients in order to test potential tissue-protective hypotheses and therapies. Cumulatively, this work has been able to provide evidence of the tissue-protective capabilities of EPO and ARA-290 *in vitro* and *in vivo* in settings of ischaemic injury.

7.2 Future studies

The potential use of ARA-290 in mediating tissue protection in a setting of ischaemic injury is an exciting observation of this work. Further studies need to be conducted to address some of the limitations of this thesis.

Though a tissue protective receptor has been suggested, there is yet to be confirmed analysis of ARA-290 binding to the suggested tissue-protective receptor. In addition, the possibility of alternative receptors needs to be explored, in conjunction with identification of additional signalling cascades. This work has demonstrated the ability of EPO and ARA-290 to provide numerous beneficial effects against ischaemia, including apoptosis, migration and proliferation. It is therefore likely that there are multiple signalling cascades at interplay, and delineating those pathways may provide useful insight into aberrations in the CLI disease state.

The functional differences in myoblasts isolated from CLI and control patients have not previously been described. Although they provide useful insight into the responses of myoblasts to chronic ischaemia, potential mechanisms underlying the observed differences need further interrogation, for the purposes of improving understanding of the deficit in muscle function often described by individuals with CLI. In addition, manipulation of the differences in CLI myoblast behaviour may provide a cornerstone for the future management of individuals with CLI. Whilst isolated myoblasts were able to survive, proliferate and differentiate *ex vivo,* further analysis will need to be conducted to evaluate in detail the observations made in this work with regard to functional differences in CLI myoblast function. It is important

to understand whether these observed difference were due to their 'pre-conditioning' in an ischaemic niche, or whether the exposure to chronic ischaemia had a resultant effect on intrinsic myoblast function, giving rise to the differences in myoblast function, and ultimately the muscle symptoms described in PAD patients. It is clear that CLI myoblasts, in their native *in vivo* conditions are incapable of physiologically normal muscle repair and regeneration. However, it is not clear whether the underlying deficit is due to the hypoxic conditions or the myoblast itself.

Elucidating the trail that leads to muscle injury and inadequate repair following chronic exposure to ischaemia is essential to combat the musculopathy observed in CLI patients. Recent attempts at cell-based therapies to transplant myogenic stem cells have yielded promising results. However, if an ischaemic niche is responsible for alterations in myoblast function, the benefit from introduction of new myogenic stem cells is likely to be short-lived. Dual introduction of myogenic and haematopoietic stem cells to improve muscle function and perfusion may ultimately be required, with simultaneous revascularisation to alleviate the local ischaemic niche sufficiently for the newly introduced stem cells to become integrated.

Though this study has examined the differences in human myoblasts between CLI and control, future work could focus on the main muscle progenitor – satellite cells. Observations made in this work have suggested that the satellite cell population becomes activated in CLI muscle, but their regenerative and reparative function and ability to differentiate into valuable myoblasts and myotubes is uncertain.

The hindlimb ischaemia model also demonstrated the promising ability of ARA-290 to ameliorate ischaemia-induced injury to muscles of the hindlimb. However, though the hindlimb ischaemia model is able to recapitulate the effects of ischaemia, it does not take into account the co-morbidities commonly present in patients with CLI, such as diabetes, hypertension and hyperlipidaemia, which can affect not only muscle regeneration and repair [341, 408-410], but also other factors, such as release of inflammatory cytokines and dampening of endothelial cell proliferation that may hinder improvements in CLI patients [411-413]. The use of transgenic and knockout animals allows investigators to address those risk factors known to be important in human disease. This may aid in the identification of novel therapies that will be equally as efficacious at the bedside as they are at the bench. In addition to

longitudinal assessment of perfusion using LDPI, many novel imaging techniques are in constant development, and their resolution and use in small animals is continuously improving. Imaging modalities such as micro and photoacoustic CT and dynamic contrast-enhanced MRI would allow evaluation of collateral formation in the ischaemic hindlimb. In addition, evaluating mitochondrial activity, which often becomes pathological following ischaemic injury could, indirectly assess muscle viability and function as a result of hindlimb ischaemia and any subsequent intervention.

Appendix

A 1: Patient information and consent form

Royal Free and University College Medical School
UNIVERSITY COLLEGE LONDON
Address for Correspondence:
University Department of Surgery
Royal Free Campus
The Royal Free Hospital
Pond Street,
London NW3 2QG
Telephone:020 77940500
Facsimile: 02074726711

PATIENT INFORMATION SHEET

Study Title: A study of muscle injury in peripheral vascular disease

You are invited to participate in a research study. This information sheet explains why we are conducting this study and how it is being done. Please take some time to read the information carefully and to decide whether you would like to take part or not. Please discuss it with your family and friends as you wish and ask us if you have any questions.

What is the purpose of this study?

The aim of this project is to study some aspects of peripheral vascular disease which are not well understood. Peripheral vascular disease is a common condition where the blood supply to the legs is impaired and the leg muscles are damaged. At present, treatment includes bypass surgery to improve the circulation. We aim to study the mechanisms that are involved in causing muscle damage secondary to peripheral vascular disease. A better understanding of these mechanisms may improve treatment for this disease in the future.

Why have I been chosen?

You have been invited to take part either because you suffer from peripheral vascular disease or because the operation you will be undergoing is similar in many ways to that done for peripheral vascular disease. This allows us to collect suitable samples for analyses and make appropriate comparisons.

Do I have to take part?

You do not have to take part in this study if you do not want to. If you decide to take part you may withdraw at any time without giving a reason. Your decision to take part or not will not affect your care in any way.

What will happen to me if I take part?

Up to 2 calf muscle samples, each the size of a small pea, will be taken during the operation. These are for the study and not part of the treatment. None of these should cause any ill effect or additional discomfort and will not affect your recovery from your operation.

What do I have to do?

You do not have to do anything more than you need to for your operation.

Royal Free and University College Medical School
UNIVERSITY COLLEGE LONDON
Address for Correspondence:
University Department of Surgery
Royal Free Campus
The Royal Free Hospital
Pond Street,
London NW3 2QG
Telephone:020 77940500
Facsimile: 02074726711

Date: 25 Sept 2008

What are the possible disadvantages and risks in taking part?

You will have small samples of your calf muscle taken. However, these will be done during the operation when you are asleep and so will not cause any discomfort. Your treatment and recovery will not be affected.

What are the possible benefits of taking part?

This study will help us improve treatment for this condition in the future. However, at this stage, there will be no immediate benefits to you.

What if something goes wrong?

This study does not involve any extra treatment or any high-risk procedures so nothing is likely to go wrong. However, if you wish to complain about any aspect of the way you have been approached or treated during the course of this study, the normal National Health Service complaints mechanisms may be available to you.

Will taking part in this study be kept confidential?

Any information collected about you during the course of the research will be kept strictly confidential.

What happens to the results of the research study?

Results from this study will be published in a medical journal in approximately a year's time. However you will not be identified in any report or publication. If you wish to know the outcome of the study, you can do so by contacting us.

Who is organising and funding the research?

This study is organised and funded by the Vascular Unit of the Department of Surgery.

Who has reviewed the study?

The Research Ethics Committee of the Royal Free Hospital has reviewed this study.

If you have any questions or queries at any stage, please contact:

Miss Janice Tsui
University Department of Surgery
Royal Free Hospital
Pond Street
London NW3 2QG
Tel: 020-7794-0500 Ext 33938

You will be given a copy of the information sheet and a signed consent form to keep. Thank you very much for taking part in this study.

Royal Free and University College Medical School
UNIVERSITY COLLEGE LONDON
Address for Correspondence:
University Department of Surgery
Royal Free Campus
The Royal Free Hospital
Pond Street,
London NW3 2QG
Telephone:020 77940500
Facsimile: 02074726711

Consent Form

Project Title: Study of Muscle Injury in Peripheral Vascular Disease

Researcher: Miss Janice Tsui & _____

1. I confirm that I have read and understood the information sheet provided for the above study and have had the opportunity to ask questions. ☐
2. I confirm that I have had sufficient time to consider whether or not I want to be included with the study. ☐
3. I understand that my participation is voluntary and that I am free to withdraw at any time, without giving any reasons, without my medical care or legal rights being affected. ☐
4. I understand that sections of my medical notes may be looked at by responsible individuals from NHS or from regulatory authorities where it is relevant to my taking part in the research. I understand that samples of my muscle may be kept up to 6 months for other studies. ☐
5. I agree to take part in the above study. ☐

Name of patient	Date	Signature

Name of person taking consent	Date	Signature

A 2: Awards, presentations and publications arising from this work

Awards

1. JSPS-British Council Summer fellowship – Japan, Summer 2012
2. Richard Wood Memorial prize, Vascular Society UK Annual General Meeting – Manchester, UK, November 2013

Presentations

1. Tissue-protective effects of EPO and EPO-derivative in isolated human myoblasts.
   Society of Academic and Research Surgery Annual Conference 2012 (oral presentation)
2. Role of PI3k/Akt Pathway in the Cytoprotective Effects of Erythropoietin and Derivatives in Ischemic Human Myotubes
   Society for Vascular Surgery Annual Conference 2012 (poster presentation)
3. Differential Proliferative and Migratory Activity of Human Myoblasts Isolated from CLI and Control Patients
   Society for Vascular Surgery Annual Conference 2013 (poster presentation)
4. Signalling Pathways Involved in the Tissue-protective Effects of Erythropoietin and Erythropoietin-derivatives in Ischemic Human Myotubes
   Society for Vascular Surgery Annual Conference 2013 (poster presentation)
5. Enhanced proliferative and migratory differences in human myoblasts isolated from CLI and control patients
   European Society for Vascular Surgery Spring Meeting 2013 (oral presentation)
6. Tissue-protective effects of an erythropoietin-derivative in a model of hindlimb ischaemia
   Vascular Society UK Annual General Meeting 2013 (oral presentation)

Publications and published abstracts

1. Potential of Novel EPO Derivatives in Limb Ischemia.
   Cardiology research and practice, 2012. **2012**: p. 213785. Joshi D, Tsui J, **Yu R**, Shiwen X, Selvakumar S, Abraham D. J. Baker, D. M.
2. Tissue protective effects of EPO and EPO-derivative in isolated human myoblasts (2012)
   British Journal of Surgery, 99, 7-123
3. Role of PI3k/Akt Pathway in the Cytoprotective Effects of Erythropoietin and Derivatives in Ischemic Human Myotubes (2012)
   Journal of Vascular Surgery, 55, 76-76
4. Differential Proliferative and Migratory Activity of Human Myoblasts Isolated from CLI and Control Patients (2013)
   Journal of Vascular Surgery, 57, 81S – 82S
5. Signalling Pathways Involved in the Tissue-protective Effects of Erythropoietin and Erythropoietin-derivatives in Ischemic Human Myotubes (2013)
   Journal of Vascular Surgery, 57, 78S – 78S

Bibliography

1. Hiatt, W.R., S. Hoag, and R.F. Hamman, Effect of diagnostic criteria on the prevalence of peripheral arterial disease. The San Luis Valley Diabetes Study. Circulation, 1995. **91**(5): p. 1472-9.

2. Criqui, M.H., et al., The prevalence of peripheral arterial disease in a defined population. Circulation, 1985. **71**(3): p. 510-5.

3. Selvin, E. and T.P. Erlinger, Prevalence of and risk factors for peripheral arterial disease in the United States: results from the National Health and Nutrition Examination Survey, 1999-2000. Circulation, 2004. **110**(6): p. 738-43.

4. Norgren, L., et al., Inter-Society Consensus for the Management of Peripheral Arterial Disease (TASC II). J Vasc Surg, 2007. **45 Suppl S**: p. S5-67.

5. Hiatt, W.R., Medical treatment of peripheral arterial disease and claudication. N Engl J Med, 2001. **344**(21): p. 1608-21.

6. Hankey, G.J., P.E. Norman, and J.W. Eikelboom, Medical treatment of peripheral arterial disease. JAMA, 2006. **295**(5): p. 547-53.

7. Kumakura, H., et al., Differences in Brain Natriuretic Peptide and Other Factors between Japanese Peripheral Arterial Disease Patients with Critical Limb Ischemia and Intermittent Claudication. Journal of atherosclerosis and thrombosis, 2013.

8. Amaranto, D.J., et al., An evaluation of gender and racial disparity in the decision to treat surgically arterial disease. J Vasc Surg, 2009. **50**(6): p. 1340-7.

9. Hankey, G.J., Vascular disease of the heart, brain and limbs: new insights into a looming epidemic. Lancet, 2005. **366**(9499): p. 1753-4.

10. Frosst, P., et al., A candidate genetic risk factor for vascular disease: a common mutation in methylenetetrahydrofolate reductase. Nat Genet, 1995. **10**(1): p. 111-3.

11. Clarke, R., et al., Hyperhomocysteinemia: an independent risk factor for vascular disease. N Engl J Med, 1991. **324**(17): p. 1149-55.

12. Hughson, W.G., J.I. Mann, and A. Garrod, Intermittent claudication: prevalence and risk factors. Br Med J, 1978. **1**(6124): p. 1379-81.

13. Price, J.F., et al., Relationship between smoking and cardiovascular risk factors in the development of peripheral arterial disease and coronary artery disease: Edinburgh Artery Study. Eur Heart J, 1999. **20**(5): p. 344-53.

14. Criqui, M.H., et al., The epidemiology of peripheral arterial disease: importance of identifying the population at risk. Vasc Med, 1997. **2**(3): p. 221-6.

15. Meijer, W.T., et al., Peripheral arterial disease in the elderly: The Rotterdam Study. Arterioscler Thromb Vasc Biol, 1998. **18**(2): p. 185-92.

16. Hirsch, A.T., et al., The role of tobacco cessation, antiplatelet and lipid-lowering therapies in the treatment of peripheral arterial disease. Vasc Med, 1997. **2**(3): p. 243-51.

17. Bhatt, D.L., et al., International prevalence, recognition, and treatment of cardiovascular risk factors in outpatients with atherothrombosis. JAMA, 2006. **295**(2): p. 180-9.

18. Norgren, L., et al., Inter-Society Consensus for the Management of Peripheral Arterial Disease (TASC II). Eur J Vasc Endovasc Surg, 2007. **33 Suppl 1**: p. S1-75.

19. Sim, E.K., et al., Prevalence of peripheral artery disease in patients with coronary artery disease. Ann Acad Med Singapore, 1993. **22**(6): p. 898-900.

20. Mautner, G.C., S.L. Mautner, and W.C. Roberts, Amounts of coronary arterial narrowing by atherosclerotic plaque at necropsy in patients with lower extremity amputation. Am J Cardiol, 1992. **70**(13): p. 1147-51.

21. Criqui, M.H. and J.O. Denenberg, The generalized nature of atherosclerosis: how peripheral arterial disease may predict adverse events from coronary artery disease. Vasc Med, 1998. **3**(3): p. 241-5.

22. Hertzer, N.R., et al., Coronary artery disease in peripheral vascular patients. A classification of 1000 coronary angiograms and results of surgical management. Ann Surg, 1984. **199**(2): p. 223-33.

23. Mendelson, G., W.S. Aronow, and C. Ahn, Prevalence of coronary artery disease, atherothrombotic brain infarction, and peripheral arterial disease: associated risk factors in older Hispanics in an academic hospital-based geriatrics practice. J Am Geriatr Soc, 1998. **46**(4): p. 481-3.

24. Dormandy, J., et al., Fate of the patient with chronic leg ischaemia. A review article. J Cardiovasc Surg (Torino), 1989. **30**(1): p. 50-7.

25. Verstaete, M., Meeting Report Evolving European consensuson critical limb ischaemia. European Heart Journal, 1990. **11**(5): p. 479-480.

26. Muluk, S.C., et al., Outcome events in patients with claudication: a 15-year study in 2777 patients. J Vasc Surg, 2001. **33**(2): p. 251-7; discussion 257-8.

27. Schroeder, T.V., The TASC supplement - international recommendations for management of peripheral arterial disease. Eur J Vasc Endovasc Surg, 2000. **19**(6): p. 563.

28. Hirsch, A.T., et al., ACC/AHA 2005 Practice Guidelines for the management of patients with peripheral arterial disease (lower extremity, renal, mesenteric, and abdominal aortic): a collaborative report from the American Association for Vascular Surgery/Society for Vascular Surgery, Society for Cardiovascular Angiography and Interventions, Society for Vascular Medicine and Biology, Society of Interventional Radiology, and the ACC/AHA Task Force on Practice Guidelines (Writing Committee to Develop Guidelines for the Management of Patients With Peripheral Arterial Disease): endorsed by the American Association of Cardiovascular and Pulmonary Rehabilitation; National Heart, Lung, and Blood Institute; Society for Vascular Nursing; TransAtlantic Inter-Society Consensus; and Vascular Disease Foundation. Circulation, 2006. **113**(11): p. e463-654.

29. Fontaine, R., M. Kim, and R. Kieny, [Surgical treatment of peripheral circulation disorders]. Helvetica chirurgica acta, 1954. **21**(5-6): p. 499-533.

30. Rutherford, R.B., et al., Recommended standards for reports dealing with lower extremity ischemia: revised version. J Vasc Surg, 1997. **26**(3): p. 517-38.

31. Al-Qaisi, M., et al., Ankle brachial pressure index (ABPI): An update for practitioners. Vasc Health Risk Manag, 2009. **5**: p. 833-41.

32. Peripheral arterial disease in people with diabetes. Diabetes Care, 2003. **26**(12): p. 3333-41.

33. Cao, P., et al., Chapter II: Diagnostic methods. Eur J Vasc Endovasc Surg, 2011. **42 Suppl 2**: p. S13-32.

34. Potier, L., et al., Use and utility of ankle brachial index in patients with diabetes. Eur J Vasc Endovasc Surg, 2011. **41**(1): p. 110-6.

35. Romanos, M.T., A. Raspovic, and B.M. Perrin, The reliability of toe systolic pressure and the toe brachial index in patients with diabetes. J Foot Ankle Res, 2010. **3**: p. 31.

36. Williams, D.T., K.G. Harding, and P. Price, An evaluation of the efficacy of methods used in screening for lower-limb arterial disease in diabetes. Diabetes Care, 2005. **28**(9): p. 2206-10.

37. Williams, D.T., P. Price, and K.G. Harding, The influence of diabetes and lower limb arterial disease on cutaneous foot perfusion. J Vasc Surg, 2006. **44**(4): p. 770-5.

38. Nicolai, S.P., et al., Ankle brachial index measurement in primary care: are we doing it right? Br J Gen Pract, 2009. **59**(563): p. 422-7.

39. Alpert, J.S., O.A. Larsen, and N.A. Lassen, Exercise and intermittent claudication. Blood flow in the calf muscle during walking studied by the xenon-133 clearance method. Circulation, 1969. **39**(3): p. 353-9.

40. Allard, L., et al., Limitations of ultrasonic duplex scanning for diagnosing lower limb arterial stenoses in the presence of adjacent segment disease. J Vasc Surg, 1994. **19**(4): p. 650-7.

41. Drieghe, B., et al., Assessment of renal artery stenosis: side-by-side comparison of angiography and duplex ultrasound with pressure gradient measurements. Eur Heart J, 2008. **29**(4): p. 517-24.

42. Buth, J., et al., Color-flow duplex criteria for grading stenosis in infrainguinal vein grafts. J Vasc Surg, 1991. **14**(6): p. 716-26; discussion 726-8.

43. Ascher, E., et al., The use of duplex ultrasound arterial mapping as an alternative to conventional arteriography for primary and secondary infrapopliteal bypasses. Am J Surg, 1999. **178**(2): p. 162-5.

44. Solomon, R., The role of osmolality in the incidence of contrast-induced nephropathy: a systematic review of angiographic contrast media in high risk patients. Kidney Int, 2005. **68**(5): p. 2256-63.

45. Met, R., et al., Diagnostic performance of computed tomography angiography in peripheral arterial disease: a systematic review and meta-analysis. JAMA, 2009. **301**(4): p. 415-24.

46. Rofsky, N.M. and M.A. Adelman, MR angiography in the evaluation of atherosclerotic peripheral vascular disease. Radiology, 2000. **214**(2): p. 325-38.

47. Collins, R., et al., Duplex ultrasonography, magnetic resonance angiography, and computed tomography angiography for diagnosis and assessment of symptomatic, lower limb peripheral arterial disease: systematic review. BMJ, 2007. **334**(7606): p. 1257.

48. Hunt, C.H., R.P. Hartman, and G.K. Hesley, Frequency and severity of adverse effects of iodinated and gadolinium contrast materials: retrospective review of 456,930 doses. AJR Am J Roentgenol, 2009. **193**(4): p. 1124-7.

49. Davis, C.P., et al., MR angiography of patients with peripheral arterial disease before and after transluminal angioplasty. AJR Am J Roentgenol, 1997. **168**(4): p. 1027-34.

50. Lee, V.S., et al., Gadolinium-enhanced MR angiography: artifacts and pitfalls. AJR Am J Roentgenol, 2000. **175**(1): p. 197-205.

51. Thomsen, H.S. and P. Marckmann, Extracellular Gd-CA: differences in prevalence of NSF. European journal of radiology, 2008. **66**(2): p. 180-3.

52. Todd, D.J., et al., Cutaneous changes of nephrogenic systemic fibrosis: predictor of early mortality and association with gadolinium exposure. Arthritis and rheumatism, 2007. **56**(10): p. 3433-41.

53. A randomised, blinded, trial of clopidogrel versus aspirin in patients at risk of ischaemic events (CAPRIE). CAPRIE Steering Committee. Lancet, 1996. **348**(9038): p. 1329-39.

54. MRC/BHF Heart Protection Study of cholesterol lowering with simvastatin in 20,536 high-risk individuals: a randomised placebo-controlled trial. Lancet, 2002. **360**(9326): p. 7-22.

55. Resnick, H.E., et al., Relationship of high and low ankle brachial index to all-cause and cardiovascular disease mortality: the Strong Heart Study. Circulation, 2004. **109**(6): p. 733-9.

56. Willigendael, E.M., et al., Influence of smoking on incidence and prevalence of peripheral arterial disease. J Vasc Surg, 2004. **40**(6): p. 1158-65.

57. Critchley, J.A. and S. Capewell, Mortality risk reduction associated with smoking cessation in patients with coronary heart disease: a systematic review. JAMA, 2003. **290**(1): p. 86-97.

58. Willigendael, E.M., et al., Smoking and the patency of lower extremity bypass grafts: a meta-analysis. J Vasc Surg, 2005. **42**(1): p. 67-74.

59. Anthonisen, N.R., et al., The effects of a smoking cessation intervention on 14.5-year mortality: a randomized clinical trial. Annals of internal medicine, 2005. **142**(4): p. 233-9.

60. Aung, P.P., et al., Lipid-lowering for peripheral arterial disease of the lower limb. The Cochrane database of systematic reviews, 2007(4): p. CD000123.

61. Chobanian, A.V., et al., Seventh report of the Joint National Committee on Prevention, Detection, Evaluation, and Treatment of High Blood Pressure. Hypertension, 2003. **42**(6): p. 1206-52.

62. 2003 European Society of Hypertension-European Society of Cardiology guidelines for the management of arterial hypertension. Journal of hypertension, 2003. **21**(6): p. 1011-53.

63. Intensive blood-glucose control with sulphonylureas or insulin compared with conventional treatment and risk of complications in patients with type 2 diabetes (UKPDS 33). UK Prospective Diabetes Study (UKPDS) Group. Lancet, 1998. **352**(9131): p. 837-53.

64. Collaborative meta-analysis of randomised trials of antiplatelet therapy for prevention of death, myocardial infarction, and stroke in high risk patients. BMJ, 2002. **324**(7329): p. 71-86.

65. Robless, P., D.P. Mikhailidis, and G. Stansby, Systematic review of antiplatelet therapy for the prevention of myocardial infarction, stroke or vascular death in patients with peripheral vascular disease. The British journal of surgery, 2001. **88**(6): p. 787-800.

66. Lambert, M.A. and J.J. Belch, Medical management of critical limb ischaemia: where do we stand today? Journal of internal medicine, 2013.

67. Ruffolo, A.J., M. Romano, and A. Ciapponi, Prostanoids for critical limb ischaemia. The Cochrane database of systematic reviews, 2010(1): p. CD006544.

68. Miyashita, Y., et al., Cilostazol increases skin perfusion pressure in severely ischemic limbs. Angiology, 2011. **62**(1): p. 15-7.

69. Soga, Y., et al., Impact of cilostazol after endovascular treatment for infrainguinal disease in patients with critical limb ischemia. J Vasc Surg, 2011. **54**(6): p. 1659-67.

70. Watson, L., B. Ellis, and G.C. Leng, Exercise for intermittent claudication. The Cochrane database of systematic reviews, 2008(4): p. CD000990.

71. Rana, M.A. and P. Gloviczki, Endovascular interventions for infrapopliteal arterial disease: an update. Seminars in vascular surgery, 2012. **25**(1): p. 29-34.

72. Saqib, N.U., et al., Predictors and outcomes of restenosis following tibial artery endovascular interventions for critical limb ischemia. J Vasc Surg, 2013. **57**(3): p. 692-9.

73. Baumann, F., et al., Single-center experience in endovascular treatment for infrainguinal bypass obstructions. J Vasc Interv Radiol, 2012. **23**(8): p. 1055-62.

74. Ferraresi, R., et al., Long-term outcomes after angioplasty of isolated, below-the-knee arteries in diabetic patients with critical limb ischaemia. Eur J Vasc Endovasc Surg, 2009. **37**(3): p. 336-42.

75. Bradbury, A.W., et al., Bypass versus Angioplasty in Severe Ischaemia of the Leg (BASIL) trial: An intention-to-treat analysis of amputation-free and overall survival in patients randomized to a bypass surgery-first or a balloon angioplasty-first revascularization strategy. J Vasc Surg, 2010. **51**(5 Suppl): p. 5S-17S.

76. Adam, D.J., et al., Bypass versus angioplasty in severe ischaemia of the leg (BASIL): multicentre, randomised controlled trial. Lancet, 2005. **366**(9501): p. 1925-34.

77. Albers, M., et al., Meta-analysis of popliteal-to-distal vein bypass grafts for critical ischemia. J Vasc Surg, 2006. **43**(3): p. 498-503.

78. Balaz, P., et al., The role of hybrid procedures in the management of peripheral vascular disease. Scandinavian journal of surgery : SJS : official organ for the Finnish Surgical Society and the Scandinavian Surgical Society, 2012. **101**(4): p. 232-7.

79. Chang, R.W., et al., Long-term results of combined common femoral endarterectomy and iliac stenting/stent grafting for occlusive disease. J Vasc Surg, 2008. **48**(2): p. 362-7.

80. Matsagkas, M., et al., Hybrid procedures for patients with critical limb ischemia and severe common femoral artery atherosclerosis. Ann Vasc Surg, 2011. **25**(8): p. 1063-9.

81. Dosluoglu, H.H., et al., Role of simple and complex hybrid revascularization procedures for symptomatic lower extremity occlusive disease. J Vasc Surg, 2010. **51**(6): p. 1425-1435 e1.

82. Nishibe, T., et al., Hybrid surgical and endovascular therapy in multifocal peripheral TASC D lesions: up to three-year follow-up. J Cardiovasc Surg (Torino), 2009. **50**(4): p. 493-9.

83. Beard, J.D., ABC of arterial and venous disease: Chronic lower limb ischaemia. BMJ, 2000. **320**(7238): p. 854-7.

84. Moxey, P.W., et al., Epidemiological study of lower limb amputation in England between 2003 and 2008. The British journal of surgery, 2010. **97**(9): p. 1348-53.

85. Treatment of limb threatening ischaemia with intravenous iloprost: a randomised double-blind placebo controlled study. U.K. Severe Limb Ischaemia Study Group. Eur J Vasc Surg, 1991. **5**(5): p. 511-6.

86. Rollins, K.E., D. Jackson, and P.A. Coughlin, Meta-analysis of contemporary short- and long-term mortality rates in patients diagnosed with critical leg ischaemia. The British journal of surgery, 2013. **100**(8): p. 1002-8.

87. Fortington, L.V., et al., Short and long term mortality rates after a lower limb amputation. Eur J Vasc Endovasc Surg, 2013. **46**(1): p. 124-31.

88. Cieri, E., et al., Functional ability in patients with critical limb ischaemia is unaffected by successful revascularisation. Eur J Vasc Endovasc Surg, 2011. **41**(2): p. 256-63.

89. Taylor, S.M., et al., Clinical success using patient-oriented outcome measures after lower extremity bypass and endovascular intervention for ischemic tissue loss. J Vasc Surg, 2009. **50**(3): p. 534-41; discussion 541.

90. Rollins, K.E. and P.A. Coughlin, Functional outcomes following revascularisation for critical limb ischaemia. Eur J Vasc Endovasc Surg, 2012. **43**(4): p. 420-5.

91. Kumar, B.N. and R.P. Gambhir, Critical limb ischemia-need to look beyond limb salvage. Ann Vasc Surg, 2011. **25**(7): p. 873-7.

92. Simons, J.P., et al., Failure to achieve clinical improvement despite graft patency in patients undergoing infrainguinal lower extremity bypass for critical limb ischemia. J Vasc Surg, 2010. **51**(6): p. 1419-24.

93. Bosiers, M., et al., Randomized comparison of everolimus-eluting versus bare-metal stents in patients with critical limb ischemia and infrapopliteal arterial occlusive disease. J Vasc Surg, 2012. **55**(2): p. 390-8.

94. Parmenter, B.J., et al., Preliminary evidence that low ankle-brachial index is associated with reduced bilateral hip extensor strength and functional mobility in peripheral arterial disease. J Vasc Surg, 2013. **57**(4): p. 963-973 e1.

95. Stewart, K.J., et al., Exercise training for claudication. N Engl J Med, 2002. **347**(24): p. 1941-51.

96. Anderson, J.D., et al., Multifactorial determinants of functional capacity in peripheral arterial disease: uncoupling of calf muscle perfusion and metabolism. J Am Coll Cardiol, 2009. **54**(7): p. 628-35.

97. Pernow, B. and S. Zetterquist, Metabolic evaluation of the leg blood flow in claudicating patients with arterial obstructions at different levels. Scand J Clin Lab Invest, 1968. **21**(3): p. 277-87.

98. Larsen, O.A. and N.A. Lassen, Effect of daily muscular exercise in patients with intermittent claudication. Lancet, 1966. **2**(7473): p. 1093-6.

99. Gardner, A.W., et al., Prediction of claudication pain from clinical measurements obtained at rest. Medicine and science in sports and exercise, 1992. **24**(2): p. 163-70.

100. Regensteiner, J.G., et al., Functional benefits of peripheral vascular bypass surgery for patients with intermittent claudication. Angiology, 1993. **44**(1): p. 1-10.

101. Gardner, A.W. and L.A. Killewich, Lack of functional benefits following infrainguinal bypass in peripheral arterial occlusive disease patients. Vascular medicine, 2001. **6**(1): p. 9-14.

102. Regensteiner, J.G., J.F. Steiner, and W.R. Hiatt, Exercise training improves functional status in patients with peripheral arterial disease. J Vasc Surg, 1996. **23**(1): p. 104-15.

103. Hiatt, W.R., et al., Benefit of exercise conditioning for patients with peripheral arterial disease. Circulation, 1990. **81**(2): p. 602-9.

104. Makris, G.C., et al., Availability of supervised exercise programs and the role of structured home-based exercise in peripheral arterial disease. Eur J Vasc Endovasc Surg, 2012. **44**(6): p. 569-75; discussion 576.

105. McDermott, M.M., et al., Impairments of muscles and nerves associated with peripheral arterial disease and their relationship with lower extremity functioning: the InCHIANTI Study. J Am Geriatr Soc, 2004. **52**(3): p. 405-10.

106. Hedberg, B., K.A. Angquist, and M. Sjostrom, Peripheral arterial insufficiency and the fine structure of the gastrocnemius muscle. Int Angiol, 1988. **7**(1): p. 50-9.

107. Makitie, J. and H. Teravainen, Histochemical changes in striated muscle in patients with intermittent claudication. Arch Pathol Lab Med, 1977. **101**(12): p. 658-63.

108. Albani, M., et al., Morphological, histochemical, and interstitial pressure changes in the tibialis anterior muscle before and after aortofemoral bypass in patients with peripheral arterial occlusive disease. BMC Musculoskelet Disord, 2002. **3**: p. 8.

109. Mitchell, R.G., et al., Increased levels of apoptosis in gastrocnemius skeletal muscle in patients with peripheral arterial disease. Vasc Med, 2007. **12**(4): p. 285-90.

110. Hedberg, B., et al., Fibre loss and distribution in skeletal muscle from patients with severe peripheral arterial insufficiency. Eur J Vasc Surg, 1989. **3**(4): p. 315-22.

111. Schiaffino, S., Fibre types in skeletal muscle: a personal account. Acta Physiol (Oxf), 2010. **199**(4): p. 451-63.

112. Schiaffino, S. and C. Reggiani, Myosin isoforms in mammalian skeletal muscle. J Appl Physiol, 1994. **77**(2): p. 493-501.

113. Lucas, C.A., L.H. Kang, and J.F. Hoh, Monospecific antibodies against the three mammalian fast limb myosin heavy chains. Biochem Biophys Res Commun, 2000. **272**(1): p. 303-8.

114. Regensteiner, J.G., et al., Chronic changes in skeletal muscle histology and function in peripheral arterial disease. Circulation, 1993. **87**(2): p. 413-21.

115. Clyne, C.A., et al., Ultrastructural and capillary adaptation of gastrocnemius muscle to occlusive peripheral vascular disease. Surgery, 1982. **92**(2): p. 434-40.

116. Steinacker, J.M., et al., Expression of myosin heavy chain isoforms in skeletal muscle of patients with peripheral arterial occlusive disease. J Vasc Surg, 2000. **31**(3): p. 443-9.

117. Hou, X.Y., et al., Skeletal muscle mitochondrial ATP production rate and walking performance in peripheral arterial disease. Clin Physiol Funct Imaging, 2002. **22**(3): p. 226-32.

118. Pipinos, II, et al., The myopathy of peripheral arterial occlusive disease: part 1. Functional and histomorphological changes and evidence for mitochondrial dysfunction. Vasc Endovascular Surg, 2007. **41**(6): p. 481-9.

119. Hiatt, W.R., et al., Effect of exercise training on skeletal muscle histology and metabolism in peripheral arterial disease. J Appl Physiol, 1996. **81**(2): p. 780-8.

120. Hiatt, W.R., et al., Skeletal muscle carnitine metabolism in patients with unilateral peripheral arterial disease. J Appl Physiol, 1992. **73**(1): p. 346-53.

121. Brevetti, G., et al., Increases in walking distance in patients with peripheral vascular disease treated with L-carnitine: a double-blind, cross-over study. Circulation, 1988. **77**(4): p. 767-73.

122. Zatina, M.A., et al., 31P nuclear magnetic resonance spectroscopy: noninvasive biochemical analysis of the ischemic extremity. J Vasc Surg, 1986. **3**(3): p. 411-20.

123. Wallace, D.C., Mitochondrial defects in cardiomyopathy and neuromuscular disease. American heart journal, 2000. **139**(2 Pt 3): p. S70-85.

124. Pipinos, II, et al., The myopathy of peripheral arterial occlusive disease: Part 2. Oxidative stress, neuropathy, and shift in muscle fiber type. Vasc Endovascular Surg, 2008. **42**(2): p. 101-12.

125. McLennan, H.R. and M. Degli Esposti, The contribution of mitochondrial respiratory complexes to the production of reactive oxygen species. Journal of bioenergetics and biomembranes, 2000. **32**(2): p. 153-62.

126. Lenaz, G., et al., Mitochondrial bioenergetics in aging. Biochimica et biophysica acta, 2000. **1459**(2-3): p. 397-404.

127. Moghaddas, S., et al., Preservation of cardiolipin content during aging in rat heart interfibrillar mitochondria. The journals of gerontology. Series A, Biological sciences and medical sciences, 2002. **57**(1): p. B22-8.

128. Makris, K.I., et al., Mitochondriopathy of peripheral arterial disease. Vascular, 2007. **15**(6): p. 336-43.

129. Pipinos, II, et al., Mitochondrial defects and oxidative damage in patients with peripheral arterial disease. Free radical biology & medicine, 2006. **41**(2): p. 262-9.

130. Lang, P.M., et al., Sensory neuropathy and signs of central sensitization in patients with peripheral arterial disease. Pain, 2006. **124**(1-2): p. 190-200.

131. Carnot, P.D., C, Sur l'activite hematopoietique du serum au cours de la regeneration du sang. C. R. Acad Sci (Paris), 1906. **143**: p. 384-386.

132. Bonsdorff, E.V.A. and E. Jalavisto, A Humoral Mechanism in Anoxic Erythrocytosis. Acta Physiologica Scandinavica, 1948. **16**(2-3): p. 150-170.

133. Miyake, T., C.K. Kung, and E. Goldwasser, Purification of human erythropoietin. The Journal of biological chemistry, 1977. **252**(15): p. 5558-64.

134. Jacobs, K., et al., Isolation and characterization of genomic and cDNA clones of human erythropoietin. Nature, 1985. **313**(6005): p. 806-10.

135. Lin, F.K., et al., Cloning and expression of the human erythropoietin gene. Proc Natl Acad Sci U S A, 1985. **82**(22): p. 7580-4.

136. Locatelli, F. and P. Gascon, Is nephrology more at ease than oncology with erythropoiesis-stimulating agents? Treatment guidelines and an update on benefits and risks. The oncologist, 2009. **14 Suppl 1**: p. 57-62.

137. Ehrenreich, H., et al., Recombinant human erythropoietin in the treatment of acute ischemic stroke. Stroke, 2009. **40**(12): p. e647-56.

138. Voors, A.A., et al., A single dose of erythropoietin in ST-elevation myocardial infarction. Eur Heart J, 2010. **31**(21): p. 2593-600.

139. Namiuchi, S., et al., High serum erythropoietin level is associated with smaller infarct size in patients with acute myocardial infarction who undergo successful primary percutaneous coronary intervention. J Am Coll Cardiol, 2005. **45**(9): p. 1406-12.

140. Lipsic, E., et al., A single bolus of a long-acting erythropoietin analogue darbepoetin alfa in patients with acute myocardial infarction: a randomized feasibility and safety study. Cardiovascular drugs and therapy / sponsored by the International Society of Cardiovascular Pharmacotherapy, 2006. **20**(2): p. 135-41.

141. Koury, M.J., Erythropoietin: the story of hypoxia and a finely regulated hematopoietic hormone. Exp Hematol, 2005. **33**(11): p. 1263-70.

142. Bachmann, S., M. Le Hir, and K.U. Eckardt, Co-localization of erythropoietin mRNA and ecto-5'-nucleotidase immunoreactivity in peritubular cells of rat

renal cortex indicates that fibroblasts produce erythropoietin. J Histochem Cytochem, 1993. **41**(3): p. 335-41.

143. Jelkmann, W., Regulation of erythropoietin production. J Physiol, 2011. **589**(Pt 6): p. 1251-8.

144. Digicaylioglu, M., et al., Localization of specific erythropoietin binding sites in defined areas of the mouse brain. Proc Natl Acad Sci U S A, 1995. **92**(9): p. 3717-20.

145. Poveshchenko, A.F., et al., [Expression of erythropoietin receptor mRNA in mouse brain hemispheres]. Tsitologiia, 2001. **43**(3): p. 279-83.

146. Marti, H.H., et al., Erythropoietin gene expression in human, monkey and murine brain. The European journal of neuroscience, 1996. **8**(4): p. 666-76.

147. Grimm, C., et al., HIF-1-induced erythropoietin in the hypoxic retina protects against light-induced retinal degeneration. Nature medicine, 2002. **8**(7): p. 718-24.

148. Tan, C.C., K.U. Eckardt, and P.J. Ratcliffe, Organ distribution of erythropoietin messenger RNA in normal and uremic rats. Kidney Int, 1991. **40**(1): p. 69-76.

149. Fandrey, J. and H.F. Bunn, In vivo and in vitro regulation of erythropoietin mRNA: measurement by competitive polymerase chain reaction. Blood, 1993. **81**(3): p. 617-23.

150. Sasaki, H., et al., Carbohydrate structure of erythropoietin expressed in Chinese hamster ovary cells by a human erythropoietin cDNA. The Journal of biological chemistry, 1987. **262**(25): p. 12059-76.

151. Misaizu, T., et al., Role of antennary structure of N-linked sugar chains in renal handling of recombinant human erythropoietin. Blood, 1995. **86**(11): p. 4097-104.

152. Takeuchi, M., et al., Relationship between sugar chain structure and biological activity of recombinant human erythropoietin produced in Chinese hamster ovary cells. Proc Natl Acad Sci U S A, 1989. **86**(20): p. 7819-22.

153. Dordal, M.S., F.F. Wang, and E. Goldwasser, The role of carbohydrate in erythropoietin action. Endocrinology, 1985. **116**(6): p. 2293-9.

154. Narhi, L.O., et al., The effect of carbohydrate on the structure and stability of erythropoietin. The Journal of biological chemistry, 1991. **266**(34): p. 23022-6.

155. Cheetham, J.C., et al., NMR structure of human erythropoietin and a comparison with its receptor bound conformation. Nat Struct Biol, 1998. **5**(10): p. 861-6.

156. Wen, D., et al., Erythropoietin structure-function relationships: high degree of sequence homology among mammals. Blood, 1993. **82**(5): p. 1507-16.

157. Lin, F.K., et al., Monkey erythropoietin gene: cloning, expression and comparison with the human erythropoietin gene. Gene, 1986. **44**(2-3): p. 201-9.

158. McDonald, J.D., F.K. Lin, and E. Goldwasser, Cloning, sequencing, and evolutionary analysis of the mouse erythropoietin gene. Molecular and cellular biology, 1986. **6**(3): p. 842-8.

159. Shoemaker, C.B. and L.D. Mitsock, Murine erythropoietin gene: cloning, expression, and human gene homology. Molecular and cellular biology, 1986. **6**(3): p. 849-58.

160. Jelkmann, W., Erythropoietin after a century of research: younger than ever. European journal of haematology, 2007. **78**(3): p. 183-205.

161. Livnah, O., et al., Crystallographic evidence for preformed dimers of erythropoietin receptor before ligand activation. Science, 1999. **283**(5404): p. 987-90.

162. Watowich, S.S., The erythropoietin receptor: molecular structure and hematopoietic signaling pathways. Journal of investigative medicine : the official publication of the American Federation for Clinical Research, 2011. **59**(7): p. 1067-72.

163. Syed, R.S., et al., Efficiency of signalling through cytokine receptors depends critically on receptor orientation. Nature, 1998. **395**(6701): p. 511-6.

164. Remy, I., I.A. Wilson, and S.W. Michnick, Erythropoietin receptor activation by a ligand-induced conformation change. Science, 1999. **283**(5404): p. 990-3.

165. Tanner, J.W., et al., The conserved box 1 motif of cytokine receptors is required for association with JAK kinases. The Journal of biological chemistry, 1995. **270**(12): p. 6523-30.

166. Westenfelder, C., D.L. Biddle, and R.L. Baranowski, Human, rat, and mouse kidney cells express functional erythropoietin receptors. Kidney Int, 1999. **55**(3): p. 808-20.

167. Fenjves, E.S., et al., Human, nonhuman primate, and rat pancreatic islets express erythropoietin receptors. Transplantation, 2003. **75**(8): p. 1356-60.

168. Sawyer, S.T., S.B. Krantz, and K. Sawada, Receptors for erythropoietin in mouse and human erythroid cells and placenta. Blood, 1989. **74**(1): p. 103-9.

169. Rundqvist, H., et al., Activation of the erythropoietin receptor in human skeletal muscle. European journal of endocrinology / European Federation of Endocrine Societies, 2009. **161**(3): p. 427-34.

170. Christensen, B., et al., Evaluation of functional erythropoietin receptor status in skeletal muscle in vivo: acute and prolonged studies in healthy human subjects. PloS one, 2012. **7**(2): p. e31857.

171. Lundby, C., et al., Erythropoietin receptor in human skeletal muscle and the effects of acute and long-term injections with recombinant human erythropoietin on the skeletal muscle. Journal of applied physiology, 2008. **104**(4): p. 1154-60.

172. Ogilvie, M., et al., Erythropoietin stimulates proliferation and interferes with differentiation of myoblasts. The Journal of biological chemistry, 2000. **275**(50): p. 39754-61.

173. Semenza, G.L., Hydroxylation of HIF-1: oxygen sensing at the molecular level. Physiology, 2004. **19**: p. 176-82.

174. Marti, H.H., Erythropoietin and the hypoxic brain. The Journal of experimental biology, 2004. **207**(Pt 18): p. 3233-42.

175. Haase, V.H., Hypoxic regulation of erythropoiesis and iron metabolism. American journal of physiology. Renal physiology, 2010. **299**(1): p. F1-13.

176. Gruber, M., et al., Acute postnatal ablation of Hif-2alpha results in anemia. Proc Natl Acad Sci U S A, 2007. **104**(7): p. 2301-6.

177. Morita, M., et al., HLF/HIF-2alpha is a key factor in retinopathy of prematurity in association with erythropoietin. The EMBO journal, 2003. **22**(5): p. 1134-46.

178. Rankin, E.B., et al., Hypoxia-inducible factor-2 (HIF-2) regulates hepatic erythropoietin in vivo. J Clin Invest, 2007. **117**(4): p. 1068-77.

179. Scortegagna, M., et al., HIF-2alpha regulates murine hematopoietic development in an erythropoietin-dependent manner. Blood, 2005. **105**(8): p. 3133-40.

180. Ivan, M., et al., HIFalpha targeted for VHL-mediated destruction by proline hydroxylation: implications for O2 sensing. Science, 2001. **292**(5516): p. 464-8.

181. Epstein, A.C., et al., C. elegans EGL-9 and mammalian homologs define a family of dioxygenases that regulate HIF by prolyl hydroxylation. Cell, 2001. **107**(1): p. 43-54.

182. Jaakkola, P., et al., Targeting of HIF-alpha to the von Hippel-Lindau ubiquitylation complex by O2-regulated prolyl hydroxylation. Science, 2001. **292**(5516): p. 468-72.

183. Maxwell, P.H., et al., The tumour suppressor protein VHL targets hypoxia-inducible factors for oxygen-dependent proteolysis. Nature, 1999. **399**(6733): p. 271-5.

184. Ohh, M., et al., Ubiquitination of hypoxia-inducible factor requires direct binding to the beta-domain of the von Hippel-Lindau protein. Nature cell biology, 2000. **2**(7): p. 423-7.

185. Greer, S.N., et al., The updated biology of hypoxia-inducible factor. The EMBO journal, 2012. **31**(11): p. 2448-60.

186. Tsuchiya, T., et al., Activation of the erythropoietin promoter by a point mutation from GATA to TATA in the -30 region. J Biochem, 1997. **121**(2): p. 193-6.

187. Imagawa, S., et al., A GATA-specific inhibitor (K-7174) rescues anemia induced by IL-1beta, TNF-alpha, or L-NMMA. FASEB journal : official publication of the Federation of American Societies for Experimental Biology, 2003. **17**(12): p. 1742-4.

188. Constantinescu, S.N., S. Ghaffari, and H.F. Lodish, The Erythropoietin Receptor: Structure, Activation and Intracellular Signal Transduction. Trends in endocrinology and metabolism: TEM, 1999. **10**(1): p. 18-23.

189. Watowich, S.S., D.J. Hilton, and H.F. Lodish, Activation and inhibition of erythropoietin receptor function: role of receptor dimerization. Molecular and cellular biology, 1994. **14**(6): p. 3535-49.

190. Frank, S.J., Receptor dimerization in GH and erythropoietin action--it takes two to tango, but how? Endocrinology, 2002. **143**(1): p. 2-10.

191. Koury, M.J. and M.C. Bondurant, The molecular mechanism of erythropoietin action. Eur J Biochem, 1992. **210**(3): p. 649-63.

192. Bao, H., et al., Protein kinase B (c-Akt), phosphatidylinositol 3-kinase, and STAT5 are activated by erythropoietin (EPO) in HCD57 erythroid cells but are constitutively active in an EPO-independent, apoptosis-resistant subclone (HCD57-SREI cells). Blood, 1999. **93**(11): p. 3757-73.

193. Uddin, S., et al., Differentiation stage-specific activation of p38 mitogen-activated protein kinase isoforms in primary human erythroid cells. Proc Natl Acad Sci U S A, 2004. **101**(1): p. 147-52.

194. Jacobs-Helber, S.M., J.J. Ryan, and S.T. Sawyer, JNK and p38 are activated by erythropoietin (EPO) but are not induced in apoptosis following EPO withdrawal in EPO-dependent HCD57 cells. Blood, 2000. **96**(3): p. 933-40.

195. Buck, I., et al., Tumor necrosis factor alpha inhibits erythroid differentiation in human erythropoietin-dependent cells involving p38 MAPK pathway, GATA-1 and FOG-1 downregulation and GATA-2 upregulation. Biochemical pharmacology, 2008. **76**(10): p. 1229-39.

196. Martin, K.J., The first human cell line-derived erythropoietin, epoetin-delta (Dynepo), in the management of anemia in patients with chronic kidney disease. Clinical nephrology, 2007. **68**(1): p. 26-31.

197. Sytkowski, A.J., et al., An erythropoietin fusion protein comprised of identical repeating domains exhibits enhanced biological properties. The Journal of biological chemistry, 1999. **274**(35): p. 24773-8.

198. Goldwasser, E., C.K. Kung, and J. Eliason, On the mechanism of erythropoietin-induced differentiation. 13. The role of sialic acid in erythropoietin action. The Journal of biological chemistry, 1974. **249**(13): p. 4202-6.

199. Dhanushkodi, A., et al., A single intramuscular injection of rAAV-mediated mutant erythropoietin protects against MPTP-induced parkinsonism. Genes, brain, and behavior, 2013. **12**(2): p. 224-33.

200. Sullivan, T.A., et al., Dose-dependent treatment of optic nerve crush by exogenous systemic mutant erythropoietin. Experimental eye research, 2012. **96**(1): p. 36-41.

201. Sullivan, T.A., et al., Systemic adeno-associated virus-mediated gene therapy preserves retinal ganglion cells and visual function in DBA/2J glaucomatous mice. Hum Gene Ther, 2011. **22**(10): p. 1191-200.

202. Leist, M., et al., Derivatives of erythropoietin that are tissue protective but not erythropoietic. Science, 2004. **305**(5681): p. 239-42.

203. Colella, P., et al., Non-erythropoietic erythropoietin derivatives protect from light-induced and genetic photoreceptor degeneration. Human molecular genetics, 2011. **20**(11): p. 2251-62.

204. Sullivan, T. and T.S. Rex, Systemic gene delivery protects the photoreceptors in the retinal degeneration slow mouse. Neurochemical research, 2011. **36**(4): p. 613-8.

205. Villa, P., et al., Reduced functional deficits, neuroinflammation, and secondary tissue damage after treatment of stroke by nonerythropoietic erythropoietin derivatives. Journal of cerebral blood flow and metabolism : official journal of the International Society of Cerebral Blood Flow and Metabolism, 2007. **27**(3): p. 552-63.

206. Colella, P. and A. Auricchio, Photoreceptor degeneration in mice: adeno-associated viral vector-mediated delivery of erythropoietin. Methods in molecular biology, 2013. **982**: p. 237-63.

207. Gan, Y., et al., Mutant erythropoietin without erythropoietic activity is neuroprotective against ischemic brain injury. Stroke, 2012. **43**(11): p. 3071-7.

208. Furuhashi, M., et al., Fusing the carboxy-terminal peptide of the chorionic gonadotropin (CG) beta-subunit to the common alpha-subunit: retention of O-linked glycosylation and enhanced in vivo bioactivity of chimeric human CG. Molecular endocrinology, 1995. **9**(1): p. 54-63.

209. Lee, D.E., et al., The prolonged half-lives of new erythropoietin derivatives via peptide addition. Biochem Biophys Res Commun, 2006. **339**(1): p. 380-5.

210. Fares, F., et al., Development of a long-acting erythropoietin by fusing the carboxyl-terminal peptide of human chorionic gonadotropin beta-subunit to the coding sequence of human erythropoietin. Endocrinology, 2007. **148**(10): p. 5081-7.

211. Fares, F., A. Havron, and E. Fima, Designing a Long Acting Erythropoietin by Fusing Three Carboxyl-Terminal Peptides of Human Chorionic

Gonadotropin beta Subunit to the N-Terminal and C-Terminal Coding Sequence. International journal of cell biology, 2011. **2011**: p. 275063.

212. Pankratova, S., et al., Neuroprotective properties of a novel, non-haematopoietic agonist of the erythropoietin receptor. Brain : a journal of neurology, 2010. **133**(Pt 8): p. 2281-94.

213. Zellinger, C., et al., Impact of the erythropoietin-derived peptide mimetic Epotris on the histopathological consequences of status epilepticus. Epilepsy research, 2011. **96**(3): p. 241-9.

214. Anagnostou, A., et al., Erythropoietin has a mitogenic and positive chemotactic effect on endothelial cells. Proc Natl Acad Sci U S A, 1990. **87**(15): p. 5978-82.

215. Juul, S.E., A.T. Yachnis, and R.D. Christensen, Tissue distribution of erythropoietin and erythropoietin receptor in the developing human fetus. Early Hum Dev, 1998. **52**(3): p. 235-49.

216. Anagnostou, A., et al., Erythropoietin receptor mRNA expression in human endothelial cells. Proc Natl Acad Sci U S A, 1994. **91**(9): p. 3974-8.

217. Fraser, J.K., et al., Expression of specific high-affinity binding sites for erythropoietin on rat and mouse megakaryocytes. Exp Hematol, 1989. **17**(1): p. 10-6.

218. David, R.B., et al., Ontogeny of erythropoietin receptor mRNA expression in various tissues of the foetal and the neonatal pig. Domest Anim Endocrinol, 2005. **29**(3): p. 556-63.

219. Ishibashi, T., J.A. Koziol, and S.A. Burstein, Human recombinant erythropoietin promotes differentiation of murine megakaryocytes in vitro. J Clin Invest, 1987. **79**(1): p. 286-9.

220. An, E., et al., Interleukin-6 and erythropoietin act as direct potentiators and inducers of in vitro cytoplasmic process formation on purified mouse megakaryocytes. Exp Hematol, 1994. **22**(2): p. 149-56.

221. Konishi, Y., et al., Trophic effect of erythropoietin and other hematopoietic factors on central cholinergic neurons in vitro and in vivo. Brain Res, 1993. **609**(1-2): p. 29-35.

222. Najjar, S.S., et al., Intravenous erythropoietin in patients with ST-segment elevation myocardial infarction: REVEAL: a randomized controlled trial. JAMA, 2011. **305**(18): p. 1863-72.

223. Stein, A., et al., Erythropoietin-induced progenitor cell mobilisation in patients with acute ST-segment-elevation myocardial infarction and restenosis. Thrombosis and haemostasis, 2012. **107**(4): p. 769-74.

224. Miyajima, A., et al., Receptors for granulocyte-macrophage colony-stimulating factor, interleukin-3, and interleukin-5. Blood, 1993. **82**(7): p. 1960-74.

225. Gadina, M., et al., Signaling by type I and II cytokine receptors: ten years after. Current opinion in immunology, 2001. **13**(3): p. 363-73.

226. Watanabe, S., T. Itoh, and K. Arai, JAK2 is essential for activation of c-fos and c-myc promoters and cell proliferation through the human granulocyte-macrophage colony-stimulating factor receptor in BA/F3 cells. The Journal of biological chemistry, 1996. **271**(21): p. 12681-6.

227. Jubinsky, P.T., et al., The beta chain of the interleukin-3 receptor functionally associates with the erythropoietin receptor. Blood, 1997. **90**(5): p. 1867-73.

228. Brines, M., et al., Erythropoietin mediates tissue protection through an erythropoietin and common beta-subunit heteroreceptor. Proc Natl Acad Sci U S A, 2004. **101**(41): p. 14907-12.

229. Liu, N.M., et al., Effect of erythropoietin on mesenchymal stem cell differentiation and secretion in vitro in an acute kidney injury microenvironment. Genetics and molecular research : GMR, 2013. **12**(AOP).

230. Liu, N., et al., Effect of erythropoietin on the migration of bone marrow-derived mesenchymal stem cells to the acute kidney injury microenvironment. Experimental cell research, 2013.

231. Bader, A. and H.G. Machens, Recombinant human erythropoietin plays a pivotal role as a topical stem cell activator to reverse effects of damage to the skin in aging and trauma. Rejuvenation research, 2010. **13**(4): p. 499-500.

232. Pavlica, S., et al., Erythropoietin enhances cell proliferation and survival of human fetal neuronal progenitors in normoxia. Brain Res, 2012. **1452**: p. 18-28.

233. Ahmet, I., et al., A small nonerythropoietic helix B surface peptide based upon erythropoietin structure is cardioprotective against ischemic myocardial damage. Molecular medicine, 2011. **17**(3-4): p. 194-200.

234. Ueba, H., et al., Cardioprotection by a nonerythropoietic, tissue-protective peptide mimicking the 3D structure of erythropoietin. Proc Natl Acad Sci U S A, 2010. **107**(32): p. 14357-62.

235. Buemi, M., et al., The pleiotropic effects of erythropoietin in the central nervous system. Journal of neuropathology and experimental neurology, 2003. **62**(3): p. 228-36.

236. Masuda, S., et al., Functional erythropoietin receptor of the cells with neural characteristics. Comparison with receptor properties of erythroid cells. The Journal of biological chemistry, 1993. **268**(15): p. 11208-16.

237. Digicaylioglu, M. and S.A. Lipton, Erythropoietin-mediated neuroprotection involves cross-talk between Jak2 and NF-kappaB signalling cascades. Nature, 2001. **412**(6847): p. 641-7.

238. Joshi, D., et al., Development of an in vitro model of myotube ischemia. Lab Invest, 2011. **91**(8): p. 1241-52.

239. Gabel, R., et al., Single high-dose intramyocardial administration of erythropoietin promotes early intracardiac proliferation, proves safety and restores cardiac performance after myocardial infarction in rats. Interactive cardiovascular and thoracic surgery, 2009. **9**(1): p. 20-5; discussion 25.

240. Lipsic, E., et al., Low-dose erythropoietin improves cardiac function in experimental heart failure without increasing haematocrit. European journal of heart failure, 2008. **10**(1): p. 22-9.

241. Ammarguellat, F., J. Gogusev, and T.B. Drueke, Direct effect of erythropoietin on rat vascular smooth-muscle cell via a putative erythropoietin receptor. Nephrology, dialysis, transplantation : official publication of the European Dialysis and Transplant Association - European Renal Association, 1996. **11**(4): p. 687-92.

242. Boissel, J.P., et al., Erythropoietin structure-function relationships. Mutant proteins that test a model of tertiary structure. The Journal of biological chemistry, 1993. **268**(21): p. 15983-93.

243. Elliott, S., et al., Mapping of the active site of recombinant human erythropoietin. Blood, 1997. **89**(2): p. 493-502.

244. Mennini, T., et al., Nonhematopoietic erythropoietin derivatives prevent motoneuron degeneration in vitro and in vivo. Mol Med, 2006. **12**(7-8): p. 153-60.

245. Brines, M., et al., Nonerythropoietic, tissue-protective peptides derived from the tertiary structure of erythropoietin. Proc Natl Acad Sci U S A, 2008. **105**(31): p. 10925-30.

246. Yu, L., et al., Investigation of N-terminal glutamate cyclization of recombinant monoclonal antibody in formulation development. J Pharm Biomed Anal, 2006. **42**(4): p. 455-63.

247. Patel, N.S., et al., Pretreatment with EPO reduces the injury and dysfunction caused by ischemia/reperfusion in the mouse kidney in vivo. Kidney Int, 2004. **66**(3): p. 983-9.

248. Erbayraktar, Z., et al., Nonerythropoietic tissue protective compounds are highly effective facilitators of wound healing. Molecular medicine, 2009. **15**(7-8): p. 235-41.

249. Ueba, H., et al., Suppression of coronary atherosclerosis by helix B surface peptide, a nonerythropoietic, tissue-protective compound derived from erythropoietin. Molecular medicine, 2013.

250. Schmidt, R.E., et al., Effect of insulin and an erythropoietin-derived peptide (ARA290) on established neuritic dystrophy and neuronopathy in Akita (Ins2 Akita) diabetic mouse sympathetic ganglia. Experimental neurology, 2011. **232**(2): p. 126-35.

251. McVicar, C.M., et al., Intervention with an erythropoietin-derived peptide protects against neuroglial and vascular degeneration during diabetic retinopathy. Diabetes, 2011. **60**(11): p. 2995-3005.

252. Heij, L., et al., Safety and efficacy of ARA 290 in sarcoidosis patients with symptoms of small fiber neuropathy: a randomized, double-blind pilot study. Molecular medicine, 2012. **18**: p. 1430-6.

253. Pulman, K.G., et al., The erythropoietin-derived peptide ARA290 reverses mechanical allodynia in the neuritis model. Neuroscience, 2013. **233**: p. 174-83.

254. Swartjes, M., et al., ARA290, a peptide derived from the tertiary structure of erythropoietin, produces long-term relief of neuropathic pain: an experimental study in rats and beta-common receptor knockout mice. Anesthesiology, 2011. **115**(5): p. 1084-92.

255. Robertson, C.S., et al., Treatment of mild traumatic brain injury with an erythropoietin-mimetic peptide. Journal of neurotrauma, 2013. **30**(9): p. 765-74.

256. Robertson, C.S., et al., Neuroprotection with an erythropoietin mimetic peptide (pHBSP) in a model of mild traumatic brain injury complicated by hemorrhagic shock. Journal of neurotrauma, 2012. **29**(6): p. 1156-66.

257. Seeger, N., et al., The erythropoietin-derived peptide mimetic pHBSP affects cellular and cognitive consequences in a rat post-status epilepticus model. Epilepsia, 2011. **52**(12): p. 2333-43.

258. Patel, N.S., et al., Delayed administration of pyroglutamate helix B surface peptide (pHBSP), a novel nonerythropoietic analog of erythropoietin, attenuates acute kidney injury. Molecular medicine, 2012. **18**: p. 719-27.

259. Patel, N.S., et al., A nonerythropoietic peptide that mimics the 3D structure of erythropoietin reduces organ injury/dysfunction and inflammation in experimental hemorrhagic shock. Molecular medicine, 2011. **17**(9-10): p. 883-92.

260. van Rijt, W.G., et al., ARA290, a non-erythropoietic EPO derivative, attenuates renal ischemia/reperfusion injury. Journal of translational medicine, 2013. **11**: p. 9.

261. Yang, C., et al., Helix B surface peptide administered after insult of ischemia reperfusion improved renal function, structure and apoptosis through beta common receptor/erythropoietin receptor and PI3K/Akt pathway in a murine model. Experimental biology and medicine, 2013. **238**(1): p. 111-9.

262. Bohr, S., et al., Alternative erythropoietin-mediated signaling prevents secondary microvascular thrombosis and inflammation within cutaneous burns. Proc Natl Acad Sci U S A, 2013. **110**(9): p. 3513-8.

263. Niesters, M., The erythropoietin analog ARA 290 for treatment of sarcoidosis-induced chronic neuropathic pain. Expert Opinion on Orphan Drugs, 2013. **1**(1): p. 77-87.

264. EU Clinical Trials Register, E.-C. ARA-290 clinical trials registered with EU-CTR. 2013 [cited 2013 June 28]; Available from: http://www.clinicaltrialsregister.eu/ctr-search/search?query=ara+290.

265. Netherlands Trial Register, N. ARA-290 clinical trials registered with NTR. 2013 [cited 2013 June 28]; Available from: http://www.trialregister.nl/trialreg/admin/rctsearch.asp?Term=ara 290.

266. Netherlands Trial Register, N. ARA-290 in treatment of Rheumatoid Arthritis. 2013 [cited 2013 June 28]; Available from: http://www.trialregister.nl/trialreg/admin/rctview.asp?TC=2577.

267. Netherlands Trial Register, N. ARA-290 in treatment of No-option CLI. 2013 [cited 2013 June 28]; Available from: http://www.trialregister.nl/trialreg /admin/rctview.asp?TC=2685.

268. Netherlands Trial Register, N. ARA-290 effect on regrowth of epidermal nerve fibres in patients with sarcoidosis. 2013 [cited 2013 June 28]; Available from: http://www.trialregister.nl/trialreg/admin/rctview.asp?TC= 3575.

269. Netherlands Trial Register, N. ARA-290 effect in Diabetes Mellitus type 2 neuropathic symptom control. 2013 [cited 2013 June 28]; Available from: http://www.trialregister.nl/trialreg/admin/rctview.asp?TC=3858.

270. Netherlands Trial Register, N. ARA-290 effect on ventilatory response to hypoxia in healthy volunteers. 2013 [cited 2013 June 28]; Available from: http://www.trialregister.nl/trialreg/admin/rctview.asp?TC=3131.

271. Miranda, A.F., Stephen F; Castellano, Vincenzo; Hyams, David; Kerendian, Naghmeh; Nguyen, Todd T; Tyson, M Amber; Scremin, A M Erika; Scremin, Oscar U, Calf Muscle Oxygenation During Exercise in Healthy Adults. Clinical Kinesiology, 2010. **64**: p. 8-15.

272. Vega-Avila, E. and M.K. Pugsley, An overview of colorimetric assay methods used to assess survival or proliferation of mammalian cells. Proceedings of the Western Pharmacology Society, 2011. **54**: p. 10-4.

273. Bernhardt, G., et al., Standardized kinetic microassay to quantify differential chemosensitivity on the basis of proliferative activity. Journal of cancer research and clinical oncology, 1992. **118**(1): p. 35-43.

274. Chen, C., et al., Quinotrierixin inhibits proliferation of human retinal pigment epithelial cells. Molecular vision, 2013. **19**: p. 39-46.

275. Kurtagic, E., M.P. Jedrychowski, and M.A. Nugent, Neutrophil elastase cleaves VEGF to generate a VEGF fragment with altered activity. American journal of physiology. Lung cellular and molecular physiology, 2009. **296**(3): p. L534-46.

276. Cory, G., Scratch-wound assay. Methods in molecular biology, 2011. **769**: p. 25-30.

277. Liang, C.C., A.Y. Park, and J.L. Guan, In vitro scratch assay: a convenient and inexpensive method for analysis of cell migration in vitro. Nature protocols, 2007. **2**(2): p. 329-33.

278. Ranzato, E., et al., Scratch wound closure of C2C12 mouse myoblasts is enhanced by human platelet lysate. Cell biology international, 2009. **33**(9): p. 911-7.

279. Grinnell, F., et al., Differences in the regulation of fibroblast contraction of floating versus stressed collagen matrices. The Journal of biological chemistry, 1999. **274**(2): p. 918-23.

280. Shi-Wen, X., et al., Endothelin-1 promotes myofibroblast induction through the ETA receptor via a rac/phosphoinositide 3-kinase/Akt-dependent pathway and is essential for the enhanced contractile phenotype of fibrotic fibroblasts. Molecular biology of the cell, 2004. **15**(6): p. 2707-19.

281. Kallio, M., et al., Development of new peripheral arterial occlusive disease in patients with type 2 diabetes during a mean follow-up of 11 years. Diabetes Care, 2003. **26**(4): p. 1241-5.

282. Tarlov, I.M., Spinal cord compression studies. III. Time limits for recovery after gradual compression in dogs. A.M.A. archives of neurology and psychiatry, 1954. **71**(5): p. 588-97.

283. Chen, S., et al., Tetramethylpyrazine attenuates spinal cord ischemic injury due to aortic cross-clamping in rabbits. BMC neurology, 2002. **2**: p. 1.

284. Yu, J., et al., Endothelial nitric oxide synthase is critical for ischemic remodeling, mural cell recruitment, and blood flow reserve. Proc Natl Acad Sci U S A, 2005. **102**(31): p. 10999-1004.

285. Westvik, T.S., et al., Limb ischemia after iliac ligation in aged mice stimulates angiogenesis without arteriogenesis. J Vasc Surg, 2009. **49**(2): p. 464-73.

286. Basso, D.M., et al., Basso Mouse Scale for locomotion detects differences in recovery after spinal cord injury in five common mouse strains. Journal of neurotrauma, 2006. **23**(5): p. 635-59.

287. Brenes, R.A., et al., Toward a mouse model of hind limb ischemia to test therapeutic angiogenesis. J Vasc Surg, 2012. **56**(6): p. 1669-79; discussion 1679.

288. Grounds, M. Quantification of histopathology in haematoxylin and eosin stained muscle sections. 2014 25/01/2014 [cited 2014 06/03/2014]; Available from: http://www.treat-nmd.eu/downloads/file/sops/dmd/MDX/DMD_M.1.2.007.pdf.

289. Beauchamp, J.R., et al., Expression of CD34 and Myf5 defines the majority of quiescent adult skeletal muscle satellite cells. The Journal of cell biology, 2000. **151**(6): p. 1221-34.

290. Ieronimakis, N., et al., Absence of CD34 on murine skeletal muscle satellite cells marks a reversible state of activation during acute injury. PloS one, 2010. **5**(6): p. e10920.

291. Joshi, D., et al., Potential role of erythropoietin receptors and ligands in attenuating apoptosis and inflammation in critical limb ischemia. J Vasc Surg, 2013.

292. Elliott, S., et al., Anti-Epo receptor antibodies do not predict Epo receptor expression. Blood, 2006. **107**(5): p. 1892-5.

293. Hart, C.A., et al., Stem cells of the lower limb: Their role and potential in management of critical limb ischemia. Experimental biology and medicine, 2013.

294. Relaix, F. and P.S. Zammit, Satellite cells are essential for skeletal muscle regeneration: the cell on the edge returns centre stage. Development, 2012. **139**(16): p. 2845-56.

295. Boldrin, L., F. Muntoni, and J.E. Morgan, Are human and mouse satellite cells really the same? J Histochem Cytochem, 2010. **58**(11): p. 941-55.

296. Tedesco, F.S., et al., Repairing skeletal muscle: regenerative potential of skeletal muscle stem cells. J Clin Invest, 2010. **120**(1): p. 11-9.

297. Zammit, P.S., T.A. Partridge, and Z. Yablonka-Reuveni, The skeletal muscle satellite cell: the stem cell that came in from the cold. J Histochem Cytochem, 2006. **54**(11): p. 1177-91.

298. Fincher, M. The influence of ischaemia on the regenerative potential of skeletal muscle. in Annual Meeting of the Society of Academic and Research Surgery. 2012. Nottingham, UK: John Wiley & Sons, Ltd.

299. Rudnicki, M.A., et al., The molecular regulation of muscle stem cell function. Cold Spring Harbor symposia on quantitative biology, 2008. **73**: p. 323-31.

300. Siren, A.L., et al., Erythropoietin and erythropoietin receptor in human ischemic/hypoxic brain. Acta neuropathologica, 2001. **101**(3): p. 271-6.

301. Bernaudin, M., et al., A potential role for erythropoietin in focal permanent cerebral ischemia in mice. Journal of cerebral blood flow and metabolism : official journal of the International Society of Cerebral Blood Flow and Metabolism, 1999. **19**(6): p. 643-51.

302. Sadamoto, Y., et al., Erythropoietin prevents place navigation disability and cortical infarction in rats with permanent occlusion of the middle cerebral artery. Biochem Biophys Res Commun, 1998. **253**(1): p. 26-32.

303. Taoufik, E., et al., TNF receptor I sensitizes neurons to erythropoietin- and VEGF-mediated neuroprotection after ischemic and excitotoxic injury. Proc Natl Acad Sci U S A, 2008. **105**(16): p. 6185-90.

304. Wu, H., et al., Inactivation of erythropoietin leads to defects in cardiac morphogenesis. Development, 1999. **126**(16): p. 3597-605.

305. Prass, K., et al., Hypoxia-induced stroke tolerance in the mouse is mediated by erythropoietin. Stroke, 2003. **34**(8): p. 1981-6.

306. Sakanaka, M., et al., In vivo evidence that erythropoietin protects neurons from ischemic damage. Proc Natl Acad Sci U S A, 1998. **95**(8): p. 4635-40.

307. Tsai, P.T., et al., A critical role of erythropoietin receptor in neurogenesis and post-stroke recovery. The Journal of neuroscience : the official journal of the Society for Neuroscience, 2006. **26**(4): p. 1269-74.

308. Meads, M.B., Z.W. Li, and W.S. Dalton, A novel TNF receptor-associated factor 6 binding domain mediates NF-kappa B signaling by the common cytokine receptor beta subunit. Journal of immunology, 2010. **185**(3): p. 1606-15.

309. Ji, X., et al., Interferon alfa regulated gene expression in patients initiating interferon treatment for chronic hepatitis C. Hepatology, 2003. **37**(3): p. 610-21.

310. Charge, S.B. and M.A. Rudnicki, Cellular and molecular regulation of muscle regeneration. Physiological reviews, 2004. **84**(1): p. 209-38.

311. Putman, C.T., et al., Fiber-type transitions and satellite cell activation in low-frequency-stimulated muscles of young and aging rats. The journals of gerontology. Series A, Biological sciences and medical sciences, 2001. **56**(12): p. B510-9.

312. Schmalbruch, H. and U. Hellhammer, The number of nuclei in adult rat muscles with special reference to satellite cells. The Anatomical record, 1977. **189**(2): p. 169-75.

313. Smith, H.K. and T.L. Merry, Voluntary resistance wheel exercise during post-natal growth in rats enhances skeletal muscle satellite cell and myonuclear content at adulthood. Acta physiologica, 2012. **204**(3): p. 393-402.

314. Verdijk, L.B., et al., Satellite cell content is specifically reduced in type II skeletal muscle fibers in the elderly. American journal of physiology. Endocrinology and metabolism, 2007. **292**(1): p. E151-7.

315. Armand, O., et al., Origin of satellite cells in avian skeletal muscles. Archives d'anatomie microscopique et de morphologie experimentale, 1983. **72**(2): p. 163-81.

316. Gros, J., et al., A common somitic origin for embryonic muscle progenitors and satellite cells. Nature, 2005. **435**(7044): p. 954-8.

317. Yamaguchi, T., et al., Continuous mild heat stress induces differentiation of mammalian myoblasts, shifting fiber type from fast to slow. American journal of physiology. Cell physiology, 2010. **298**(1): p. C140-8.

318. Manabe, Y., et al., Characterization of an acute muscle contraction model using cultured C2C12 myotubes. PloS one, 2012. **7**(12): p. e52592.

319. Czifra, G., et al., Insulin-like growth factor-I-coupled mitogenic signaling in primary cultured human skeletal muscle cells and in C2C12 myoblasts. A central role of protein kinase Cdelta. Cellular signalling, 2006. **18**(9): p. 1461-72.

320. Staiger, H., et al., Muscle-derived angiopoietin-like protein 4 is induced by fatty acids via peroxisome proliferator-activated receptor (PPAR)-delta and is of metabolic relevance in humans. Diabetes, 2009. **58**(3): p. 579-89.

321. Contaldo, C., et al., Human recombinant erythropoietin protects the striated muscle microcirculation of the dorsal skinfold from postischemic injury in mice. American journal of physiology. Heart and circulatory physiology, 2007. **293**(1): p. H274-83.

322. Harder, Y., et al., Erythropoietin reduces necrosis in critically ischemic myocutaneous tissue by protecting nutritive perfusion in a dose-dependent manner. Surgery, 2009. **145**(4): p. 372-83.

323. Rezaeian, F., et al., Erythropoietin protects critically perfused flap tissue. Ann Surg, 2008. **248**(6): p. 919-29.

324. Rezaeian, F., et al., Erythropoietin-induced upregulation of endothelial nitric oxide synthase but not vascular endothelial growth factor prevents musculocutaneous tissue from ischemic damage. Lab Invest, 2010. **90**(1): p. 40-51.

325. Rotter, R., et al., Erythropoietin improves functional and histological recovery of traumatized skeletal muscle tissue. Journal of orthopaedic research : official publication of the Orthopaedic Research Society, 2008. **26**(12): p. 1618-26.

326. Koh, G.Y., et al., Differentiation and long-term survival of C2C12 myoblast grafts in heart. J Clin Invest, 1993. **92**(3): p. 1548-54.

327. Chakravarthy, M.V., E.E. Spangenburg, and F.W. Booth, Culture in low levels of oxygen enhances in vitro proliferation potential of satellite cells from old skeletal muscles. Cellular and molecular life sciences : CMLS, 2001. **58**(8): p. 1150-8.

328. Csete, M., et al., Oxygen-mediated regulation of skeletal muscle satellite cell proliferation and adipogenesis in culture. Journal of cellular physiology, 2001. **189**(2): p. 189-96.

329. Liu, W., et al., Hypoxia promotes satellite cell self-renewal and enhances the efficiency of myoblast transplantation. Development, 2012. **139**(16): p. 2857-65.

330. Millman, J.R., J.H. Tan, and C.K. Colton, The effects of low oxygen on self-renewal and differentiation of embryonic stem cells. Current opinion in organ transplantation, 2009. **14**(6): p. 694-700.

331. Duan, Z., et al., SD-1029 inhibits signal transducer and activator of transcription 3 nuclear translocation. Clinical cancer research : an official journal of the American Association for Cancer Research, 2006. **12**(22): p. 6844-52.

332. Liu, Y., et al., XZH-5 inhibits STAT3 phosphorylation and causes apoptosis in human hepatocellular carcinoma cells. Apoptosis : an international journal on programmed cell death, 2011. **16**(5): p. 502-10.

333. Yang, C., et al., A novel target for treatment of chordoma: signal transducers and activators of transcription 3. Molecular cancer therapeutics, 2009. **8**(9): p. 2597-605.

334. Nauc, V., et al., Inhibitors of phosphoinositide 3-kinase, LY294002 and wortmannin, affect sperm capacitation and associated phosphorylation of proteins differently: Ca2+-dependent divergences. Journal of andrology, 2004. **25**(4): p. 573-85.

335. Sun, H., et al., The phosphoinositide 3-kinase inhibitor LY294002 enhances cardiac myocyte contractility via a direct inhibition of Ik,slow currents. Cardiovascular research, 2004. **62**(3): p. 509-20.

336. Tsai, K.D., et al., Differential effects of LY294002 and wortmannin on inducible nitric oxide synthase expression in glomerular mesangial cells. International immunopharmacology, 2012. **12**(3): p. 471-80.

337. Ethier, M.F. and J.M. Madison, LY294002, but not wortmannin, increases intracellular calcium and inhibits calcium transients in bovine and human airway smooth muscle cells. Cell calcium, 2002. **32**(1): p. 31-8.

338. Walker, E.H., et al., Structural determinants of phosphoinositide 3-kinase inhibition by wortmannin, LY294002, quercetin, myricetin, and staurosporine. Molecular cell, 2000. **6**(4): p. 909-19.

339. Davies, S.P., et al., Specificity and mechanism of action of some commonly used protein kinase inhibitors. The Biochemical journal, 2000. **351**(Pt 1): p. 95-105.

340. Blaisdell, F.W., The pathophysiology of skeletal muscle ischemia and the reperfusion syndrome: a review. Cardiovascular surgery, 2002. **10**(6): p. 620-30.

341. Cheng, C.S., et al., Conditions that promote primary human skeletal myoblast culture and muscle differentiation in vitro. American journal of physiology. Cell physiology, 2014. **306**(4): p. C385-95.

342. Rangarajan, A. and R.A. Weinberg, Opinion: Comparative biology of mouse versus human cells: modelling human cancer in mice. Nature reviews. Cancer, 2003. **3**(12): p. 952-9.

343. di Prampero, P.E. and G. Ferretti, The energetics of anaerobic muscle metabolism: a reappraisal of older and recent concepts. Respiration physiology, 1999. **118**(2-3): p. 103-15.

344. Lanza, I.R., et al., In vivo ATP production during free-flow and ischaemic muscle contractions in humans. J Physiol, 2006. **577**(Pt 1): p. 353-67.

345. Jang, H.S., et al., Previous ischemia and reperfusion injury results in resistance of the kidney against subsequent ischemia and reperfusion insult in mice; a role for the Akt signal pathway. Nephrology, dialysis, transplantation : official publication of the European Dialysis and Transplant Association - European Renal Association, 2012. **27**(10): p. 3762-70.

346. Kharbanda, R.K., et al., Ischemic preconditioning prevents endothelial injury and systemic neutrophil activation during ischemia-reperfusion in humans in vivo. Circulation, 2001. **103**(12): p. 1624-30.

347. Brines, M. and A. Cerami, Erythropoietin-mediated tissue protection: reducing collateral damage from the primary injury response. Journal of internal medicine, 2008. **264**(5): p. 405-32.

348. Zhu, Y., D. Ye, and Z. Huang, [The correlation of cytokines TNF alpha, IFN-gamma, Epo with anemia in rheumatoid arthritis]. Zhonghua xue ye xue za zhi = Zhonghua xueyexue zazhi, 2000. **21**(11): p. 587-90.

349. Verhoef, G.E., et al., Measurement of serum cytokine levels in patients with myelodysplastic syndromes. Leukemia, 1992. **6**(12): p. 1268-72.

350. Polgarova, K., et al., The erythropoietin analogue ARA290 modulates the innate immune response and reduces Escherichia coli invasion into urothelial cells. FEMS immunology and medical microbiology, 2011. **62**(2): p. 190-6.

351. Kasperk, C., et al., Human bone cell phenotypes differ depending on their skeletal site of origin. The Journal of clinical endocrinology and metabolism, 1995. **80**(8): p. 2511-7.

352. Martinez, M.E., et al., Influence of skeletal site of origin and donor age on osteoblastic cell growth and differentiation. Calcified tissue international, 1999. **64**(4): p. 280-6.

353. Siegel, G., et al., Phenotype, donor age and gender affect function of human bone marrow-derived mesenchymal stromal cells. BMC medicine, 2013. **11**: p. 146.

354. Wang, K., et al., Advantages of in vitro cytotoxicity testing by using primary rat hepatocytes in comparison with established cell lines. The Journal of toxicological sciences, 2002. **27**(3): p. 229-37.

355. Owens, J., K. Moreira, and G. Bain, Characterization of primary human skeletal muscle cells from multiple commercial sources. In vitro cellular & developmental biology. Animal, 2013. **49**(9): p. 695-705.

356. Longland, C.J., Collateral circulation in the limb. Postgraduate medical journal, 1953. **29**(335): p. 456-8.

357. Longland, C.J., The collateral circulation of the limb; Arris and Gale lecture delivered at the Royal College of Surgeons of England on 4th February, 1953. Annals of the Royal College of Surgeons of England, 1953. **13**(3): p. 161-76.

358. Hellingman, A.A., et al., Variations in surgical procedures for hind limb ischaemia mouse models result in differences in collateral formation. Eur J Vasc Endovasc Surg, 2010. **40**(6): p. 796-803.

359. Aicher, A., et al., Essential role of endothelial nitric oxide synthase for mobilization of stem and progenitor cells. Nature medicine, 2003. **9**(11): p. 1370-6.

360. Couffinhal, T., et al., Mouse model of angiogenesis. The American journal of pathology, 1998. **152**(6): p. 1667-79.

361. Masaki, I., et al., Angiogenic gene therapy for experimental critical limb ischemia: acceleration of limb loss by overexpression of vascular endothelial growth factor 165 but not of fibroblast growth factor-2. Circulation research, 2002. **90**(9): p. 966-73.

362. Stabile, E., et al., Impaired arteriogenic response to acute hindlimb ischemia in CD4-knockout mice. Circulation, 2003. **108**(2): p. 205-10.

363. van Weel, V., et al., Natural killer cells and CD4+ T-cells modulate collateral artery development. Arterioscler Thromb Vasc Biol, 2007. **27**(11): p. 2310-8.

364. Zhuang, Z.W., et al., Challenging the surgical rodent hindlimb ischemia model with the miniinterventional technique. J Vasc Interv Radiol, 2011. **22**(10): p. 1437-46.

365. Brevetti, L.S., et al., Exercise-induced hyperemia unmasks regional blood flow deficit in experimental hindlimb ischemia. The Journal of surgical research, 2001. **98**(1): p. 21-6.

366. Lotfi, S., et al., Towards a more relevant hind limb model of muscle ischaemia. Atherosclerosis, 2013. **227**(1): p. 1-8.

367. Zbinden, S., et al., Interanimal variability in preexisting collaterals is a major factor determining outcome in experimental angiogenesis trials. American journal of physiology. Heart and circulatory physiology, 2007. **292**(4): p. H1891-7.

368. Goto, T., et al., Search for appropriate experimental methods to create stable hind-limb ischemia in mouse. The Tokai journal of experimental and clinical medicine, 2006. **31**(3): p. 128-32.

369. Skjeldal, S., et al., Model for skeletal muscle ischemia in rat hindlimb: evaluation of reperfusion and necrosis. European surgical research. Europaische chirurgische Forschung. Recherches chirurgicales europeennes, 1991. **23**(5-6): p. 355-65.

370. Helisch, A., et al., Impact of mouse strain differences in innate hindlimb collateral vasculature. Arterioscler Thromb Vasc Biol, 2006. **26**(3): p. 520-6.

371. Chalothorn, D. and J.E. Faber, Strain-dependent variation in collateral circulatory function in mouse hindlimb. Physiological genomics, 2010. **42**(3): p. 469-79.

372. Annex, B.H., Therapeutic angiogenesis for critical limb ischaemia. Nature reviews. Cardiology, 2013. **10**(7): p. 387-96.

373. Shimada, T., et al., Angiogenesis and vasculogenesis are impaired in the precocious-aging klotho mouse. Circulation, 2004. **110**(9): p. 1148-55.

374. Kirkeby, A., et al., High-dose erythropoietin alters platelet reactivity and bleeding time in rodents in contrast to the neuroprotective variant carbamyl-erythropoietin (CEPO). Thrombosis and haemostasis, 2008. **99**(4): p. 720-8.

375. Ahmet, I., et al., Chronic administration of small nonerythropoietic peptide sequence of erythropoietin effectively ameliorates the progression of postmyocardial infarction-dilated cardiomyopathy. The Journal of pharmacology and experimental therapeutics, 2013. **345**(3): p. 446-56.

376. Kato, S., et al., Effect of erythropoietin on angiogenesis with the increased adhesion of platelets to the microvessels in the hind-limb ischemia model in mice. Journal of pharmacological sciences, 2010. **112**(2): p. 167-75.

377. Yanagawa, T., et al., Erythropoietin induces angiogenesis in a manner dependent on the intrinsic auto/paracrine production of interleukin-6 in vitro. International journal of cardiology, 2013.

378. Ribatti, D., In vivo angiogenic activity of erythropoietin. Methods in molecular biology, 2013. **982**: p. 227-35.

379. Chong, Z.Z., J.Q. Kang, and K. Maiese, Angiogenesis and plasticity: role of erythropoietin in vascular systems. Journal of hematotherapy & stem cell research, 2002. **11**(6): p. 863-71.

380. Ribatti, D., Angiogenic effects of erythropoietin. International review of cell and molecular biology, 2012. **299**: p. 199-234.

381. Joshi D, T.J., Shiwen X, Patel H, Selvakumar S, Lawrence D, Abraham D, Baker D. Helix-B peptide of erythropoietin could be used as pharmacotherapy in critical limb ischaemia. in British Journal Surgery: 45th Annual Scientific Meeting of the Vascular-Society-of-Great-Britain-and-Ireland. 2011. British Journal Surgery.

382. Bahlmann, F.H., et al., Erythropoietin regulates endothelial progenitor cells. Blood, 2004. **103**(3): p. 921-6.

383. Heeschen, C., et al., Erythropoietin is a potent physiologic stimulus for endothelial progenitor cell mobilization. Blood, 2003. **102**(4): p. 1340-6.

384. Urbich, C. and S. Dimmeler, Endothelial progenitor cells: characterization and role in vascular biology. Circulation research, 2004. **95**(4): p. 343-53.

385. Fu, W., et al., Recombinant human erythropoietin preconditioning attenuates liver ischemia reperfusion injury through the phosphatidylinositol-3 kinase/AKT/endothelial nitric oxide synthase pathway. The Journal of surgical research, 2013. **183**(2): p. 876-84.

386. Elsherbiny, A., et al., EPO reverses defective wound repair in hypercholesterolaemic mice by increasing functional angiogenesis. Journal of plastic, reconstructive & aesthetic surgery : JPRAS, 2012. **65**(11): p. 1559-68.

387. Carr, C.L., et al., Dysregulated selectin expression and monocyte recruitment during ischemia-related vascular remodeling in diabetes mellitus. Arterioscler Thromb Vasc Biol, 2011. **31**(11): p. 2526-33.

388. Crawford, R.S., et al., Divergent systemic and local inflammatory response to hind limb demand ischemia in wild-type and ApoE-/- mice. The Journal of surgical research, 2013. **183**(2): p. 952-62.

389. Landazuri, N., et al., Growth and regression of vasculature in healthy and diabetic mice after hindlimb ischemia. American journal of physiology. Regulatory, integrative and comparative physiology, 2012. **303**(1): p. R48-56.

390. Pattillo, C.B., et al., Dipyridamole reverses peripheral ischemia and induces angiogenesis in the Db/Db diabetic mouse hind-limb model by decreasing oxidative stress. Free radical biology & medicine, 2011. **50**(2): p. 262-9.

391. Tekabe, Y., et al., Imaging the effect of receptor for advanced glycation endproducts on angiogenic response to hindlimb ischemia in diabetes. EJNMMI research, 2011. **1**(1): p. 3.

392. Terry, T., et al., CD34(+)/M-cadherin(+) bone marrow progenitor cells promote arteriogenesis in ischemic hindlimbs of ApoE(-)/(-) mice. PloS one, 2011. **6**(6): p. e20673.

393. Ruiter, M.S., et al., Diabetes impairs arteriogenesis in the peripheral circulation: review of molecular mechanisms. Clinical science, 2010. **119**(6): p. 225-38.

394. Hazarika, S., et al., Impaired angiogenesis after hindlimb ischemia in type 2 diabetes mellitus: differential regulation of vascular endothelial growth factor receptor 1 and soluble vascular endothelial growth factor receptor 1. Circulation research, 2007. **101**(9): p. 948-56.

395. Brown, W.M., et al., Erythropoietin receptor expression in non-small cell lung carcinoma: a question of antibody specificity. Stem cells, 2007. **25**(3): p. 718-22.

396. Kirkeby, A., et al., Functional and immunochemical characterisation of different antibodies against the erythropoietin receptor. Journal of neuroscience methods, 2007. **164**(1): p. 50-8.

397. Sturiale, A., et al., Erythropoietin and its lost receptor. Nephrology, dialysis, transplantation : official publication of the European Dialysis and Transplant Association - European Renal Association, 2007. **22**(5): p. 1484-5.

398. Kase, S., et al., Expression of erythropoietin receptor in human epiretinal membrane of proliferative diabetic retinopathy. The British journal of ophthalmology, 2007. **91**(10): p. 1376-8.

399. Spandou, E., et al., Hypoxia-ischemia affects erythropoietin and erythropoietin receptor expression pattern in the neonatal rat brain. Brain Res, 2004. **1021**(2): p. 167-72.

400. Wright, G.L., et al., Erythropoietin receptor expression in adult rat cardiomyocytes is associated with an acute cardioprotective effect for recombinant erythropoietin during ischemia-reperfusion injury. FASEB journal : official publication of the Federation of American Societies for Experimental Biology, 2004. **18**(9): p. 1031-3.

401. Bahlmann, F.H., et al., Endothelial progenitor cell proliferation and differentiation is regulated by erythropoietin. Kidney Int, 2003. **64**(5): p. 1648-52.

402. Abdel-Mageed, A.B., et al., Erythropoietin-induced metallothionein gene expression: role in proliferation of K562 cells. Experimental biology and medicine, 2003. **228**(9): p. 1033-9.

403. Westenfelder, C. and R.L. Baranowski, Erythropoietin stimulates proliferation of human renal carcinoma cells. Kidney Int, 2000. **58**(2): p. 647-57.

404. Guo, L., et al., Effects of erythropoietin on osteoblast proliferation and function. Clinical and experimental medicine, 2012.

405. Mourkioti, F. and N. Rosenthal, IGF-1, inflammation and stem cells: interactions during muscle regeneration. Trends in immunology, 2005. **26**(10): p. 535-42.

406. Muscaritoli, M., et al., Prevention and treatment of cancer cachexia: new insights into an old problem. European journal of cancer, 2006. **42**(1): p. 31-41.

407. Brevetti, G., et al., IGF system and peripheral arterial disease: relationship with disease severity and inflammatory status of the affected limb. Clinical endocrinology, 2008. **69**(6): p. 894-900.

408. Akhmedov, D. and R. Berdeaux, The effects of obesity on skeletal muscle regeneration. Frontiers in physiology, 2013. **4**: p. 371.

409. Krause, M.P., et al., Impaired macrophage and satellite cell infiltration occurs in a muscle-specific fashion following injury in diabetic skeletal muscle. PloS one, 2013. **8**(8): p. e70971.

410. Nguyen, M.H., M. Cheng, and T.J. Koh, Impaired muscle regeneration in ob/ob and db/db mice. TheScientificWorldJournal, 2011. **11**: p. 1525-35.

411. Fadini, G.P., et al., Circulating endothelial progenitor cells are reduced in peripheral vascular complications of type 2 diabetes mellitus. J Am Coll Cardiol, 2005. **45**(9): p. 1449-57.

412. Kougias, P., et al., Effects of adipocyte-derived cytokines on endothelial functions: implication of vascular disease. The Journal of surgical research, 2005. **126**(1): p. 121-9.

413. Virdis, A. and E.L. Schiffrin, Vascular inflammation: a role in vascular disease in hypertension? Current opinion in nephrology and hypertension, 2003. **12**(2): p. 181-7.